HAEMATIN-QUINOLINE INTERACTIONS AND STRUCTURE-ACTIVITY RELATIONSHIPS IN THE ANTIMALARIAL CHLOROQUINE AND RELATED COMPOUNDS

BY

CATHERINE HART KASCHULA

Thesis Presented for the Degree of

DOCTOR OF PHILOSOPHY

In the Department of Chemistry

UNIVERSITY OF CAPE TOWN

March 2002

Supervisors: Dr T.J.Egan and Associate Professor R. Hunter

ABSTRACT

The nature of the ferriprotoporphyrin IX (Fe(III)PPIX) antimalarial drug target and its interactions with aminoquinolines was investigated spectrophotometrically. Fe(III)PPIX was found to be extensively dimerised in aqueous solution (log $K_D = 7.2 \pm 0.2$) and is proposed to exist as a stacked, π-π dimer and not a μ-oxo dimer as previously thought. Sensitivity of the spectrum charge transfer region of the visible spectrum to pH further conforms that the dimer is not a μ-oxo dimer. A series of 17 synthesised compounds and 7 commercially available quinolines were investigated for their ability to interact with Fe(III)PPIX, inhibit β-haematin formation and for antiplasmodial activity against the D10 chloroquine-sensitive strain of malaria parasite. 2- And 4-aminoquinoline were found to be unique in their ability to form strong complexes with Fe(III)PPIX (log $K = 4.23 \pm 0.02$ and 4.49 ± 0.01 respectively) whilst quinoline, 3-, 5-, 6- and 8-aminoquinoline fail to form any detectible complexes with Fe(III)PPIX. The association with Fe(III)PPIX was found to be a necessary, but not sufficient requirement for inhibition of β-haematin formation. The presence of a chloro-group at the 7-position on the quinoline ring was found to be a requirement for this inhibition. In turn, inhibition of β-haematin formation was found to be a necessary but not sufficient requirement for antiplasmodial activity. A basic side-chain was found to be the additional component needed for this activity. In a further series of eleven N^2-(7-X-4-quinolinyl)-N^1,N^1-diethyl-1,2-ethanediamines where X = NH_2, OH, OCH_3, H, CH_3, F, I, Br, Cl, CF_3 and NO_2 that were synthesised, it was found that the pK_a of the quinoline ring nitrogen and the tertiary amino nitrogen are both lowered by electron withdrawing sustituents at the 7-posiiton. The quinoline nitrogen pK_a ranges from 6.28 in the nitro derivative to 8.36 in the amino derivative, whilst the tertiary amino nitrogen has a pK_a ranging between 7.65 in the trifluoromethyl derivative and 10.02 in the amino derivative. Calculation suggests that the resulting pH trapping of these compounds in the parasite food vacuole ranges between about 9% of that observed in chloroquine for the nitro derivative and 97% in the amino derivative. It was found that the critical structural feature in chloroquine and related 4-aminoquinolines responsible for strong β-haematin inhibition is the chloro-group at the 7-position on the 4-aminoquinoline ring. In the series of eleven 7-substituted 4-aminoquinolines a direct correlation was observed between antiplasmodial activity which had been normalised for the extent of pH trapping and β-haematin inhibitory activity ($r^2 = 0.83$, $p = 0.004$). The β-haematin inhibitory activity was found to correlate with the Fe(III)PPIX-quinoline association constant and the Hammett constant of the substituent at the 7-posiiton. The association constant was found to correlate with the lipophilicity of the group at the 7-position.

DECLARATION

I declare that "***Haematin-Quinoline Interactions and Structure-Activity Relationships in the Antimalarial Chloroquine and Related Compounds***" is my own work and that all sources that I have used or quoted have been indicated and acknowledged by means of complete references.

Signed by candidate

Catherine Hart Kaschula

ACKNOWLEDGEMENTS

I would like to thank the following people for their contributions towards this thesis:

Dr T. J. Egan for the large amount of time and energy he has invested in me, and for his endless enthusiam and interest in my PhD project;

Associate Professor Roger Hunter who always made himself available to give advice on synthetic aspects of my project;

All my past and present colleagues in the Department of Chemistry, particularly those in the Organic Synthesis laboratories;

Professor Donatella Taramelli, Dr Diego Monti, Erica Pasini, Nicoletta Basilico and Silvia Parapini at the University of Milan making me feel so welcome during my stay in Italy;

Professor Helder Marques and the postgraduate students in the Bioinorganic laboratories at the University of the Witwatersrand for allowing me to use their laboratory facilities;

Thembalani Nomkoko for his help in determining the pK_a's of my compounds;

Piero Benincasa, Dr Phillip Boshoff, Noel Hendricks and Pete Roberts for their analytical services.

I would also like to that the National Research Foundation and my supervisors for their financial assistance without which, this thesis would not have been possible.

Finally I would like to thank my parents for always encouraging me to do what I wanted and Nick-Desmond Smith for his continued support, especially towards the end when it was most needed and for his time he spent proofreading this thesis.

CONFERENCE PROCEEDINGS AND PUBLICATIONS ARISING FROM THIS WORK

CONFERENCE PROCEEDINGS

1998: 06 – 10 July, 7th International Chemistry Conference in Africa and 34th Convention of the South African Chemical Institute, University of Natal, Durban, South Africa.
Poster – "Synthesis of 4-Aminoquinolines for Investigation of the Mechanism of Action of Chloroquine".

1999: 08 – 09 April, University of Cape Town International Research Conference – " Trends in Organic Synthesis"
Lecture – "Synthetic and Physical Studies into the Mode of Action of Chloroquine".

1999: 20 – 22 September, British Society of Parasitology, Imperial College, London.
Poster – "Structure – Function Relations in Chloroquine and Related Antimalarials: a Detailed Model of the Mode of Action of Chloroquine".

2001: 7 - January, 1st Binational RSC/SACI International Conference – Organic Chemistry, University of Cape Town, South Africa.
Poster – "Chloroquine – Type Antimalarials act by Inhibiting the Haem Detoxification Pathway (β-Haematin Formation) in the Malaria Parasite.

PUBLICATIONS

Egan, T. J., Hunter, R., Kaschula, C. H., Mavuso, W. W. Towards the Rational Design of Antimalarial Drugs. *S. Afr. J. Sci.*, **1998**, 94, 1 – 2.

Egan, T. J., Hunter, R., Kaschula, C. H., Marques, H. M., Misplon, A., Walden, J. Structure – Function Relationships in Aminoquinolines: Effect of Amino and Chloro Groups on Quinoline – Haematin Complex Formation, Inhibition of β-Haematin Formation, and Antiplasmodial Actiivity. *J. Med. Chem.*, **2000**, 43, 283 – 291.

Egan, T. J., Hunter, R., Kaschula, C. H., Ncokazi, K. K. A Bioinorganic Approach Towards the Rational Discovery of New Antimalarials. *J. Inorg. Biochem.*, **2001**, 86, 43.

Kaschula, C. H., Egan, T. J., Hunter, R., Basilico, N., Parapini, S., Taramelli, D., Pasini, E., Monti, D. Structure – Function Relationships in 4-Aminoquinolines Antiplasmodials. The Role of the Group at the 7-Position. *J. Med. Chem.* **2002**, 45, 3531 – 3539.

TABLE OF CONTENTS

INTRODUCTION

1.1. HISTORICAL OUTLINE 1

1.2. CURRENT GLOBAL MALARIA SITUATION 1

1.2.1. The Global Malaria Eradication Campaign 1
1.2.2. The Current Global Situation 2

1.3. THE LIFE CYCLE OF THE MALARIA PARASITE 3

1.4. CURRENT UTILISATION OF QUINOLINE ANTIMALARIALS 5

1.4.1. The Discovery of Important Antimalarials 5
1.4.2. Clinical Use 8

1.5. MECHANISM OF ACTION OF QUINOLINE ANTIMALARIALS 9

1.5.1. Evidence that the Food Vacuole is the Locus of Antimalarial Activity 9
1.5.2. Biochemical Processes Occurring in the Food Vacuole 10
1.5.2.1. Haemoglobin Degradation 10
1.5.2.1.1. The pH of the Food Vacuole 10
1.5.2.1.2. Proteases Involved in Haemoglobin Degradation 10
1.5.2.1.3. The Haem Detoxification Pathway 11
1.5.2.2. The Structure of Malaria Pigment 12
1.5.2.3. Mechanism of β-Haematin and Haemozoin Formation 12
1.5.2.3.1. Mechanism of β-Haematin Formation 12
1.5.2.3.2. Mechanism of Haemozoin Formation 14
1.5.3. Hypotheses on the Mode of Action of Quinoline Antimalarials 14
1.5.3.1. Extravacuolar Hypotheses 15
1.5.3.1.1. DNA Binding 15
1.5.3.1.2. Inhibition of Polyamine Synthesis 15
1.5.3.2. Intravacuolar Hypotheses 15
1.5.3.2.1. Inhibition of Haemoglobin Degradation 15
1.5.3.2.1.1. Inhibition of Phospholipase Activity 16
1.5.3.2.1.2. Inhibition of Protease Activity 16
1.5.3.2.2. Increased Vacuolar pH 16
1.5.3.2.3. Binding to Haematin 17

1.5.3.3. Accumulation of Chloroquine in the Food Vacuole 17
1.5.3.3.1. Non-Saturable Uptake via Weak Base Properties (Intravacuolar) 17
1.5.3.3.2. Saturable Uptake via Haematin Binding 20
1.5.3.4. The Nature of Fe(III)PPIX-Quinoline Interactions 22
1.5.3.5. Association Constants for Fe(III)PPIX-Quinoline Interactions 25
1.5.4. Hypotheses on how Complex Formation is Related to Antiplasmodial Activity 27
1.5.4.1. Inhibition of Protein Synthesis 27
1.5.4.2. Inhibition of β-Haematin Formation 28
1.5.4.2.1. Inhibition of a Haem Polymerase Enzyme 28
1.5.4.2.2. Inhibition of Crystallisation Activity 28
1.5.4.3. Interaction of Haematin with Biological Membranes 33
1.5.4.4. Alternative Hypotheses on the Fate of Intravacuolar Haematin 34

1.6. RESISTANCE MECHANISMS 35

1.6.1. Reduced Uptake vs Enhanced Efflux 35
1.6.2. Other Hypotheses on Reduced Chloroquine Accumulation 37
1.6.2.1. Reduced NHE activity 37
1.6.2.2. Reduced Vacuolar pH 37
1.6.2.3. Reduced Access to Haematin 37
1.6.3. Concluding Remarks 38
1.6.4. Structural Modifications that Circumvent Resistance 38
1.6.4.1. Changes to the Aminoalkyl Side-Chain of Chloroquine 38
1.6.4.2. Changes to the Quinoline Ring 40

1.7. AIMS AND OBJECTIVES 42

1.7.1. Aims 42
1.7.2. Objectives 42
1.7.2.1. Investigation of the Target 42
1.7.2.1.1. The Nature of Fe(III)PPIX in Aqueous Solution 42
1.7.2.1.2. Structural Features of *CQ* Critical for Fe(III)PPIX- *CQ* Binding 42
1.7.2.2. Mechanism of Action of 4-Aminoquinolines 43
1.7.2.2.1. Accumulation Through pH Trapping 43
1.7.2.2.2. Inhibition of β-Haematin Formation 43

SYNTHESIS

2.1. BACKGROUND 44

2.1.1 Synthetic Targets Chosen for the Study 45

2.2. OVERVIEW OF QUINOLINE REACTIVITY 46

2.2.1. Reactivity Towards Nucleophiles 46
2.2.2. Reactivity Towards Electrophiles 47
2.2.3. Reactivity of Quinoline 1-oxide 47

2.3. GENERAL ROUTES TO 2-AND 7-X-4-AMINOQUINOLINES 48

2.3.1. Routes to 2-Chloroquinoline 48
2.3.2. Route to 7-X-4-Chloroquinolines 49
2.3.2.1. Method 1. Via Quinoline 1-oxide 50
2.3.2.2. Method 2. Price and Roberts 52
2.3.2.2.1. Mechanistic Comments 57
2.3.3. Synthesis of 2- and 4-Aminoquinoline Analogues 60
2.3.4. Characterisation of 2-Aminoquinolines 63
2.3.5. Characterisation of 4-Aminoquinolines and 7-X-4-Aminoquinolines 65
2.3.6. Alternative Routes to 4-Aminoquinoline 71
2.3.7. Synthesis of the Remaining Analogues 72

THE BEHAVIOUR OF Fe(III)PPIX IN AQUEOUS SOLUTION

3.1. BACKGROUND 74

3.1.1. The Behaviour of Fe(III)PPIX in Haemoglobin 74
3.1.2. Characterisation of the μ-oxo dimer 76
3.1.3. Evidence for the Existence of Higher Aggregates in Aqueous Solution 79
3.1.4. Evidence for the Existence of the μ-oxo dimer in Aqueous Solution 80
3.1.4.1. Spectroscopic Study by Brown *et al.* 80
3.1.4.2. Determination of log K_{obs} 83
3.1.4.3. Determination of K and n 83
3.1.4.4. Reasons for Repeating the Study of Brown *et al.* 84

3.2. RESULTS AND DISCUSSION 87

3.2.1. Determination of α, β and log K_{obs} by Non-Linear Least Squares Fitting 87
3.2.1.1. Spectra of Haematin in Aqueous Solution 87
3.2.1.2. Derivation of the Dimerisation Equation 89
3.2.1.3. Analysis of Data 90
3.2.2. Independent Determination of α 90
3.2.3. Determination of log K_{obs} and β by Fixing α 101
3.2.4. Reanalysis of the Data of Brown *et al.* 102
4.2.4. Spectral Evidence 105

3.3. CONCLUSIONS 108

STRUCTURE-ACTIVITY RELATIONSHIPS IN 4-AMINOQUINOLINES

4.1. BACKGROUND 109

4.2. EXPERIMENTAL METHODS 111

4.2.1. Synthesis of the Chloroquine Analogues 111
4.2.2. Spectrophotometric Titrations 111
4.2.3. β-Haematin Inhibition 114
4.2.4. Antiplasmodial Testing 116

4.3. RESULTS 116

4.4. DISCUSSION 118

4.4.1. Structural Requirements for Haematin Binding 118
4.4.2. Structural Requirements for β-Haematin Inhibition 122
4.4.3. Structural Requirements for Antiplasmodial Activity 124

4.5. CONCLUSIONS 129

QUANTITATIVE STRUCTURE-ACTIVITY RELATIONSHIPS IN 4-AMINOQUINOLINE ANTIPLASMODIALS

5.1 BACKGROUND 132

3.2.1. Determination of α, β and log K_{obs} by Non-Linear Least Squares Fitting 87
3.2.1.1. Spectra of Haematin in Aqueous Solution 87
3.2.1.2. Derivation of the Dimerisation Equation 89
3.2.1.3. Analysis of Data 90
3.2.2. Independent Determination of α 90
3.2.3. Determination of log K_{obs} and β by Fixing α 101
3.2.4. Reanalysis of the Data of Brown *et al.* 102
4.2.4. Spectral Evidence 105

3.3. CONCLUSIONS 108

STRUCTURE-ACTIVITY RELATIONSHIPS IN 4-AMINOQUINOLINES

4.1. BACKGROUND 109

4.2. EXPERIMENTAL METHODS 111

4.2.1. Synthesis of the Chloroquine Analogues 111
4.2.2. Spectrophotometric Titrations 111
4.2.3. β-Haematin Inhibition 114
4.2.4. Antiplasmodial Testing 116

4.3. RESULTS 116

4.4. DISCUSSION 118

4.4.1. Structural Requirements for Haematin Binding 118
4.4.2. Structural Requirements for β-Haematin Inhibition 122
4.4.3. Structural Requirements for Antiplasmodial Activity 124

4.5. CONCLUSIONS 129

QUANTITATIVE STRUCTURE-ACTIVITY RELATIONSHIPS IN 4-AMINOQUINOLINE ANTIPLASMODIALS

5.1 BACKGROUND 132

5.2. EXPERIMENTAL METHODS 135

5.2.1. Synthesis of the N^2-(7-X-4-quinolinyl)-N^1,N^1-diethyl-1,2-ethanediamine Analogues 135
5.2.2. Spectrophotometric Titrations 135
5.2.3. β-Haematin Inhibition 135
5.2.3.1. IR Method (Egan *et al.* 1994) 135
5.2.3.2. BHIA Method (Parapini *et al.* 2000) 135
5.2.4. pK_a Determinations 136
5.2.5. Antiplasmodial Testing 136
5.2.6. Statistical Correlations 136

5.3. RESULTS 137

5.4. DISCUSSION 138
5.4.1. Effect of the group at the 7-Position on pK_{a1} and pK_{a2} 138
5.4.2. Relationship Between β-Haematin inhibition and Antiplasmodial Activity 141
5.4.3. Insights into the Molecular Basis for Complex Formation and β-Haematin Inhibition 145

5.5. CONCLUSIONS 147

CONCLUSIONS AND FUTURE WORK

6.1. CONCLUSIONS 149

6.2. FUTURE WORK 153

EXPERIMENTAL

7.1. SYNTHESIS 156

7.1.1. General Procedures 156
7.1.2. Synthesis, Purification and Characterisation of Compounds 158

7.2. PHYSICAL DETERMINATIONS 193

7.2.1. Commercially Available Chemicals Used 193
7.2.2. Haematin Dimerisation Methods 194
7.2.2.1. Instrumentation and General Methods 194
7.2.2.2. Methods for Determination of K_{obs}, α and β 194
7.2.2.2.1. Preparation of HEPES Buffers 194

7.2.2.2.2. Calculation of Ionic Strength 194
7.2.2.2.3. Preparation of Haematin Solutions 196
7.2.2.2.4. Collection of Titration Data 197
7.2.2.2.5. Derivation of the Haematin Dimerisation Model 197
7.2.2.2.5.1. Methods for Determination of K_{obs}, α and β 197
7.2.2.2.5.2. Methods for Determination of K and n 200
7.2.2.3. Derivation of the Model for Single Deprotonation 200
7.2.2.4. Methods for Determination of α in Detergent and Methanol Solutions 202
7.2.2.4.1. Preparation of Buffer Solutions 202
7.2.2.4.1.1. Preparation of SDS Solution 202
7.2.2.4.1.2. Preparation of TRITON X-100 and TWEEN 20 Solutions 203
7.2.2.4.1.3. Preparation of MES, HEPES and CHES Buffers 203
7.2.2.4.2. Preparation of Haematin Stock Solutions and Water-Methanol Solutions 204
7.2.2.4.3. Collection of Spectra 205
7.2.2.5. Determination of Haematin Solubility in Aqueous Solution 205
7.2.2.5.1. Preparation of KHP, MES and HEPES Buffers 205
7.2.2.5.2. Preparation of Haematin Stock Solution and Collection of Spectra 206
7.2.2.6. Spectra of Haematin Solutions Between 700nm and 450nm 206
7.2.2.6.1. Spectra of Haematin in HEPES Buffer with Pyridine, NaCl or $NaClO_4$ 206
7.2.2.6.2. Spectra of Haematin in 20% HEPES-Methanol Mixtures 206

7.2.3. Methods for Determination of Haematin-Quinoline Association Constants 206
7.2.3.1. Instrumentation Used 206
7.2.3.2. Preparation of Buffers 207
7.2.3.3. Preparation of Stock Solutions 207
7.2.3.4. Collection of Spectra 208
7.2.3.5. Spectroscopic Titrations 208
7.2.3.5.1. The 1:1 (quinoline:haematin) Association Model (Model 1) 208
7.2.3.5.2. The 2:1 (quinoline:haematin) Association Model (Model 2) 209
7.2.3. Derivation of the Equation for Vacuolar Accumulation Ratio 210
7.2.4. β-Haematin Inhibition 211
7.2.4.1. IR Method (Egan *et al.* 1994) 211
7.2.4.1.1. Instrumentation and General Methods 211
7.2.4.1.2. Assay 211
7.2.4.2. BHIA Method (Parapini *et al.* 2000) 212
7.2.5. pK_a Determinations 212
7.2.6. Antiplasmodial Testing 213

APPENDIX 1 i

APPENDIX 2 xii

APPENDIX 3 xvi

REFERENCES xix

ABBREVIATIONS

A	Absorbance
Å	Angstrom
AQ	Amodiaquine
2-*AQ*	2-Aminoquinoline
3-*AQ*	3-Aminoquinoline
4-*AQ*	4-Aminoquinoline
5-*AQ*	5-Aminoquinoline
6-*AQ*	6-Aminoquinoline
8-*AQ*	8-Aminoquinoline
BHIA	Beta-haematin inhibitory assay
$BHIA_{50}$	50% Inhibitory concentration (molar equivalents relative to haematin)
CHES	2-[N-Cyclohexylamino]ethanesulfonic acid
Cl-Fe(III)PPIX	Chloroferriprotoporphyrin IX (haemin)
CQ	Chloroquine
DDT	Dichlorodiphenyltrichloroethane
DMSO	Dimethyl sulphoxide
ε	Molar extinction coefficient
Fe(III)PPIX	Ferriprotoporphyrin IX
HEPES	N-[2-Hydroxyethyl]piperazine-N-2-ethanesulfonic acid]
HO-Fe(III)PPIX or H_2O-Fe(III)PPIX	Hydroxo- or Aquaferriprotoporphyrin IX (haematin)
IC_{50}	50% Inhibitory concentration
K	Molar equilibrium constant
KHP	Potasium hydrogen phthalate
μ	Ionic strength
MES	2-{N-Morpholino}ethanesulfonic sodium salt
MeOH	Methanol
π	Lipophilicity constant
σ_m	Meta-Hammett constant
σ_p	Para-Hammett constant
SDS	Sodium dodecyl sulphate
T	Transmittance

TRITON X-100	Polyoxoethylethylene (10) isooctylpentyl ether
TWEEN-20	Polyoxoethylene sorbitan monolaurate
Uv-vis	Ultraviolet-visible
ν	Wavenumber
λ	Wavelength
WHO	World Health Organisation

INTRODUCTION

1.1. HISTORICAL OUTLINE

The antiquity of malaria, which is caused by protozoan parasites of the genus *Plasmodium*, is demonstrated by the host specificity of over 100 parasite species found in reptiles, birds and mammals. The four species of plasmodia that infect man are *P. vivax, P. malariae, P. ovale and P. falciparum*; of which *P. falciparum* is the most deadly (Bruce-Chwatt 1981).

It is thought that malaria was prevalent in ancient Egypt, India, China and Greece where its symptoms were described and documented. The Romans named the disease "*mal' aria*" as at that time, the disease was attributed to the "*bad air*" surrounding stagnant waters. Association of the disease with swamps, led to various methods of drainage practiced by the Greeks and Romans from the sixth century BC and continued in Europe throughout the middle ages (Bruce-Chwatt 1985, Sherman 1998).

1.2. CURRENT GLOBAL MALARIA SITUATION

1.2.1. The Global Malaria Eradication Campaign

Huge progress was made in reducing the number of malaria cases in the 1950's following the discovery of the insecticide dichlorodiphenyltrichloroethane (DDT), chloroquine chemotherapy and the establishment of the World Health Organisation (WHO) who embarked on a Global Malaria Eradication Campaign. The strategy was to interrupt malaria transmission from vector to host by attacking the mosquitoes likely to have contact with humans, namely inside homes. This was done by employing a very large taskforce of people to spray DDT in eighty percent of houses in infected areas. With dramatic results, malaria was eliminated completely from Taiwan, the Caribbean, the Balkans, parts of North Africa, in most parts of Europe, Northern Australia and a large portion of the South Pacific. Also a significant decrease in malaria cases was observed in Sri Lanka and India (Russel *et al.* 1963, WHO Health Report 1999, Gladwell 2001).

By the mid-1960's resistance to DDT and chloroquine had emerged and the indiscriminate use of DDT as an insecticide for agriculture had impacted in the Western American environment. These factors, along with dwindling enthusiasm for the campaign, prompted

the WHO to drop the eradication program and put in place control strategies which form the basis of their malaria policy today (Gladwell 200, WHO Health Report 1999).

Contrary to the rest of the world, the Global Eradication Campaign had very little impact in the Amazon basin and Sub-Saharan Africa where social and economic conditions meant the program was either not implemented or not sustainable (WHO Health Report 1999).

1.2.2. The Current Global Situation

The downward trend in malaria-related mortality achieved during the 1950's has undergone a reversal since the late 1980's. This resurgence is confined mainly to underdeveloped countries where inadequate or deteriorating health systems are unable to provide rapid diagnosis and treatment. Areas of civil conflict and large scale human migrations have resulted in malaria epidemics due to increased vector-human contact or movement of unprotected and non immune populations into malarious areas. Epidemics have also broken out due to climatic and environmental changes which have caused an increase in the number of vectors. Of growing concern is the increasing antimalarial drug resistance which is rendering current antimalarial treatment ineffective (Pasvol 1995, Sherman 1998, WHO Health Report 1999).

Today Malaria is the world's most important parasitic disease. Each year around 300 million people are infected with the disease and between 1.5 to 2.7 million people die. Almost 90% of the deaths occur in Sub-Saharan Africa where young children are the most affected. Malaria is directly responsible for one in five childhood deaths in Africa and indirectly contributes to illness and death from respiratory infections, diarrhoeal disease and malnutrition (WHO Health Report 1999). It is estimated that Malaria claims 100 000 lives per year elsewhere in the world and these deaths occur in all age groups, mainly among individuals who lack immunity and are infected by *P. falciparum* in areas where appropriate diagnosis and treatment are not available (Sherman 1998). The current worldwide distribution of malaria is shown in (Figure 1.1).

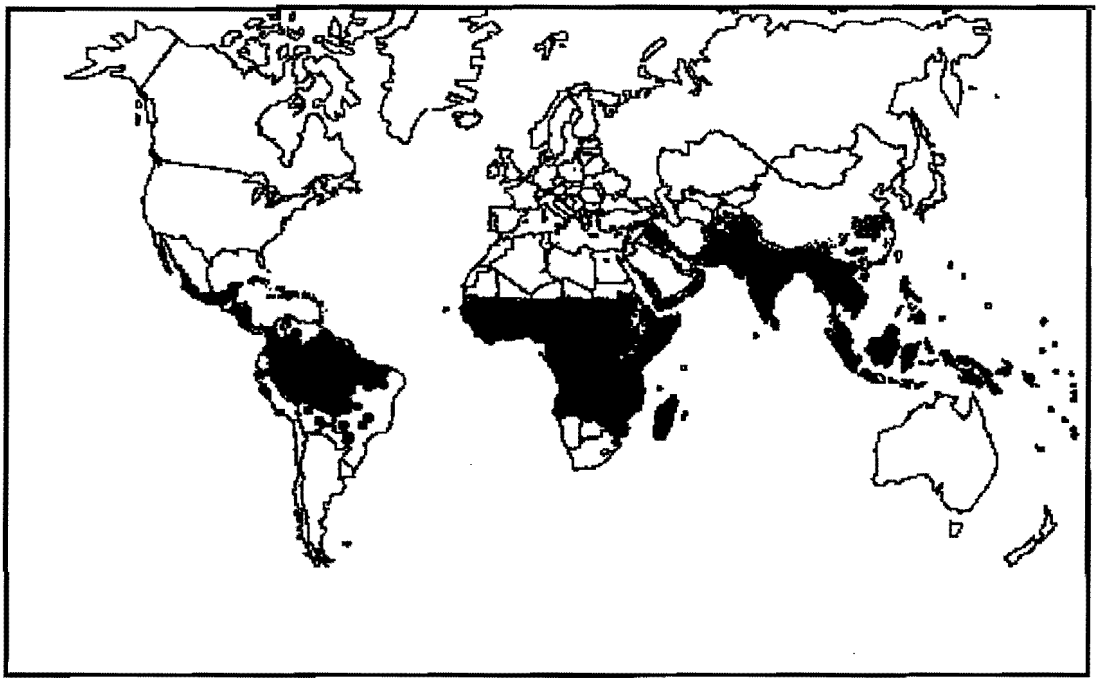

Figure 1.1. Global malaria distribution in 1994 (Sherman 1998).

1.3. THE LIFE CYCLE OF THE MALARIA PARASITE

The life cycle of all species of human malaria parasites are essentially the same (except that hypnozoites do not occur in *P. falcipaum*) and is represented in Figure 1.2.

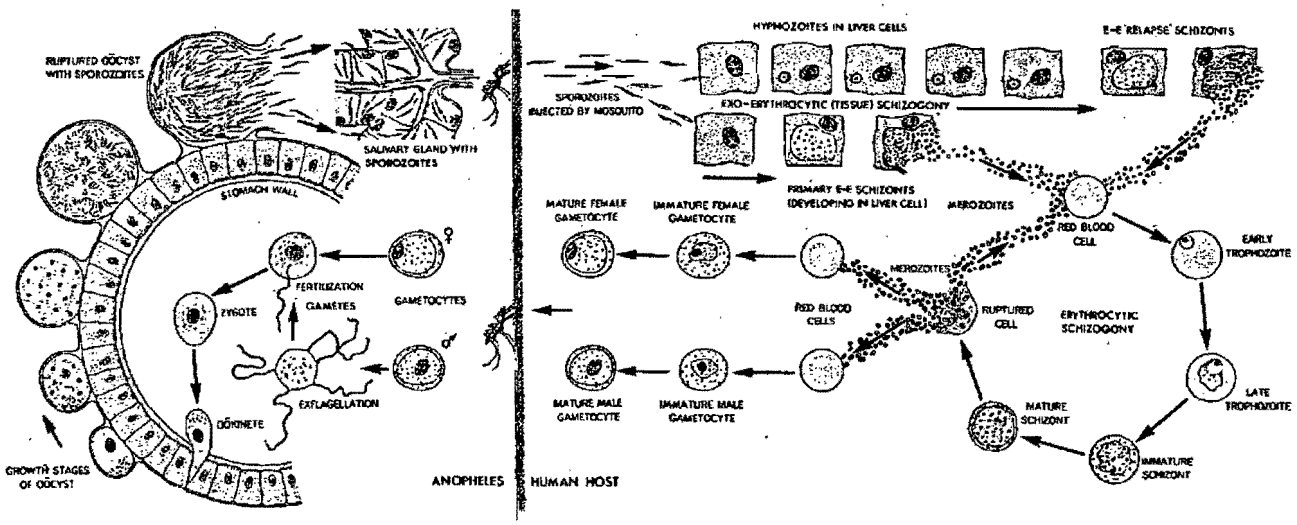

Figure 1.2. The life cycle of malaria parasites in the mosquito and human host (Bruce-Chwatt 1985)

Sporozoites, or infective stages are transmitted to a human host through the bite of around 60 different species of the female *Anopheles* mosquito. These sporozoites rapidly pass to the liver and penetrate parenchymal cells where they multiply 30 000 fold and form liver schizonts which burst open to release merozoites after 5 days in the case of *P. falciparum* (Pasvol 1995). The merozoites invade red blood cells and develop into small, rounded bodies with a parasitophorous vacuole called rings, which develop into larger, more irregular shaped trophozoites. This stage of the life cycle is associated with host haemoglobin degradation and the formation of the black, granular malaria pigment within an acidic secondary lysosome known as the food vacuole (Bruce-Chwatt 1985) (Figure 1.3).

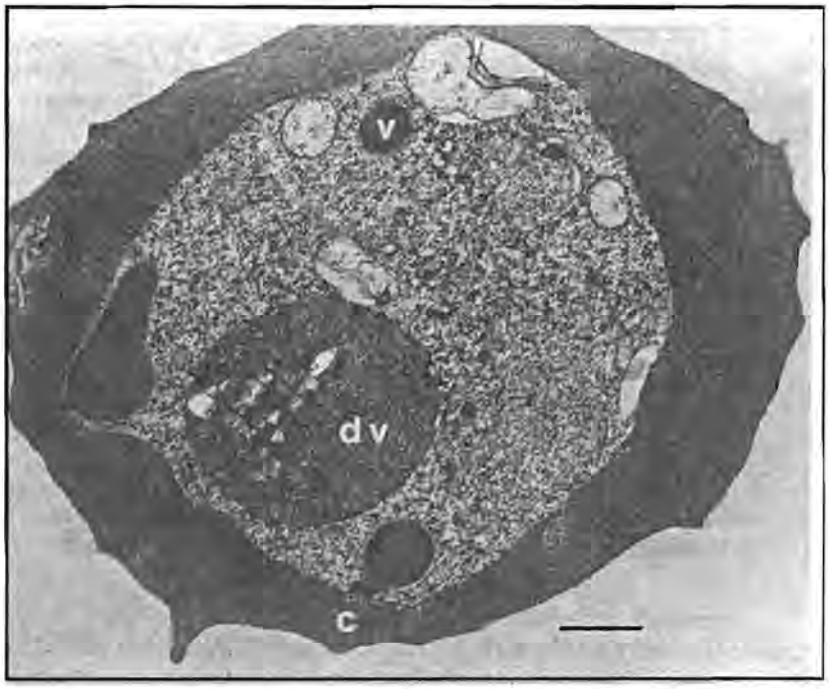

Figure 1.3. *P. falciparum* trophozoite actively digesting haemoglobin. dv, digestive vacuole; c, cystome; v, transport vesicle (Goldberg and Slater 1992).

The trophozoite divides asexually many times to form a blood schizont which, when mature, causes the red cell to burst open and release merozoites into the bloodstream. These merozoites then invade fresh red blood cells to produce another generation of parasites leading to a progressive increase in parasitemia which continues until host response regulation or death of the patient (Pasvol 1985, Bruce-Chwatt 1985). This blood stage cycle takes 48 hours in *P. falciparum*, *P.vivax* and *P. Ovale* and 72 hours in *P. malariae*, of which cell rupturing and freeing of merozoites into the blood stream is responsible for the periodic fevers associated with the disease (Pasvol 1995). In the case of *P. falciparum*, the blood

schizonts cause the erythrocytes to become sticky and adherent to the capillary endothelium of deep organs which can result in coma, known as cerebral malaria, severe anaemia or multiple organ failure (Pasvol 1995, Ridley 1998).

Some erythrocytic schizonts are intended to develop into male and female gametocytes which may then be taken up by an *Anopholes* mosquito through its bite. Once inside the gut of the mosquito, male and female gametes fuse to form a zygote which develops into an oocyst, and later into sporozoites. These sporozoites travel to the salivary glands where they wait to be discharged into the next human host when the mosquito takes another blood meal (Russell 1963, Bruce-Chwatt 1985).

P. falciparum is the most dangerous of the four human malarias because it can invade red blood cells of any age and produce overwhelming, potentially lethal parasitemias. There is virtually no risk of death from the other species that infect humans because they produce more limited parasitemias and can invade only young (*P.* vivax and *P.* ovale) or old (*P. malariae*) red blood cells with the latter being the mildest of the three (Pasvol 1995). *P. vivax* can complete its cycle inside the mosquito at lower temperatures than *P. falciparum* and was the malaria species transmitted in the UK and Netherlands in the 1800's (Pasvol 1995, Sherman 1998). Liver stage *P. vivax* parasites tend to persist in the liver parenchymal cells as hypnozoites and may give rise to late relapses, even after several years. *P. ovale* is similar to *P. vivax* and is found predominantly in West Africa (Pasvol 1995).

1.4. CURRENT UTILISATION OF QUINOLINE ANTIMALARIALS

1.4.1. The Discovery of Important Antimalarials

The first effective treatment for malaria in Europe was brought from Peru by the Spanish priests in the mid-sixteen hundreds. Whether the curative properties of the bark of the "fever trees" growing on the mountainous slopes of the Peruvian Andes were known to the local inhabitants before the Spanish conquest remains uncertain and controversial. Demand for the powdered bark, known as "Jesuit's powder" became so great in the seventeen hundreds that accessible South American forests of "fever trees" were soon stripped. The Dutch successfully planted *Cinchona ledgeriana* trees from Bolivia in Java and by the 1930's were producing 97% of the world's production (Bruce-Chwatt 1981). "Jesuit's powder" contains four quinine related alkaloids which differ with respect to symmetry about the chiral centres at C-8 and C-9, namely quinine (**1a**, 9R, 8S), quinidine (**1b**, 9S, 8R), 9-epiquinine (**1c**, 9S, 8S) and 9-epiquinidine (**1d**, 9R, 8R) (Figure 1.4). Of these four alkaloids, only quinine and

quinidine have strong antimalarial properties (Winstanley and Breckenridge 1987, White *et al.* 1981).

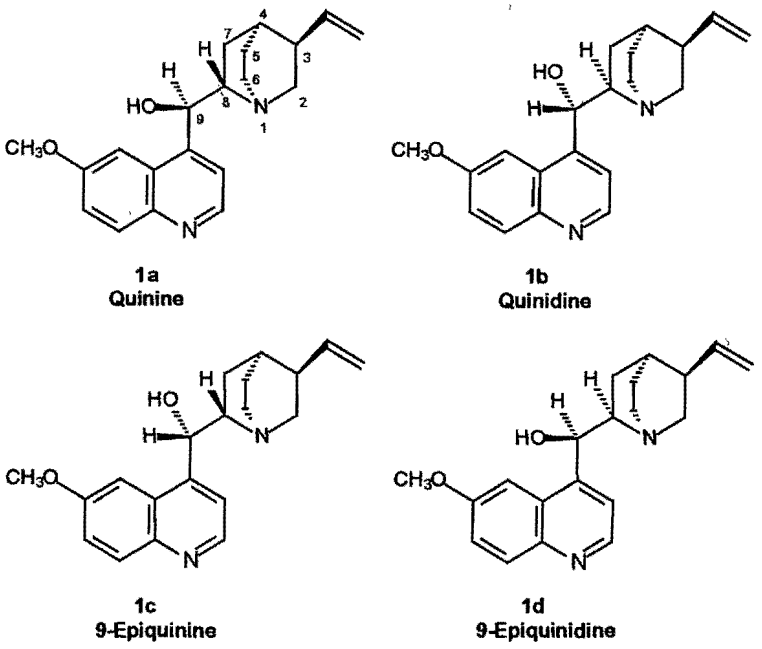

Figure 1.4. The four quinine alkaloids present in the bark of the Cinchona tree. Quinine (**1a**), quinidine (**1b**), 9-epiquinine (**1c**) and 9-epiquinidine (**1d**).

During the First World War, the Germans, having found themselves cut off from the world's supply of natural quinine alkaloids, began synthesising synthetic antimalarials. These efforts resulted in the discovery of the first 8-aminoquinoline, pamaquine (**2**) in 1932 and quinacrine (**3**) in 1933. **3** was used as the first Malaria prophylactic by the allied forces during World War II (Coatney 1963, Bruce-Chwatt 1985).

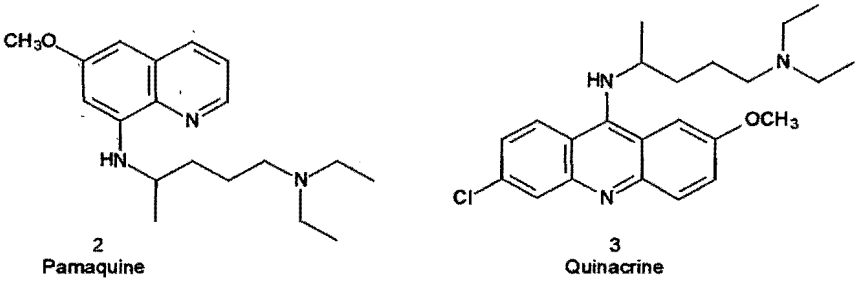

In 1935, Germans chemists working at Bayer I.G. synthesised analogues based on **2** and discovered sontoquine (**4**) and resochin (later known as chloroquine (*CQ*)) (Kenyon 1949, Coatney 1963). **4** was used as a prophylactic by the German troops and *CQ* was abandoned due to toxicity problems observed in preliminary trials (Coatney 1963). When a stock of **4** fell into US hands in 1941, *CQ* was rediscovered along with the development of amodiaquine (*AQ*) and the 8-aminoquinoline primaquine (**5**) (Kenyon 1949). Both *AQ* and **5** exhibit toxicity

which limits their widespread use. *CQ* however turned out to be one of the most successful drugs ever developed and formed the mainstay treatment and prophylaxis for over five decades.

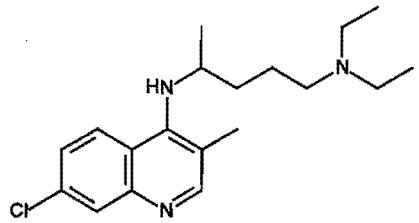

4
Sontoquine

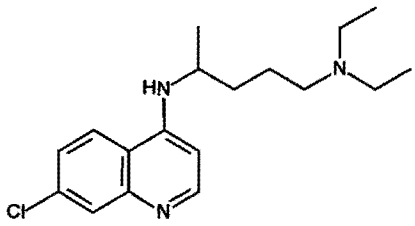

CQ
Chloroquine

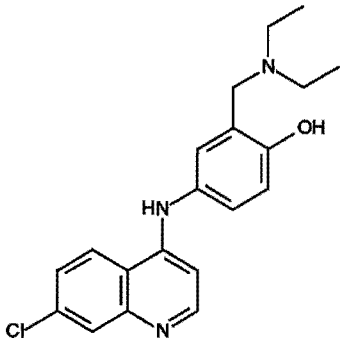

AQ
Amodiaquine

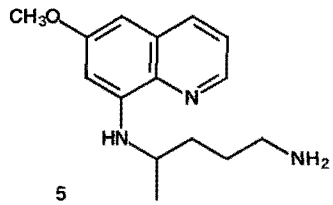

5
Primaquine

In the 1960's, *CQ* resistance to *P. falciparum* started to emerge simultaneously in Columbia, Brazil and Thailand. A very large program was launched with WHO sponsorship at the Walter Reed Army Institute of Research where 250 000 compounds were synthesised and screened for antimalarial activity. The result of this effort was the discovery of the phenanthrenemethanols of which halofantrine (**6**) is noteworthy and the quinolinemethanols which include mefloquine (**7**) (Bruce-Chwatt 1981, Egan 2001).

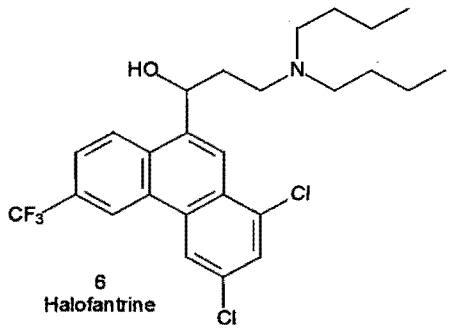

6
Halofantrine

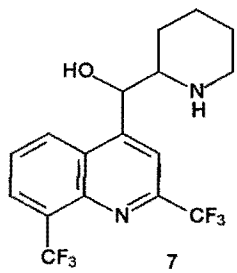

7
Mefloquine

Antimalarials currently being developed by the WHO include pyronaridine (**8**) which is based on the template of (**3**) and artemesinin derivatives which are based on artemesinin (**9**), an extract from the Chinese herb, *Artemisia annua.* **9**, has poor antiplasmodial activity due to

limited water solubility however the synthetic analogues artemether (**10**) and artesunate (**11**) have shown promising activity and are currently undergoing clinical trials (Sherman 1998).

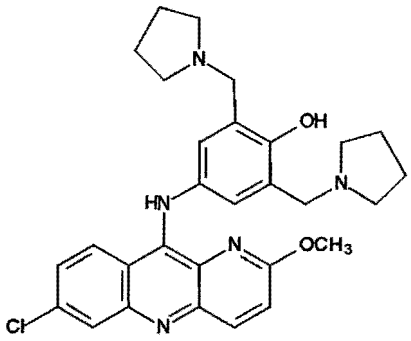

8
Pyronaridine

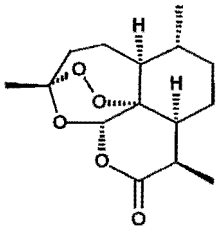

9
Artemesinin

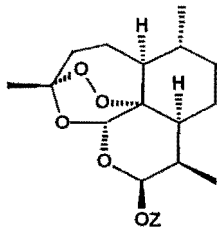

No	Name	Z
10	Artemether	CH_3
11	Sodium Artesunate	$COCH_2CH_2COONa$

1.4.2. Clinical Use

The 4-aminoquinolines, acridines and quinolinemethanols, which include chloroquine, amodiaquine, quinacrine, quinine and mefloquine, all act solely on the blood stage of the infection and are termed blood schizonticides. They clear the malaria parasites from the blood that give rise to the clinical symptoms of headaches, fevers and chills and therefore cure the disease. In cases of low toxicity, these blood schzonticides can be used prophylactically (Ridley 1998).

In contrast, the 8-aminoquinolines primaquine and pamaquine act only on the early liver stage and are termed tissue schizonticides. Their clinical utility is for radical cure of certain species of the malaria parasite, such as *P. vivax*, by eliminating the residual hypnozoites that can lead to recurrent infections. These tissue schizontocides are too toxic for routine use as prophylactics. For a summary of clinical use see Table 1.1.

Table 1.1. Clinical utility of quinoline antimalarial drugs currently in use.

Drug	Class of Compound	Site of Action		Clinical Utility
		Blood Stage	Liver Stage	
Chloroquine	4-aminoquinoline	+		T, P[a]
Amodiaquine	4-aminoquinoline	+		T
Quinacrine	9-aminoacridine	+		T[b]
Quinine	quinoline methanol	+		T
Mefloquine	quinoline methanol	+		T, P
Primaquine	8-aminoquinoline		+	T
Pamaquine	8-aminoquinoline		+	T[b]

T = treatment, P = prophylaxis, [a] limited by resistance, [b] no longer in clinical use

Chloroquine cross-resistance has been observed clinically in the structurally related 4-aminoquinoline drug amodiaquine and experimentally in pyronaridine. To delay the spread of resistance and prolong the utility of drugs, they are now marketed as combination therapies. This has been done successfully for mefloquine where resistance, which is now widespread in Thailand, has been successfully delayed by administration of Fansimef; a cocktail of mefloquine and the antibacterial agents pyrimethamine and sulfadoxone (Ridley 1998). When pyronaridine is marketed, it will probably be in combination with artesunate (Peters and Robinson 2000). Although quinine gives rise to serious toxic side effects, it is used along with mefloquine to treat chloroquine-resistant malaria (Egan 2001b).

1.5. MECHANISM OF ACTION OF QUINOLINE ANTIMALARIALS

1.5.1. Evidence that the Food Vacuole is the Locus of Antimalarial Activity

The utility of quinoline blood schizontocide drugs is limited to the stages actively involved in haemoglobin degradation, namely trophozoites and early schizonts (Yayon *et al.* 1983, Zhang *et al.* 1986). After exposure of these stage-specific parasites to *CQ*, the food vacuoles enlarge (Langareth *et al.* 1978) and according to some studies produce reduced amounts of haemozoin (Macomber and Sprinz 1967, Homewood *et al.* 1972, Zhang 1987, Zhang 1999) although it has been suggested that this may be secondary to parasite killing (Asawamahasakda *et al.* 1994). In addition, the parasite cytoplasm demonstrates ribosomal aggregation, mitochondrial swelling and swelling of the rough endoplasmic reticulum (Jacobs *et al.* 1988). Endocytosis and trafficking of erythrocytic haemoglobin to the central food vacuole continues normally in the presence of *CQ* but the intact vesicles accumulate in

the food vacuole without further digestion (Yayon *et al.* 1984). *CQ* accumulates (Aikawa 1972, Geary and Ginsburg 1989) in the damaged food vacuole of malaria trophozoites, and has been shown to associate with haemozoin (Sullivan *et al.* 1996b). Given the morphological changes and locus of accumulation upon *CQ* administration, it would appear that the primary drug target of *CQ* and related quinoline antimalarials is located within the food vacuole.

1.5.2. Biochemical Processes Occurring in the Food Vacuole

1.5.2.1. Haemoglobin Degradation

Malaria parasites obtain most of their amino acids required for protein synthesis from degrading 25 to 75% of host haemoglobin in the occupied erythrocyte (Goldberg *et al.* 1990, Loria *et al.* 1999). In this process, large quantities of erythrocyte cytoplasm are ingested by fluid phase endocytosis and transported in vesicles to a secondary lysosome known as the food vacuole (Sherman 1998).

1.5.2.1.1. The pH of the Food Vacuole

The pH of the food vacuole (pH_{vac}) was originally thought to range between pH 5.2 and 5.4 based on cuvette measurements of pH-sensitive fluorescent probes that had been endocytosed into the food vacuole of intra- (Krogstad *et al.* 1985) and extra-erythrocytic parasites (Yayon *et al.* 1984). Recently Dzekunov *et al.* found the pH_{vac} of the *CQ*-sensitive HB3 strain is 5.6 based on single-cell fluorescence measurements of parasitised erythrocytes stained with the fluorescent weak base, acridine orange (AO) (Dzekunov *et al.* 2000). Their experimental methods have since been called into question by Bray *et al.* who claim that the fluorescence pattern observed by Dzekunov *et al.* arises wholly from the parasites cytosol and not from the food vacuole (Bray *et al.* 2002a). Technical aspects of the microscopy techniques used to monitor AO fluorescence between the two laboratories, interpretation of the fluorescence patterns and hence the reported pH_{vac} of 5.6 is still a matter of intense debate (Dzekunov *et al.* 2002, Bray *et al.* 2002b).

1.5.2.1.2. Proteases Involved in Haemoglobin Degradation

The food vacuole contains multiple proteases that degrade haemoglobin to peptide fragments in an ordered process (Goldberg *et al.* 1990). Two aspartic proteases plasmepsins I and II (PM I and II), that initiate degradation by cleaving native haemoglobin in

a highly conserved hinge region, have been identified and extensively characterised (Goldberg *et al.* 1990, Goldberg *et al.* 1991, Tyas *et al.* 1999, Moon *et al.* 1997). Recently two additional proteases, namely a histidine-aspartic protease (HAP) containing an active site histidine, and plasmepsin IV (PM IV) have also been identified and implicated in the metabolism of haemoglobin (Banerjee *et al.* 2002). Two cysteine proteases falcipain 2 (Gluzman *et al.* 1994) and falcipain 3 (Sijwali *et al.* 2001) and a metallopeptidase falcilysin (Eggleson *et al.* 1999) are thought to act by degrading haemoglobin into smaller peptide fragments further downstream (Rosenthal and Meshnick 1996, Goldberg 1990). This degradation process is complicated by the release of ferrous haem which is rapidly oxidised to the ferric form known as haematin (aquaferriprotoporphyrin IX or H_2O-Fe(III)PPIX) (Figure 1.5). Solubilised haematin is cytotoxic and has been shown to damage biological membranes (Tappel 1953, Orjih *et al.* 1981, Ginsburg and Demel 1983, Van Der Zee *et al.* 1996) and inhibit a variety of enzymes (Yasuhara *et al.* 1991) including vacuolar proteases (Vander Jagt *et al.* 1987).

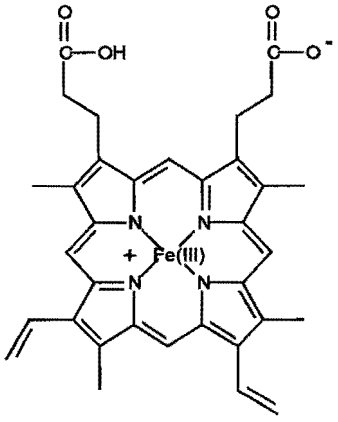

H_2O-Fe(III)PPIX

Figure 1.5. Structure of aqua-ferriprotoporphyrin IX (H_2O-Fe(III)PPIX)

1.5.2.1.3. The Haem Detoxification Pathway

The malaria parasite has evolved a pathway to detoxify haematin by conversion, at least in part, to the highly insoluble, black, granular substance known as malaria pigment or haemozoin. This substance is responsible for organ discolouration in malaria patients and was first described by Lancisi in 1716 and later by Bright in 1831 (Sherman 1998). Haemozoin formation is not unique to erythrocytic stage malaria parasites, but has also been identified in other animals that degrade haemoglobin where it presumably serves the same purpose. These organisms are a blood sucking insect *Rhodinus prolixus*, which is an important vector of *Trypanosoma cruzi*, the causative agent of Chaga's disease (Oliviera *et*

al. 1999, Oliviera *et al.* 2000a); *Shistosoma mansoni*, a worm in humans causing schistosomiasis (Oliveira *et al.* 2000b, Chen *et al.* 2000) and *Haemoproteus columbae*, a protozoan parasite common in birds (Chen *et al.* 2001).

1.5.2.2. The Structure of Malaria Pigment

Malaria pigment can be synthesised *in vitro* by precipitation of haematin under acid conditions (Slater *et al.* 1991, Egan *et al.* 1994) to form the synthetic equivalent known as β-haematin. The native and synthetic forms of haemozoin are chemically and structurally equivalent as shown spectroscopically by infra-red, EXAFS and ESR spectroscopy as well as X-ray powder diffraction (Slater *et al.* 1991, Scott Bohle *et al.* 1998, Egan *et al.* 1999a). For many years β-haematin was believed to be a polymer of haematin, however publication of the recently solved X-ray diffraction pattern (Pagola *et al.* 2000) has shown that β-haematin is composed of crystalline dimers linked together through a Fe(III)-carboxylate bond (Figure 1.6). These dimeric units interact in the crystal through hydrogen bonding between the remaining propionic acid group on each Fe(III)PPIX.

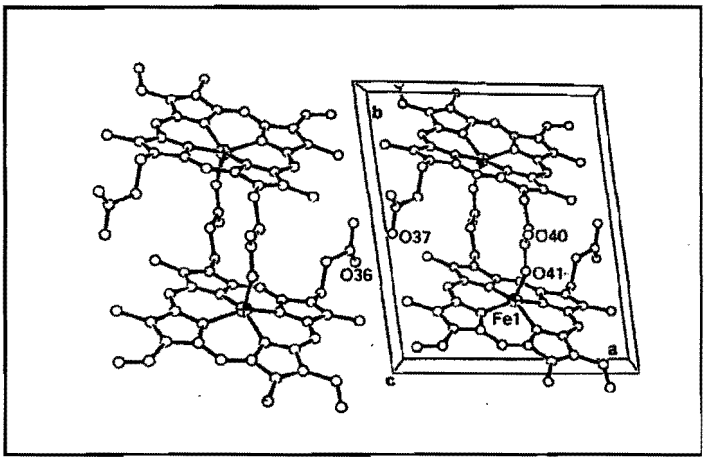

Figure 1.6. Structure of the β-haematin dimer (Pagola *et al.* 2000).

1.5.2.3. Mechanism of β-Haematin and Haemozoin Formation

1.5.2.3.1. Mechanism of β-Haematin Formation

β-Haematin can be precipitated from aqueous 0.1 - 4.5M acetate solution between pH 2.6 and 5, at temperatures ranging from 6 to 70°C and reaction times between 30mins and overnight (Slater *et al.* 1991, Egan *et al.* 1994, Slater 1998). The optimum set of conditions

for this process is a vigorously stirred solution of haematin in 4.5M acetate, pH 4.5 at 60°C for 1h (Egan *et al.* 2001c). In this observed pH window, one of the deprotonated carboxylate groups is available for coordination to the Fe(III) centre of a second haematin molecule, with the remaining protonated carboxylate group available for intermolecular hydrogen bonding between two dimers. Formation of the product can be monitored by the appearance of two peaks in the infrared spectrum around 1660cm^{-1} and 1210cm^{-1} which are believed to arise from C=O and C-O stretching of the Fe(III)-coordinated propionate groups respectively (Slater *et al.* 1991) (Figure 1.7).

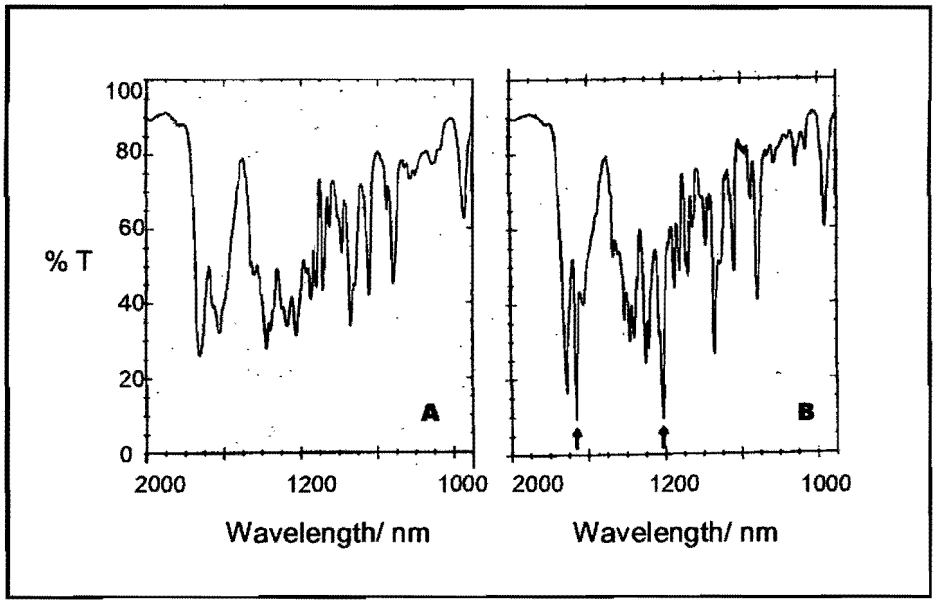

Figure 1.7. Infrared spectra of haematin after 0 (**A**) and 30min incubation (**B**) 4.5M acetate, pH 4.5, 60°C. The definitive peaks for β-haematin around 1660cm^{-1} and 1210cm^{-1} are marked by arrows (Egan *et al.* 1994).

Conversion of haematin to β-haematin is spontaneous under the range of conditions mentioned although the reaction is markedly slower in acetate solutions below 4.5M and at pHs and temperatures below 3.0 and 60°C respectively (Egan *et al.* 1994, Egan *et al.* 2001c). The process of β-haematin formation occurs via rapid precipitation of noncrystalline haematin followed by slow conversion to the crystalline product. The acetate is thought to facilitate the dimerisation reaction by solubilising haematin through formation of a Fe(III)PPIX-acetate complex (Egan *et al.* 1994, Egan *et al.* 2001c). The reaction kinetics follow a sigmoidal relationship which has been explained in terms of a biomineralisation process in which a rapidly precipitated, noncrystalline solid slowly converts to a more thermodynamically stable, crystalline product through an ordered process involving nucleation and crystal growth (Egan *et al.* 2001c).

1.5.2.3.2. Mechanism of Haemozoin Formation

There is still much uncertainty regarding the mechanism of haemozoin formation *in vivo*. β-Haematin can form spontaneously from haematin under physiological conditions (37°C and pH 4.8) but the reaction only goes to completion after 12 days (Dorn *et al.* 1998a). Slater and Cerami suggested that haemozoin formation is enzyme catalysed *in vivo* and demonstrated the catalytic activity of this putative enzyme present in *P. falciparum* trophozoites extracts (Slater and Cerami 1992). That the reaction is enzyme mediated was questioned by Dorn *et al.* who noted that heat treatment of the extracts had little effect on the reaction and suggested the initiator is haemozoin itself (Dorn *et al.* 1995). Bendrat *et al.* suggested that this reaction promoting material is a lipid contaminating the haemozoin extracts (Bendrat *et al.* 1995, Ridley *et al.* 1995). This has been supported by subsequent work in which acetonitrile extracts of malarial trophozoites and uninfected erythrocytes promote β-haematin formation (Dorn *et al.* 1998a). It has been suggested that the active promoters in these extracts are lipids which themselves can catalyse the reaction (Dorn *et al.* 1998, Fitch *et al.* 1999, Fitch *et al.* 2000). This is further supported by the ability of perimicrovillar membranes from the midgut of the haemozoin producing insect *R. prolixus* to promote β-haematin formation (Oliveira *et al.* 1999, Oliveira *et al.* 2000a).

Sullivan *et al.* managed to identify and clone two histidine-rich proteins (HRP II and HRP III) in purified digestive vacuoles which promote β-haematin formation *in vitro.* (Sullivan *et al.* 1996a). This protein, which bears a similarity to human histidine-rich glycoprotein (HRG), can bind around 50 haem units which all share a similar environment as indicated by electronic absorption, resonance Raman and EPR spectroscopy (Choi *et al.* 1999). These authors claim all the ferrihaems in the HRP II-Fe(III)PPIX complex are low spin, six coordinate with two histidine ligands and that this complex is stable between pH 5.5 and 7.0. These results are at odds with the findings of Lynn *et al.*, who observed two types of pH-dependent Fe(III)PPIX binding in HRP-II. Below pH 6, Fe(III) is supposedly coordinated to aspartate through a weak carboxylate-metal interaction which is capable of promoting haemozoin formation. Above pH 6, it is thought that formation of a strong Fe(III)-histidine complex correlates to the lack of haemozoin formation in this pH range (Lynn *et al.* 1999).

Since recent findings on the mechanism of β-haematin formation *in vitro* have compared this process to biomineralisation, it is possible that the role of HRP *in vivo* may be to provide a scaffold on which nucleation and growth of the crystal can occur (Egan *et al.* 2001c).

1.5.3. Hypotheses on the Mode-of-Action of Quinoline Antimalarials

1.5.3.1. Extravacuolar Hypotheses

From the morphological changes and specific accumulation associated with the food vacuole upon *CQ* administration, it would appear that this is the primary locus of drug activity. Various extravacuolar hypotheses have however been proposed over the last four decades but none have found widespread acceptance.

1.5.3.1.1. DNA Binding

CQ was originally thought to exert its antimalarial activity through DNA intercalation and hence inhibition of DNA replication and RNA synthesis. *In vitro CQ* binds to DNA (O'Brien *et al.* 1966) but at concentrations significantly higher (100μM) than the *in vitro* concentration (typically 10nM) (Slater 1993). This theory has been further rejected on the basis that the quinoline antimalarial, mefloquine, does not bind to DNA (Davidson *et al.* 1975), and that there is no selectivity between the *CQ* - DNA interactions of host and parasite DNA (Angerman *et al.* 1972).

1.5.3.1.2. Inhibition of Polyamine Synthesis

CQ inhibits ornithine decarboxylase activity present in trophozoite extracts (Königk *et al.* 1981). Since inhibition of this enzyme would block polyamine synthesis, it has been suggested that *CQ* may exert its antiplasmodial activity through this effect. There have been no further follow-up experiments to lend weight to this hypothesis which does not account for the erythrocytic stage specificity of this drug, as liver stage parasites also presumably have orthinine decarboxylase (Slater 1993).

1.5.3.2. Intravacuolar Hypotheses

1.5.3.2.1. Inhibition of Haemoglobin Degradation

One of the morphological changes observed in malaria parasites upon *CQ* administration is an accumulation of undigested haemoglobin-containing endocytic vesicles in the food vacuole (Yayon *et al.* 1984b). This observation has led to hypotheses that *CQ* may interfere with the parasites feeding mechanism by inhibiting haemoglobin degradation. In support of this, Zarchin *et al.* have found a correlation between antiplasmodial activity of quinoline-

containing antimalarial drugs and the parasite's ability to produce amino acids (Zarchin *et al.* 1986). Several proposals as to how this inhibition occurs have been made.

1.5.3.2.1.1. Inhibition of Phospholipase Activity

Vacular phospholipases have been identified within the food vacuole which are responsible for degrading endocytic vesicle membranes in order to release their haemoglobin content into the food vacuole. *CQ* has been shown to inhibit phospholipase activity *in vitro* (Ginsburg and Krugliak 1992), but at concentrations substantially higher than those likely to occur in the vacuole (Slater 1993).

1.5.3.2.1.2. Inhibition of Protease Activity

CQ has also been shown to inhibit the activity of partially purified aspartic protease from *P. falciparum* extracts (Gyang *et al.* 1982) but again only at concentrations above the clinical range. Furthermore, haematin itself is a very good inhibitor of acid proteases (roughly 10μM) and this activity is unchanged in the presence of *CQ* (Vander Jagt *et al.* 1987).

Hypotheses that *CQ* interferes with the parasite's feeding mechanism have further been questioned by Ginsburg and Krugliak who noted that treatment of *CQ*-treated parasites with membrane permeable amino-acids, is unable to alleviate inhibition of parasite growth (Ginsburg and Krugliak 1992).

1.5.3.2.2. Increased Vacuolar pH

CQ has been shown to accumulate in the food vacuole, at least in part, through it's ability to act as a weak base (Section 1.5.3.3.1.). Homewood *et al.* originally postulated that a rapid influx of *CQ* into the food vacuole through this weak base effect could deplete the vacuole of protons and thereby cause an increase in vacuolar pH (Homewood *et al.* 1972). This hypothesis was supported by Goldberg *et al.* who showed that proteases operating in the food vacuole showed reduced activity above pH 6 (Goldberg *et al.* 1990). The strongest evidence in support of this hypothesis came from Krogstad *et al.* who showed temporary alkalinisation of the parasite's food vacuole following *CQ* treatment (Krogstad *et al.* 1992) which correlated to antiplasmodial activity (Krogstad *et al.* 1985). These results have since been questioned by Ginsburg and colleagues who claim that the pH measurements of Krogstad *et al.* were probably complicated by physiological alterations to the parasite during the isolation procedure (Ginsburg *et al.* 1989). Further experiments using fluorescinated

dextrans to monitor the vacuolar pH have shown that vacuolar alkalinisation is only observed at levels above the clinical concentration of the antimalarial drugs (Yayon *et al.* 1984, Yayon *et al.* 1985, Geary and Ginsburg 1986, Ginsburg *et al.* 1989).

This theory further fails to explain the inactivity of the stereoisomers of quinine which presumably have similar pK_a's and hence alkalinising abilities, but exhibit very different antiplasmodial activities.

1.5.3.2.3. Binding to Haematin

Fitch originally observed that *CQ* uptake into parasitised red blood cells is saturable (Fitch 1970) and dependent on haemoglobin degradation (Fitch *et al.* 1974). This has been supported by several recent findings that antiplasmodial activity of the blood stage antimalarial drugs *CQ*, *AQ*, quinine and mefloquine, are dependent on haemoglobin degradation (Mungthin *et al.* 1998, Bray *et al.* 1998, Bray *et al.* 1999). These observations support the existence of a haemoglobin-derived or related drug receptor within the food vacuole (Fitch *et al.* 1974). In theory, this receptor could be a protease responsible for haemoglobin degradation, a haemoglobin-derived peptide, or the haematin end product. It is unlikely that *CQ* inhibits proteases (Section 1.5.3.2.1.2.) and there is no evidence to suggest that *CQ* and related antimalarials act by interacting with haemoglobin-derived peptide fragments (Egan 2001a). *CQ* does however, form a non-covalent complex with haematin (Cohen *et al.* 1964). This complex has also been shown to exist in the parasite (Balasubramanian and Mohan Rao 1984) and has been isolated from parasitised erythrocytes (Fitch *et al.* 1980). There is therefore strong evidence that *CQ* acts by binding to a haematin target.

1.5.3.3. Accumulation of Chloroquine in the Food Vacuole

Food vacuoles have an incredible ability to accumulate *CQ* where it is estimated to reach millimolar concentrations at clinical doses (Yayon *et al.* 1985, Geary *et al.* 1986, Ginsburg and Geary 1987). This ability has been explained in terms of non-saturable weak-base properties and saturable binding to a drug target.

1.5.3.3.1. Non-Saturable Uptake via Weak-Base Properties (Intravacuolar)

CQ accumulation is sensitive to the proton gradient between the acidic food vacuole and the extracellular environment (Fitch *et al.* 1974). Perturbation of these transmembrane proton

gradients with specific inhibitors of vacuolar proton pumps (Bray *et al.* 1992b, Hawley *et al.* 1996), or by lowering the external pH or alkalinising the intravacuolar pH (*e.g.* with NH_4Cl) results in less *CQ* accumulation in mammalian lysosomes (MacIntyre and Cutler 1993) and parasitised red cells (Yayon 1984, Krogstad *et al.* 1985). This pH-dependent accumulation has been explained in terms of *CQ*'s ability to accumulate as a weak base (Homewood *et al.* 1972).

CQ has two sites that are capable of being protonated under physiological conditions, namely, the quinoline ring nitrogen (pK_{a1} = 8.3) and the diethylamino group on the side chain (pK_{a2} = 10.2) (Irvin and Irvin 1947, Schlesinger *et al.* 1988). These two protonatable sites can give rise to three pH-dependent species *B*, BH^+ and BH_2^{2+} (Figure 1.8). The relative percentages of these three species as a function of pH can be calculated from knowledge of the pK_a's and are plotted in Figure 1.8 below.

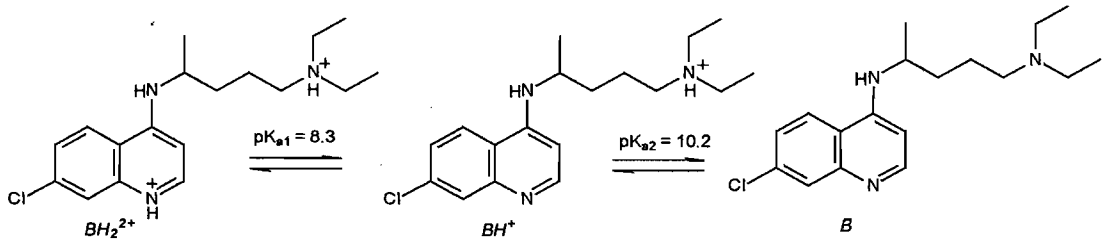

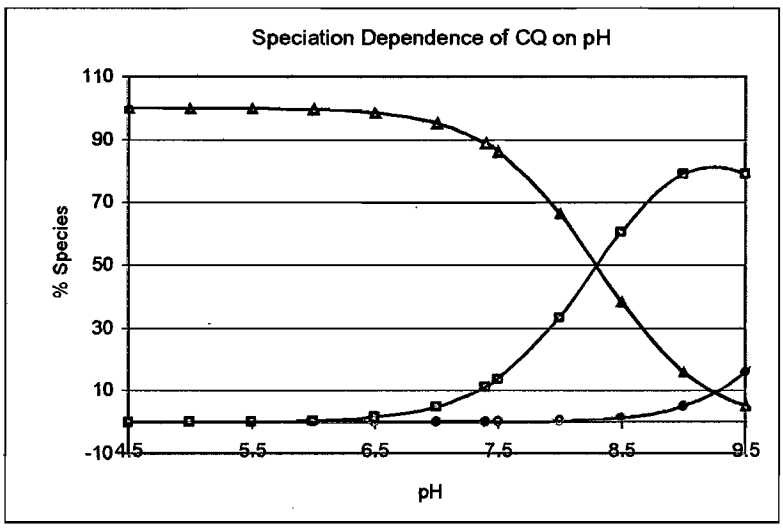

Figure 1.8. (top) the three pH dependent species of *CQ*. (bottom) a speciation plot of the relative percentages of (—) BH_2^{2+}, (—) BH^+ and (—) *B* as a function of pH.

In the food vacuole (pH 5.2 to 5.6 (see Section 1.2.2.1.1)), *CQ* exists in the form of BH_2^{2+}, whereas in the serum (pH 7.4), *CQ* exists 0.02% in the form of *B*, and between 11.2% and 88.8% in the charged forms, BH^+ and BH_2^{2+} respectively (Table 1.2).

Table 1.2. Calculated percentages of the three pH-dependent *CQ* species present in the food vacuole (between pH 5.2 and 5.6) and in the serum (pH 7.4) based on pK_{a1} (8.3) and pK_{a2} (10.2)

Location	pH	% *B*	% BH^+	% BH_2^{2+}
Food vacuole	5.2	7.9×10^{-7}	0.08	99.9
	5.3	1.3×10^{-6}	0.10	99.9
	5.4	2.0×10^{-6}	0.13	99.9
	5.5	3.2×10^{-6}	0.16	99.8
	5.6	5.0×10^{-6}	0.20	99.8
Serum	7.4	0.02	11.2	88.8

Since the lipophilicity of charged *CQ* species is greatly reduced (Hansch and Leo 1979), predominantly *B* will pass by passive diffusion into the acidic food vacuole where it will be converted to the charged BH^+ and BH_2^{2+} species which cannot pass back out across the membrane. This depletion of intravacuolar *B* will cause more of this species to diffuse into the food vacuole until the *B* equilibrium concentrations on both sides of the membrane are equal. Since both BH^+ and BH_2^{2+} contribute to the total *CQ* concentration, the intravacuolar concentration will become substantially higher than the external concentration.

Krogstad *et al.* observed that *CQ* accumulation into mammalian vesicles is virtually identical to that predicted through pH trapping but that *CQ* accumulation in the vesicles of susceptible parasites is substantially more than predicted by pH trapping (Krogstad *et al.* 1992). This observation has been confirmed by Bray *et al.* who showed that *CQ* accumulates roughly 1700 fold into red cells infected with the *CQ*-sensitive strain HB3 (expressed as the cellular accumulation ratio (CAR), Bray *et al.* 1996, Bray *et al.* 1998). Assumuing that the food vacuole occupies roughtly 2% of the volume of a red cell (Dzekunov *et al.* 2000), *CQ* is predicted to accumulate 85 000 fold into the food vacuole (expressed as the vacuolar accumulation ratio (VAR)). The predicted CAR for *CQ* based on pH trapping alone lies between 71 and 446 (presuming the pH of the food vacuole to be between pH 5.2 and 5.6, Equation 1 and Table 1.3). Since these predicted CAR values can only account for 4-26% of the observed accumulation, there must be an additional *CQ* uptake mechanism to pH trapping alone.

$$\frac{[CQ]_v}{[CQ]_e} = \left\{ \frac{1 + \frac{[H^+]_v}{K_{a2}} + \frac{[H^+]_v^2}{K_{a1}K_{a2}}}{1 + \frac{[H^+]_e}{K_{a2}} + \frac{[H^+]_e^2}{K_{a1}Ka2}} \right\} \quad (1)$$

In equation **1**, $[CQ]_v$ refers to the total vacuolar concentration of CQ and $[CQ]_e$ refers to its total extravacuolar concentration. The terms $[H^+]_v$ and $[H^+]_e$ refer to the vacuolar and extravacuolar hydrogen ion concentrations respectively and K_{a1} = 5.01 × 10^{-9} M (pK_a = 8.3) and K_{a2} = 6.31 × 10^{-11} M (pK_a = 10.2)

In contrast, Hawley *et al.* found that the CAR of CQ could be accounted for based on pH-trapping alone by assuming a vacuolar pH of 5.0 and a fractional vacuolar volume that is 3.5% of that of the parasitised red blood cell (Hawley *et al.* 1996). This pH value for the vacuole would however appear to be too low, lying well below those that have been reported on the basis of experimental data.

Table 1.3. Predicted and observed CQ accumulation ratio in the red cell (pH 7.4) and food vacuole (between pH 5.2 and 5.6)

Predicted				Observed	
pH_v	pH_e	VAR	CAR	VAR	CAR
5.2	7.4	22324	446	85000	1700[a]
5.3		14088	282		
5.4		8891	178		
5.5		5612	112		
5.6		3542	71		

VAR = vacuolar accumulation ratio between pH 5.2-5.6 and an external pH of 7.4, CAR = cellular accumulation ratio (for the parasitised red cell), [a] Bray *et al.* 1996.

1.5.3.3.2. Saturable Uptake via Haematin Binding

Fitch originally noted that CQ uptake is saturable and competitively inhibited by structurally related quinolines. This observation prompted him to propose the existence of a structurally defined drug receptor within the food vacuole (Fitch 1970, Fitch *et al.* 1974). Binding of CQ to this receptor will deplete the free CQ concentration inside the food vacuole, thereby causing more CQ to diffuse across the membrane until all the binding sites are saturated.

Although accumulation of *CQ* through pH trapping can only account for 4-26% of the total accumuation, it's importance in driving the total accumulation must not be underestimated (Egan 2001a). If one considers formation of a 1:1 haematin-quinoline complex, an appropriate equilibrium expression can be formulated (Equation **2**):

$$H + CQ_f \underset{}{\overset{K}{\rightleftharpoons}} CQ_b \qquad \textbf{(2)}$$

$$K = \frac{[CQ]_b}{[H][CQ]_f}, [CQ]_b = K[H][CQ]_f$$

$$CQ_{tot} = CQ_f + CQ_b$$

Here, $[H]$ represents the free haematin concentration, $[CQ]_f$ represents the free *CQ* concentration, $[CQ]_b$ represents the concentration of bound *CQ* and CQ_{tot} is the total *CQ* concentration. The free haematin concentration is unknown although it has recently been estimated at about 20μM (Dzekunov *et al.* 2000) and the K value for *CQ* in 40% aqueous DMSO is $3.3\times10^5\ M^{-1}$ (Egan *et al.* 1997, discussed in Section 1.5.3.5.). In the presence of pH trapping, *CQ* is predicted to accumulate between 3542 and 22324 fold (Table 1.3) which equates to a vacuolar *CQ* concentration of $3.5\times10^{-5} - 2.2\times10^{-4}$ M at the IC_{50} (10nM) (Table 1.4). The bound *CQ* is predicted to be roughly $2.3\times10^{-4} - 1.5\times10^{-3}$ M (Equation **2**) which gives a total *CQ* concentration in the food vacuole of roughly 2.7×10^{-4} - 1.7×10^{-4} M (26900 –169700 fold VAR accumulation). Since the food vacuole only occupies 2% of the total volume of the red cell, this amounts to a CAR of roughly 538-3394 fold (which is in general agreement with the experimentally reported value of 1700 (Bray *et al.* 1996).

Table 1.4. Calculated CAR of *CQ* based on pH trapping and haematin binding

pH_V	Predicted VAR[a]	$[CQ]_f$	$[CQ]_b$	$[CQ]_{tot}$	Predicted VAR[b]	Predicted CAR	Found CAR
5.2	22324	2.2×10^{-4}	1.5×10^{-3}	1.7×10^{-4}	169700	3394	1700[c]
5.3	14088	1.4×10^{-4}	9.3×10^{-4}	1.1×10^{-4}	107050	2141	
5.4	8891	8.9×10^{-5}	5.9×10^{-4}	6.8×10^{-4}	67550	1351	
5.5	5612	5.6×10^{-5}	3.7×10^{-4}	4.3×10^{-4}	42650	853	
5.6	3542	3.5×10^{-5}	2.3×10^{-4}	2.7×10^{-4}	26900	538	

[a] Calculated from pH trapping alone (Table 1.3)
[b] Calculated from pH trapping and complex formation with Fe(III)PPIX
[c] Bray *et al.* 1996

In the absence of pH trapping, the free *CQ* concentration in the food vacuole will be roughly the same as the external clinical concentration of 10nM. The concentration of bound *CQ* will be roughly 6.6×10^{-8} M (Equation **2**, Table 1.5.) which amounts to a total *CQ* concentration of 7.6×10^{-8} M which gives a CAR of approximately 8 (compared to the observed CAR of 1700).

Table 1.5. Calculated CAR of *CQ* based on haematin binding alone

$[CQ]_f$	$[CQ]_b$	$[CQ]_{tot}$	**Predicted VAR**	**Predicted CAR**	**Found CAR**
1.0×10^{-8}	6.6×10^{-8}	7.6×10^{-8}	400	8	1700[a]

[c] Bray *et al.* 1996

Therefore, even though accumulation via pH trapping only contributes to approximately 4-26% of the total accumulation, it is essential to drive the saturable accumulation component through Le Chatelier's principle (Egan *et al.* 2001a).

1.5.3.4. The Nature of Fe(III)PPIX-Quinoline Interactions

Fe(III)PPIX-Quinoline interactions are difficult to study in aqueous solution as Fe(III)PPIX tends to aggregate (Davies 1940, Shack and Clarke 1947) and undergoes slow autoxidation (Brown *et al.* 1968, Shack and Clarke 1947). Furthermore, this molecule precipitates out of solution below pH 6 (Dzekunov *et al.* 2000) and has been observed to adhere to surfaces (Brown *et al.* 1968). The most extensive study on the state of Fe(III)PPIX in aqueous solution was carried out by Brown *et al.* in 1970 (Brown *et al.* 1970) who found that Fe(III)PPIX is extensively dimerised in aqueous solution (log K = 0.65) and claimed it to be a μ-oxo dimer (Equation **3** and Figure 1.9).

$$2M \underset{}{\overset{K=4.5}{\rightleftharpoons}} D + H^+ \qquad (3)$$

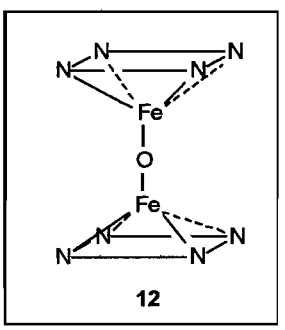

12

Figure 1.9. Dimerisation equilibrium of Fe(III)PPIX in aqueous solution proposed by Brown *et al.* 1970 where M is the haematin monomer and D is the μ-oxo dimer (**12**)

Because of the problems associated with studying haematin in aqueous solution, alternative binding models have been used. Studies have been performed either in non-aqueous systems (Warhurst 1981, Warhurst 1987) or in aqueous detergent systems (Bachhawat *et al.* 2000) where haematin is reported to be monomeric (Simplicio *et al.* 1975). Also the iron porphyrins that have a lesser tendency to aggregate have been used in studies (Constantinidis and Satterlee 1988a, Constantinidis and Satterlee 1988b, Marques *et al.* 1996).

Initial studies showed that the blood stage antimalarial drugs *CQ*, *AQ*, quinacrine, quinine and mefloquine are all capable of binding to Fe(III)PPIX in aqueous solution at pH 7.4 (Fitch *et al.* 1980). Qualitative experiments later questioned the ability of *AQ* to form a complex in benzene (Warhurst 1987), although subsequent studies using electronic and Mössbauer spectroscopies showed that a complex can be formed in aqueous solution (Blauer 1988, Blauer *et al.* 1993). There were also early studies showing that 9-epiquinine, the inactive enantiomer of quinine, could not form a complex with Fe(III)PPIX in benzene (Warhurst 1987, Warhurst 1981). This is not the case in aqueous solution as quinine, quinidine, 9-epiquinine and 9-epiquinidine all form complexes with Fe(III)PPIX (Egan *et al.* 1997, Egan *et al.* 1999a, Mavuso, PhD thesis 2001, Bachhawat *et al.* 2000).

The binding interactions in *CQ* are thought to be coplanar π-π interactions between the aromatic ring system of *CQ* and the porphyrin (Constantinidis and Satterlee 1988b, Moreau *et al.* 1982, Adams *et al.* 1996, Marques *et al.* 1996, Egan *et al.* 1997). Evidence that complexation does not involve metal-coordination is shown by the ability of *CQ* to form complexes with the metal free porphyrins, protoporphyrin IX (Moreau *et* al. 1985) and uroporphyrin I (Constantinidis and Satterlee 1988b) which are almost as strong as the corresponding metal porphyrin complexes. Furthermore, the strength of the complex is virtually unchanged between pH 5.6 and 7.4 (Egan *et. al.* 1997) which implies that the protonation state of the drug and hence metal-coordination is not important.

The term π-π complex does not necessarily imply that complex stability arises solely from overlap of π-orbitals, hydrophobic interactions are also important (Hunter and Sanders 1990). The strength of the complex and hence hydrophobic interactions have been found to depend on the nature of the surrounding solvent. This is observed by a weakening in the association constant between *CQ* and Fe(III)PPIX with increasing concentrations of acetonitrile in water (Egan *et al.* 1997). The importance of the solvent in complex stability may also explain why early researchers failed to observe complex formation between Fe(III)PPIX, and *AQ* or 9-epiquinine in benzene (Warhurst 1987, Warhurst 1981).

Since haematin is predominantly dimeric in aqueous solution, the current view is that *CQ* binds to haematin μ-oxo dimers in a cofacial π-π sandwich type complex (Figure 1.10) (Moreau *et al.* 1982, Dorn *et al.* 1998a, Vippagunta *et al.* 1999).

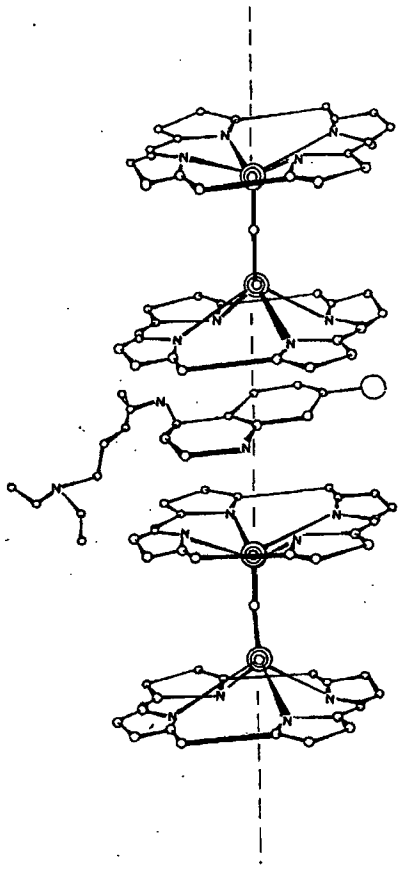

Figure 1.10. Model of the interaction between *CQ* and Fe(III)PPIX in aqueous solution (Moreau *et al.* 1982)

Interactions between quinine and haematin also have a large π-π component (Moreau *et al.* 1985, Constantinidis and Satterlee 1988a), but NMR spectra of the urohemin I complex (Constantinidis and Satterlee 1988a) and the uv-vis spectrum of a haem-peptide complex (Marques *et al.* 1996) indicates that additional coordination of the 9-OH group to the iron centre is likely to occur.

Further evidence that *CQ*-haematin and quinine-haematin complexes are different is supported by Mössbauer spectroscopy (Adams *et al.* 1996). Also thermodynamic parameters obtained for *CQ*-haematin complex formation indicates the process to be largely entropically driven whereas the quinine-haematin complex formation is enthalpically driven (Egan *et al.* 1997).

1.5.3.5. Association Constants for Fe(III)PPIX-Quinoline Complexes

Fitch *et al.* originally reported association constants in aqueous medium based on an equilibrium dialysis method (Fitch *et al.* 1980). Association constants have subsequently been measured in an aqueous environment using titration calorimetry where large haematin:drug stoichiometries are observed (Dorn *et al.* 1998a) (Table 1.6). This is supposedly because the drug is sandwiched between two or more haematin μ-oxo dimers. Since these large stoichiometries render the results difficult to interpret, efforts have been made to obtain association constants in strictly monomeric Fe(III)PPIX. Bachhawat *et al.* obtained a similar value for *CQ* using titration calorimetry in a detergent system in which haematin is likely to be monomerised into micelles (Bachhawat *et al.* 2000). Similar association constants for the various drugs with haematin have also been obtained in our laboratories in 40% DMSO (aq) systems in which haematin is strictly monomeric (Egan *et al.* 1997, Egan *et al.* 1999a) (Table 1.6).

Table 1.6. Association constants for interaction of quinoline antimalarials with Fe(III)PPIX (haematin:drug stoichiometry in parenthesis)

Compound	**log K**		
	Dorn *et al.*	**Bachhawat *et al.***	**Egan *et al.***
Chloroquine	5.60 ± 0.2 (4:1)	5.64 (2:1), 2.90	5.52 ± 0.03 (1:1)
Amodiaquine	4.97 ± 0.1 (4:1)		5.39 ± 0.04 (1:1)
Quinacrine	5.70 ± 0.04 (4:1)		
Pyronadine	5.48 ± 0.03 (7:1)		
Quinine	4.32 ± 0.04 (5:1)		4.10 ± 0.02 (1:1)
Quinidine			5.02 ± 0.03 (1:1)
9-Epiquinine			4.04 ± 0.03 (1:1)
9-Epiquinidine			4.37 ± 0.02 (1:1)
Mefloquine	4.08 ± 0.1 (3:1)		3.90 ± 0.08 (1:1)
Halofantrine	4.66 (1:1)*		5.29 ± 0.02 (1:1)

* In 80% ethanol; Dorn *et al.* haematin 0.25M phosphate buffer, pH 6.5, 37°C (Dorn *et al.* 1998a); Bachhawat *et al.* Haematin in 0.2% Triton X-100, pH 7.4, 5mM phosphate buffer, 27.5°C (Bachhawat *et al.* 2000); Egan *et al.* haematin in 40% DMSO (aq), pH 7.4, 0.02M HEPES, 25°C (Egan *et al.* 1997, Mavuso, PhD thesis 2001)

Little is known about the structural features in *CQ* and related 4-aminoquinolines responsible for complex formation with Fe(III)PPIX. O'Neill *et al.* used molecular mechanics to model the interaction between Fe(III)PPIX and the *AQ* analogue tebuquine (O'Neill *et al.* 1997). These authors found complex stability depended on a combination of the coplanar interaction

between the quinoline nucleus and the porphyrin ring, and an apparent hydrogen bonding interaction between the side chain terminal amine of the drug and the Fe(III)PPIX propionate groups. A subsequent study has found that the hydrogen bonding interaction is not critical as *CQ* analogues lacking a basic terminal amino group in the side chain (**14**) or lacking a side chain (**15**) still form complexes with Fe(III)PPIX (Vippagunta *et al.* 1999) (Figure 1.11A). These authors claim that the 7-chloro substituent on the quinoline ring of *CQ* is a critical structural determinant for binding as the 6-chloro analogue (**17**) of *CQ* failed to bind to Fe(III)PPIX (Figure 1.11B). This is supported by Egan *et al.* who found that quinoline, 5-, 6- and 8-aminoquinoline (*5AQ*, *6AQ* and *8AQ* respectively) also failed to bind to Fe(III)PPIX (Figure 1.11B) (Egan *et al.* 1997).

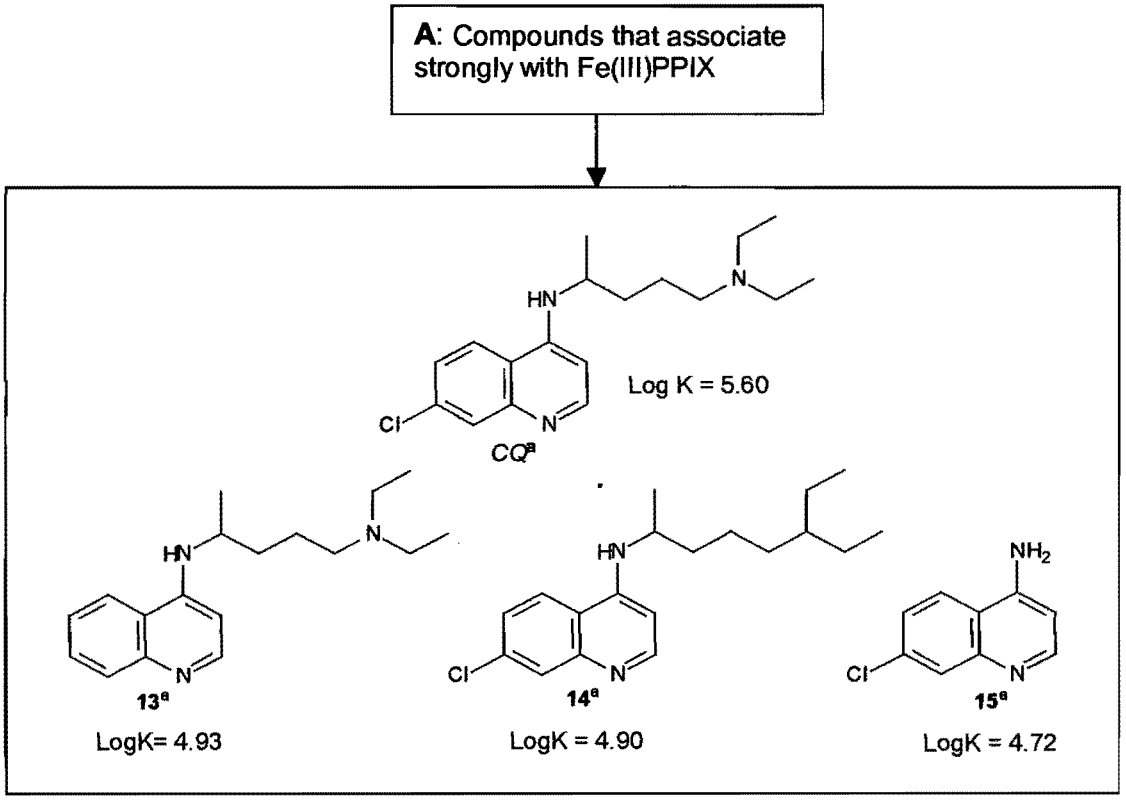

Figure 1.11A. Reported analogues of *CQ* that all bind strongly to Fe(III)PPIX. [a] Vippagunta *et al.* 1999.

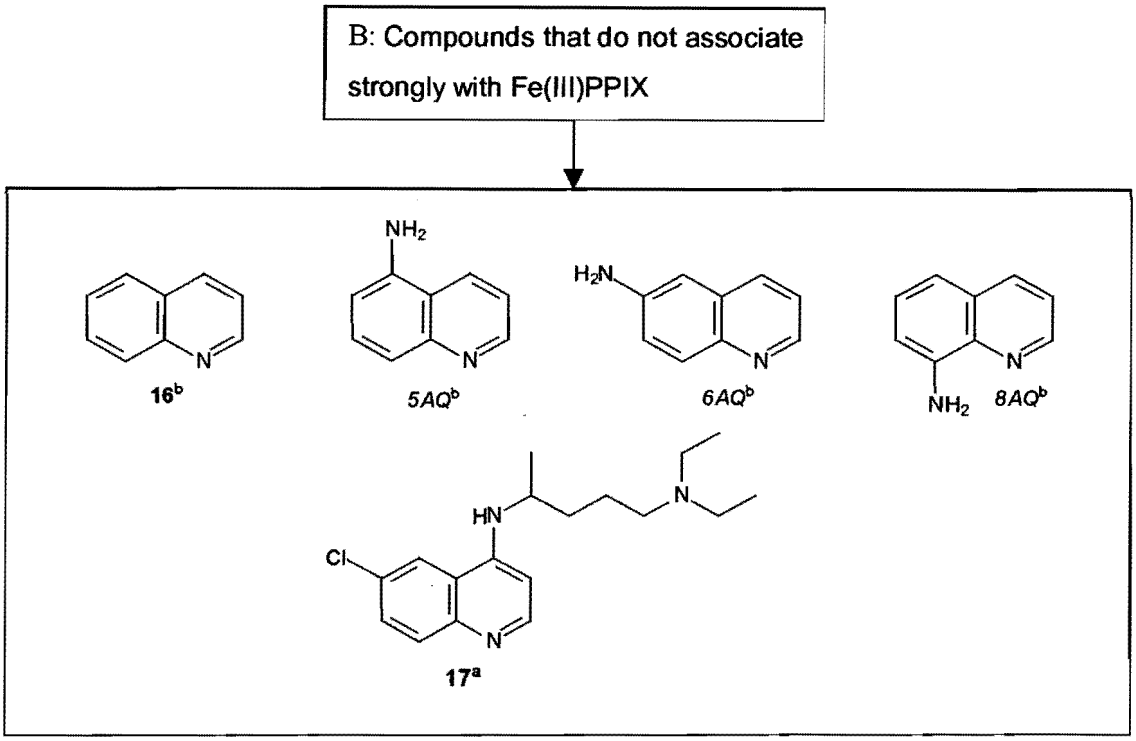

Figure 1.11B. Reported analogues of *CQ* that fail to bind to Fe(III)PPIX. [a] Vippagunta *et al.* 1999, [b] Egan *et al.* 1997.

There is no evidence that the strength of haematin binding is quantitatively related to antiplasmodial activity (Vippagunta *et al.* 1999, O'Neill *et al.* 1997, Egan *et al.* 1997, Dorn *et al.* 1998a) although all the *CQ* and related quinoline antimalarials form strong complexes with haematin.

1.5.4. Hypotheses on how Complex Formation is Related to Antiplasmodial Activity

1.5.4.1. Inhibition of Protein Synthesis

Suriola and Padmanaban found that Fe(III)PPIX stimulates protein synthesis and proposed that *CQ* inhibits this process by forming a *CQ*-Fe(III)PPIX complex (Suriola and Padmanaban 1991). This hypothesis has not found widespread acceptance as the *CQ* concentrations required to inhibit protein synthesis are substantially higher (micromolar) than those required for antiplasmodial activity (nanomolar). Furthermore, there is no evidence that malaria protein synthesis is dependent on Fe(III)PPIX (Slater 1991).

1.5.4.2. Inhibition of β-Haematin Formation

1.5.4.2.1. Inhibition of Haem Polymerase Activity

Slater and Cerami originally suggested that *CQ* and related antimalarial drugs may act by inhibiting the haem detoxification pathway (*i.e.* haemozoin formation) in malaria parasites (Slater and Cerami 1992). At that time, haemozoin was thought to be a polymer that required a "haem polymerase" enzyme to form. This enzyme was supposedly present in extracts from *P. falciparum* trophozoites and *CQ* was shown to inhibit this process presumably by inhibiting the enzyme. Other researchers have supported the existence of a haem polymerase enzyme (Fitch and Chou 1996, Coy and Fitch 1997) even though no such enzyme has ever been isolated. Furthermore, under conditions where β-haematin has been shown to form spontaneously in the absence of biological material, its formation is still inhibited by *CQ* (Egan *et al.* 1994).

1.5.4.2.2. Inhibition of Crystallisation Activity

In the absence of a haem polymerase enzyme, it has been suggested that *CQ* inhibits β–haematin formation directly (Egan *et al.* 1994, Sullivan *et al.* 1996, Sullivan *et al.* 1998). It was proposed that the *CQ*-Fe(III)PPIX complex prevents the incorporation of haematin into β–haematin (Dorn *et al.* 1995) by capping the growing polymer chain (Sullivan *et al.* 1996). This was supported by observations that [^{3}H] *CQ* associates with haemozoin *in vivo* and that association *in vitro* is dependent on the presence of free haematin (Sullivan *et al.* 1996, Sullivan *et al.* 1998). Recently Pagola *et al.* have shown that β–haematin is not a polymer but a crystalline haematin dimer (Pagola *et al.* 2000) which has led to the suggestion that *CQ* may instead inhibit β-haematin formation by blocking the fastest growing crystal face (Pagola *et al.* 2000) or inhibiting crystal nucleation (Egan *et al.* 2001a, Egan *et al.* 2001c).

That β-haematin inhibition is responsible for the antiplasmodial activity of *CQ* is supported by independent findings in the haemozoin-producing insect, *R. prolixus*. Following the feeding of the insect on blood supplemented with *CQ*; midgut swelling is observed, haemozoin production is inhibited and free Fe(III)PPIX is seen to appear in the insect's haemolymph (Oliveira *et al.* 2000a). Furthermore, evidence of lipid peroxidation is seen (although the insects do not die).

CQ and related 4-aminoquinolines, quinolinemethanols, a wide range of phenanthrenemethanols and bisquinoline antimalarials and antiplasmodials have been

shown to strongly inhibit β-haematin formation (Table 1.7A) (Egan *et al.* 1994, Raynes *et al.* 1996, Egan *et al.* 1999a, Dorn *et al.* 1998, Hawley *et al.* 1998, Vennerstroom *et al.* 1998, Vippagunta *et al.* 1999). In these classes of compounds, complex formation with haematin appears to be a prerequisite but not a sufficient requirement for β-haematin inhibition (Table 1.7B). This distinction is highlighted by the inability of the inactive stereoisomers of quinine, namely 9-epiquinine and 9-epiquinidine, to inhibit β-haematin formation even though they form complexes of similar strength to quinine and quinidine with haematin (Egan *et al.* 1997, Egan *et al.* 1999a, Mavuso PhD thesis 2001). In agreement with these observations, quinoline and related compounds that do not bind to Fe(III)PPIX or inhibit β–haematin formation fail to exhibit strong antiplasmodial activity (Table 1.7C).

Table 1.7A. Compounds that form strong complexes with Fe(III)PPIX, inhibit β–haematin formation and have strong antiplasmodial or antimalarial activity

Compound	Complex Formation	β–Haematin Inhibition	Antiplasmodial Activity
Chloroquine	+[a,d]	+[a,b,c,d]	+
Amodiaquine	+[a,d]	+[a,b,c,d]	+
Desbutylhalofantrine	+[a]	+[a]	+
Halofantrine	+[a,d]	+[a,b,c,d]	+
Mefloquine	+[a,d]	+[a,b,c,d]	+
Quinine	+[a,d]	+[a,b,c,d]	+
Quinidine	+[a]	+[a,c]	+
Quinacrine	+[d]	+[b,d]	+
Pyronaridine	+[d,]	+[b,c,d]	+
Ro 48-6910	+[d]	+[b,d]	+

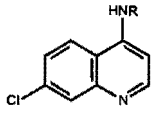

R = H	+[g]	+[g]	+[g]
R = CH_2CH_3	+[g]	+[g]	+[g]
R = $CH(CH_3)CH_2NEt_2$	+[g]	+[g]	+[g]
R = $CH(CH_3)CH_2CH_2NEt_2$	+[g]	+[g]	+[g]
R =$CH(CH_3)CH_2CH_2CH_2CH_2NEt_2$	+[g]	+[g]	+[g]
R = $CH(CH_3)CH_2CH_2CH_2CHEt_2$	+[g]	+[g]	+[g]

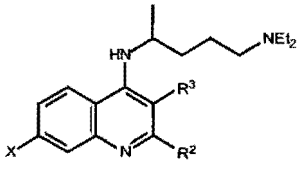

X	R^2	R^3			
NO_2	H	H	+[g]	+[g]	+[g]
Br	H	H	+[g]	+[g]	+[g]
Cl	CH_3	H	+[g]	+[g]	+[g]
Cl	H	CH_3	+[g]	+[g]	+[g]

[a] Egan *et al.* 1994, Egan *et al.* 1997 and Egan *et al.* 1999a, [b] Dorn *et al.* 1998, [c] Hawley *et al.* 1998, [d] Dorn *et al.* 1998, [e] Ridley and Hudson 1998, [f] Egan 2001, [g] Vippagunta *et al.* 1999.

Table 1.7B. Compounds that form strong complexes with Fe(III)PPIX, do not strongly inhibit β–haematin formation and do not have strong antiplasmodial activity.

Compound	Complex Formation	β-Haematin Inhibition	Antiplasmodial Activity[e,f]
9-Epiquinine	+[a]	_[a]	_[a]
9-Epiquinidine	+[a]	_[a]	_[a]
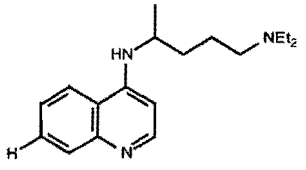	+[g]	_[g]	_[g]
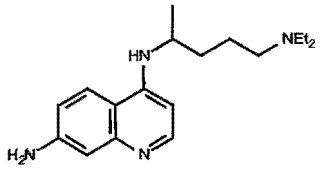	+[g]	_[g]	_[g]

[a] Egan *et al.* 1994, Egan *et al.* 1997, Egan *et al.* 1999a and Mavuso PhD thesis 2001, [g] Vippagunta *et al.* 1999.

Table 1.7C. Compounds that do not form a strong complexe with Fe(III)PPIX, do not inhibit β–haematin formation or have strong antiplasmodial activity

Compound	Complex Formation	β–Haematin Inhibition	Antiplasmodial Activity[e,f]
Quinoline	_[a]	_[a]	_[a]
5-Aminoquinoline	_[a]	_[a]	_[a]
6-Aminoquinoline	_[a]	_[a]	_[a]
8-Aminoquinoline	_[a]	_[a]	_[a]
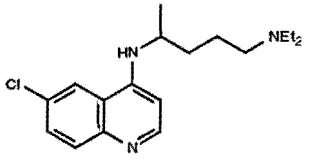	_[g]	_[g]	_[g]

[a] Egan *et al.* 1994, Egan *et al.* 1997 and Egan *et al.* 1999a, [g] Vippagunta *et al.* 1999.

Strong evidence that β-haematin inhibition is primarily responsible for antiplasmodial activity is demonstrated in a wide variety of quinoline antimalarial (Dorn *et al.* 1998b) and antiplasmodials (Hawley *et* al. 1998, Vippagunta *et al.* 1999). Dorn *et al.* found a correlation between β-haematin inhibition and antiplasmodial activity for the blood stage antimalarial drugs: *CQ*, *AQ*, halofantrine, pyronaridine, quinine, quinacrine, mefloquine and Ro 48-6910 (Figure 1.12A) (Dorn *et al.* 1998b). Furthermore, these authors observed a correlation

between the haematin binding constant and the ability of these compounds to inhibit β-haematin formation. This is in line with the hypothesis that *CQ*-haematin binding is important for antiplasmodial activity through β-haematin inhibition. Similar observations have also been found in a series of *AQ* analogues and *CQ* where antiplasmodial activity was strongly correlated to β-haematin inhibition when activity was normalised for the extent of cellular drug accumulation (Figure 1.12B) (Hawley *et al.* 1998). Vippagunta *et al.* also observed a modest correlation between antiplasmodial activity and β-haematin inhibition for eleven *CQ* analogues when β-haematin inhibition was normalised for μ-oxo dimer binding affinities (Figure 1.12C). In this case, no direct correlation was found between the strength of haematin association and the ability to inhibit β-haematin formation although it was suggested that variable accumulation may have accounted for the lack of correlation (Vippagunta *et al.* 1999). Finally, a correlation has been observed between the antiplasmodial activity of a series of bis-quinolines and their ability to inhibit β-haematin formation (Figure 1.12D) (Raynes *et al.* 1996).

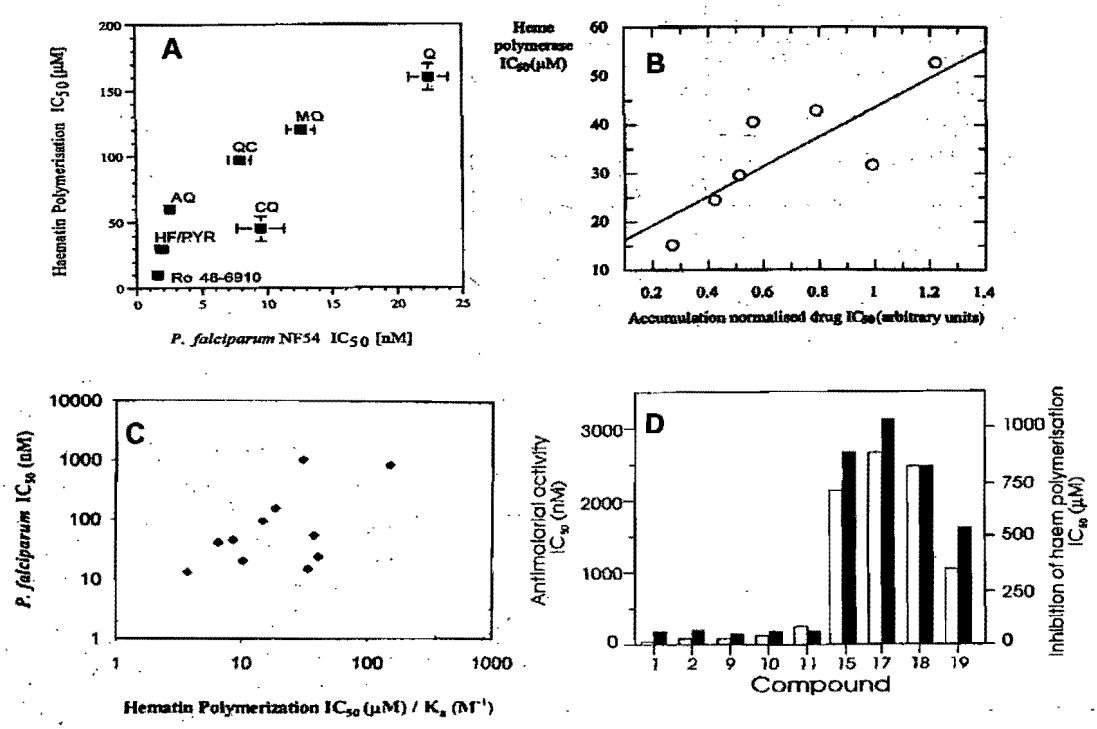

Figure 1.12. Correlation between β-haematin inhibition and antiplasmodial activity in: (A) the *CQ* sensitive strain NF54 for eight antimalarial drugs (Dorn *et al.* 1998b); (B) the *CQ*-sensitive strain 3D7 for seven *AQ* analogues in which antiplasmodial activity was normalised for extent of cellular accumulation (CAR) (Hawley *et al.* 1998); (C) the *CQ*-sensitive strain NF54 for eleven *CQ* analogues in which β-haematin inhibition was normalised for haematin μ-oxo dimer binding affinities (Vippagunta *et al.* 1999) and (D) the *CQ*-sensitive strain D10-for nine bis-quinoline analogues (open bars = antiplasmodial IC_{50}, solid bars = β-haematin inhibition IC_{50}) (Raynes *et al.* 1996).

From the currently available literature, it is not obvious what structural features in *CQ* are responsible for β–haematin inhibition. It would appear that the chloro-group at the 7-position in *CQ* may play a role as replacement with hydrogen or amino (Table 1.7B) renders the compounds inactive and unable to inhibit β–haematin formation, whereas replacement with nitro or bromo (Table 1.7A) does not.

1.5.4.3. Interaction of Haematin with Biological Membranes

If formation of a *CQ*-haematin complex interferes with the parasite mechanism to sequester haematin, vacuolar haematin concentrations would be expected to increase following *CQ* administration. It has been proposed that haematin or the *CQ*-haematin complex exerts a toxic effect on the parasite by compromising the integrity of the vacuolar membrane (Chou and Fitch 1981, Orjih *et al.* 1981). This is in agreement with the observed morphological changes upon *CQ* administration which include a loss of internal detail and swelling of the food vacuole (Fitch *et al.* 1982). *In vitro* studies on erythrocytic membranes in *P. berghei* (Orjih *et al.* 1981) and *P. falciparum* (Fitch *et* al. 1982) have shown that both haematin and the *CQ*-haematin complex cause membrane lysis. Being hydrophobic, haematin has a strong affinity to intercalate within erythrocytic membranes (Atamna and Ginsburg 1995) and lipid bilayers (Tipping *et al.* 1979, Ginsburg and Demel 1983, Cannon *et al.* 1984) which is likely to upset membrane order and increase permeability (Chou and Fitch 1981). *In vitro*, haematin has been demonstrated to impair the ability of erythrocytic membranes to maintain cationic gradients (Chou and Fitch 1981) and causes leakage of solutes trapped in inner vesicles and liposomes in a concentration-dependent manner (Schmitt *et al.* 1993).

Another mechanism through which haematin may cause membrane damage is by promoting lipid peroxidation (Tappel 1953, Tappel 1955). This has been shown to occur *in vitro* where haematin-catalysed lipid peroxidation displays a bell-shaped dependence on haematin concentration as measured by thiobarbituric acid reactive substances (TBARS) (Schmitt *et al.* 1993, Omodeo-Sale *et al.* 2001). The extent of lipid peroxidation appears to be dependent on the pre-existence of hydroperoxides in the membrane (Omodeo-Sale 2001) which is in agreement with a proposed mechanism in which haematin reacts with membrane hydroperoxides to generate alkoxyl and peroxyl radicals (Van der Zee *et al.* 1996) which subsequently degrade the membrane (Dahle *et al.* 1962). Furthermore, complex formation between *CQ* and haematin has an increased ability to promote lipid peroxidation relative to haematin alone (Sugioka *et al.* 1987, Sugioka and Suzuki 1991, Omodeo-Sale *et al.* 2001).

1.5.4.4. Alternative Hypotheses for the Fate of Intravacuolar Haematin

Despite considerable evidence that quinoline antimalarials act by inhibiting haemozoin formation, unequivocal evidence for this hypothesis has not been provided *in vivo*. Recently two independent research groups have provided evidence suggesting that only less than 30% of haemoglobin derived haem is converted to haemozoin in *P. falciparum* infected erythrocytes (Ginsburg *et al.* 1998, Loria *et al.* 1999). These observations have led to the recent advancement of two alternative hypotheses on haematin detoxification.

Ginsburg *et al.* suggested that at least 70% of the haematin is not converted to haemozoin, but exits the food vacuole into the cytosol where it is subsequently degraded by glutathione and that *CQ* and related 4-aminoquinoline antimalarials inhibit this process (Ginsburg *et al.* 1998). Non-degraded haematin then exerts a toxic effect on the parasite by associating with the membranes. Glutathione has been shown to degrade haematin *in vitro* (Atamna and Ginsburg 1995) and *CQ* inhibits this process (Ginsburg *et al.* 1998). Furthermore, a correlation has been observed between increased membrane-associated haematin following *CQ* administration and antiplasmodial activity (Ginsburg *et al.* 1998). A problem with this hypothesis is that it assumes the existence of a *CQ*-haematin complex in the parasite's cytosol where no pH trapping is expected to occur. Here the free *CQ* concentration is expected to be similar to the clinical concentration (10nM) which would result in the existence of almost no *CQ*-haematin complex (discussed in Section 1.5.3.3.2).

In an alternative hypothesis by Loria *et al.*, it is proposed that haematin is degraded in the food vacuole by reaction with hydrogen peroxide (Loria *et al.* 1999). Hydrogen peroxide may arise from the oxidation of ferrohaem, released from haemoglobin, to ferrihaem (haematin) (Equations **4**, **5** and **6**) (Atamna and Ginsburg 1995).

$$Fe^{2+} + O_2 \rightleftharpoons Fe^{3+} + O_2^- \quad (4)$$

$$O_2^- + H^+ \rightleftharpoons HO_2^\bullet \quad (5)$$

$$HO_2^\bullet + O_2^- + H^+ \longrightarrow H_2O_2 + O_2 \quad (6)$$

Haematin is known to display catalase-like and peroxidase-like activities with hydrogen peroxide *in vitro* (Orjih *et al.* 1988, de Almeida Ribeiro *et al.* 1995, de Almeida Ribeiro *et al.* 1997) resulting in the destruction of the porphyrin ring (Brown *et al.* 1968), and *CQ* and

related antimalarials have been shown to inhibit this degradation process *in vitro* (de Almeida Ribeiro *et al.* 1995, de Almeida Ribeiro *et al.* 1997, Loria *et al.* 1999).

A potential problem with both these hypotheses is that the experimental methods used to assay for haematin do not unequivocally identify the putative non-haem iron species in the parasite-infected erythrocytes. The hypotheses rest on the accuracy of the haematin assay alone. In a recent study in which the total iron content in infected erythrocyes isolated from trophozoites, food vacuoles and haemozoin, was assayed using a ferrocene calorimetric assay (Jill Combrink, Hons Project, Department of Pharmacology, University of Cape Town, 2001), 92% of the iron present in an infected erythrocyte was found to be located in the trophozoite food vacuole and 88% of this was in the form of haemozoin. Furthermore, a Mössbauer spectrum of the iron in trophozoites is identical to that of β-haematin with no additional peaks observed, which implies that virtually all the iron in the parasite is haemozoin-iron (Egan, unpublished results). This calls into question the existence of a haematin detoxification route apart from conversion to β-haematin.

1.6. RESISTANCE MECHANISMS

Resistance to *CQ* was slow to develop suggesting that multiple mutations were required to produce the resistance phenotype. Two resistance foci appeared simultaneously in South East Asia and South America in the 1960's, and these have since spread to every country where malaria is endemic (Foote and Cowman 1994, Foley and Tilley 1997). Once established, the *CQ*-resistance phenotype appears to be stable and persists even in the absence of drug pressure (Le Bras *et al.* 1983).

1.6.1. Reduced Uptake vs Enhanced Efflux

A common feature of *CQ* resistance is that *CQ*-resistant parasites accumulate less drug than their sensitive counterparts (Macomber *et al.* 1966, Fitch 1969, Krogstad *et al.* 1987). Much debate has centred around whether this reduced accumulation is due to reduced drug uptake or enhanced drug efflux from the parasitised cell (Bray and Ward 1993). *CQ* resistance can be reversed by its co-administration with compounds such as verapamil (Martin *et al.* 1987), desipramine and chlorpromazine (Bitonti *et al.* 1988) which are known to reverse multi-drug resistance (MDR) in cancer cells. MDR is thought to arise from the presence of an ATP-dependent, membrane bound drug effluxer protein known as P-glycoprotein (Martin et al. 1987, Bray and Ward 1993). Verapamil is thought to compete with

the anticancer drugs for P-glycoprotein binding and hence prevent their active efflux from the cell. The similarities between MDR and *CQ* resistance in malaria parasites has suggested that a similar energy dependent efflux protein may be present in *CQ*-resistant parasites (Krogstad *et al.* 1987, Warhurst 1988, Krogstad *et al.* 1992). Two MDR genes have been found in *P. falciparum* (Wilson *et al.* 1989), one of which, *pfmdr*1, has a high degree of homology to mammalian MDR genes (Foote *et al.* 1990). However the level of *CQ* resistance in a number of strains of *P. falciparum* do not correlate with the level of *pfmdr*1 expression arguing against a direct role for this protein in *CQ* resistance (Foote *et al.* 1990, Cowman *et al.* 1994). In addition, offspring from a genetic cross of *CQ*-resistant and *CQ*-sensitive cloned isolates could establish no linkage between the *pfmdr*1 gene and the rapid efflux phenotype (Wellems 1990, Wellems 1991).

Chloroquine resistance has also been mapped to complex polymorphisms related to two genes (*cg1* and *cg2*) on chromosome 7 of the malaria parasite (Wellems *et al.* 1991). A recent study in which the *cg1* and *cg2* sequences in resistant parasites were replaced with the *cg1* and *cg2* sequences from sensitive parasites, however showed no subsequent change in the degree of *CQ* resistance thereby arguing against this hypothesis (Fidock *et al.* 2000a). These authors instead suggested that a gene located close to *cg1* and *cg2*, namely *pfcrt*, is probably responsible for *CQ* resistance (Fidock *et al.* 2000b). There is an increasing body of evidence implicating the PfCRT protein in *CQ* resistance (Fidock *et al.* 2000b, Ward and Bray 2000, Warhurst 2001). This protein is located in the vacuolar membrane and resembles other 10 transmembrane domain proteins that facilitate transport of organic cations (Zhang *et al.* 1997). Although 10 codon changes were found in the *pfcrt* sequance in *CQ* resistant isolates from South America, Africa and Asia, only the point mutation from lysine to threonine in codon 76 appears to be common to all *CQ* resistant strains (Warhurst 2001). Furthermore, the *CQ*-resistant phenotype has been expressed from a *CQ*-sensitive strain by transfection with a plasmid containing the 'resistance" *pfcrt* sequence (Fidock *et al.* 2000b).

There is various evidence that reduced *CQ* accumulation in resistant parasites is due to reduced drug uptake and not enhanced drug efflux (Geary *et al.* 1986, Ferrari and Cutler 1991, Bray *et al.* 1992a and b, Martiney *et al.* 1995) which is supported by a number of mathematical models (Ferrari and Cutler 1991, Ginsburg and Stein 1991).

1.6.2. Other Hypotheses on Reduced Chloroquine Accumulation

1.6.2.1. Reduced NHE activity

Since the initial rate of *CQ* uptake into *CQ*–sensitive parasites is rapid, it has been proposed that *CQ* is actively transported into the parasite (Ferrari and Cutler 1991, Sanchez *et* al. 1997). This is supported by evidence that specific inhibitors of a Na^+/H^+ exchanger (NHE) inhibit *CQ* uptake. It has therefore been proposed that *CQ* resistance is the result of an impaired NHE pump and that verapamil reverses this effect (Sanchez 1997, Wünsch *et al.* 1998). This hypothesis has recently been discredited by Bray *et al.* who showed that *CQ* uptake is unchanged in the absence of sodium ions and that inhibition of *CQ* uptake by NHE inhibitors (amiloride derivatives) occurs via inhibition of *CQ*-haematin binding as opposed to inhibition of NHE (Bray *et al.* 1999, Bray *et al.* 1998).

1.6.2.2. Increased Vacuolar pH

Reduced *CQ* accumulation into resistant parasites has also been attributed to an increased vacuolar pH in resistant parasites due to a weakened proton pump (Geary *et al.* 1986, Ginsburg and Stein 1991). This was further supported by Bray *et al.* who found that inhibition of the vacuolar ATPase system with bafilomycin A1 caused a greater reduction of [^{3}H] *CQ* uptake into *CQ*–sensitive as opposed to *CQ*–resistant parasites (Bray *et al.* 1992). Krogstad *et al.* however found no significant differences in vacuolar pH between resistant and sensitive parasites (Krogstad *et al.* 1985). Recently Dzenukov *et al.* found that the vacuolar pH in resistant parasites is actually lower, and not higher, than their sensitive counterparts (Dzenukov *et al.* 2000), although their experimental methods have recently been called into question (Bray *et al.* 2002a, Dzekunov *et al.* 2002, Bray *et al.* 2002b).

1.6.2.3. Reduced Access to Haematin

A recent study by Bray *et al.* found that saturable *CQ* uptake is due solely to the binding of *CQ* to haematin and that the number of binding sites in both resistant and sensitive parasites are the same. The difference in *CQ* accumulation is accounted for by a reduction in *CQ* binding affinity which can be reversed in the presence of verapamil (Bray *et al* 1998, Bray *et al.* 1999). It has been suggested that the *CQ*-resistance mechanism probably regulates the access of *CQ* to haematin which is consistent with the resistance hypotheses arguing that prevention of *CQ* accumulation at the local site of action is the basis of activity.

1.6.3. Concluding Remarks

The mechanism of *CQ* drug resistance appears to be multifaceted and is still the subject of much debate. It appears that alteration in *pfmdr*1 and/or *pfcrt* gene sequences may play a role, however the search for a genetic event capable of explaining resistance in all isolates is probably too simplistic (Ward *et al.* 1997). In highly *CQ*-resistant parasites, it has been proposed that at least two mechanisms are present; a verapamil-sensitive component which is responsible for the shift in IC_{50} from moderate resistance to high resistance, and a verapamil-insensitive component responsible for the initial loss in sensitivity compared to the truly sensitive isolates (Ward *et al.* 1995). This is demonstrated by *AQ* resistance, which shows a degree of cross-resistance to *CQ* but lacks the verapamil-sensitive resistance component (Bray *et al.* 1996). It has been suggested that the existence of more than one resistance mechanism in highly *CQ*-resistant malaria has contributed to many of the controversies that surround the subject (Ward *et al.* 1995).

1.6.4. Structural Modifications that Circumvent Resistance

1.6.4.1. Changes to the Aminoalkyl Side-Chain of *CQ*

Although the *CQ*-resistance mechanism is still the subject of much debate, it appears to arise from reduced drug accumulation and not modification of the target. The resistance mechanism is extremely structure specific and seems to recognise the aminoalkyl side-chain of *CQ*. This was demonstrated elegantly by Krogstad *et al.* who showed that close analogues of *CQ* with either shortened (2-3C long) or lengthened (10-12C long) side-chains maintain full activity against *CQ* resistant strains whereas those with chain lengths closer to that of *CQ* have intermediate activities (Figure 1.13) (De *et al.* 1996).

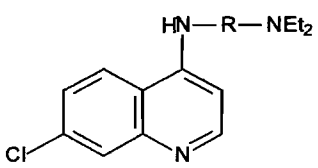

R = ethyl, propyl, isopropyl, butyl, pentyl, isopentyl, hexyl, octyl, decyl and dodecyl

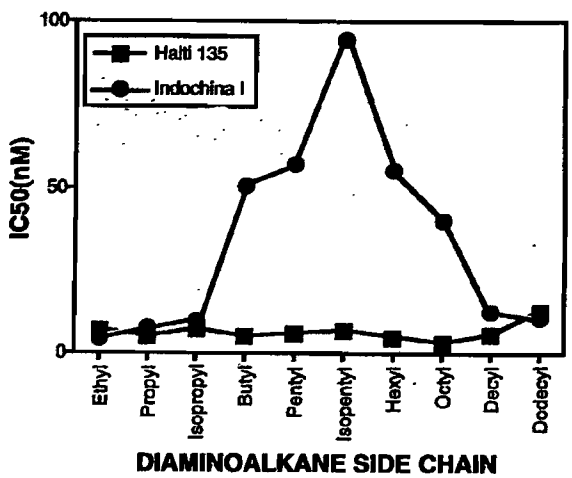

Figure 1.13. Relationship between length of the aminoalkyl side-chain and activity against chloroquine-sensitive (Haiti 135) and chloroquine-resistant *P. falciparum* (De *et al.* 1996).

It appears that a high degree of variability can be tolerated in the side-chain as can be seen from the introduction of a short side-chain similar to that of *CQ* in **18** and **Ro 47-0543**, or the introduction of an organometallic substituent in **19** (Figure 1.14). **Ro 47-0543** and three other short chain analogues of *CQ* were selected for in depth scrutiny as potential replacements of *CQ*. They exhibited comparable activity to *CQ* in the mouse model but showed partial cross resistance with *CQ*. In addition, the metabolites of these compounds, which contribute to *in vivo* activity, are inactive against *CQ*-resistant strains bringing into question the ultimate efficacy of these compounds as *CQ* replacements in the clinic (Ridley *et al.* 1996, Ridley *et al.* 1997, Ridley and Hudson 1998).

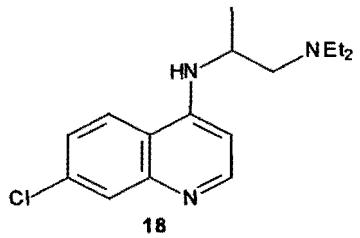

18

IC_{50} / nM (**18**) = 8 (Haiti 135(*S*)), 11 (Dd2 (*R*))

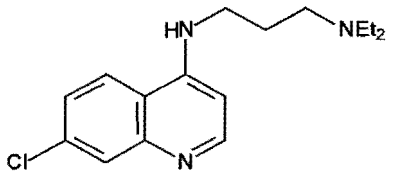

Ro 47-0543

IC_{50} / nM (Ro 47-0543) = 18 (NF54 (*S*)), 59 (K1 (*R*))

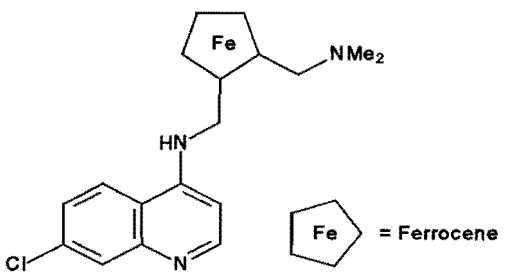

19

IC_{50} / $\mu g.ml^{-1}$ (**19**) = 0.057 (FG4 (*S*)), 0.067(FG1(*R*))

Figure 1.14. Analogues of *CQ* with different side chains that retain activity against *CQ*-resistant *P. falciparum*. **18** (De *et al.* 1996), **Ro 47-0543** (Ridley *et al.* 1996), **19** (Biot *et al.* 1997). *S* represents a *CQ*-sensitive strain and *R* represents a *CQ*-resistant strain of *P. falciparum*.

Many bis-quinolines with varying side chains also have good activity against *CQ*-resistant *P. falciparum* (Figure 1.15) (Chen 1991, Vennerstrom *et al.* 1992, Raynes *et al.* 1995, Raynes *et al.* 1996, Ridley *et al.* 1997, Vennerstrom *et al.* 1998). In particular **22** underwent extensive preclinical evaluation at Hoffmann-LaRoche Ltd, but was rejected on toxicological grounds (Ridley *et al.* 1997, Vennestrom *et al.* 1998).

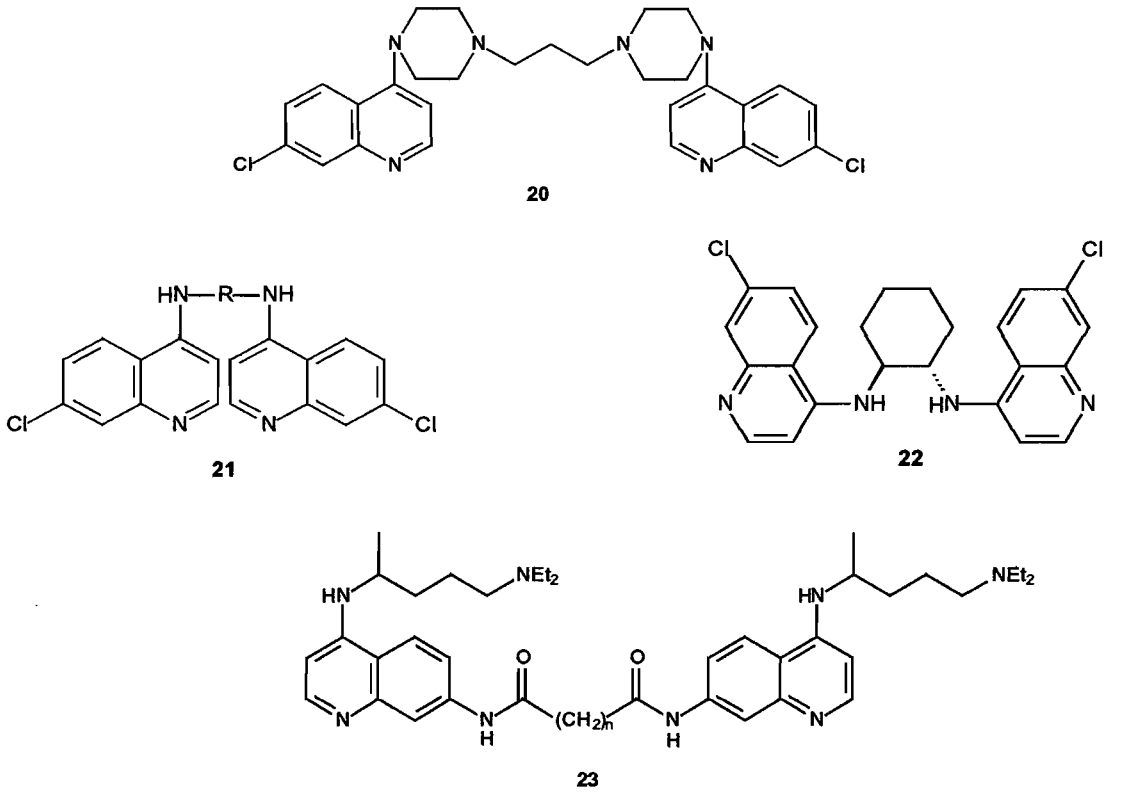

Figure 1.15. Bis-quinoline analogues of *CQ* with different side chains that retain activity against *CQ* resistant strains of *P. falciparum.* **20** (Chen 1991, **21** (Vennerstroom *et al.* 1992), **22** (Ridley *et al.* 1997, Vennerstroom *et al* 1998) and **23** (Raynes *et al.* 1995).

1.6.4.2. Changes to the Quinoline Ring

Structural changes to the quinoline ring system appear to have little effect on antiplasmodial activity of *CQ* against both *CQ*-sensitive and *CQ*-resistant parasites if the 7-chloro group is substituted with iodo, bromo or nitro groups (Table 1.8). Substitution with fluoro or trifluoromethyl groups at the 7-position significantly reduces *CQ*'s activity against both the *CQ*-resistant and *CQ*-sensitive parasites, and substitution with methoxy, hydro or amino groups substantially reduces *CQ*'s activity against both *CQ*-resistant and *CQ*-sensitive parasites. From these observations, It appears that changes to the quinoline ring system have little effect on the *CQ*-resistance mechanism but are essential for *CQ*'s antimalarial activity. From these 7-substituted *CQ* analogues it would appear that antiplasmodial activitiy may be related to the electron withdrawing ability and/or lipophilicity of the group at the 7-position.

Table 1.8. Effect of changing quinoline-ring substituents on the antiplasmodial activity of *CQ*

Compound	**IC_{50} / nM**	
	***CQ*-sensitive**	***CQ*-resistant**
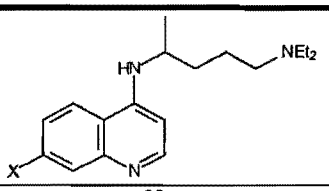		
X	**Haiti 135**	**Indochina I**
Cl (*CQ*)[a]	8	95
I[a]	4	35
Br[a]	5	90
F[a]	20	500
CF_3[a]	16	45
OMe[a]	55	3000
H[b]	90	5000
	NF54	**KI**
Cl (*CQ*)[c]	13	350
NO_2[c]	15	68
NH_2[c]	2600	4300
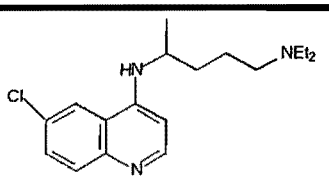	30 (Haiti 135)[b] 170 (NF54)[c]	250 (Indochina 1)[b] 4900 (KI)[c]
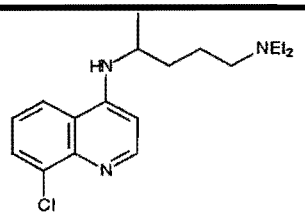	1000 (Haiti 135)[b]	1050 (Indochina 1)[b]

[a] De *et al.* 1998, [b] De *et al.* 1996, [c] Vippagunta *et al.* 1999.

In summary, since close analogues of *CQ* maintain activity against *CQ*-resistant parasite strains it appears that the resistance mechanism does not involve any change to the target of this class of drug, but rather involves a compound-specific resistance. As a result, it remains of considerable importance to understand the mode-of-action of *CQ* with a view to rational design of new antimalarials based on the same mechanism of action. This is especially true given that the putative haemozoin inhibition process occurs only in the parasite and not in the host and so represents an ideal drug target.

1.7. AIMS AND OBJECTIVES

1.7.1. Aims

The aims of the project are to investigate the nature of the ferriprotoporphyrin IX (Fe(III)PPIX) target and to determine the critical structural features in 4-aminoquinoline antiplasmodials responsible for their complexation with Fe(III)PPIX and the relationship to antiplasmodial activity. An attempt will also be made to identify the structural features in 4-aminoquinolines responsible for β-haematin inhibition with an aim to probing whether these compounds act by inhibiting β-haematin formation. In addition, it will be investigated if accumulation of the 4-aminoquinoline antiplasmodials in the food vacuole is dependent on pH trapping and whether pH trapping is important for antiplasmodial activity.

1.7.2. Objectives

1.7.2.1. Investigation of the Target

1.7.2.1.1. The Nature of Fe(III)PPIX in Aqueous Solution

There is considerable evidence that ferriprotoporphyrin IX (Fe(III)PPIX), released from haemoglobin into an acidic aqueous environment is the target of *CQ* and related 4-aminoquinoline antimalarials and antiplasmodials. Fe(III)PPIX in aqueous solution is generally thought to consist of monomers and μ-oxo dimers with a dimerisation constant strongly in favour of the dimer (K = 4.5) (Brown *et al.* 1970). Since behaviour of Fe(III)PPIX in aqueous solution is central to understanding the mechanism of action of quinoline antimalarials, and there have been no follow-up investigations since the study by Brown *et al.*, the nature of the Fe(III)PPIX target in aqueous solution will be investigated.

1.7.2.1.2. Structural Features of *CQ* critical for Fe(III)PPIX- *CQ* Binding

Little is known about the structural features in *CQ* responsible for Fe(III)PPIX binding. In this study, the following structural features in *CQ* will be probed to ascertain the effect they have on Fe(III)PPIX- *CQ* binding: (i) the position of the amino-group on the quinoline ring, (ii) the presence of a 7-chloro group and (iii) the presence of a side chain with terminal amino functionality. The existence of a quantitative relationship between strength of Fe(III)PPIX association and antiplasmodial activity will also be investigated.

1.7.2.2. Mechanism of Antiplasmodial Action of 4-Aminoquinolines

1.7.2.2.1. Accumulation Through pH Trapping

Since *CQ* accumulates roughly 10 000 fold in the food vacuole at the IC_{50}, it would appear that these enhanced internal concentrations are necessary for antiplasmodial activity. It has recently been suggested that this vacuolar accumulation is driven predominantly by Fe(III)PPIX complex formation and that pH trapping plays a lesser role. In this study, the structural significance of the terminal amino-group will be probed to ascertain if pH trapping is important in antiplasmodial activity. Furthermore, the extent of pH trapping will be predicted for a series of structurally related compounds in order to ascertain if accumulation through pH trapping is quantitatively related to antiplasmodial activity.

1.7.2.2.1. Inhibition of β-Haematin Formation

Although there is considerable evidence that *CQ* and related 4-aminoquinolines bind to Fe(III)PPIX, the resulting toxicity of this complex is still the subject of much debate. In this study, the hypothesis that *CQ*–type antimalarials act by inhibiting β-haematin formation will be investigated. An attempt will be made to identify the critical structural features in *CQ* and related 4-aminoquinolines responsible for β-haematin inhibition in order to probe whether this class of compounds acts by inhibiting β-haematin formation.

SYNTHESIS

2.1. BACKGROUND

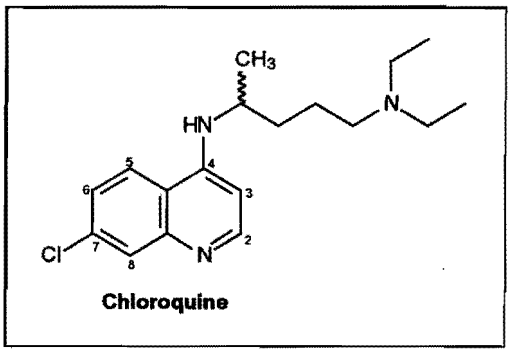

For more than 40 years, chloroquine (*CQ*) has been the drug most widely used in the prophylaxis and treatment of malaria. The recent spread of *CQ* resistance has compromised its utility and spurred on the need to develop new antimalarials. Instead of searching for a completely new motif, there has been a trend towards understanding the structure-activity relations in *CQ* with a view to rationally designing superior quinoline antimalarials. In this project, it was decided to dismantle the *CQ* molecule to probe how the following three structural features are related to antiplasmodial activity (Figure 2.1.):

1. Position of the amino-group on the quinoline ring
2. Functionality of the group at the terminal position on the side-chain, Y
3. Functionality of the group at the 7-position on the quinoline ring, X.

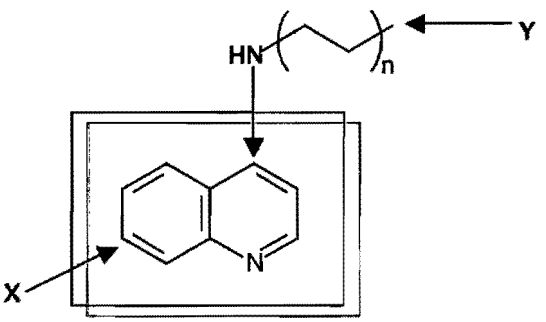

Figure 2.1. Schematic representation of the three structural features of interest in chloroquine (*CQ*). NH: position of the amino-group, Y: terminal functionality of the group in the side-chain, and X: functionality of the group at the 7-position.

2.1.1 Synthetic Targets Chosen for the Study

The following four classes (1-4 below) of aminoquinolines were obtained or synthesised in order to probe the following structural features in *CQ*.

1. Position of the amino-group on the quinoline ring:

Quinoline, 3-, 5-, 6- and 8-aminoquinoline are commercially available, whilst 2- and 4-aminoquinoline were synthesised (Figure 2.2.).

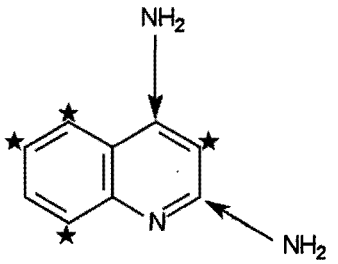

★Commercially avaliable

Figure 2.2. Aminoquinolines required for the study

2. Influence of the group at the 7-position of 4-aminoquinoline (Figure 2.3.).

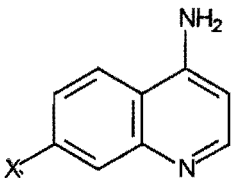

X
Cl
CH_3

Figure 2.3. 7-X-4-aminoquinolines required for the study

3. Functionality of the group at the terminal position in the side chain (Figure 2.4.).

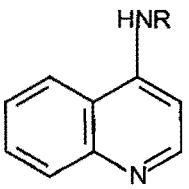

R
CH_3
CH_2CH_2OH
$CH_2CH_2HNCOCH_3$
$CH_2CH_2NH_2$
$CH_2CH_2NEt_2$

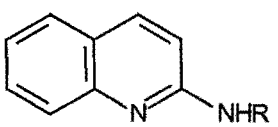

R
CH_3
$CH_2CH_2NH_2$

Figure 2.4. Derivatives with an amino-group at the 2- and 4-positions, containing a short alkyl side chain and terminal functionality

4. Functionality of the group at the 7-position on the quinoline ring (Figure 2.5.).

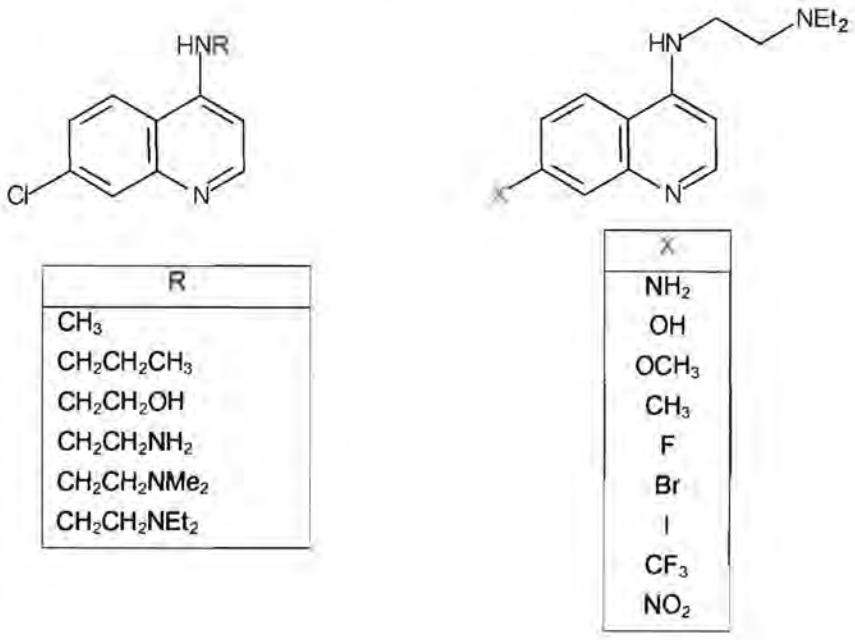

R
CH_3
$CH_2CH_2CH_3$
CH_2CH_2OH
$CH_2CH_2NH_2$
$CH_2CH_2NMe_2$
$CH_2CH_2NEt_2$

X
NH_2
OH
OCH_3
CH_3
F
Br
I
CF_3
NO_2

Figure 2.5. (left) derivatives of 4-amino-7-chloroquinoline with different terminal side chain groups and, (right) derivatives of N^2-(7-X-4-quinolinyl)-N^1,N^1-diethyl-1,2-ethanediamine where X = NH_2, OH, OCH_3, CH_3, F, Br, I, CF_3 and NO_2.

2.2. OVERVIEW OF QUINOLINE REACTIVITY

2.2.1. Reactivity Towards Nucleophiles

If quinoline is considered as benzo[b]pyridine, much of its chemistry can be rationalised in terms of benzene and pyridine. Like pyridine, the quinoline pyridine ring is π-deficient due to the electron-withdrawing inductive and mesomeric effects of the nitrogen atom. These effects are pronounced at positions 2 and 4 (Figure 2.6.), which are the preferred nucleophilic sites of attack. A halogen group at positions 2 or 4 on the quinoline pyridine ring further activates these positions towards nucleophilic attack. Quinoline is more reactive towards nucleophiles than pyridine as a result of stabilisation of the reaction intermediate by the presence of a second aromatic ring.

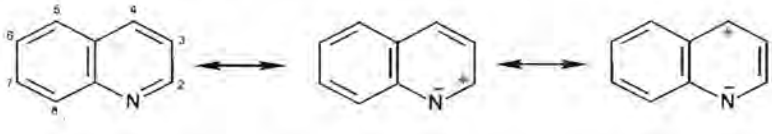

Figure 2.6. Mesomeric effects in quinoline providing a rational for the preferred sites of nucleophilic attack

2.2.2. Reactivity Towards Electrophiles

Quinoline is more π-deficient than benzene and hence not very susceptible towards electrophiles. Electrophiles will first attack the electron-rich nitrogen atom of the quinoline pyridine ring but once this is protonated or quaternised, substitution will occur at positions 5 and 8 on the quinoline benzene ring. These positions are favoured as the resulting intermediates can be represented by two canonical structures while preserving the aromatic character of the heterocyclic ring as opposed to only one resulting from electrophilic attack at positions 6 and 7 (Figure 2.7.).

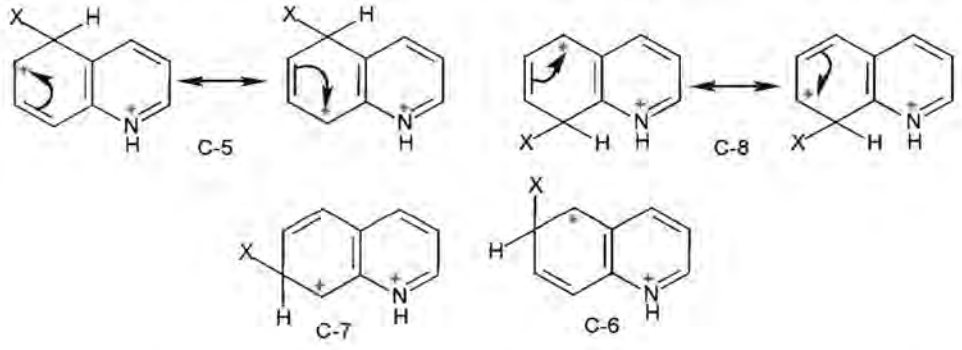

Figure 2.7. Mesomeric effects in quinoline providing a rational for the preferred sites of electrophilic attack

2.2.3. Reactivity of Quinoline-1-oxide

The quinoline ring can be activated towards electrophilic attack by transformation to its N-oxide, quinoline-1-oxide. The N-oxide can act as an electron donor into the ring, thereby making it more π-rich. (Katritzky and Lagowski 1971) (Figure 2.8.). Electrophilic substitution of quinoline 1-oxide usually occurs at position 4 in the quinoline pyridine ring (Barton and Ollis 1979).

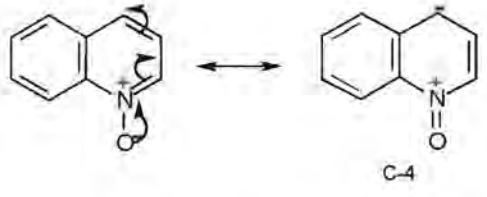

Figure 2.8. Representation of quinoline-1-oxide acting as an electron donor

2.3. GENERAL ROUTES TO 2-AND 7-X-4-AMINOQUINOLINES

The 2-aminoquinolines (2AQ) and 7-X-4-aminoquinolines (7X4AQ) were synthesised by nucleophilic attack of the appropriate amine, in an addition-elimination pathway, with 2-chloroquinoline **24** and 7X4AQ respectively (Scheme 2.1.). Since nucleophilic substitution of a halogen occurs more readily at positions 2 and 4 than in the quinoline benzene ring (Comprehensive Heterocyclic Chemistry II 1996), no unwanted 7-substituted side products were observed in the substitution reactions of 7X4AQ.

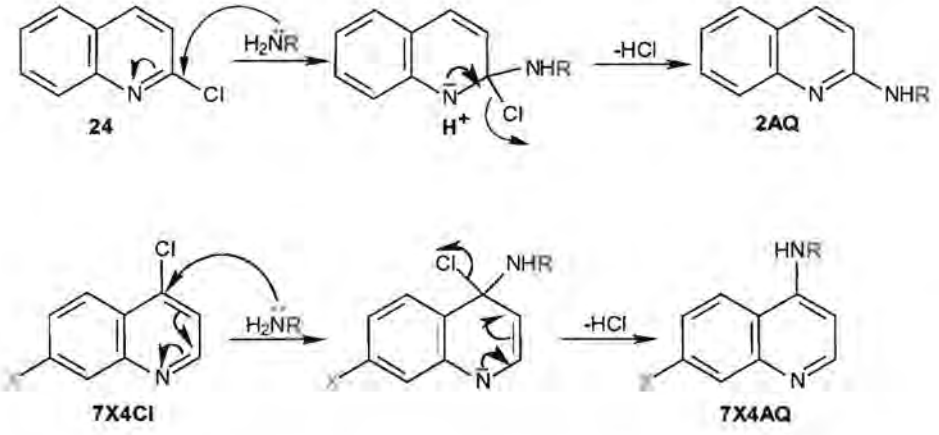

Scheme 2.1. General routes to 2- and 7-X-4-aminoquinolines from 2- and 7-X-4-chloroquinoline respectively

In order to make all the *CQ* analogues, both **24** and the various 7X4AQ were synthesised. The routes to these chloroquinolines are outlined below.

2.3.1. Routes to 2-Chloroquinoline

2-Chloroquinoline was synthesised using two methods. Firstly (Riegel *et al.* 1946) (Scheme 2.2.) by treatment of commercially available 2-hydroxyquinoline **25**[a], with phosphorus oxychloride at 100°C for 2h to give **24** in a 79% yield.

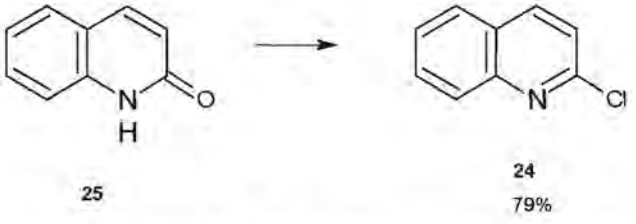

Scheme 2.2. Preparation of 2-chloroquinoline. *Reagents and Conditions:* i. $POCl_3$, 100°C.

[a] 2- and 4-hydroxyquinoline exist in tautomeric equilibrium with their quinolone forms (shown for 2-quinolone (25)). For simplicity, the quinoline tautomer has been shown throughout the thesis.

In a second route, quinoline-1-oxide, whose synthesis is described in Section 2.3.2.1. was treated with phosphorus oxychloride (Bachman 1944, Badger 1961) at 65°C for 1h. The products were isolated by chromatogrphy to give a mixture of 2- and 4-chloroquinolines in a 3.3:1 ratio (Scheme 2.3.). In this Meisenheimer type reaction (Meisenheimer 1929), it is proposed (Comprehensive Heterocyclic Chemistry II 1996) that the electrophilic phosphorus reagent first reacts with the N-oxide thus promoting chloride attack at positions 2 or 4 on the quinoline pyridine ring giving a mixture of 2- and 4-chloroquinoline (**24** and **26** respectively).

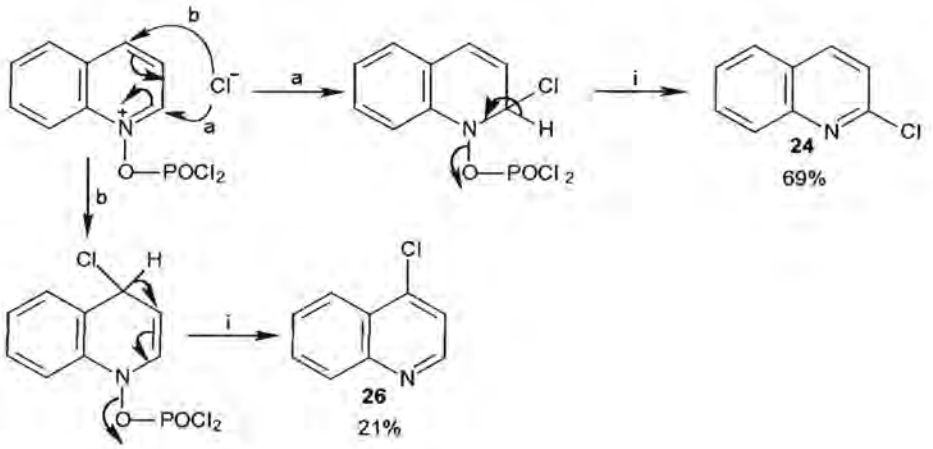

Scheme 2.3. Formation of a mixture of 2- and 4-chloroquinoline. *Reagents and Conditions:* i. $POCl_3$, 65°C.

2.3.2. Route to 7-X-4-Chloroquinolines

The 7-X-4-chloroquinolines were synthesied by two methods (Table 2.1.). For compounds X = H and X = CH_3, Method 1 was used. Compounds X = Cl and CF_3 were obtained commercially and X = F, Br, I, OCH_3 and NO_2 were synthesised according to Method 2.

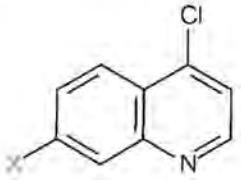

Table 2.1. Routes used to 7-X-4-chloroquinolines

X	H	CH_3	Cl	CF_3	F	Br	I	OCH_3	NO_2
Method	1	1	ca	ca	2	2	2	2	2

ca. commercially available

Treatment of **27a-b** with peracetic acid at 65 - 70°C for 26 - 40h (Ochiai 1953) gave **28a-b** in 89 - 93% yield. Selective nitration at the 4-position was achieved using potassium nitrate in trifluoroacetic acid (Yokoyama *et al.* 1997) to give **29a-b** in a 77 - 79% yield (Scheme 2.5.).

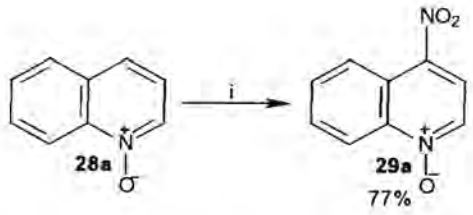

Scheme 2.5. Selective 4-nitration of **28a**. *Reagents and Conditions:* i. CF_3COOH, KNO_3, 60°C.

Chlorination of **29a-b**, using PCl_3 in dry dichloromethane for 6 - 20h at room temperature followed by a further 40 - 50h at 60°C, resulted in formation of three products which were isolated by chromatography to give **30a** and **30b** as the major products in 78% and 75% yields respectively. The other two products in the "**a**" reaction were isolated and characterised as 2,4-dichloroquinoline **32** and 2-chloro-4-nitroquinoline **33** in 7% and 3% yields respectively (Scheme 2.6.). In the "**b**" reaction the two side products were observed by TLC, but were not isolated. Attempts to scale-up the "**a**" reaction from 1g to 2.6g resulted in a lower yield of **30a** (56%) and hence the reaction was only carried out on 1g quantities.

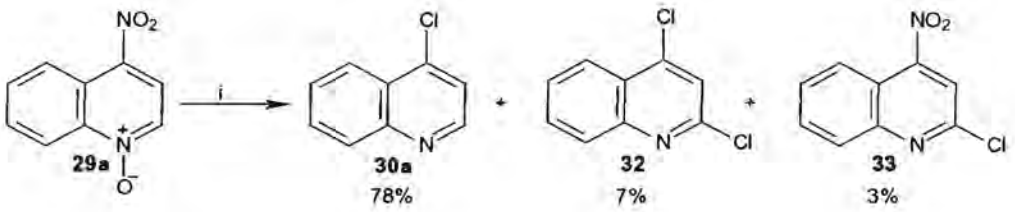

Scheme 2.6. Preparation of 4-chloroquinoline **29a**. *Reagents and Conditions:* i. PCl_3, CH_2Cl_2, 60°C.

2.3.2.2. Method 2: Price and Roberts

The 7-X-4-chloroquinolines, X = F, Br, I, OCH_3 and NO_2 were synthesised according to methodology developed to synthesise and derivatise *CQ*. These routes will be discussed briefly as they give the background to Method 2.

Surrey and Hammer developed a route to 7-X-4-aminoquinolines for X = Cl, Br and I, that was used for the production of *CQ* in the United States (Surrey and Hammer 1946, Kenyon 1949) (Scheme 2.7.).

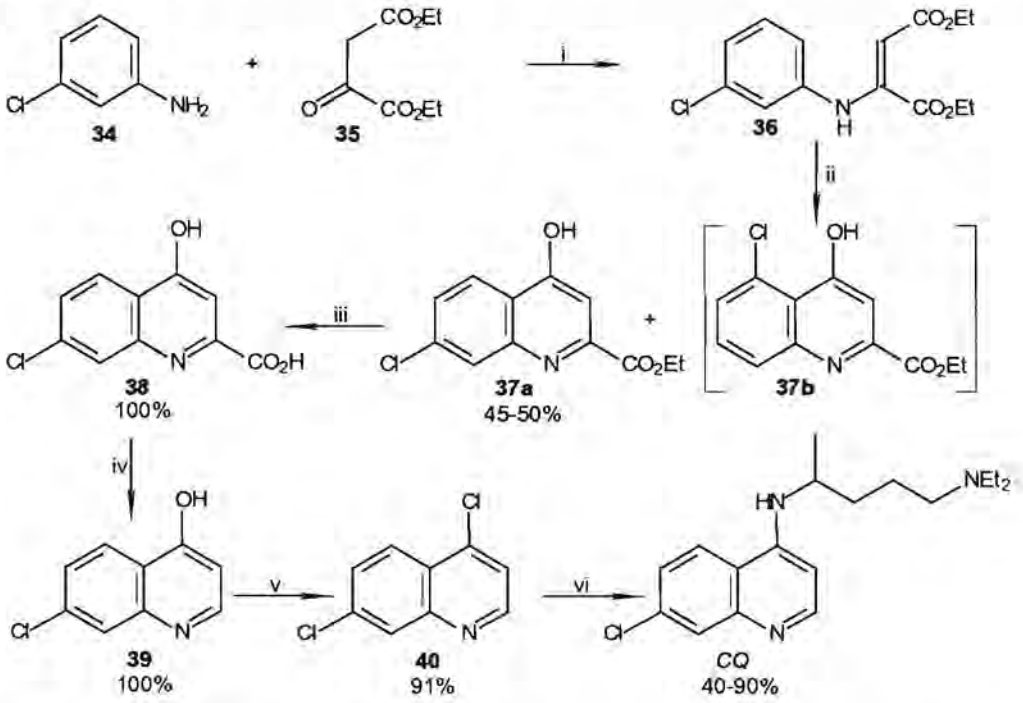

Scheme 2.7. Commercial route to *CQ* developed by Surrey and Hammer in 1946. *Reagents and Conditions:* i. CH_3COOH (aq), 40 - 50°C, 15 - 18h; ii. mineral oil, 250°C, 20min; iii. 35% NaOH, reflux, 2h; iv. mineral oil, 270°C, 5min; v. $POCl_3$, reflux, 2h; vi. 4-amino-1-diethylaminopentane, 160 - 180°C, 7h (Surrey and Hammer 1946).

In the case of *CQ*, *m*-chloroaniline **34** was condensed with diethyl 2-oxo-succinate **35** to form **36**. Thermal cyclisation of **36** gave a 1:1 mixture of 2-(ethoxycarbonyl)-4-hydroxy-7-chloroquinoline **37a** and its 5-chloroisomer **37b** from which the desired **37a** was isolated by selective crystallisation. Hydrolysis to the acid followed by decarboxylation and chlorination of the resultant 7-chloro-4-hydroxyquinoline **39** gave 4,7-dichloroquinoline **40**, which underwent 4-substitution with excess 4-amino-1-diethylaminopentane (novol diamine, NDA) for 3 - 5h at 160 - 170°C to afford *CQ* as the free base which was isolated as the diphosphate salt by treatment with phosphoric acid.

Some interesting adaptations from Surrey and Hammer's laboratory synthesis to plant production of *CQ* were reviewed by Kenyon in 1949. One improvement was the use of Dowtherm instead of mineral oil for the cyclisation and decarboxylation steps ii and iv respectively as mineral oil is difficult to remove due to it's high viscosity and tendency to carbonise. Another improvement was addition of phenol to **40** prior to coupling with NDA (step vi). Phenol reacts with **40** to form 7-chloro-4-phenoxyquinoline **41** (Surrey 1951) (Scheme 2.8.) which then couples more readily with NDA enabling the use of stochiometric amounts of NDA and lower reaction temperatures. This then eliminated the need to isolate *CQ* as its free base prior to formation of the diphosphate salt.

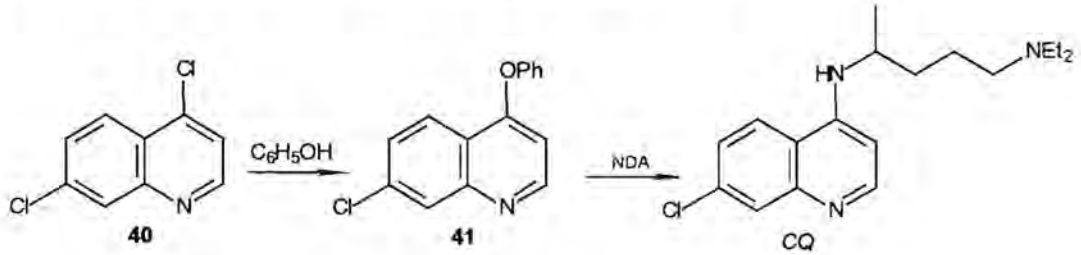

NDA = $H_2NCH(CH_3)CH_2CH_2CH_2N(C_2H_5)_2$

Scheme 2.8. Improved preparation of *CQ* from **40**.

Subsequently, Johnson and Buell provided another route that gave, upon cyclisation, only the desired 7-chloroisomer. In this route, methyl acrylate and *m*-chloroaniline were condensed to give **42** (Johnson and Buell 1952) (Scheme 2.9.). Tosylation and saponification then gave the acid **43** which was cyclised and detosylated to give **44**. Condensation with NDA in the presence of an oxidising agent then gave *CQ*. The authors claim that an overall 25% yield from *m*-chloroaniline can be obtained which compares favourably to the Surrey and Hammer process.

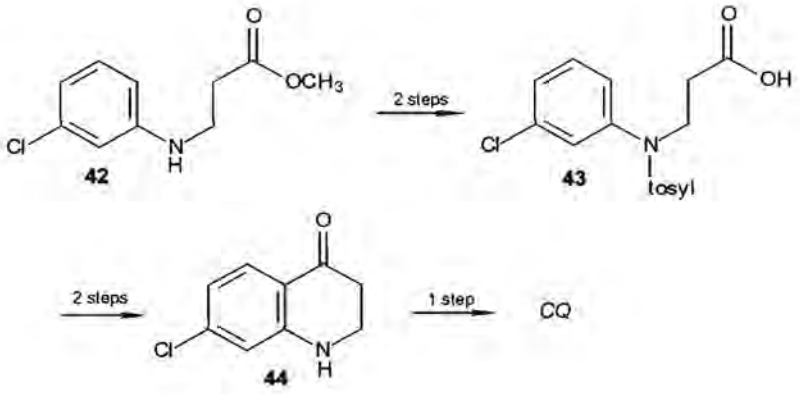

Scheme 2.9. Synthesis of *CQ* by Johnson and Buell (Johnson and Buell 1952)

A superior route to 4,7-dichloroquinoline was developed by Price and Roberts 1946 that involved condensation of diethyl ethoxymethylenemalonate **45** with *m*-chloroaniline **34** (Scheme 2.10.). In this method, cyclisation of **46** formed predominantly the 7-chloroisomer **47** (80 - 90%) with only traces of the unwanted 5-chloroisomer. Both the cyclisation and decarboxylation steps ii and iv were carried out using Dowtherm A.

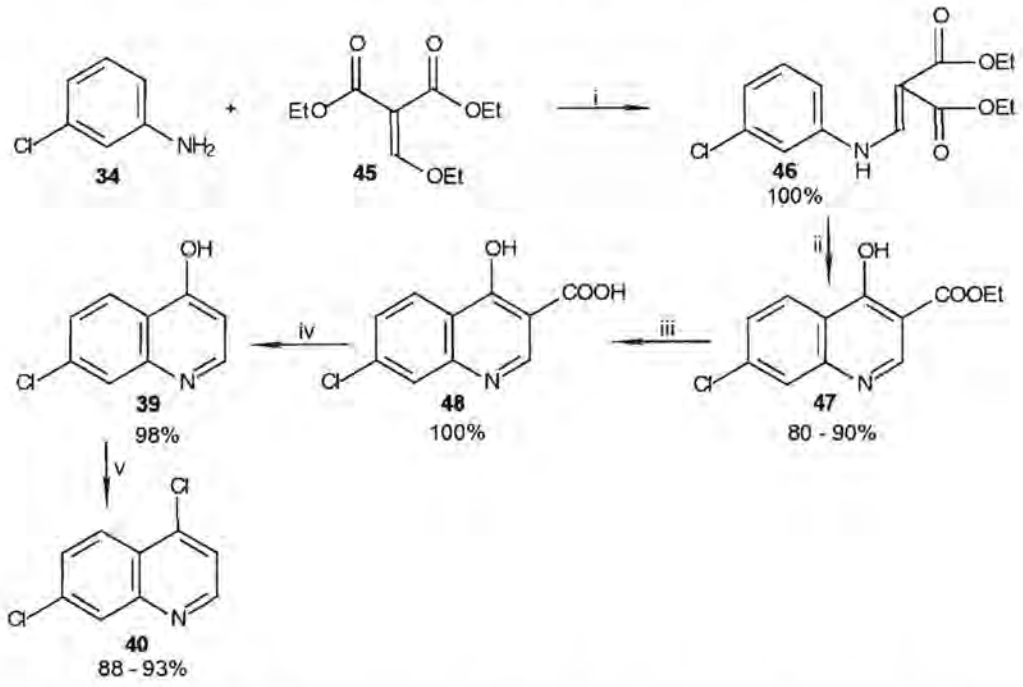

Scheme 2.10. Improved route to 2,4-dichloroquinoline (Price and Roberts 1946). *Reagents and Conditions:* i. 100°C, 1h; ii. Dowtherm A, reflux, 45min; iii. 10% NaOH (aq), reflux, 1h; iv. 240-270°C; v. $POCl_3$, reflux, 2h.

The method of Price and Roberts was used to synthesise the 7-X-4-chloroquinolines required for this study where, X = F, I, Br, OCH_3 and NO_2 (Scheme 2.11.).

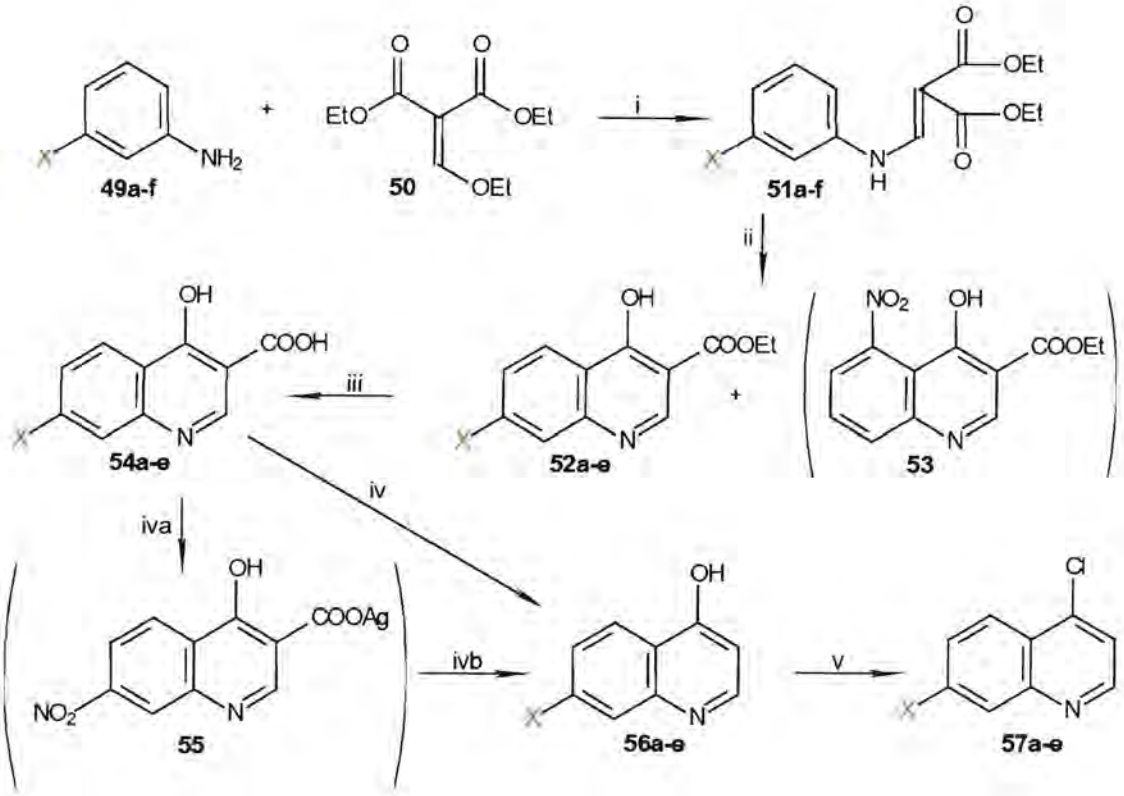

No.	a	b	c	d	e	F
X	F	Br	I	OCH_3	NO_2	OH

Scheme 2.11. Route to 7-X-4-chloroquinolines, X = F, Br, I, OCH_3 and NO_2. *Reagents and Conditions*. i. 60 - 110°C, 0.5 – 2h; ii. phenyl ether, reflux, 20min – 5h; iii. 10% NaOH (aq), reflux, 1 – 3h; iva. 25% NH_3 (aq), H_2O, reflux, 10min → $AgNO_3$, reflux, 16h; iv and ivb. phenyl ether, reflux, 30 – 50min; v. $POCl_3$, 115°C, 1h.

The appropriate *m*-substituted aniline **49a-f** and diethyl ethoxymethylenemalonate **50** were heated at 60 - 110°C for 0.5 - 2h to afford the acrylates **51a-f** which were crystallised from ethanol in 83 - 96% yield. Each purified **51a-e** was then added, slowly, over 10 - 20min to vigorously stirred, refluxing phenyl ether and the mixture refluxed for a further 20 - 40min to give the desired 7-substituted quinoline products **52a-d** regioselectively in 30 - 77% yields. Owing to the difficulty in removing all the phenyl ether from **52a-d**, the regioselectivity of these derivatives was confirmed by nmr in the next step. By comparison, the nitro and hydroxy derivatives **51e-f**, required longer, 5h, reaction times and both the 7- and 5-substituted regioisomers formed. In this case, the remaining phenyl ether was removed by extensive washing with cold acetone. The 7- and 5-nitro regioisomers had different Rf's on TLC (methanol : ethyl acetate (10 : 90)) of 0.48 and 0.33 respectively, but were both too insoluble for chromatography. Some of the slightly more soluble 5-nitroisomer **53** was

separated by hot extraction into methanol and crystallised out of this solvent upon cooling to room temperature. The 7-nitroisomer **52e** was then selectively crystallised from large volumes of DMSO in an optimised 23% yield.

The hydroxy derivatives appeared separable on TLC using a mixture of methanol : dichloromethane (10 : 90). Chromatography however proved difficult as the products were insoluble in dichloromethane and only sparingly soluble in methanol. Hence, an alternative route to synthesising the 7-hydroxy derivative was used (described in Scheme 2.17. later in this chapter).

Saponification of **52a-e** by refluxing in 10% NaOH (aq) for 1 - 3h gave the sodium salts of **54a-e** which were precipitated out of solution as their acids by addition of 10% HCl (aq). In the case of the nitro derivative, the precipitate was a yellow sludge from which **54e** was selectively extracted into large volumes of boiling ethyl acetate. The 7-substituted regioselectivity of compounds **54a-e** was confirmed by the ^{1}H nmr splitting patterns and coupling constants of the protons in the quinoline benzene ring. H-5 and H-8 appeared as doublets and H-6 as a doublet of doublets with ortho and meta coupling constants of 8.8 and 2Hz respectively (Figure 2.10.). The analogous arrangement of hydrogens in the ^{1}H nmr spectrum for the 5-regioisomers revealed a completely different pattern.

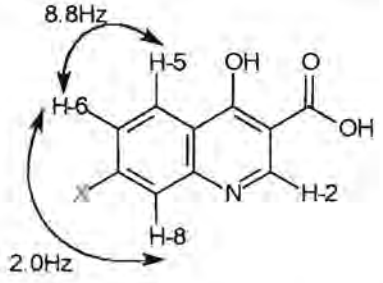

Figure 2.10. Characteristic ^{1}H nmr coupling constants of the quinoline benzene protons in the 7-substituted quinolines.

54a-d were decarboxylated in refluxing phenyl ether for 30 – 50min to give the respective 7-X-4-hydroxyquinolines **56a-d** in quantitative yields. **54e** was decarboxylated via the silver salt, **55** (Baker *et al.* 1946) to give **31e** in an optimised 13% yield. The 7-X-4-hydroxyquinolines **56a-e** showed the characteristic ortho and meta couplings between the protons in the quinoline benzene ring as well as a pair of AB doublets (J = 7.3Hz) corresponding to H-2 and H-3 in the quinoline pyridine ring (Figure 2.11.). This large coupling constant arises due to the existence of 4-hydroxyquinoline in the tautomeric

quinolone form. H-2 resonated at a higher chemical shift owing to the deshielding effect of the adjacent ring nitrogen of the quinoline pyridine ring .

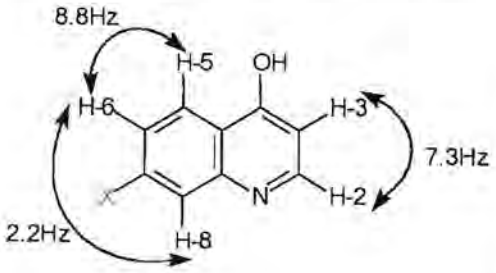

H	δ / ppm	Multiplicity	J / Hz
H-2	5.9 – 6.0	d	7.3
H-3	7.8 – 7.9	d	7.3
H-5	variable	d	8.8
H-6	variable	dd	8.8 and 2.2
H-8	variable	d	2.2

Figure 2.11. Characteristic ^{1}H nmr multiplicities and coupling constants for 7-X-4-hydroxyquinolines **56a-e**.

Chlorination of **56a-e** in phosphorus oxychloride at 110 - 120°C for 20min - 1h gave 7-X-4-chloroquinolines **57a-e** in yields of 73 - 91%. The ^{1}H nmr spectra of these compounds again showed the characteristic ortho and meta couplings between the protons in the quinoline benzene ring. H-2 and H-3 had characteristic chemical shifts of 7.5 – 7.7ppm and 8.7 – 8.9ppm respectively and their common coupling constant was lowered to 4.7Hz (Figure 2.12.).

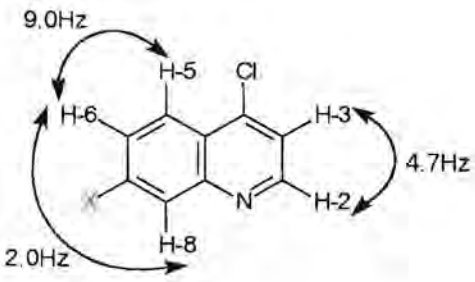

H	δ / ppm	Multiplicity	J / Hz
H-2	8.7 – 8.9	d	4.7
H-3	7.5 – 7.7	d	4.7
H-5	variable	d	9.0
H-6	variable	dd	9.0 and 2.0
H-8	variable	d	2.0

Figure 2.12. Characteristic ^{1}H nmr multiplicities and coupling constants for 7-X-4-chloroquinolines **57a-e**

2.3.2.2.1. Mechanistic Comments

Although the route to 7-X-4-chloroquinoline developed by Price and Roberts in 1946 has been widely used to make 4-aminoquinoline antimalarials, there has been no comment on the thermal cyclisation mechanism. The current study has not attempted to study this mechanism but comments are presented on two possibilities.

The first possibility involves a polar intramolecular nucleophilic substitution pathway (ionic mechanism) (Scheme 2.12.). In this case, attack of the aromatic ring on the carbonyl group would produce the polar intermediate (**A**) in the rate determining step (*rds*). Subsequent expulsion of ethanol followed by rapid tautomerism would give the products **52a-f**.

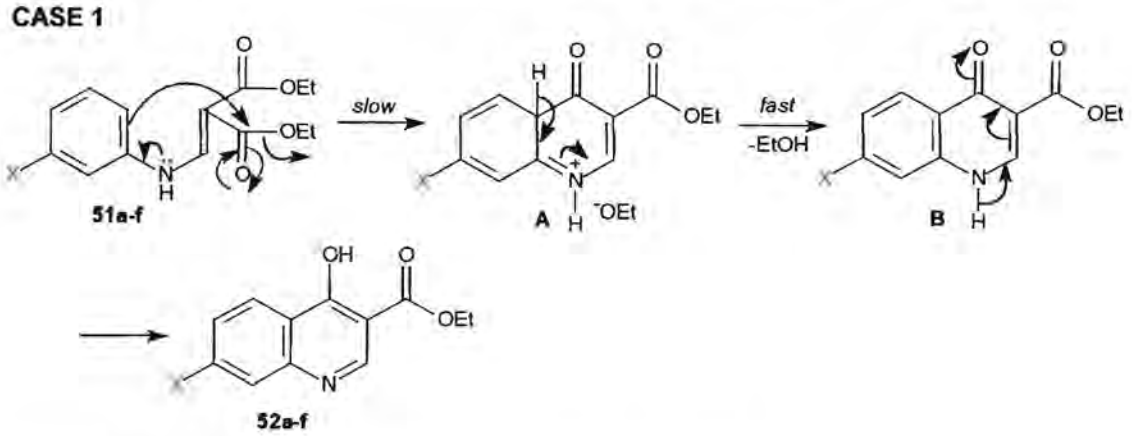

Scheme 2.12. Proposed cyclisation mechanism 1 via a polar intermediate **A**.

Another possibility is that the reaction proceeds via a 6π-electrocyclic mechanism (Scheme 2.13.). In this case, a reactive ketene intermediate **C** would need to form by an entropically-driven (favoured by high temperature) expulsion of ethanol. A subsequent 6π-electrocyclic rearrangement followed by tautomerism would give the products **52a-f**.

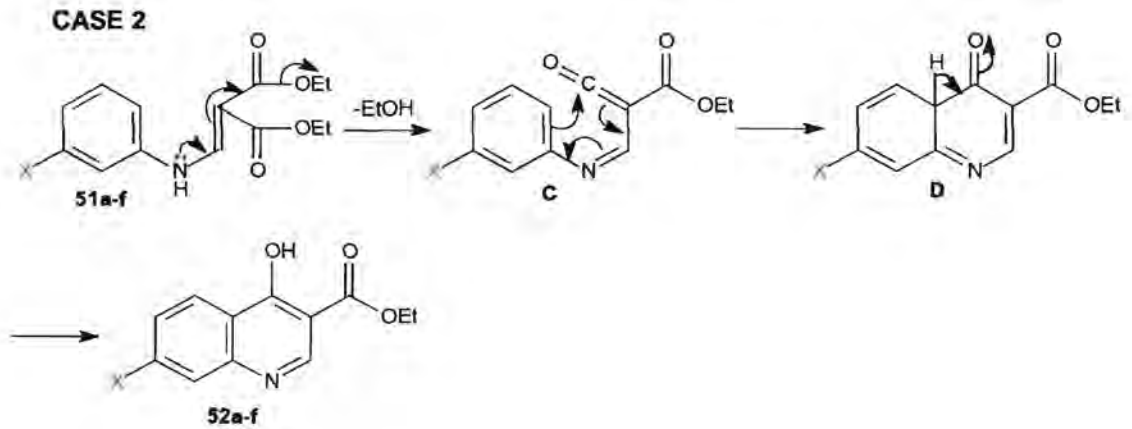

Scheme 2.13. Proposed 6π-electrocyclic cyclisation mechanism 2 via the ketene intermediate **C**.

If the cyclisation reaction proceeds via a polar mechanism, then strongly electron-releasing substituents (eg OH which has a strongly negative Hammett constant, Table 2.2) would favour the formation of **A**, via the resonance contribution of **E** promoting a fast rate of reaction (Scheme 2.14.). Conversely, strongly electron-withdrawing substituents (eg NO_2

which has a strongly positive Hammett constant, Table 2.2) would disfavour the formation of **A** thereby leading to a reduced rate (Scheme 2.14.).

The progress of the cyclisation reactions were monitored approximately every 20 mins by viewing the disappearance of the starting material (**51a-f**) by TLC. In the reactions involving the NO_2 and OH-substituted aromatic rings (**51e** and **51f** respectively), it was found that longer reaction times (approximately 5h vs 20 - 60mins for the other derivatives) were required to produce the cyclised products which formed in lower yields (approximately < 30% vs > 90% for the other derivatives) (Table 2.2.). Since these results are not consistent with the predicted outcome for a polar mechanism, it is likely that the cyclisation reaction does not proceed via this mechanism.

Table 2.2. Experimental and reported observations on the cyclisation reaction

-x	σ_p	**Reaction Times (viewed by TLC)**	**Yield**	**Regioselectivity**
-OH	-0.37	5h	<20%	5 and 7
-OMe	-0.27	30 ± 20 min	>90%	7
-F	0.06	40 ± 20 min	>90%	7
-I	0.18	60 ± 20 min	>90%	7
-Cl	0.23	20-40 min[a]	>90%[a]	7
-Br	0.23	45 ± 20 min	>90%	7
$-CF_3$	0.54	20–40 min[b]	>90%[b]	7
$-NO_2$	0.78	5h	34%	5 and 7

σ_p = para constant (Hansch and Leo 1979), [a] Price and Roberts 1946, [b] Snyder *et al.* 1947.

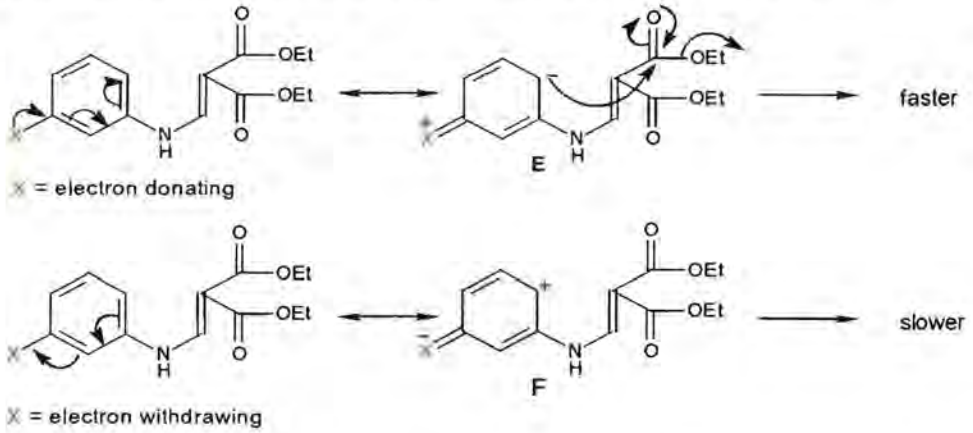

Scheme 2.14. Resonance forms resulting from the presence of (top) an electron donating and (bottom) an electron withdrawing group at the 3-position on the aromatic ring.

From the available experimental data, it is not possible to ascertain if the reaction proceeds via a 6π-electrocyclic mechanism (**CASE 2**) since it is not evident which step is rate determining. According to Frontier Molecular Orbital Theory (FMO theory), one would need to have information on the effect of the aromatic ring substituents on the HOMO and LUMO energies of the electrocyclic system as well as on the coefficients of the ketene carbon and C-4 of the aromatic ring (Scheme 2.13., intermediate **C**). Calculation of these parameters in addition to rate experiments would be required to ascertain if this reaction proceeds via a pericyclic mechanism.

It is also not obvious what controls the observed 5- and 7-substitution regioselectivity. Presumably the 7-isomer is sterically preferred and the 5-isomer may thus form as a result of an interaction between the carboxylic acid groups and the NO_2 or OH substituents (Scheme 2.15).

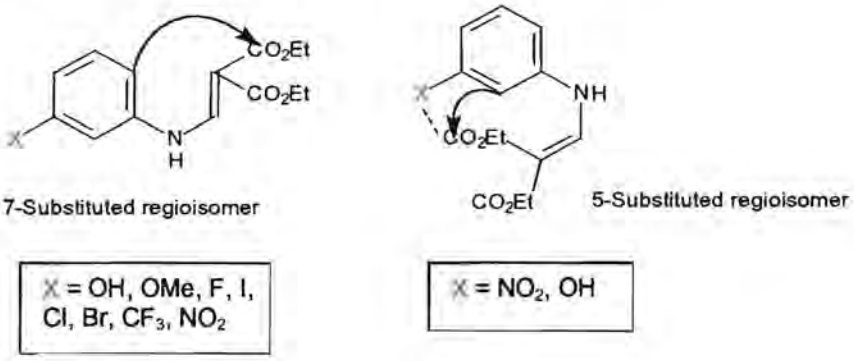

Scheme 2.15. Proposed formation of 5- and 7-substituted regioisomers

2.3.3. Synthesis of the 2- and 4-Aminoquinoline Analogues

The 2- and 4-aminoquinoline analogues were synthesised from their respective 2- and 4-chloroquinolines by nucleophilic substitution with the appropriate amine. In the literature (J. Am. Chem. Soc 1946), the 2- and 4-aminoquinoline analogues were often synthesised from carefully prepared diamine side chains and hence stoichiometric amounts of reagents were desired. This could be achieved using careful temperature control in the presence of phenol. The reaction mixture was heated until a sudden rise in temperature was noted. Thereafter the temperature was maintained a few degrees below this point for one to two hours (Drake *et al.* 1946). This method was not used in this study as our coupling amines were all commercially available. Instead, the chloroquinolines were heated with excess amine in a sealed tube at 105 - 140°C for 20 – 65h to give the 2-aminoquinolines **58-60** (Scheme 2.12.) and 120 - 160°C for 5 – 8h to give the 4-aminoquinolines **61-80** (Scheme 2.13.). In general,

the 2-substitutions were slower than the 4-susbstitutions and took longer reaction times. Substitutions with 25% ammonia (aq) were slower as a result of the lower nucleophilicity of ammonia relative to a primary amine. The heat sensitivity of N^2-(7-nitro-4-quinolinyl)-N^1,N^1-diethyl-1,2-ethanediamine **79**, resulted in thes coupling reaction (iv)e being carried out under the milder refluxing conditions of 85°C for 5h.

In general, most of the excess amine was removed under reduced pressure and then hot benzene was used to selectively extract out the product. The compounds were then chromatographed or crystallised directly to give analytically pure hydrochloride salts of **60** and **64**, and the free bases of **58**, **59**, **61-63**, **65-80**.

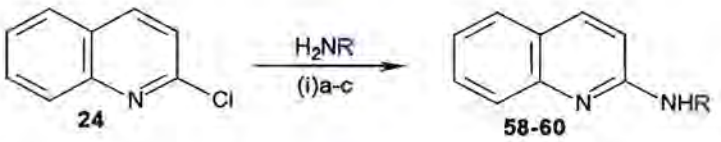

24 **58-60**

Rxn	No	R	Yield / %
(i)a	**33**	H	78
(i)b	**34**	CH_3[a]	81
(i)c	**35**	$CH_2CH_2NH_2$	82

[a] (Ashley Misplon, honours project, Department of Chemistry, University of Cape Town, 1998)

Scheme 2.12. General route to 2-substituted aminoquinolines. *Reagents and Conditions:* (i)a. 25% NH_3(aq), $ZnCl_2$, 140°C, 65h; (i)b. 33% H_2NCH_3 (methanol), 120°C, 20h; (i)c. 90% $H_2NCH_2CH_2NH_2$ (methanol), 105°C, 19h.

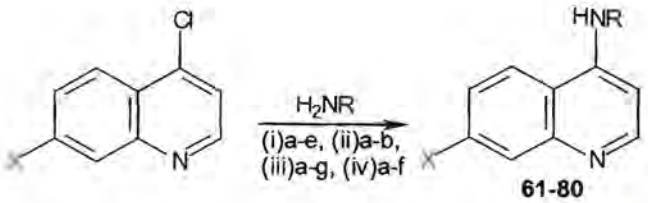

Reaction	No	X	R	Yield
(i)a	**61**	H	H	60%
(i)b	**62**		CH_3	94%
(i)c	**63**		CH_2CH_2OH	86%
(i)d	**64**		$CH_2CH_2NH_2$	92%
(i)e	**65**		$CH_2CH_2NEt_2$	77%
(ii)a	**66**	CH_3	H	64%
(ii)b	**67**		$CH_2CH_2NEt_2$	78%
(iii)a	**68**	Cl	H	[a]
(iii)b	**69**		CH_3	[a]
(iii)c	**70**		$CH_2CH_2CH_3$	37%
(iii)d	**71**		CH_2CH_2OH	[a]
(iii)e	**72**		$CH_2CH_2NH_2$	[a]
(iii)f	**73**		$CH_2CH_2NMe_2$	54%
(iii)g	**74**		$CH_2CH_2NEt_2$	33%
(iv)a	**75**	F	$CH_2CH_2NEt_2$	62%
(iv)b	**76**	Br	$CH_2CH_2NEt_2$	57%
(iv)c	**77**	I	$CH_2CH_2NEt_2$	67%
(iv)d	**78**	OCH_3	$CH_2CH_2NEt_2$	75%
(iv)e	**79**	NO_2	$CH_2CH_2NEt_2$	63%
(iv)f	**80**	CF_3	$CH_2CH_2NEt_2$	56%

[a] Yields between 60 and 80%

Scheme 2.13. Synthesis of 7-X-4-aminoquinolines. *Reagents and Conditions:* (i)a. 25% NH_3 (aq), $ZnCl_2$, 150°C, 35h; (i)b. 33% CH_3NH_2 (methanol), 154°C, 20h; (i)c. $NH_2CH_2CH_2OH$, 120°C, 4.5h; (i)d. 90% $NH_2CH_2CH_2NH_2$ (aq), 120°C, 5h; (i)e. $NH_2CH_2CH_2NEt_2$, 150°C, 8h; (ii)a. 25% NH_3 (aq), $ZnCl_2$, 145°C, 18h → 160°C, 24h; (ii)b. $NH_2CH_2CH_2NEt_2$, 130°C, 18h → 150°C, 6h; (iii)c. $NH_2CH_2CH_2CH_3$, 95°C, 20h; (iii)f. $NH_2CH_2CH_2NMe_2$, 140°C, 3.5h; (iii)g. $NH_2CH_2CH_2NEt_2$, 150°, 5h; (iv)a. $NH_2CH_2CH_2NEt_2$, 160°C, 6h; (iv)b. $NH_2CH_2CH_2NEt_2$, 135°C, 6h; (iv)c. $NH_2CH_2CH_2NEt_2$, 120°C, 8h; (iv)d. $NH_2CH_2CH_2NEt_2$, 140°C, 5h; (iv)e. $NH_2CH_2CH_2NEt_2$, 85°C, 5h (iv)f. $NH_2CH_2CH_2NEt_2$, 145°C, 7h.

2.3.4. Characterisation of 2-Aminoquinolines

^{1}H nmr spectra of ***60***

The 2-aminoquinolines all showed characteristic ^{1}H nmr splitting patterns (Figure 2.13) and ^{13}C nmr chemical shifts which will be discussed in detail for analogue **60**.

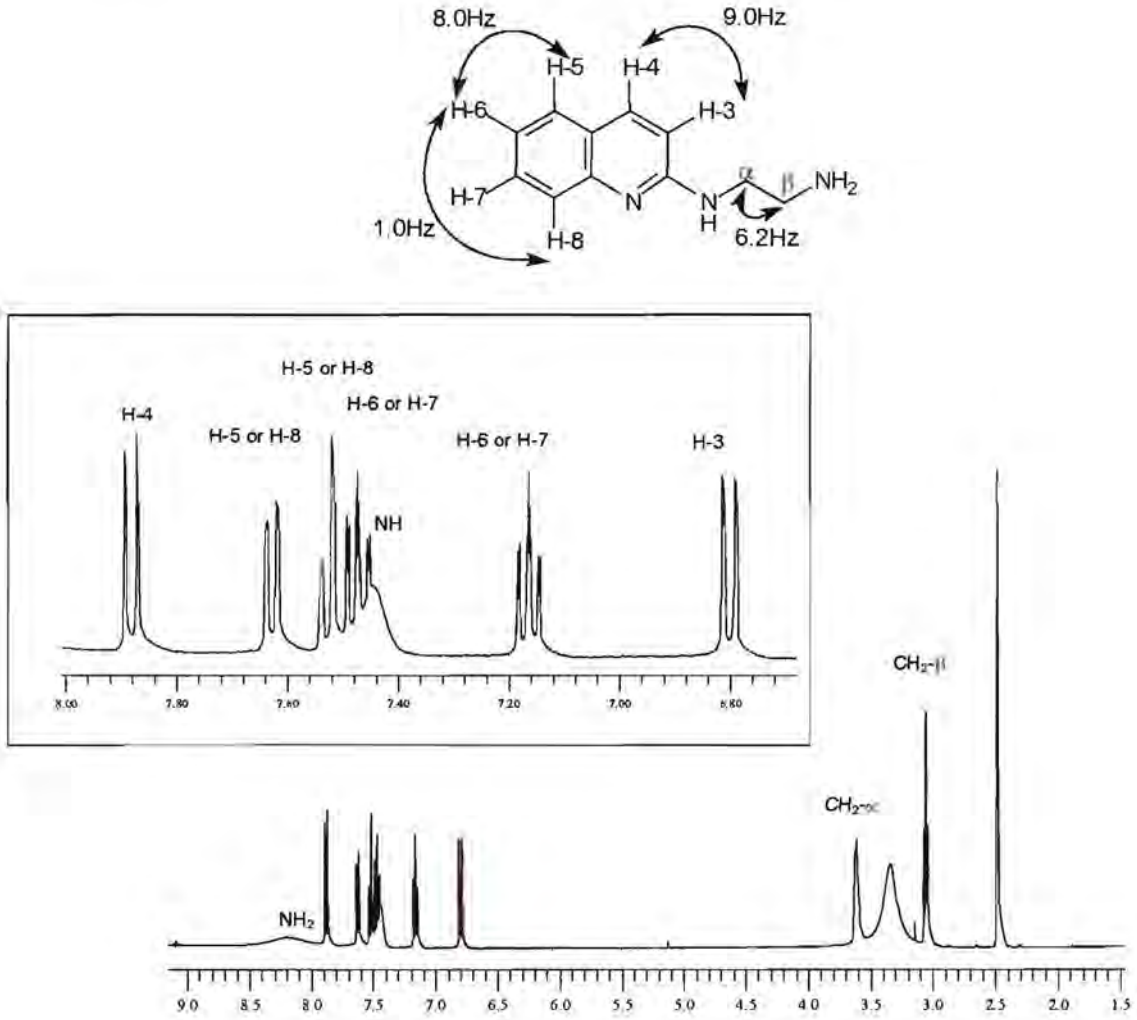

Figure 2.13. ^{1}H nmr spectrum of **60** in d_6 DMSO. Inset: expanded aromatic region between 6.7 and 8.0ppm.

The CH_2 peak at 3.61ppm was assigned to CH_2-α on the basis of a strong interaction with NH identified in the COSY spectrum. The remaining CH_2 peak at 3.06ppm was thus assigned to CH_2-β. The two doublets at 6.80ppm and 7.88ppm share a common coupling constant of 9.0Hz and were assigned to H-3 and H-4, the former being shielded by mesomeric release from the 2-amino substituent. The ortho and meta coupling constants for

the four quinoline benzene ring protons gave rise to two types of splitting patterns; a *dd* at 7.63 and 7.56 for H-5 and H-8, and a *td* at 7.48 and 7.16 for H-6 and H-7. These protons could not be individually assigned from the HMBC spectrum although it was evident from the COSY that the *dd* signal at 7.63ppm is ortho to the *td* signal at 7.16ppm.

*^{13}C nmr spectra of **60***

From the HSQC spectrum of **60**, the ^{13}C nmr signals could be assigned collectively (Table 2.3). C-2 could be assigned from the HMBC spectrum owing to an interaction with CH_2-α. Since all the 2-aminoquinoline analogues had similar ^{13}C nmr spectra, the chemical shifts for **58** and **59** were assigned from **60** (Table 2.3).

Table2.3. ^{13}C nmr peaks of **60** (—) assigned from HSQC and HMBC spectra, and **58** and **59** (—) assigned from **60**

C	58	59	60
C-2	156.9	157.6	157.2
C-3, C-4	111.6, 138.0	111.1, 137.2	113.7, 136.9
C-5, C-8	126.0, 127.5	126.1, 127.4	125.9, 127.9
C-6, C-7	122.7, 129.7	121.9, 129.5	122.0, 129.6
C-4a, C-8a	123.6, 147.7	123.3, 148.1	123.4, 147.8

Melting Points and Microanalysis of 2-Aminoquinolines

The melting points were compared to literature values where appropriate, and combustion analysis was obtained to ensure analytical purity of the compounds (Table 2.4).

Table 2.4. Characterisation 2-Aminoquinolines **58-60**

No.	Observed mp / °C	Literature mp / °C	Microanalysis					
			Calcuated / %			Found / %		
			C	H	N	C	H	N
33	129	128 – 129, Brown and Plasz 1970.	75.0	5.6	19.4	75.3	5.6	19.5
34	70 – 72	69 – 71, Watanabe *et al.* 1980.	75.9	6.4	17.7	76.1	6.5	17.4
35	174 - 178	Novel	59.1	6.3	18.8	59.0	6.3	18.8

2.3.5. Characterisation of 4-Aminoquinolines and 7-X-4-Aminoquinolines

Both the 4-aminoquinoline and 7-X-4-aminoquinoline series showed characteristic ^{1}H nmr splitting patterns and ^{13}C nmr chemical shifts which will be discussed for the representative analogues **64** and **74** respectively.

*^{1}H nmr spectra of **64** and **74***

The ^{1}H nmr spectra for analogues **64** and **74** (Figures 2.13 and 2.14 respectively) revealed the characteristic pair of AB doublets corresponding to H-2 and H-3 sharing a common coupling constant of 5.4Hz. In this case, H-3 is assigned the lower chemical shift due to a shielding effect by mesomeric release from the 4-amino substituent. The aromatic multiplicities in the quinoline benzene ring for **64** were the same as observed for the 2-series but with the signals further apart and hence better defined. In the case of **64**, H-6 was assigned from a HMBC interaction with CH_3 which enabled absolute assignments of the remaining quinoline benzene protons.

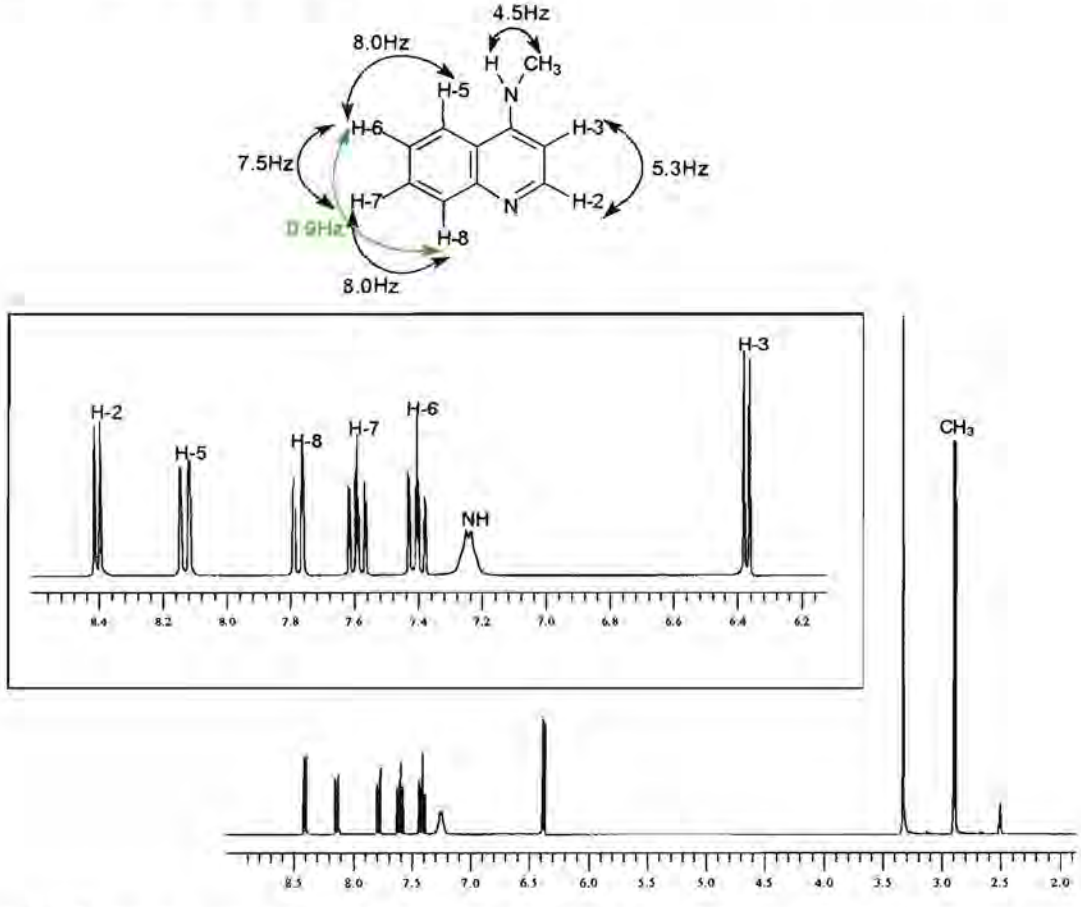

Figure 2.14. ^{1}H nmr spectrum and coupling constants for **64**. Inset: expanded aromatic region between 6.2 and 8.6ppm.

The ^{1}H nmr spectrum for analogue **74** (Figure 2.15) showed the characteristic 7-substitution in the quinoline benzene ring which allowed for unambiguous assigment of all the aromatic protons.

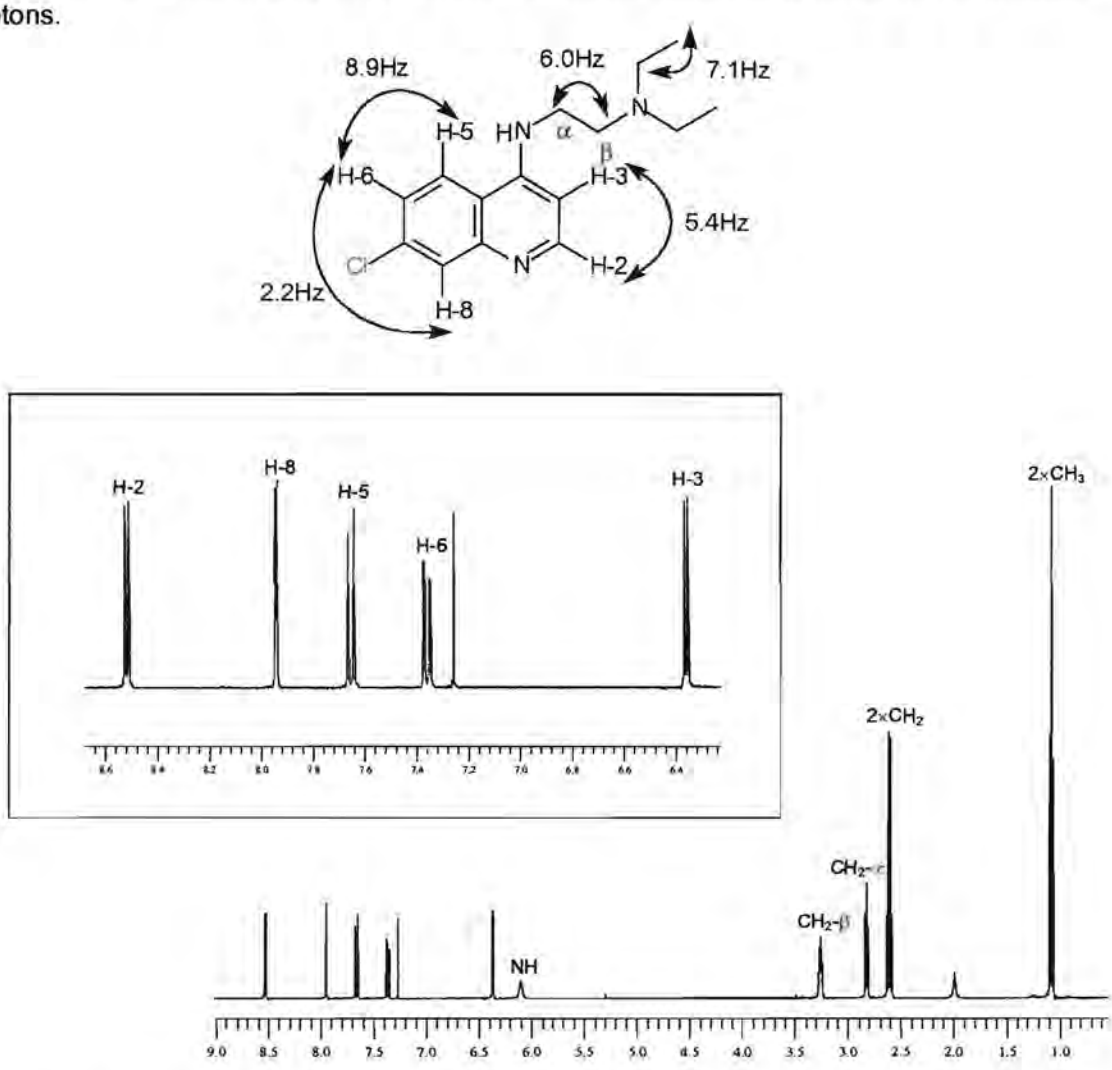

Figure 2.15. ^{1}H nmr spectrum for **74** in $CDCl_3$. Inset: expanded aromatic region between 6.3 and 8.6ppm.

^{13}C nmr assignments of the 4-aminoquinolines and 7-X-4aminoquinolines

In all cases, the HSQC spectrum of each compound in both series enabled assignment of the CH carbon signals, C-2, C-3, C-5, C-6 and C-8, in the ^{13}C spectrum (Table 2.7 and Table 2.8). The quarternary carbons, C-4, C-4a, C-7 and C-8a, for both the 4-aminoquinolines and the 7-X-4-aminoquinolines were similar and were solved from the long range HMBC interactions for compound **78** (Table 2.5). In this case, C-7 was unambiguously assigned from its strong interaction with the methyl protons of the methoxy group at position-7. C-4 revealed a strong interaction with CH_2-α, and the ring junction carbons (C-4a and C-8a) from their interactions with H-3 and H-5, and H-2 respectively.

Table 2.5. Long range couplings for **78** extracted from the HMBC spectrum

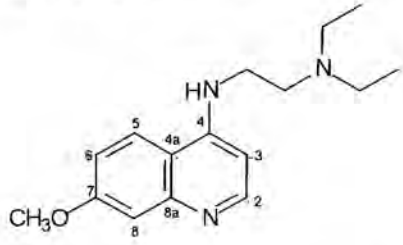

C	Coupling H
C-4	CH_2-α and H-5
C-4a	H-3, H-5, H-6 and H-8
C-7	OCH_3
C-8a	H-2

Further support for all the ring carbon assignments comes from the C-F coupling constants identified from the ^{13}C nmr spectra for all the 7-fluoroquinoline compounds (Table 2.6).

Table 2.6. ^{13}C nmr assignments and coupling constants of 7-fluoroquinoline ring carbons.

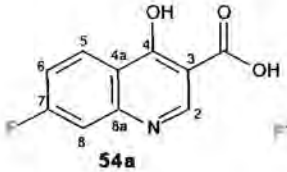

54a

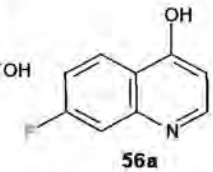

56a

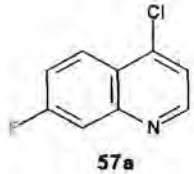

57a

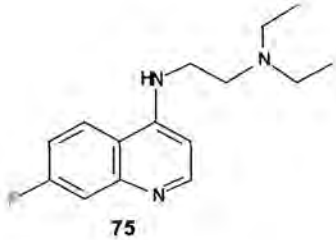

75

No	54a		56a		57a		75	
	δ/ ppm	J/Hz	δ/ ppm	J/Hz	δ/ ppm	J/Hz	δ/ ppm	J/Hz
C-2	146.8		140.6		151.8		152.2	
C-3	108.6		109.7		121.1		98.7	
C-4	178.5		177.0		141.3		150.0	
C-4a	122.2	2	123.6		122.8		115.9	
C-5	129.3	11	129.0	11	126.6	10	121.8	10
C-6	115.9	24	112.6	24	118.3	25	114.3	25
C-7	165.5	253	164.4	248	162.8	250	162.9	249
C-8	105.8	25	104.0	25	113.0	21	113.3	20
C-8a	141.8	13	142.1	13	149.5	13	149.9	12

The C-7 assignment was confirmed from the large coupling constant of 250Hz to F. The assignments for the C-6 and C-8 carbons was confirmed by their similar coupling constants of about 24Hz, being both equidistant from F. C-5 and C-8a both revealed a characteristic ^3J

value of 12 Hz. Finally, in the case of **54a** (Figure 2.15), C-4a shows a weak ^{4}J coupling constant of 2Hz to F, further supporting the HMBC assignment for **78** at C-4a.

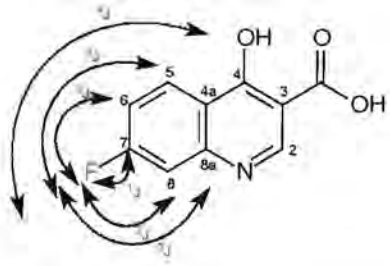

Jce	J / Hz
^{1}J	253
^{2}J	25
^{3}J	12
^{4}J	2

Figure 2.15. Observed coupling constants between -C and -F in the ^{13}C nmr spectrum for **54a**.

The quarternary carbon signals for all the 4-aminoquinolines and 7-X-4-aminoquinolines could therefore be assigned on the basis of the HMBC assignments for **78**, and the C-F coupling constants identified from the ^{13}C nmr of the 7-fluoroquinoline compounds. The ^{13}C nmr peaks for C-4 and C-8a were not individually assigned as both had similar chemical shifts of about 150ppm. The synthesis of compounds **82** and **83** is described later in this chapter.

Table 2.7 (top) ^{13}C nmr assignments of the 7-X-4-aminoquinolines differing only with respect to the group at the 7-position, quarternary carbons assigned from **74, 75** and **78** (—) and, Table 2.7 (bottom) ^{13}C nmr assignments of the 4-aminoquinolines . Quarternary carbons assigned from trends noted in the 7-X-4-aminoquinolines (—).

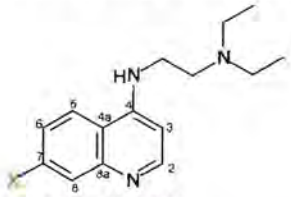

65, 67, 74-80, 82-83

C	H	CH_3	Cl	F	Br	I	OCH_3	NO_2	CF_3	OH	NH_2
	65	**67**	**74**	**75**	**76**	**77**	**78**	**79**	**80**	**82**	**83**
2xCH_3	12.1	12.1	12.0	12.1	12.1	12.1	12.1	12.1	12.1	12.5	12.0
CH_2-β	50.8	50.8	50.6	50.7	50.7	50.7	50.8	50.5	50.6	51.4	50.9
2xCH_2	46.6	46.5	46.5	46.5	46.5	46.5	46.6	46.5	46.6	47.4	46.5
CH_2-α	39.8	39.8	39.7	39.7	39.8	39.8	39.8	39.8	39.8	41.5	39.8
C-2	151.1	151.1	152.1	152.2	152.1	151.8	151.3	153.2	152.3	148.5	151.3
C-3	99.0	98.5	99.3	98.7	99.4	99.5	98.1	101.1	100.3	97.3	97.1
C-4a	119.6	116.9	117.4	115.9	117.8	118.2	113.5	122.5	120.1	112.3	112.3
C-5	119.1	119.3	121.1	121.8	121.2	121.1	120.9	121.5	121.0	124.0	120.9
C-6	124.5	126.6	125.2	114.3	127.8	133.0	116.9	117.7	120.1	117.3	116.0
C-7	128.9	139.0	134.7	162.9	123.0	94.8	160.3	147.9	127.6	159.9	147.2
C-8	129.8	128.9	128.7	113.3	132.1	138.7	108.1	125.9	127.6	108.5	110.4
C-4,	148.4	148.6	149.1	150.0	149.9	150.0	150.2	147.9	147.7	147.6	150.0
C-8a	149.9	149.9	149.8	149.9	149.4	149.5	150.1	149.6	149.7	152.3	150.0

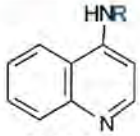

61-65, 81

C	61	62	63	64	65	81
C-2	151.6	151.2	151.1	150.7	151.1	151.1
C-3	103.6	98.3	98.6	98.8	99.0	98.5
C-4a	118.8	119.2	119.2	119.3	119.6	119.2
C-5	120.3	121.8	122.0	122.6	119.1	121.8
C-6	124.7	124.2	124.2	124.4	124.5	124.3
C-7	129.3	129.1	129.1	129.4	128.9	129.1
C-8	129.7	129.4	129.4	129.0	129.8	129.4
C-4	148.8	148.5	148.7	148.2	148.4	148.7
C-8a	149.8	151.2	150.5	150.3	149.9	150.2

Melting Points and Microanalysis of 4-Aminoquinolines and 7-X-4-Aminoquinolines

The melting points of all the crystalline compounds were compared to literature values where appropriate and combustion analysis was obtained to ensure analytical purity (Table 2.8).

Table 2.8. Characterisation of 4-Aminoquinolines and 7-X-4-Aminoquinolines

No.	Observed mp / °C	Literature mp / °C	Microanalysis					
			Calcuated / %			Found / %		
			C	H	N	C	H	N
61	151 - 153	151 – 152, Den Hertog *et al.* 1967; 149 – 150, Tondys *et al.* 1985.	75.0	5.6	19.4	74.8	5.7	19.6
62	233 dec.	227 – 227.5, Luthy *et al.* 1949; 231 – 232, Watanabe *et al.* 1980.	75.9	6.4	17.7	75.8	6.6	17.9
63	139	Novel	70.2	6.4	14.9	69.6	6.7	14.0
64	211 – 212	Novel	59.1	6.3	18.8	59.0	6.5	18.6
65	82	Novel	74.0	8.7	17.3	74.0	8.8	17.2
66	164 – 165	Novel	75.9	6.4	17.7	75.7	6.5	17.7
67	102 – 105	99 – 103.6, Patent US2940974 1960.	74.7	9.0	16.3	74.6	9.4	16.3
68	134	105 – 110, Price *et al.* 1946, 152 – 154.4, Roseman *et al.* 1970, 146 – 147, Lin and Loo 1978.		[a]			[a]	
69	245	245 – 246, Craig and Pearson 1968.	62.3	4.7	14.5	62.5	4.6	14.5
70	146 – 148	Novel						
71	217 – 218	214, Elderfield *et al.* 1946.	59.3	5.0	12.6	59.2	5.0	12.5
72	137 – 139	137 – 139, Pearson *et al.* 1946.	59.6	5.5	19.0	59.6	5.6	18.9
73	122 – 124	121 – 122.8, Surrey *et al* 1959.	62.5	6.5	16.8	61.7	6.6	16.4
74	106 – 108	92, De *et al.* 1997.	64.9	7.3	15.1	64.7	7.3	15.1
75	81 – 82	72 – 73, De *et al.* 1998.	68.9	7.7	16.1	69.1	7.8	16.2
76	120 – 121	111 – 112, De *et al.* 1998.	55.9	6.3	13.0	56.0	6.4	13.0
77	133 – 136	131 – 132, De *et al.* 1998.	48.8	5.5	11.4	48.8	5.7	11.4
78	98 – 99	94 - 95, De *et al.* 1998.	70.3	8.5	15.4	70.4	8.8	15.2
79	110 – 113	Novel	62.5	7.0	19.4	62.8	6.7	19.1
80	121 - 123	122 – 123, De *et al.* 1998.	61.7	6.5	13.5	61.9	6.4	13.4

[a]The melting point is strongly dependent on the degree of hydration of the compound. When hydrated the melting point is 105 - 110°C, but rises substantially after extensive drying (Price *et al.* 1946). Due to this phenomenon, the microanalysis was not recorded.

2.3.6. Alternative Routes to 4-Aminoquinoline

4-Aminoquinoline was also synthesised in this project by the Chichibabin reaction (Chichibabin and Seide 1914) in which treatment of a heterocyclic base, such as quinoline, with a metal amide in the presence of a hydride ion acceptor gives predominantly the 2-substituted amino-product. The amination procedure of Tondys *et al.* was followed in which thermodynamic control results in production of 4-aminoquinoline as the main product (Scheme 2.14) (Tondys *et al.* 1985). The immediate product of the reaction is **61a**, the metal salt of **61** (McGill and Rappa 1988). Protonation of this metal salt during aqueous work-up then generates 4-aminoquinoline **61**. Prior to aqueous work-up, the reaction mixture was warmed to 0°C, resulting in rapid evaporation of the ammonia which caused spluttering of the product, explaining why **61** was recovered, after chromatography, in a low 26% yield.

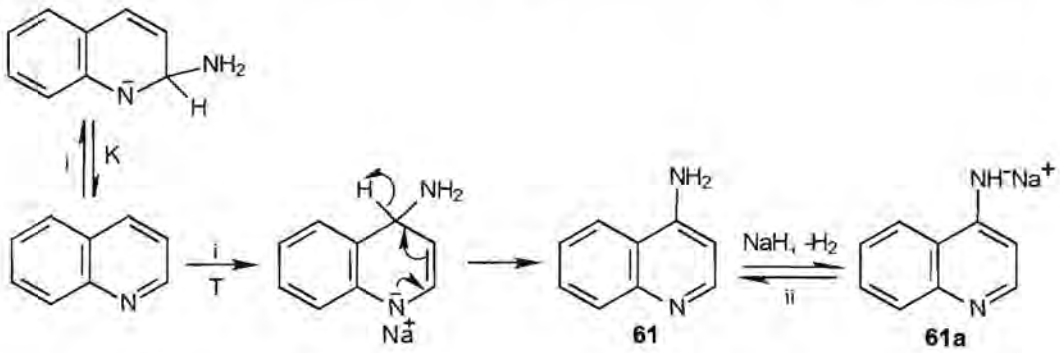

Scheme 2.14. Synthetic route to 4-aminoquinoline where T represents thermodynamic and K represents kinetic control. *Reagents and Conditions:* i. NH_3/KNH_2, ii. $KMNO_4$, aq work-up.

A third route to 4-aminoquinoline was achieved by reducing 4-nitroquinoline-1-oxide in a solution of H_2, 10% Pd-C, acetic acid, acetic anhydride and ethanol at room temperature for 7.5h (Ochiai 1953) to give **61** in a 65% yield (Scheme 2.15). Longer reaction times resulted in unwanted side products due to over reduction.

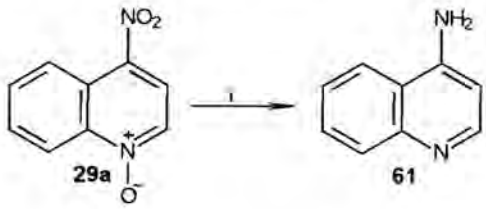

Scheme 2.15. Reduction of **29a** to 4-aminoquinoline. *Reagents and Conditions*: i. H_2, 10% Pd-C, CH_3COOH, acetic anhydride, CH_3CH_2OH, rt, 7.5h.

2.3.7. Synthesis of the Remaining Analogues

The remaining analogues **81**, **82** and **83** were synthesised according to Schemes 2.16., 2.17. and 2.18. respectively and are characterised in Table 2.9.

The terminal amino group of **64** was acetylated using acetic anhydride and triethylamine to give analogue **81** in a 78% yield (Scheme 2.16).

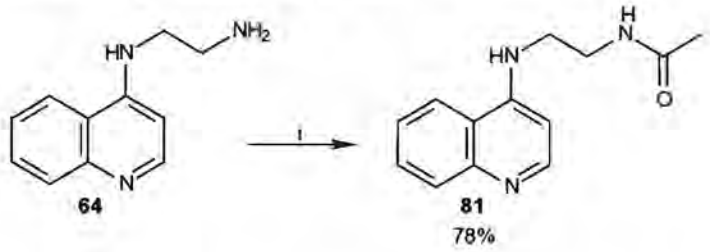

Scheme 2.16. Acetylation of **64**. *Reagents and Conditions:* i. Acetic anhydride, Et_3N, THF, 0°C.

Since difficulties were experienced in synthesising 7-hydroxy-4-chloroquinoline via the cyclisation route of Price and Roberts, **82** was synthesised by treatment of the methoxy-analogue **78** with boron tribromide at -13°C for 40h to form the hydroxy product (Scheme 2.17).

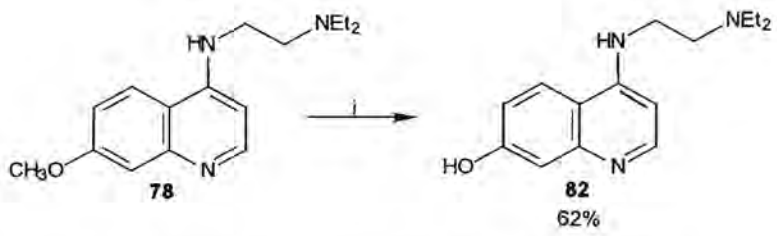

Scheme 2.17. Preparation of **82**. *Reagents and Conditions:* i. BBr_3, CH_2Cl_2, -78°C

Analogue **83** was synthesised by room temperature reduction of **79** in a hydrogen atmosphere over 10% Pd-C for 22h (Vippagunta *et al.* 1999). The product was then isolated and purified using neutral alumina chromatography to give **83** in a 78% yield (Scheme 2.18).

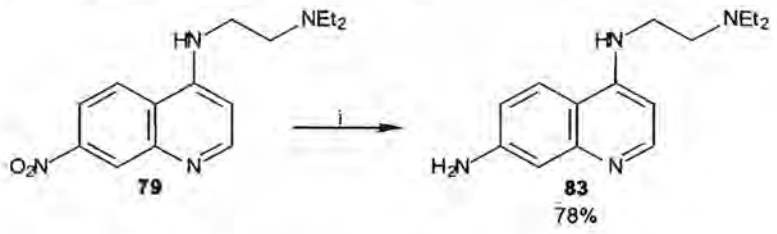

Scheme 2.18. Reduction of 79. *Reagents and Conditions:* i. H_2, 10% Pd-C, ethanol, rt.

Compound **81** was purified by crystallisation and characterised by a sharp melting point combustion analysis (Table 2.9). Compounds **82** and **83** were oils and were characterised by High Resolution Mass Spectroscopy (HRMS).

Table 2.9. Characterisation of Compounds **81-83**

No.	Observed mp / °C	Literature mp / °C	Microanalysis					
			Calculated / %			Found / %		
			C	H	N	C	H	N
81	200 - 202	Novel	68.1	6.6	18.3	67.9	6.6	18.3
			HRMS					
			Calculated / g.mol^{-1}			Found / g.mol^{-1}		
82	oil	Novel	259.16846			259.16770		
83	oil	Novel	258.18445			258.18425		

THE BEHAVIOUR OF Fe(III)PPIX IN AQUEOUS SOLUTION

3.1. BACKGROUND

As described in Chapter 1, there is considerable evidence that haem (Fe(III)PPIX), released from haemoglobin into an aqueous environment (pH 5.4) is the target of chloroquine and related antimalarial drugs. Chloroquine interacts with the aqua- or hydroxy- form of haem known as haematin (H_2O-Fe(III)PPIX or HO-Fe(III)PPIX) to form a π-π Fe(III)PPIX-chloroquine complex which then ultimately leads to a toxic effect on the parasite. In order to probe which structural features of chloroquine are important in complex formation, we needed to understand the behaviour of Fe(III)PPIX in aqueous solution.

3.1.1. The Behaviour of Fe(III)PPIX in Haemoglobin

Haemoglobin (**Hb**) acts as an oxygen-transport protein by reversibly binding oxygen to haem iron (Figure 3.1.). There are four haem groups per protein and they are situated in hydrophobic pockets within the globin structure. Haem in deoxy-**Hb** (**84**) (Figure 3.1.) consists of high-spin ferrous iron (HS Fe(II)) situated out of the plane of a tetrapyrrole protoporphyrin ring with a proximal histidine ligand occupying the fifth coordination site. Owing to the steric positioning of a nearby distal histidine residue, oxygen binds weakly to the sixth coordination site through a bent bond. This weak interaction causes only partial oxidation of HS Fe(II) to the smaller low-spin ferric iron (LS Fe(III)), which then moves into the plane of the porphyrin ring **85** (Rawn 1989, Buchler 1978).

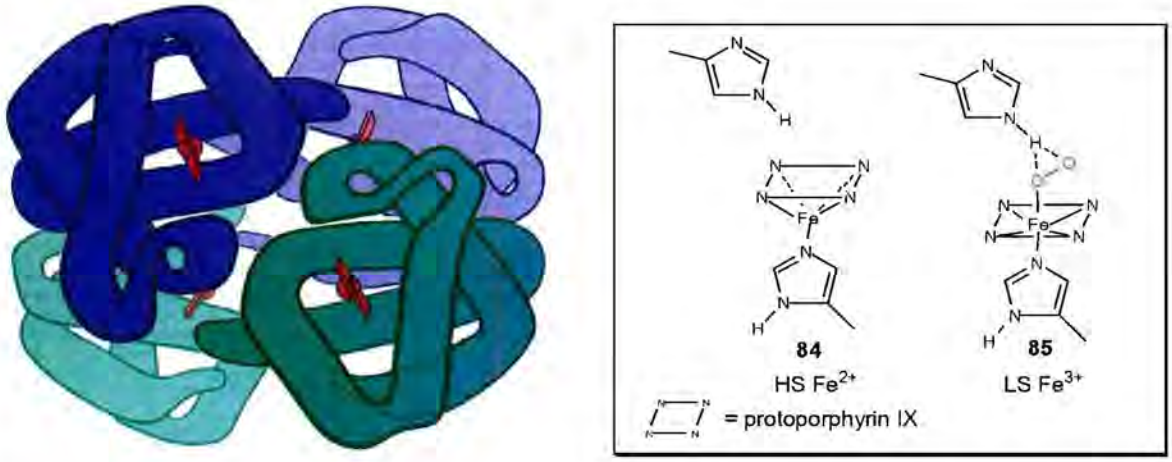

Figure 3.1. (left) structure of haemoglobin containing four haem units (Campbell 1991). (right) reversible binding of oxygen in a sterically induced bent bond to haem iron, showing the oxy- **85** and deoxy- **84** forms.

The large globin protein provides a sterically hindered, hydrophobic cage that protects the porphyrin ring and the haem iron from irreversible oxidation. When haem is released from haemoglobin into an aqueous environment, the ferrous iron rapidly binds oxygen in a strong linear bond (Figure 3.2.) (Hoard 1971) and is irreversibly oxidised to HS ferric iron with the production of superoxide (Gutteridge 1989). In water, the vacant fifth coordination site is occupied by OH^- or H_2O ligands forming hydroxo- or aquaferriprotoporphyrin IX (**86** or **87** respectively), also known as haematin.

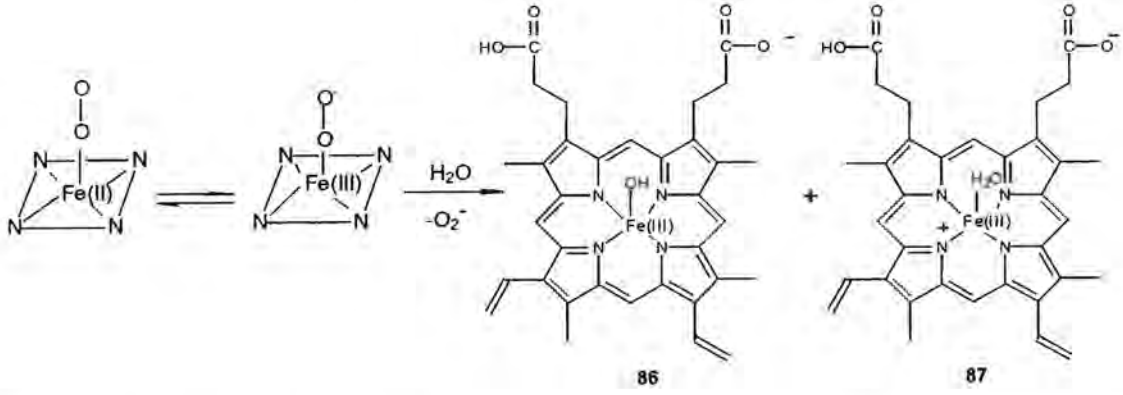

Figure 3.2. Irreversible oxidation of haem iron in water to form hydroxoferriprotoporphyrin IX (**86**) and aquaferriprotoporphyrin IX (**87**).

Crystal structures and Mössbauer spectra of chloroferriprotoporphyrin IX (haemin) and related HS ferric porphyrins have confirmed that the geometry of these complexes are 5-coordinate, square pyramidal (C_{4V}) with the ferric ion displaced out-of-the-plane of the porphyrin ring (Figure 3.3.) (Koenig 1965, Hoard *et al.* 1965, Hoffman *et al* 1972, Hoard 1971, Fleischer and Srivastava 1969, Moss *at al.* 1969).

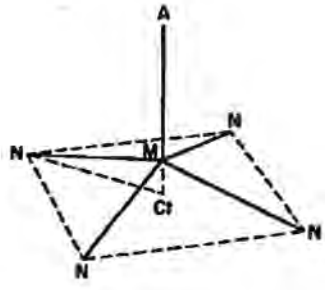

Figure 3.3. The square-pyrimidal (C_{4v}) geometry that characterises the coordination in HS iron porphyrins (Hoard 1971).

3.1.2. Characterisation of the μ-oxo dimer

Aqueous haematin solutions are difficult to work with as haematin is known to adhere to surfaces (Brown 1968) and precipitate below pH 6 (Dzekunov *et al.* 2000). Furthermore, aged solutions undergo slow spectroscopic changes indicative of either higher aggregation (Davies 1940, Shack and Clarke 1947) or molecular modification (Brown *et al.* 1968, Shack and Clarke 1947). This behaviour of haematin is attributed to the strongly polar carboxyl groups and the labile vinyl groups on the protoporphyrin IX ring. To overcome these limitations, synthetic derivatives of haematin are often used. Removal of the vinyl groups gives ferrideuteroporphyrin IX (**88**) or conversion of the carboxyl groups to the less polar dimethyl ester derivatives gives ferriprotoporphyrin IX dimethyl ester (**89**), ferrimesoporphyrin IX dimethyl ester (**90**) and ferrideuteroporohyrin IX dimethyl ester (**91**) (Figure 3.4.). Ferritetraphenylporphyrin IX (**92**), which can be prepared from pyrrole in one step, (Fuhrhop 1974) is also commonly used as a model system for haematin.

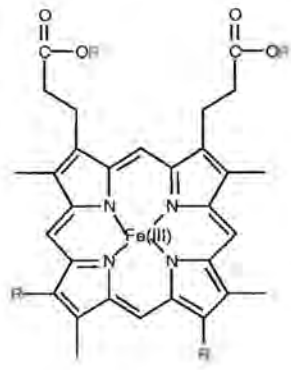

87-91

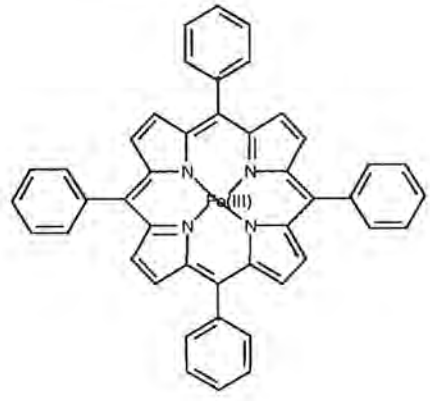

92

No	R	R	Abbreviation
87	$CH{=}CH_2$	H	Fe(III)PPIX
88	H	H	Fe(III)DP
89	$CH{=}CH_2$	CH_3	Fe(III)PPIX-DME
90	CH_2CH_3	CH_3	Fe(III)MESO-DME
91	H	CH_3	Fe(III)DP-DME

Figure 3.4. Synthetic modification of haematin **87** to the more stable porphyrin derivatives **88-91**.

It has long been known that fresh aqueous solutions of haematin consist of monomers and dimers (Davies 1940, Shack and Clarke 1947). In water-dimethyl sulphoxide (DMSO) mixtures, haematin is monomerised at acid or neutral pH, presumably by formation of a Fe(III)PPIX-DMSO complex, and aggregated at alkaline pH (Brown and Lantzke 1969).

Since precipitation of haematin from aqueous alkaline solution using solid sodium hydroxide gives a μ-oxo dimer (**12**) (Brown *et al.* 1969) (Figure 3.5.), it has long been thought that this is the dimeric species present in aqueous alkaline solution (Brown *et al.* 1970).

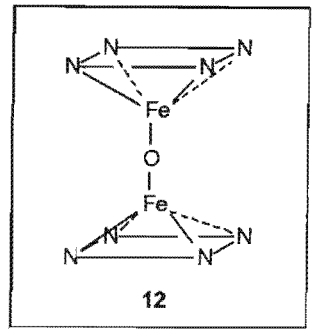

12

Figure 3.5. μ-oxo dimer of haematin **12**.

This μ-oxo dimer, can also be synthesised by (i) addition of water or alumina to the monomer in chloroform (Sadasivan *et al.* 1969, Fleischer and Srivastava 1969); (ii) treatment of the monomer with pyridine followed by alumina chromatography (O'Keeffe and Barlow 1975) or (iii) autoxidation of the dipyridine Fe(II)DP-DME monomer in benzene (Alben *et al.* 1968).

The crystal structure of the μ-oxo dimer of **92** is consistent with the square-pyramidal five coordinate geometry that is typical for high-spin ferric porphyrins. In this case, both the iron centres are displaced 0.5Å from the plane of the porphyrin ring towards the axial oxo-ligand with the two iron centres antiferromagnetically coupled through a near linear 174.5° oxo-linkage (Hoffman *et al.* 1972, Fleischer and Srivastava 1969). Magnetic susceptibilities and Mössbauer spectra of the haematin μ-oxo dimer (Lucas and Silver 1983, Lucas *et al.* 1982) and various μ-oxo Fe(III)DP-DME dimers (O'Keeffe and Barlow 1975, Torrens *et al.* 1972, Cohen 1969) are consistent with two high spin (S = 5/2) Fe(III) ions antiferromagnetically coupled to each other. A distinctive infrared absorption band between 800cm^{-1} and 900cm^{-1}, assigned to a ν_3 asymmetric stretching vibration of the Fe-O-Fe bond (Brown *et al.* 1969), has often been used for quick identification of the μ-oxo-dimer. The Uv-vis spectrum of the μ-oxo Fe(III)DP-DME dimer in chloroform shows a peak at 567nm and a shoulder at 590nm (Sadasivan *et al.* 1969) (Figure 3.6. left). The data in Figure 3.6 (right) show that this peak and shoulder are largely substituent independent. Comparison of Figure 3.6 (left) with spectrum (D) in Figure 3.6 (right) shows that it is also solvent independent.

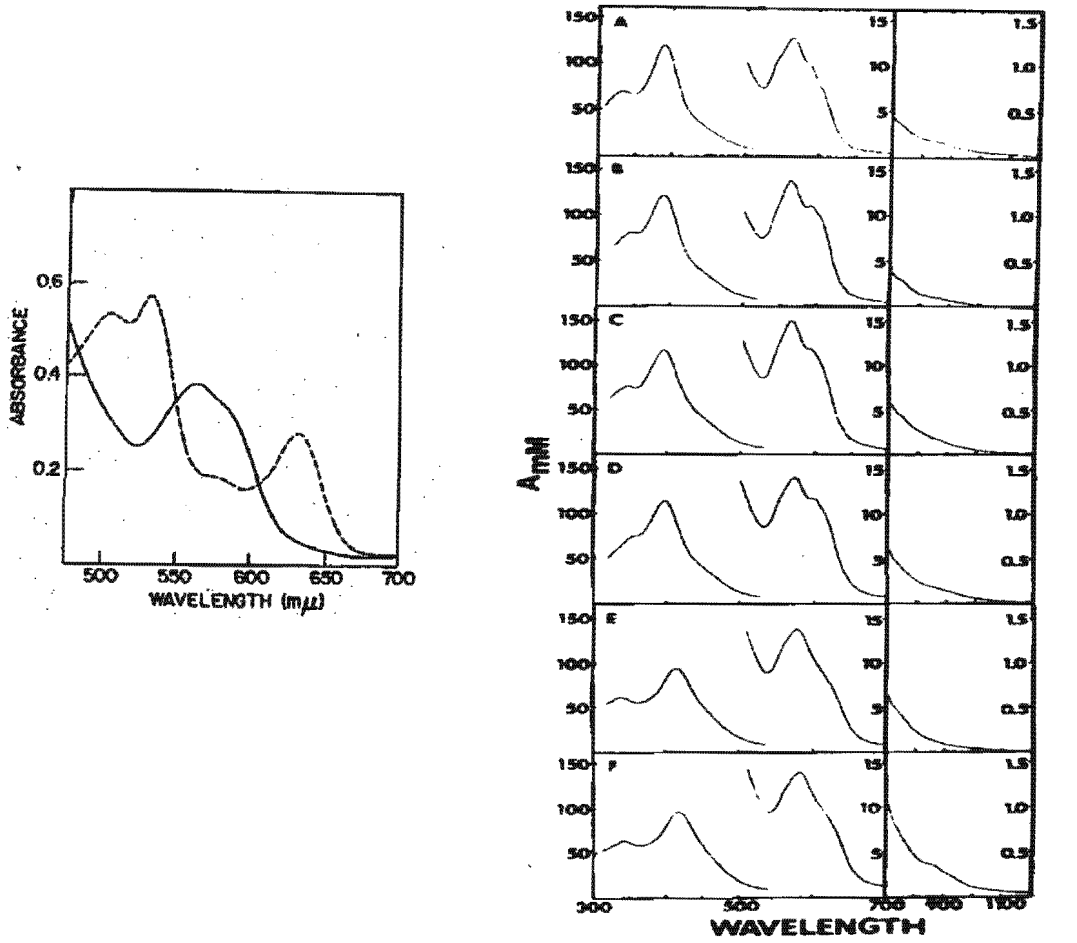

Figure 3.6. (left). Uv-vis spectrum of (—) Fe(III)DP μ-oxo dimer and (...) Cl-Fe(III)DP monomer in chloroform (Sadasivan *et al.* 1969). (right). Uv-vis spectra of μ-oxo Fe(III)DP-DME derivatives in benzene where the hydrogens at positions 2- and 4- are substituted for: A, hydrogen; B, ethyl; C, 2-(ethoxycarbonyl)cyclopropyl; D, vinyl: E, propionyl; F, acetyl (O'Keeffe and Barlow 1975).

3.1.3. Evidence for the Existence of Higher Aggregates in Aqueous Solution

Inada and Shibata, and Srinivas and Rao, both observed two rate constants for the formation of dimers and higher aggregates in aged, non-buffered haematin solutions (Inada and Shibata 1962, Srinivas and Rao 1990). Kuzalova *et al.* further supported these findings in phosphate-buffered (pH 7.4) solutions by measuring the binding kinetics of monomeric haematin to albumen. In fresh solutions the rate of binding was dependent on the dissociation of dimers to monomers (Kuzalova *et al.* 1997). This dissociation process was biphasic in aged solutions and thus suggested to provide support for the formation of higher aggregates over time.

Haematin has however been shown to undergo slow autoxidation in phosphate buffered solutions (pH 11) (Figure 3.7.) (Brown *et al.* 1968, Shack and Clarke 1947). This has been attributed to the slow oxidation of the vinyl groups of haematin as Fe(III)DP (Brown *et al.* 1968) and ferrihematoporphyrin (Marques 1992), in which the vinyl groups are replaced by hydrogens or hydroxyethyl groups respectively, show no such behaviour. Since the authors studying the higher aggregation of haematin did not take precautions against autoxidation, their spectral changes assigned to aggregation may have been due to the appearance of an oxidised product. Definitive evidence of higher aggregation in aqueous solution is thus lacking. By contrast, it is well established that metal free protoporphyrin undergoes extensive aggregation in aqueous solution (Brown and Shillcock 1976).

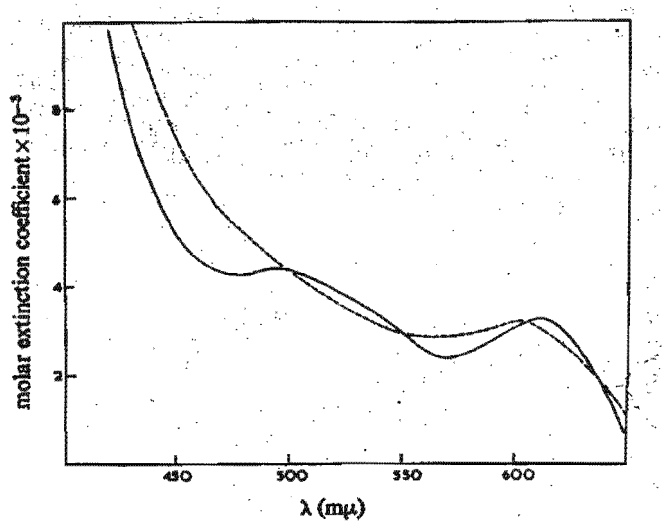

Figure 3.7. Spectroscopic changes associated with ageing haematin in phosphate buffer, pH 11; (——) fresh haematin; (.....) aged haematin (Brown *et al.* 1968).

3.1.4. Existence of the μ-oxo-dimer in Aqueous Solution

Although there is unequivocal proof for the existence of the μ-oxo-dimer, it is less clear that this is the dimeric species present in fresh aqueous solution. Silver and Lucas have provided evidence indicating that Mössbauer spectra of frozen haematin solutions are composed of monomers at low pH and μ-oxo-dimers at high pH (Silver and Lucas 1983). The authors also recorded uv-vis spectra of 50μM haematin in fresh aqueous solution and assigned the limiting spectrum at low pH to the monomer and the spectrum at high pH to the μ-oxo-dimer suggesting that formation of the two species are pH-dependent (Figure 3.8.). These authors found no evidence for aggregates higher than dimers in their frozen aqueous systems.

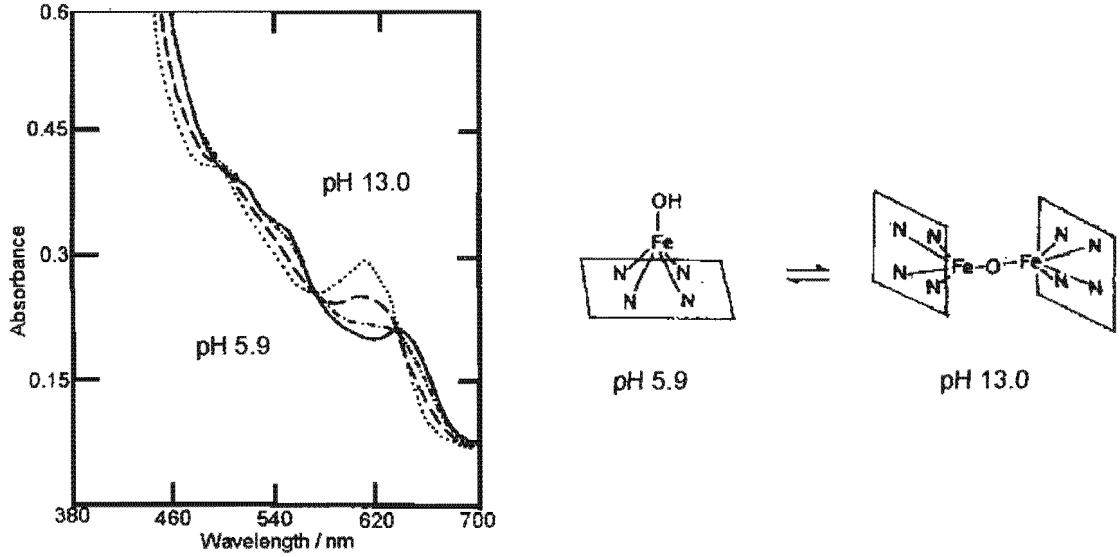

Figure 3.8. (left) Uv-vis spectra of 50μM haematin in aqueous solution at pHs (___) 5.9, (_._._) 7.6, (_ _ _) 8.2 and (.....) 13.0. Note the peak maximum at 610nm which does not correspond to the distinctive peak and shoulder in the μ-oxo-dimer at 590 and 567nm. (Right) pH dependent monomer and μ-oxo-dimer haematin species proposed to exist in aqueous solution (Silver and Lucas 1983).

3.1.4.1. Spectrophotometric Study by Brown *et al.*

The most extensive study of haematin dimerisation was carried out by Brown *et al.* in 1970. It has frequently been cited as evidence of μ-oxo dimer formation in aqueous solution (Brown *et al.* 1970). In this study, the authors measured a pH dependent dimerisation constant in aqueous solution. Brown *et al.* collected spectra of the Soret region of Fe(III)DP (384nm) and Fe(III)PPIX (394nm) in the concentration range 2×10^{-7} – 2×10^{-4}M at pH 6.98, and noted that Beer's Law is not obeyed (Figure 3.9). There is a drop in the extinction

coefficient and a flattening of the Soret band with increasing ferrihaem concentration. This was interpreted as evidence for the existence of monomers at low concentration and dimers at high concentration. In the case of Fe(III)PPIX, the Soret band is flattened even at the lowest concentrations indicative of more extensive dimerisation than in Fe(III)DP.

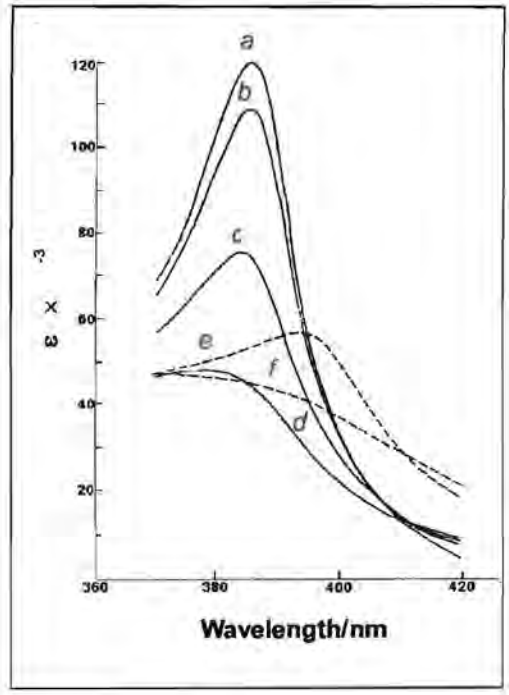

Figure 3.9. Illustration of the drop in extinction coefficient of ferrihaems (pH 6.98) with increasing concentration for (——) Fe(III)DP and (.....) Fe(III)PPIX. Concentrations: *a*, 2×10^{-7}M; *b*, 7×10^{-7}M; *c*, 7×10^{-6}M; *d*, 2×10^{-4}M; *e*, 2×10^{-7}M; *f*, 2×10^{-4}M (Brown *et al.* 1970).

This process was also shown to be apparently pH dependent with increased sharpening of the Soret bands at low pH. The extinction coefficient of the Soret band of Fe(III)PPIX and Fe(III)DP were recorded between concentrations of 2×10^{-7} and 2×10^{-4}M in the pH range 6.5 to 11.0 and found to follow a sigmoidal relationship when plotted on a log scale (Figure 3.10A and B respectively).

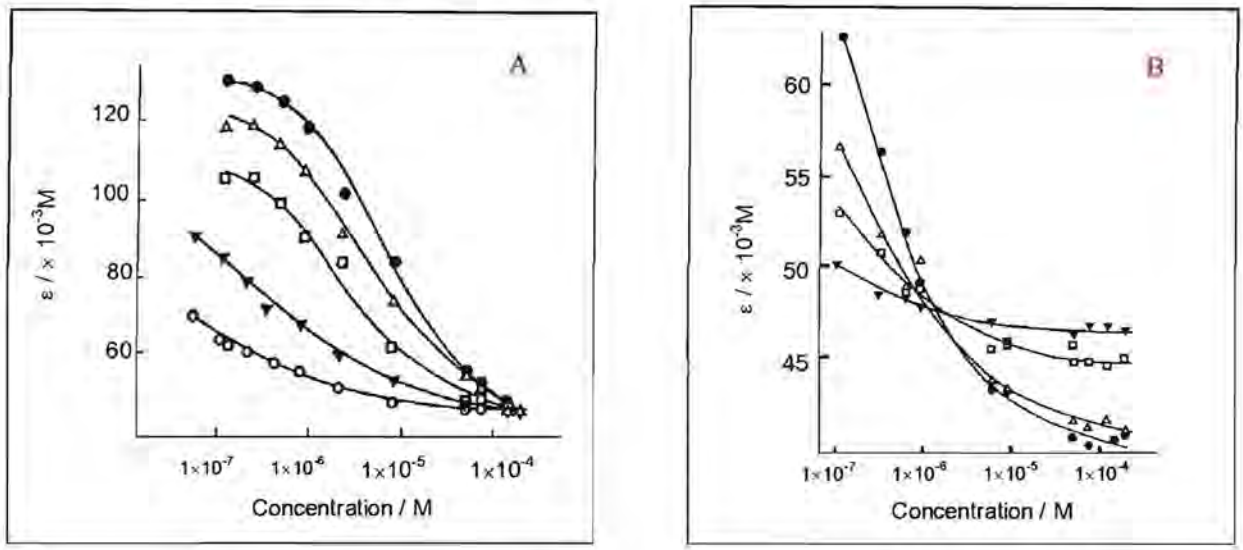

Figure 3.10. Concentration and pH dependence of ε_{384} for (A) Fe(III)DP. •, pH 6.64; Δ, pH 6.98; □, pH 7.38; ▼, pH 8.04; °, 11.0 and (B) Fe(III)PPIX. •, pH 6.98; Δ, pH 7.38; □, pH 8.04; ▼, pH 11.0 (Brown *et al.* 1970).

The absence of intermediate steps in the curves was taken as evidence that aggregation beyond μ-oxo dimers does not occur and the following pH dependent relationship was envisaged:

$$2M \underset{}{\overset{K}{\rightleftharpoons}} D + nH^{+} \qquad (1)$$

where M represents the Fe(III)PPIX and Fe(III)DP monomers and D their respective dimers. K is the dimerisation constant and n an integer corresponding to the number of protons released upon dimer formation.

The equilibrium expression for (**1**) can be written as follows:

$$K = \frac{[D][H^{+}]^{n}}{[M]^{2}} \qquad (2)$$

At fixed pH, K_{obs} is a conditional equilibrium constant given by (**3**)

$$K_{obs} = \frac{K}{[H]^n} = \frac{[D]}{[M]^2} \qquad (3)$$

Taking the log of (**3**) gives a linear relationship between log K_{obs} and pH with a slope equal to the number of protons released in the dimerisation process and the y-intercept equal to log K.

$$\boxed{log\, K_{obs} = log\, K + npH} \qquad (4)$$

3.1.4.2.Determination of log K_{obs}

The extinction coefficients of the monomers (ε_M) and dimers (ε_D) at the various pH's were read off or extrapolated from the curves in Figure 3.9 and used to obtain the respective K_{obs} values by linearisation methods. This was done relatively easily for Fe(III)DP where the limiting values of ε_M and ε_D could be read off the curves directly.

For Fe(III)PPIX, the extent of dimerisation is high even at the lowest pH and concentration and hence it was possible to obtain limiting extinction coefficients for the dimer but not for the monomer. Here the authors assumed that the values of ε_M for Fe(III)PPIX are similar to those of Fe(III)DP and used these values to calculate K_{obs} for Fe(III)PPIX.

3.1.4.3. Determination of K and n

Plots of log K_{obs} against pH for both Fe(III)DP and Fe(III)PPIX were fitted to straight lines with unit slopes and K was found to be 1.9×10^{-2} for Fe(III)DP and 4.5 for Fe(III)PPIX by extrapolation to the origin (Figure 3.11.).

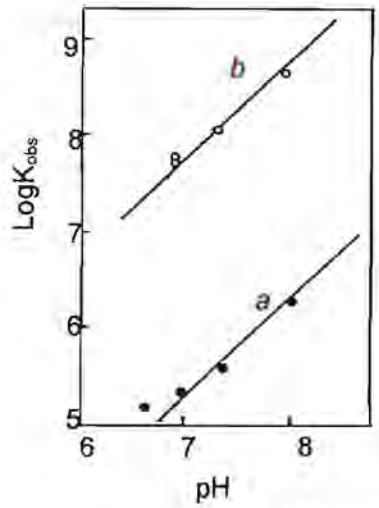

Figure 3.11. Dependence of K_{obs} on pH for *a*. • Fe(III)DP and *b*. ° Fe(III)PPIX (Brown *et al.* 1970)

In addition to Fe(III)PPIX and Fe(III)DP, a range of other iron porphyrins have been found undergo a pH dependent dimerisation with the release of a single proton (Brown *et al.* 1976). Fleischer *et al.* found that the water soluble tetrasulfonated tetraphenylporphyrin IX (Fe(III)TPPS), releases two protons upon dimer formation (Fleischer *et al.* 1971).

The haematin dimerisation constant obtained by Brown *et al.* has been accepted and used in malaria related research to describe interactions between chloroquine and the drug target (Vippagunta *et al.* 1999, Dorn *et al.* 1998).

3.1.4.4. Reasons for Repeating the Study of Brown *et al.*

It was decided to repeat the study by Brown *et al.* for the following reasons:

1. The authors did not have access to computerised non-linear least squares fitting procedures in the 1970's and therefore manipulated their data by linearisation methods which can introduce distortions into the analysis through unequal weighting of data points (Motulski 1995). Another advantage of non-linear regression is that parameters do not need to be fixed on the basis of extrapolated values, but all parameters can be refined simultaneously, removing further sources of error from the analysis.

2. Since the authors were unable to obtain values of ε_M for Fe(III)PPIX, they made assumptions that ε_M for Fe(III)PPIX are the same as those for Fe(III)DP. This may not be

true, considering the very different behaviour and solubilities of the two porphyrins in aqueous solution. Today we have access to more sensitive uv-vis spectrophotometers and better data fitting techniques which may enable us to obtain these limiting values for the Fe(III)PPIX monomer.

3. The authors studied haematin in phosphate buffer and used sodium chloride to adjust the ionic strength. This may have introduced additional species into their systems as both phosphate (Parapini *et al.* 2000) and chloride (Koenig 1965) can act as axial ligands to haematin. This can now be circumvented by using non-coordinating buffers (*e.g.* MES, HEPES and CHES) and by the judicious choice of salts (*e.g.* sodium perchlorate).

4. Owing to the low solubility of Fe(III)PPIX below pH 6 and the inability to obtain an estimate of ε_M for Fe(III)DP above pH 8, the authors obtained only three log K_{obs} values for Fe(III)PPIX between pH 7 and 8. Their final determination of K is therefore dependent on a straight line fit through only three data points extrapolated from pH 7 to the origin at pH 0.

5. Finally, since today haematin and the haematin μ-oxo dimer are known to be five-coordinate (Koenig 1965, Hoard 1971, Fleisher and Srivastava 1969, Hoffman *et al.* 1972), it is difficult to interpret the finding of Brown *et al.* that dimerisation involves a single deprotonation (Equation **5**).

$$2M \underset{}{\overset{K}{\rightleftharpoons}} D + H^+ \qquad (1)$$

In aqueous solution, haematin is likely to exist as two pH-dependent forms with either H_2O or HO^- as the axial ligands whereas the μ-oxo dimer likely exists as one species only, irrespective of pH. In theory, these three species should give rise to two pH-dependent and one pH-independent equilibria in aqueous solution (Figure 3.12.) with Equation **5** predominating at low pH, Equation **6** around the pK_a of the axial ligand and Equation **7** at high pH. The slope of log K_{obs} against pH is predicted to correspond to two deprotonations at low pH, one around the pK_a and none at high pH. On the contrary, Brown *et al.* observed a slope of one over their entire pH range even though they covered a large enough range to observe non-linearity. By contrast to Fe(III)PPIX, Fe(III)TPPS dimerises with release of two protons, indicating that this iron porphyrin does indeed form a μ-oxo dimer (Fleischer *et al.* 1971). This further demonstrates that extrapolation of the behaviour of one iron porphyrin to another must be done with considerable care.

A

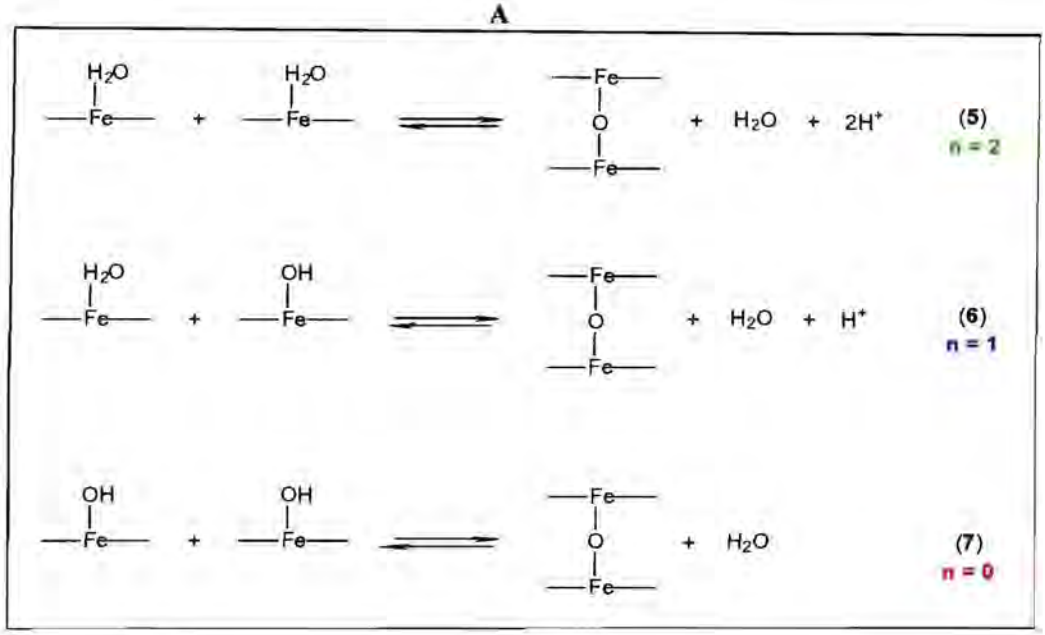

—Fe— = ferriprotoporphyrin IX

$$log\ K_{obs} = log\ K + npH \qquad (4)$$

B

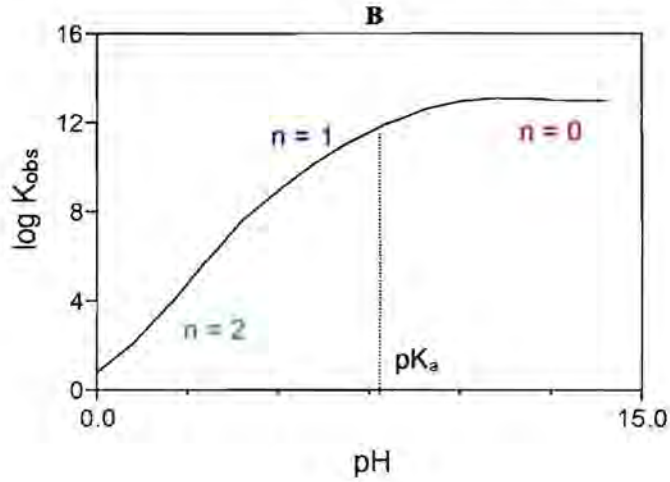

Figure 3.12. (A). Predicted equilibria between monomeric and μ-oxo dimeric ferrihaem in aqueous solution (Equations **5**, **6** and **7**). (B) The expected relationship between $logK_{obs}$ and pH (Equation **4**) should be a straight line with a limiting slope of 2 at low pH (n = 2), 1 around the pK_a of the axial ligand (n = 1) and 0 at high pH (n = 0). This predicted plot of $logK_{obs}$ vs pH is different from that observed by Brown *et al.* who found a slope of 1 over their entire pH range (Brown *et al.* 1970).

3.2. RESULTS AND DISCUSSION

3.2.1. Determination of α, β and log K_{obs} by Non-Linear Least Squares Fitting

3.2.1.1. Spectra of Haematin in Aqueous solution

Spectra were collected for haematin in 50mM HEPES buffer in the same pH range as Brown *et al.*, namely between pH 6.9 to 8.0. The ionic strength was corrected to the physiological ionic strength of 154mM using sodium perchlorate (Figure 3.13.).

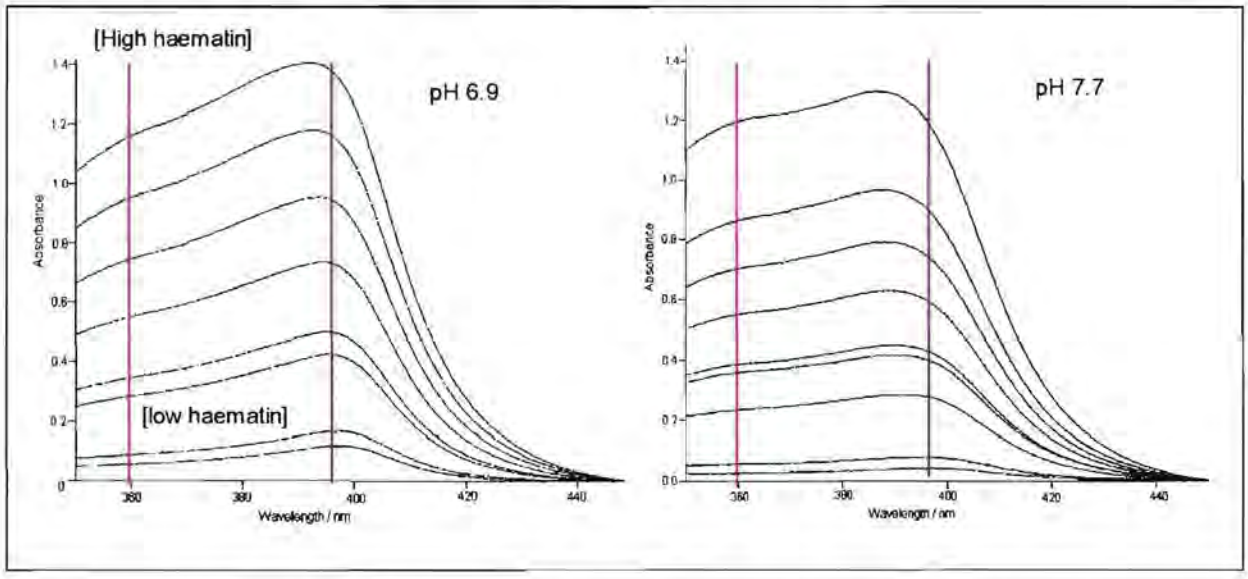

Figure 3.13. Spectra of haematin in 50mM HEPES buffer, μ = 154mM at pH 6.9 (left) and 7.7 (right) from 2.0×10^{-7} to 4.2×10^{-6}M haematin showing the position of the (—) N (0,0) band (361nm) and the (—) Soret B (1,0) band (395nm).

As observed by Brown *et al.*, a drop in intensity of the Soret band (—) relative to the N-band (—), and broadening of the Soret band occurs with increasing haematin concentration and pH. This flattening of the Soret is further accompanied by a simultaneous relative increase in intensity of the N band. Furthermore the apparent position of the Soret band appears to shift from 398nm at low concentration to 387nm at higher concentrations. Spectra were collected under an argon atmosphere to prevent haematin from undergoing slow autoxidation (Brown and Shillcock 1976). We were prevented from obtaining data below the limiting haematin concentration of 2×10^{-7}M used by Brown *et al.* due to excessive data scatter in this region. A plot of absorbance at 389nm against haematin concentration shows deviations from Beers law (Figure 3.14.).

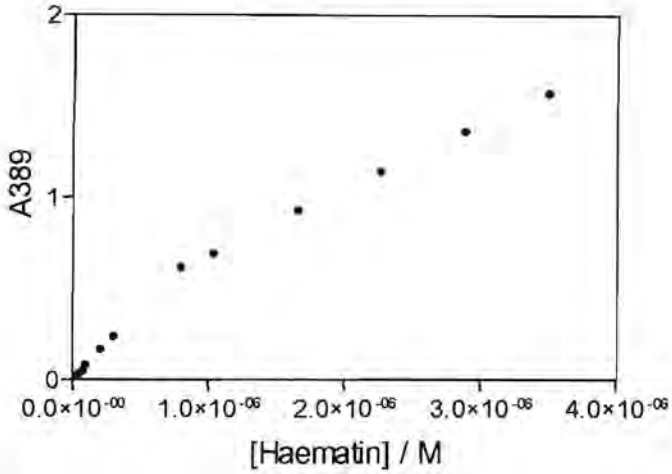

Figure 3.14. A Beers law plot of A_{389} vs haematin concentration in aqueous buffer at pH 6.92

In principle, such deviations can be used to model dimerisation and aggregation behaviour in porphyrins (White 1978, Munro and Marques 1996). In the case of haematin, however, this approach could not be used as the limiting extinction coefficient for the monomer was too poorly defined due to significant aggregation at even the lowest concentration. An alternative approach, where the extinction coefficient was plotted as a function of concentration also gave unsatisfactory results because of excessive data scatter at low concentrations. For this reason absorbance ratios as opposed to absolute absorbances were plotted at the apparent positions of the Soret (B (1,0)) (395nm) and the N (0,0) (361nm) bands (Mavuso pHD thesis 2001) in which the latter absorbance approximates to an isosbestic point (Figure 3.1.5.)

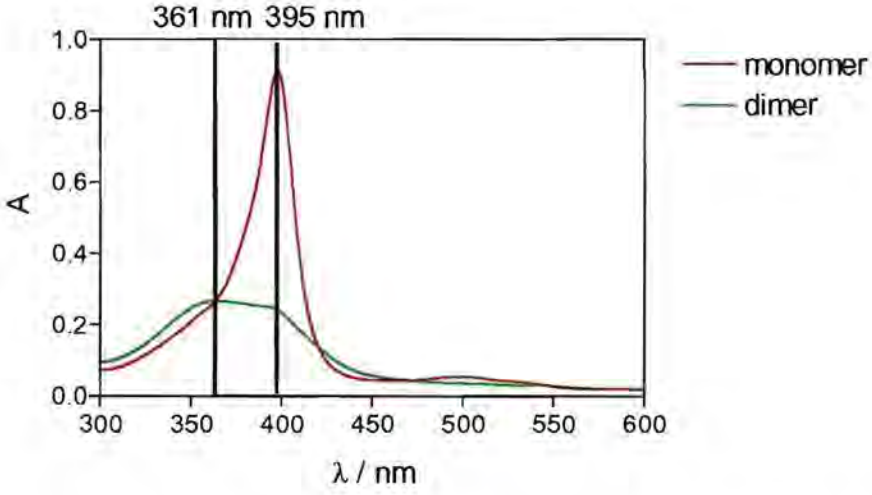

Figure 3.15. Position of the wavelengths used in to obtain the absorbance ratios (A_{395}/A_{361}) for determination of the haematin dimerisation equation (Figure supplied courtesy of Dr T. J. Egan).

3.2.1.2. Derivation of the Dimerisation Equation

The following Beer's law relationship applies:

$$\frac{A_1}{A_2} = \frac{A_1^a + A_1^b}{A_2^a + A_2^b} = \frac{\varepsilon_1^a c_a + \varepsilon_1^b c_b}{\varepsilon_2^a c_a + \varepsilon_2^b c_b} \qquad (5)$$

Where A_1^a, A_1^b, A_2^a and A_2^b are the absorbances of the monomer (^{a}) and dimer (^{b}) at 395nm ($_1$) and 361nm ($_2$). Similarily, ε_1^a, ε_1^b, ε_2^a and ε_2^b refer to the corresponding extinction coefficients of the monomer (^{a}) and dimer (^{b}) at 395nm ($_1$) and 361nm ($_2$). c_a and c_b represent the concentrations of the monomer (^{a}) and dimer (^{b}) respectively.

Dividing the top and bottom by $(c_a + c_b)$ leads to

$$= \frac{\varepsilon_1^a \left\{\frac{c_a}{c_a + c_b}\right\} + \varepsilon_1^b \left\{\frac{c_b}{c_a + c_b}\right\}}{\varepsilon_2^a \left\{\frac{c_a}{c_a + c_b}\right\} + \varepsilon_2^b \left\{\frac{c_b}{c_a + c_b}\right\}}$$

$$= \frac{\varepsilon_1^a \left\{\frac{c_a}{c_a + c_b}\right\}}{\varepsilon_2^a \left\{\frac{c_a}{c_a + c_b}\right\} + \varepsilon_2^b \left\{\frac{c_b}{c_a + c_b}\right\}} + \frac{\varepsilon_1^b \left\{\frac{c_b}{c_a + c_b}\right\}}{\varepsilon_2^a \left\{\frac{c_a}{c_a + c_b}\right\} + \varepsilon_2^b \left\{\frac{c_b}{c_a + c_b}\right\}}$$

$$\boxed{\frac{A_1}{A_2} = \frac{\varepsilon_1^a}{\varepsilon_2^a + \varepsilon_2^b \left\{\frac{c_b}{c_a}\right\}} + \frac{\varepsilon_1^b}{\varepsilon_2^b + \varepsilon_2^a \left\{\frac{c_a}{c_b}\right\}}} \qquad (6)$$

In the special case where the absorbance at 361nm (^{b}) is an isosbestic point $\varepsilon_2^a \approx \varepsilon_2^b$. In this instance, ε_2^a and ε_2^b can be interchanged in the demononator of Equation **6** to give Equation **7**.

$$\frac{A_1}{A_2} = \frac{\varepsilon_1^a}{\varepsilon_2^a + \varepsilon_2^a \left\{\frac{c_b}{c_a}\right\}} + \frac{\varepsilon_1^b}{\varepsilon_2^b + \varepsilon_2^b \left\{\frac{c_a}{c_b}\right\}} \qquad (7)$$

Multiplying out the terms gives:

$$\frac{A_1}{A_2} = \frac{\varepsilon_1^a c_a}{\varepsilon_2^a c_a + \varepsilon_2^a c_b} + \frac{\varepsilon_1^b c_b}{\varepsilon_2^b c_a + \varepsilon_2^b c_b}$$

Regrouping:

$$\frac{A_1}{A_2} = \frac{c_a}{c_a + c_b}\left\{\frac{\varepsilon_1^a}{\varepsilon_2^a}\right\} + \frac{c_b}{c_a + c_b}\left\{\frac{\varepsilon_1^b}{\varepsilon_2^b}\right\}$$

Since $\frac{\varepsilon_1^a}{\varepsilon_2^a} = \frac{\varepsilon_1^a c_a}{\varepsilon_2^a c_a} = \frac{A_1^a}{A_2^a}$ and $\frac{\varepsilon_1^b}{\varepsilon_2^b} = \frac{\varepsilon_1^b c_b}{\varepsilon_2^b c_b} = \frac{A_1^b}{A_2^b}$

And $\frac{c_a}{c_a + c_b}$ = the fraction of haematin in the form of the monomer (f_a) and $\frac{c_b}{c_a + c_b}$ = the fraction of haematin in the form of the dimer (f_d), Equation **8** can be written which is only true in the case where the absorbance at 361nm is an isosbestic point.

$$\frac{A_1}{A_2} = f_a\left\{\frac{A_1^a}{A_2^a}\right\} + f_b\left\{\frac{A_1^b}{A_2^b}\right\} \qquad \textbf{(8)}$$

Equation **8** was therefore used to fit the absorbance ratios collected at 395nm and 361nm to the dimerisation equation (See Section 7.2.2.2.5. for derivation of the model).

3.2.1.3. Analysis of Data

Absorbance ratios (A_1/A_2) were collected for haematin in the same pH range as Brown *et al.*, namely between pH 6.9 to 8.0, and fitted to the dimerisation equation using non-linear least squares fitting procedures (See Section 7.2.2.2.5. for derivation of the model). In agreement with Brown *et al.*, the data collected gave excellent fits to the dimerisation equation with no evidence of higher aggregation (Figure 3.16.).

As observed by Brown *et al.*, the limiting absorbance ratio of the monomer is never reached although this value appears to increase with decreasing pH. At high haematin concentrations, the curves flatten off significantly to the limiting absorbance ratio of the dimer which appears to increase slightly with increasing pH. Three parameters describing this behaviour were extracted from the dimerisation equation namely: α, the absorbance ratio of the pure monomer; β, the absorbance ratio of the pure dimer and log K_{obs}, the log of the pH-conditional dimerisation constant (Table 3.5.).

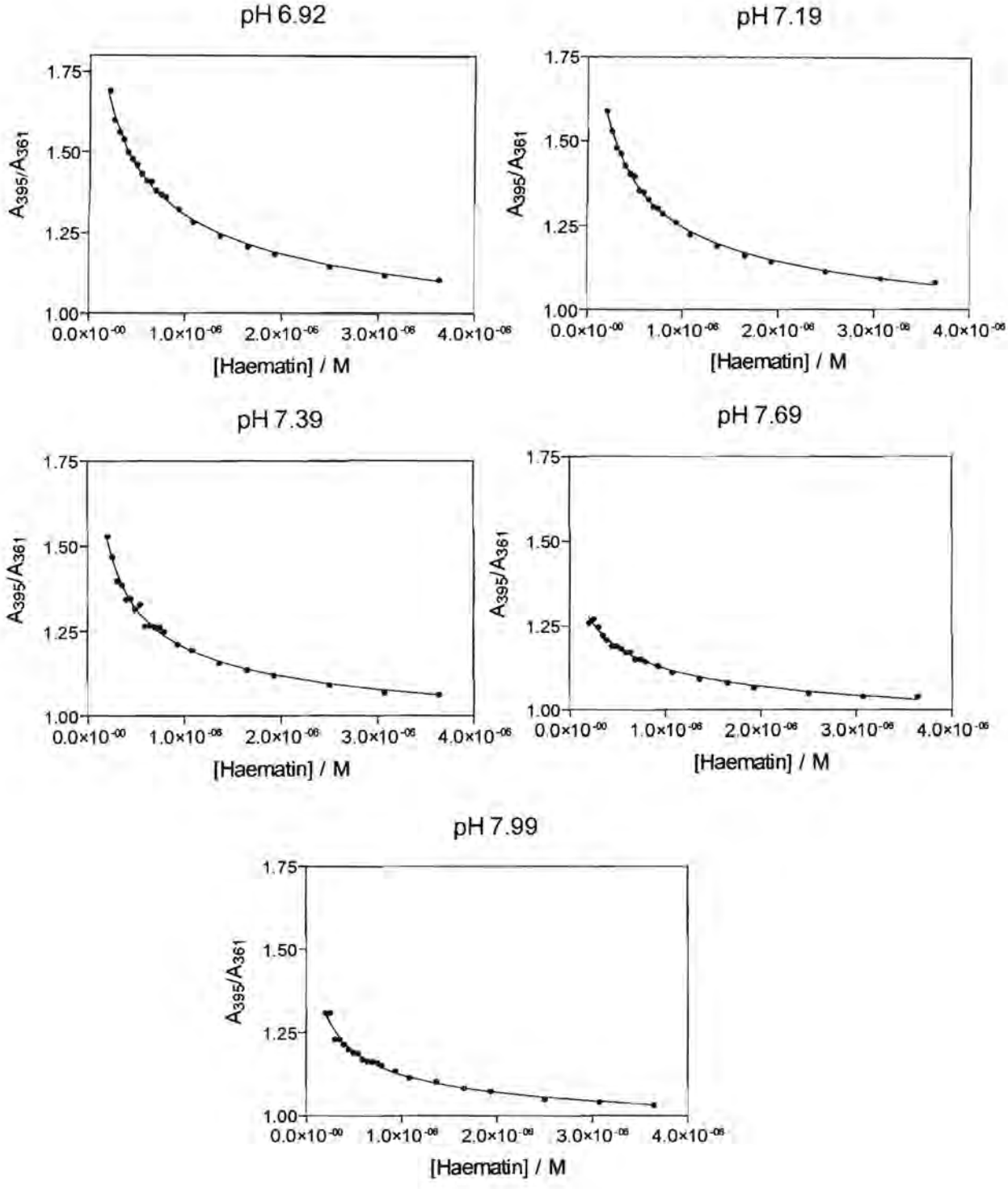

Figure 3.16. Graphs of experimental data (▪) fitted to the dimerisation equation (—) using non-linear least squares fitting for pH 6.92, 7.19, 7.39, 7.69 and 7.99.

Table 3.5. Mean ± SD for α, β and log K_{obs} calculated by non-linear least squares fitting to the dimerisation equation.

pH	α	β	log K_{obs}
6.92	2.7 ± 1	0.82 ± 0.06	6.6 ± 0.5
7.19	2.6 ± 0.3	0.87 ± 0.03	7.0 ± 0.4
7.39	2.5 ± 0.3	0.89 ± 0.01	7.1 ± 0.2
7.69	1.9 ± 0.5	0.91 ± 0.01	6.8 ± 0.5
7.99	2.0 ± 0.1	0.91 ± 0.02	6.97 ± 0.04
Mean	2.34 ± 0.36		6.89 ± 0.20

Since there is relatively little monomer present even at the lowest concentrations, scatter in the α values is large. Furthermore, a strong cross-correlation exists between log K_{obs} and α which further adds to the uncertainty in these α values. Contrary to the findings of Brown *et al.*, no significant correlation was found to exist between log K_{obs} and pH even though a large enough pH range was covered, implying that K is pH-independent and dimerisation does not involve deprotonation (Figure 3.17.).

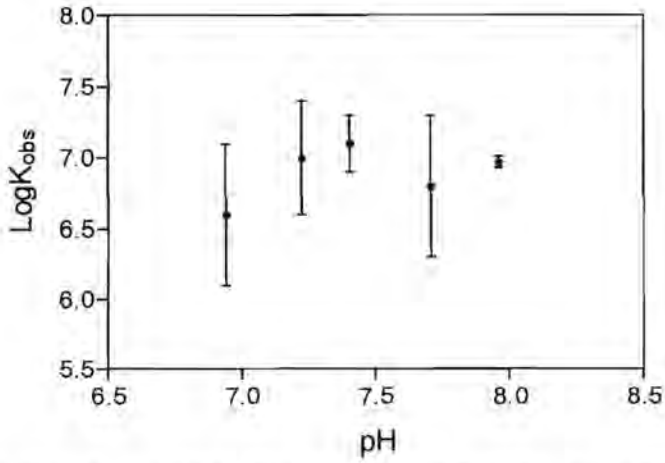

Figure 3.17. Plot of log K_{obs} vs pH for fitted data obtained from the dimerisation equation allowing all three parameters α, β and log K_{obs} to refine freely.

Considering the strong cross-correlation between α and log K_{obs}, the possibility that this lack of dependence could be artifactual was then explored. If it is assumed that the decreasing value of α with pH is an artifact of its correlation with log K_{obs}, and α is fixed at the mean α value of 2.34, log K_{obs} and β can be recalculated from the dimerisation equation to obtain a new set of well defined values (Table 3.6.).

Table 3.6. Mean ±SD for β and log K_{obs} calculated by fixing α = 2.34 in the dimerisation equation.

pH	β	log K_{obs}
6.92	0.8 ± 0.1	6.4 ± 0.3
7.19	0.87 ± 0.03	6.9 ± 0.2
7.39	0.88 ± 0.01	6.9 ± 0.1
7.69	0.93 ± 0.02	7.4 ± 0.2
7.99	0.92 ± 0.02	7.3 ± 0.1

A plot of log K_{obs} vs pH now gives a straight line with slope of 0.9 ± 0.2 which is similar to the slope of 1 obtained by Brown *et al.* (Figure 3.18.). If this slope is then fixed at 1, a dimerisation constant of K = 0.35 is obtained. This constant is more than an order of magnitude lower than the value of K = 4.5 reported by Brown *et al.*

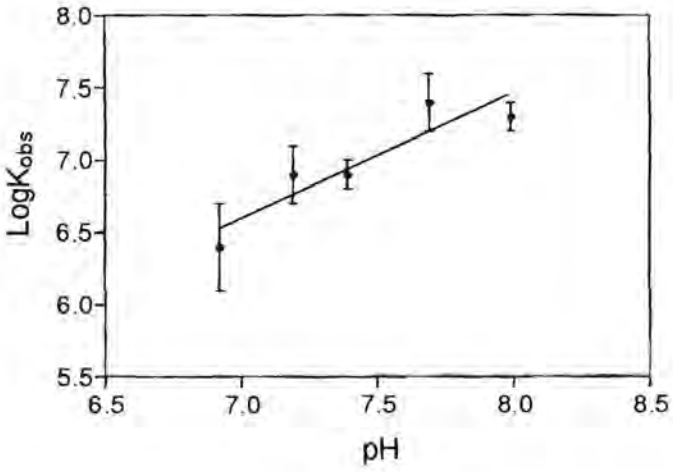

Figure 3.18. Plot of log K_{obs} vs pH for LogK_{obs} calculated by fixing α = 2.34 in the dimerisation equation.

3.2.2. Independent Determination of α

Since the values of log K_{obs} are only well defined when α is fixed, use of the mean from fitted data is arbitrary and difficult to justify. A method was sought to measure α for the pure haematin monomer, independently. This is problematic as the limit of the monomer cannot be reached in aqueous solution and non-aqueous solvents may displace the axial H_2O or OH^- ligands of haematin. Dimethyl sulfoxide (DMSO) monomerises haematin presumably by coordinating Fe(III) (Brown and Lantzke 1969) which gives an α value of 3.22 (Figure 3.19.).

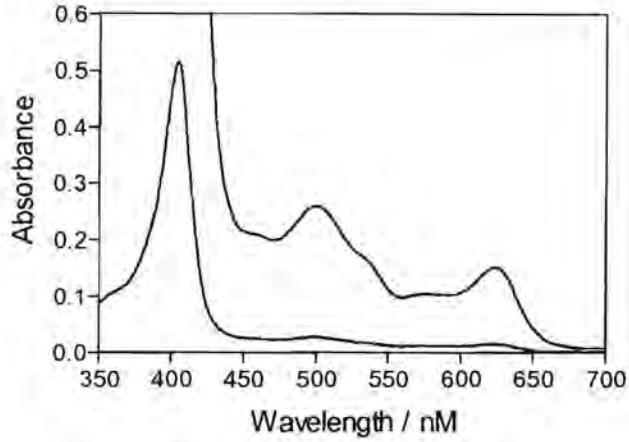

Figure 3.19. Uv-vis spectrum of haematin in DMSO, α = 3.22.

The detergent sodium dodecyl sulphate (SDS) has been shown spectrophotometrically to monomerise haematin by formation of a 1:1 haematin-micelle complex (Simplicio 1972, Simplicio and Schwenzer 1973, Figure 3.20.). It was therefore decidied to dissolve haematin in 2% SDS as a method to obtain monomeric haematin in an aqueous milieu. The nmr spectrum of 2% SDS in D_2O shows smallest paramagnetic shifts in the peak positions of the methylene protons adjacent to the sulfonate group ($\Delta\delta$ = 0.033ppm) upon addition of 0.24mM haematin, with larger shifts in the terminal methyl ($\Delta\delta$ = 0.038ppm) and methylene protons ($\Delta\delta$ = 0.047ppm). This indicates that monomerisation is induced by haematin embedded within the micelle and not by axial coordination of a sulfonate group to Fe(III).

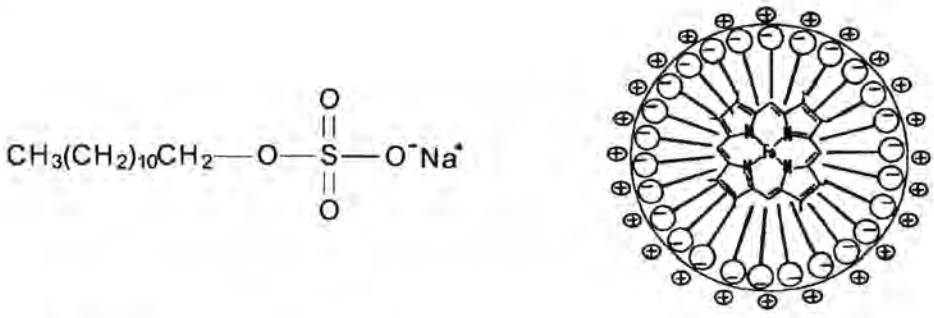

Figure 3.20. (left). structure of SDS. (right). proposed monomerisation of haematin in SDS by formation of a 1:1 haematin-micelle complex (Simplicio 1972).

Spectra of haematin in SDS and two other detergents, polyoxoethylene (10) isooctylpentyl ether (TRITON X-100) and polyoxoethylenesorbitan monolaurate (TWEEN-20) were recorded in HEPES buffer at pH 7.2 and 8.0. The soret region was not very informative as in all cases it remained flattened except in the case of SDS where it became sharpened (spectra not shown). Since the longer wavelength region gave more informative information

on the nature of the haematin species in aqueous solution, only this part of the spectrum was studied (Figure 3.21.).

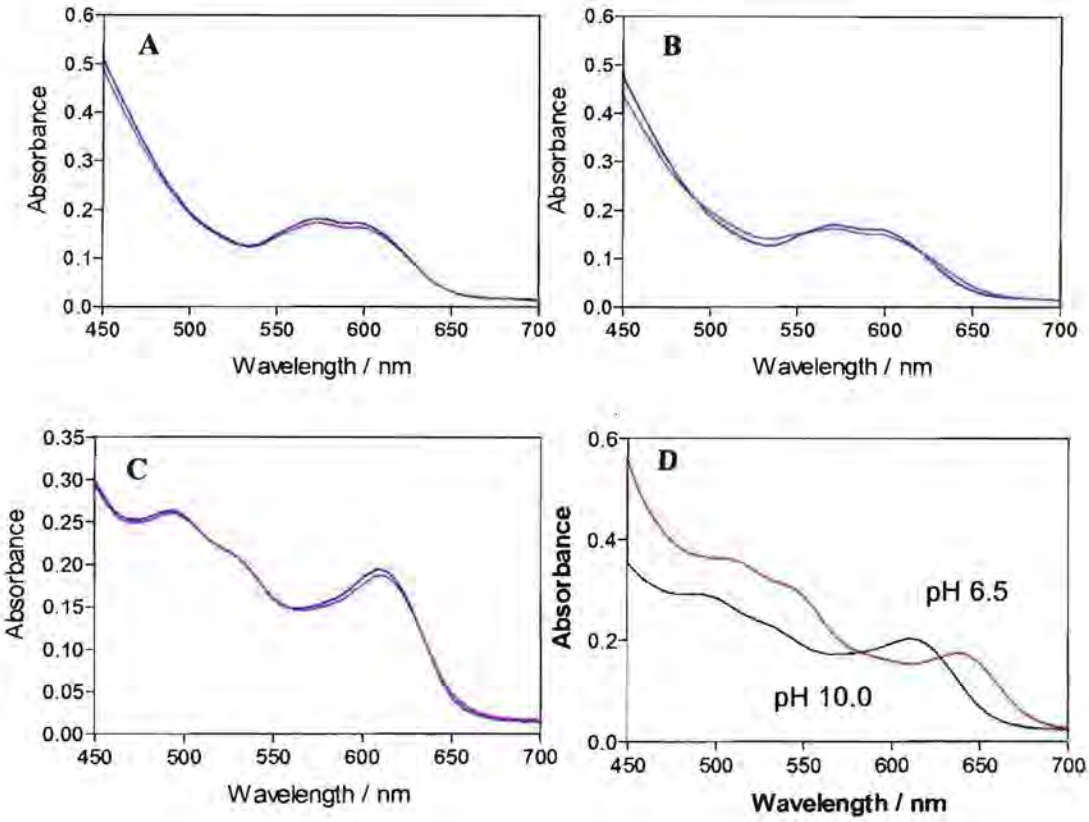

Figure 3.21. Visible spectra of haematin in (A) 3% TRITON X-100, (B) 2% TWEEN-20 and (C) 2% SDS at pH 7.2 and pH 8.0. For comparison (D) visible spectrum of haematin in HEPES buffer (pH 6.5) and CHES buffer (pH 10) (D).

Spectra of haematin in 3% TRITON X-100 and 2% TWEEN-20 (Figure 3.21A. and 3.21B.) are characteristic of the μ-oxo dimer at both pH 7.2 and 8.0, indicating that these two detergents, in fact, induce μ-oxo dimer formation and not monomerisation. Spectra of haematin in 2% SDS at pH 7.2 and 8.0 (Figure 3.21C.) appear to represent the proposed haematin-micelle complex as they are different from both the μ-oxo dimer and haematin in purely aqueous solution. In this case, α = 1.74 at both pHs, implying that the presence of this haematin monomer is pH-independent. In order to ensure that 2% SDS, pH 8.0 is the limiting spectrum of the monomer, α was recorded in varying percentages of SDS from 0.25% to 3.0% in the pH range from 7.2 to 10.1. In all cases a ratio close to 1.74 was obtained (Table 3.7.).

Table 3.7. α ratios for haematin in 0.25 – 3% SDS in the pH range 7.2 to 10.1.

% SDS	pH	α
2	7.2	1.74
2	8.0	1.73
2	10.1	1.76
0.25	8.0	1.75
0.5	8.0	1.71
1.0	8.0	1.75
2.5	8.0	1.76
3.0	8.0	1.75
Mean		1.74 ± 0.02

This value of α = 1.74 is lower than some of the experimental values for mixtures of the monomer and dimer in aqueous solution and hence cannot be a pH-independent value for monomeric haematin in aqueous solution at pH 5. It was therefore decided to investigate another non-coordinating solvent, methanol.

The spectrum of haematin in dry methanol is again different from the μ-oxo dimer and haematin in aqueous solution (Figure 3.22A) and the value of α is again 1.74. In this system, α is very sensitive to the presence of water, with only a few percent causing a large increase in the value of α at low pH. This effect is further dependent on pH, with the largest increases in the value of α at low pH (Figure 3.22B) and little change at pH 10.

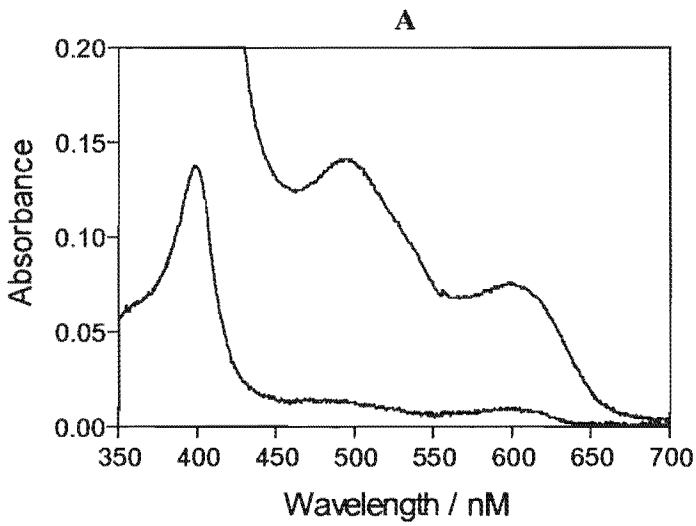

Figure 3.22. (A) Uv-vis spectrum of haematin in dry methanol, α = 1.74.

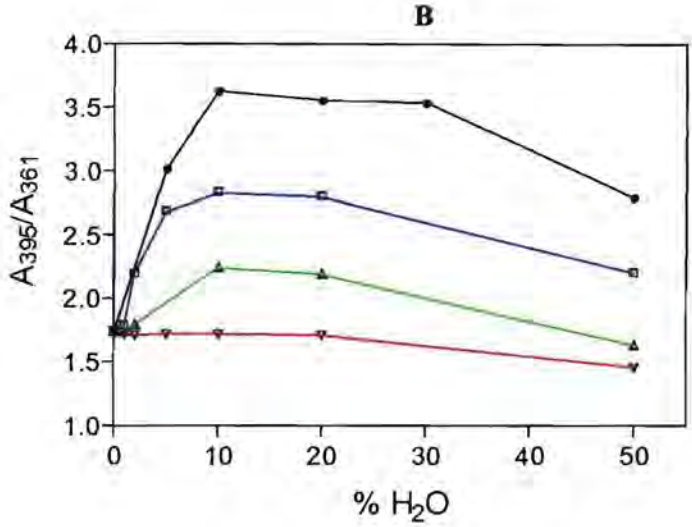

Figure 3.22. (B) Effect of percentage water and pH on α in buffered water-methanol systems at pH (—) 10.03, (—) 8.00, (—) 7.41 and (—) 5.99.

At neutral and low pH, there is a sharp rise in the α ratio from 1.74 in pure methanol to a value which plateaus in 10 - 30% water-methanol and then declines in higher water percentages indicative of the onset of dimerisation. This increase in the α value is most pronounced at low pH and is completely absent at pH 10 where the ratio remains at 1.74 until the dimer starts to form. The fact that the value of α in non-aqueous environments (strictly dry methanol and the hydrophobic core of SDS micelles) is essentially identical to that in basic aqueous methanol solution (around 1.74) indicates that this α value is solvent independent and corresponds to a haematin monomer in which hydroxide is the ligand. In hydrophobic environments, it is possible that the pK_a of the propionate groups and axial water increase and decrease respectively to generate a formally neutral, non-polar haematin monomer **86** (Figure 3.23.). Upon addition of a few percent of acidic or neutral aqueous medium to methanol, the pH dependent zwitterionic and charged species **87a** is likely to form. Upon the addition of alkaline aqueous medium to the dry methanol solution, it is likely that the carboxylic acid side chain deprotonates and hydroxide remains as the axial ligand to give species **87b** which has the same α value as the spectrum arises from the porphyrin core. The intermediate α values (Table 3.8.) probably correspond to mixtures of the two species in aqueous medium which are present at intermediate pHs.

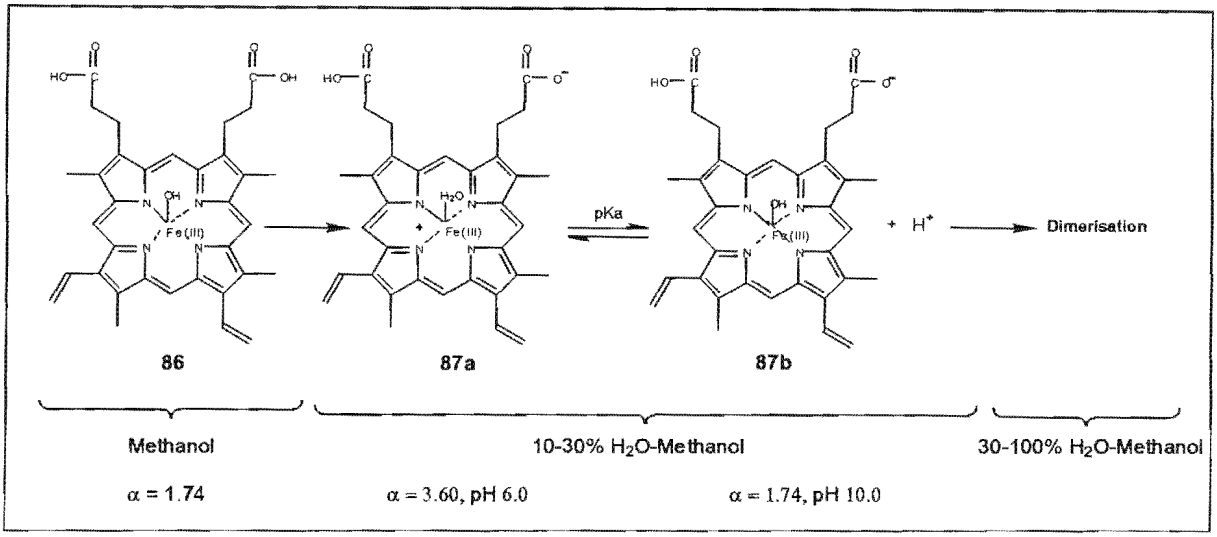

Figure 3.23. The haematin monomers present in methanol (**86**) and 10-30% H_2O-Methanol mixtures (**87a** and **87b**). Since Fe(III) carries a +3 charge, the porphyrin nitrogens carry a -2 charge and the HO^- ligand carries a -1 charge, the overall charge on **86** and **87a** is zero, since **87a** Zwitterionic. Similarily, the overall charge on **87b** is 1- as the charge on the H_2O ligand is zero.

Table 3.8. Limiting α values of haematin in 10 – 30% water-methanol mixtures as a function of pH

pH	α
5.99	3.60 ± 0.08
6.51	3.25 ± 0.08
6.89	3.23 ± 0.02
7.19	2.96 ± 0.01
7.41	2.82 ± 0.01
7.73	2.48 ± 0.01
8.00	2.22 ± 0.01
9.22	1.80 ± 0.01
10.03	1.71 ± 0.01

Relatively large errors are associated with the α values at the two lowest pHs investigated. This is probably due to the onset of haematin precipitation in the low pH range. To check where the onset of haematin precipitation begins, samples of 1.95μM haematin in HEPES buffer between pH 5.1 and 8.0 were stirred for 30mins and then centrifuged. This haematin concentration was chosen as it is the same as that used in the Fe(III)PPIX-quinoline binding assays. In the low pH samples a black pellet formed on the bottom of the tube after centrifugation indicative of precipitation. A plot of the absorbance of the Soret band as a function of pH indeed shows that haematin starts to precipitate around pH 6 (Figure 3.24.).

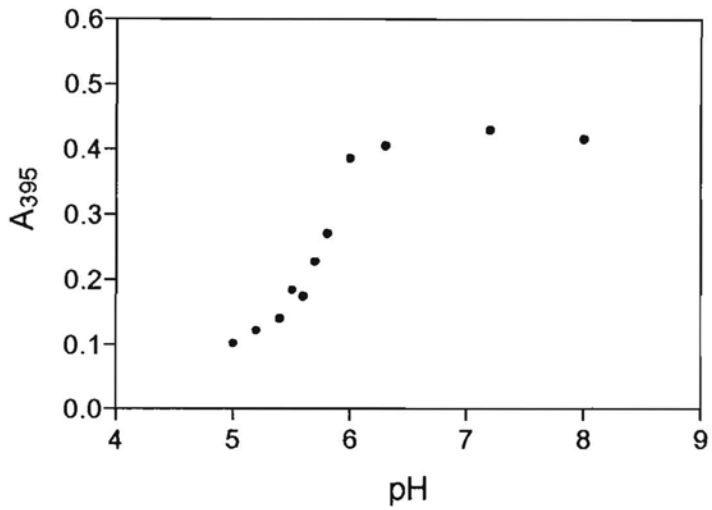

Figure 3.24. Absorbance of the Soret band for 1.95μM haematin as a function of pH.

If the limiting α values reported in Table 3.8. represent average values for mixtures of protonated and deprotonated monomer species, (**87a** and **87b** respectively), the equilibrium constant for this deprotonation process should give the pKa of the axial H_2O ligand in the 10 - 30% water-methanol mixtures.

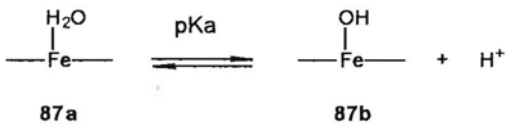

87a 87b (8)

When the absorbance ratios were fitted to an equilibrium equation (Derived in Chapter 7.2) for a single deprotonation using non-linear least squares fitting procedures an excellent fit was obtained with the pK_a of the axial ligand being 7.56 ± 0.07 (Figure 3.24.). This is in good agreement with the pK_a value of 7.6 reported by Shack and Clarke for ferriprotoporphyrin IX (Shack and Clarke 1947). Similar pK_a values of the aqua ligand have been reported for the haematin analogues ferrimesoporphyrin (pK_a = 7.01) (Cowgill and Clarke 1952 and ferricoprotoporphyrin (pK_a = 7.44) (Clarke and Perkins 1940), and various haemproteins (pK_a's = 8.05 - 8.99) (Baldwin 1986). Furthermore, the fitted α values reported in Table 3.5. closely parallel this curve despite their large uncertainty.

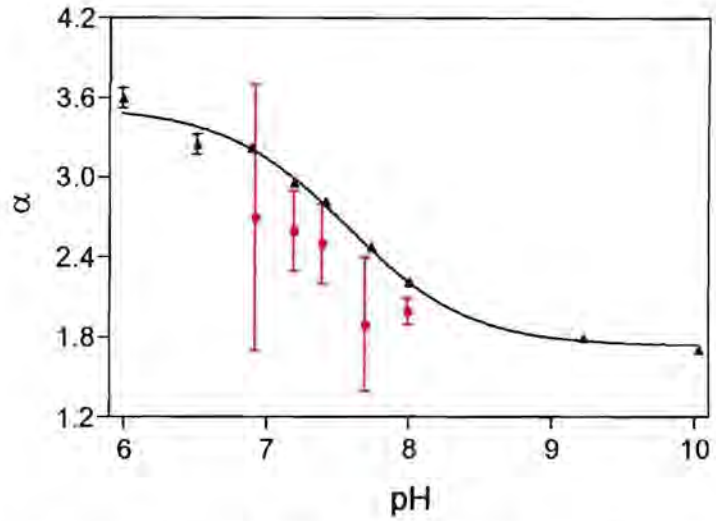

Figure 3.25. Limiting α values obtained in 20% water-methanol mixtures (▲) fitted to a pH titration curve for a single deprotonation (—) using non-linear least squares fitting. The fitted α values from Table 3.5. are shown for comparison (●).

Spectroscopic evidence for two protonatable states of haematin is provided by visible spectra of haematin in 20% water-methanol between pH 6.0 and 10.0 in which conversion of one species to another gives rise to two isosbestic points at 628nm and 653nm (Figure 3.26.). The spectrum of the monomer when H_2O is the axial ligand shows a peak maximum at 623nm which shifts to 599nm for axially coordinated HO^-. This shift to shorter wavelength is consistent with greater nucleophilicity towards Fe(III) of HO^- compared to H_2O.

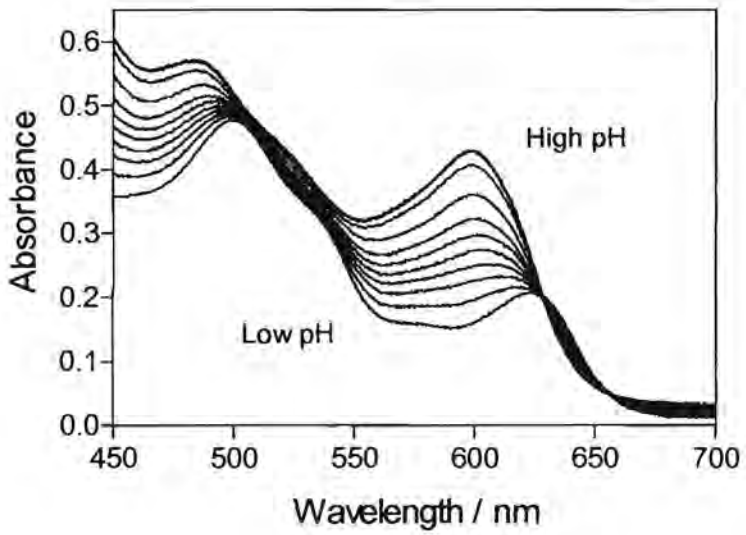

Figure 3.26. Visible spectra of haematin in 20% water-methanol mixtures from pH 6.0 to 10

Since the two monomeric species of haematin in 10 - 30 % water-methanol appear to be those expected in pure water, namely HO-Fe(III)PPIX and H_2O-Fe(III)PPIX, we can assume that the limiting α values for the monomer in the mixed water-methanol systems are good approximations of the corresponding α values in aqueous solution. The α values at the pHs of our titrations can be read off the pK_a curve and fixed in the haematin dimerisation equation in order to recalculate log K_{obs} using non-linear least squares fitting.

3.2.3. Determination of log K_{obs} and β by Fixing α

The recalculated values of log K_{obs} and β obtained when α is fixed at the limiting values for the monomer obtained in 10 - 30% water-methanol systems are presented in Table 3.9.

Table 3.9. log K_{obs} and β obtained by non-linear least squares fitting with α fixed to the limiting water-methanol values

pH	α	β	log K_{obs}
6.92	3.20	0.86 ± 0.03	7.00 ± 0.09
7.19	3.00	0.89 ± 0.02	7.3 ± 0.2
7.39	2.81	0.89 ± 0.01	7.2 ± 0.1
7.69	2.50	0.93 ± 0.02	7.5 ± 0.2
7.99	2.22	0.92 ± 0.02	7.2 ± 0.1
Mean			7.2 ± 0.2

A plot of log K_{obs} vs pH confirms our original findings that there is no significant dependence of log K_{obs} on pH (Table 3.10. and Figure 3.27.) and that dimerisation does not involve deprotonation.

Table 3.10. Slope and statistical parameters obtained from a linear regression fit to log K_{obs} vs pH for values of log K_{obs} obtained by free fitting and methanol fitting procedures

Parameters	Free Fitted log K_{obs}	Methanol Fitted log K_{obs}
Slope	0.2 ± 0.3	0.3 ± 0.2
r^2	0.175	0.486
P value	0.483	0.191
Deviation from zero	Not Significant	Not Significant

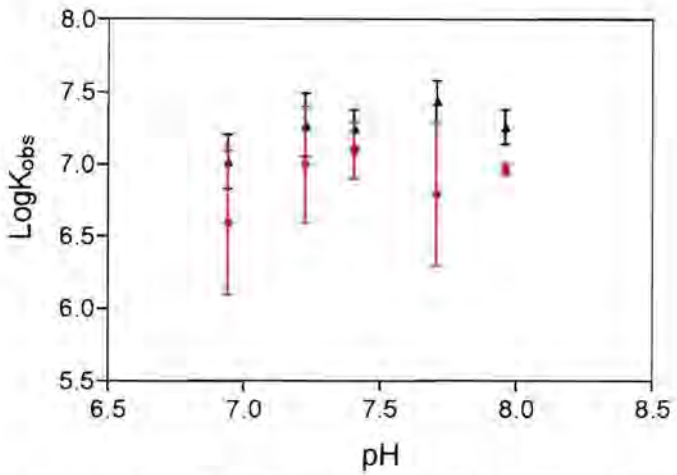

Figure 3.27. Plot of log K_{obs} vs pH for free fitted data from Table 3.5. (—) and data fitted using the limiting α values from the water-methanol mixtures (—).

3.2.4. Reanalysis of the Data of Brown *et al.*

Since analysis of the data using both freely refined parameters and fixed α values independently determined give a different result to Brown *et al.*, it was decided to reanalyse their data using non-linear least squares fitting. Data points of the extinction coefficient at varying haematin concentrations were extracted off their sigmoidal curves (Figure 3.10A and 3.10B) for Fe(III)DP and Fe(III)PPIX (Appendix 1) and were converted to absorbances. The absolute absorbances were then fitted to the dimerisation equation (See Section 7.2.2.2.5. for derivation of the model). The data for Fe(III)DP converged using the dimerisation equation and values for ε_M, ε_D and log K_{obs} were obtained (Table 3.10.). For Fe(III)PPIX the same problems reported by Brown *et al.* were encountered with the ε_M's being too poorly defined to obtain corresponding values of log K_{obs}. These values were then fixed at the limiting monomer extinction coefficients of Fe(III)DP, as done by Brown *et al.*, to obtain the values of ε_D and log K_{obs} reported in Table 3.11.

Table 3.10. Values of ε_M, ε_D and log K_{obs} obtained for Fe(III)DP by i. linearisation methods (Brown *et al*. 1970) and ii. non-linear least squares fitting.

pH	ε_M / mM	ε_D / mM	log K_{obs}
Brown *et al*. 1970			
6.64	132 500	35 000	4.83
6.98	121 500	37 000	4.73
7.38	110 000	40 000	4.46
8.04	95 000	44 000	3.78
11.0	89 000	46 400	nd
Refitted by Non-linear Least Squares Fitting			
6.64	137 000 ± 5000	38 300 ± 5000	5.7 ± 0.2
6.98	127 000 ± 6000	38 000 ± 4000	5.8 ± 0.2
7.38	115 000 ± 12000	41 000 ± 6000	6.0 ± 0.4
8.04	96 000 ± 6000	44 200 ± 2000	6.6 ± 0.2
11.0	76 000 ± 4000	44 000 ± 1000	6.9 ± 0.2

Table 3.11. Values of ε_D and log K_{obs} obtained for Fe(III)PPIX by i. linearisation methods (Brown *et al* 1970) and ii. non-linear least squares fitting.

pH	ε_D / mM	log K_{obs}
Brown *et al*. 1970		
6.98	39 300	6.33
7.38	40 800	5.98
8.04	44 600	5.41
11.0	46 600	nd
Refitted by Non-linear Least Squares Fitting		
6.98	39 200 ± 900	7.84 ± 0.08
7.38	40 700 ± 700	8.01 ± 0.08
8.04	44 400 ± 500	8.3 ± 0.1
11.0	46 400 ± 300	8.7 ± 0.1

Although a plot of $\log K_{obs}$ against pH for the refitted data of Fe(III)PPIX and Fe(III)DP does increase slightly with pH, the slopes are only 0.19 ± 0.04 and 0.27 ± 0.07 respectively which, contrary to the findings of Brown *et al.*, is indicative of n = 0 and not n = 1 (Figure 3.28.). The discrepancy with the data analysis of Brown *et al.* is likely due to the errors involved in extrapolating the limiting monomer extinction coefficient for Fe(III)DP from their curves, and fixing this value as the limiting monomer extinction coefficient for Fe(III)PPIX. As can been seen from our data analysis (Tables 3.5. and 3.6.), the value of log K_{obs} and hence the overall slope of log K_{obs} against pH, is highly sensitive to this limiting value obtained for the monomer.

We can therefore conclude that there are discrepancies in the data analysis of Brown *et al.* and that dimer formation is pH-independent and does not involve deprotonation.

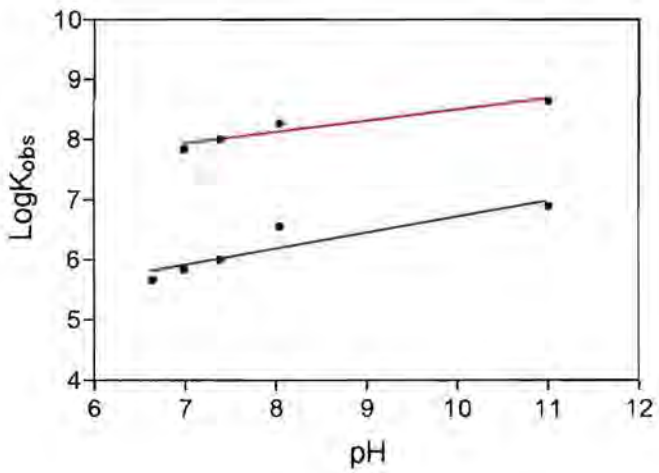

Figure 3.27. Plot of log K_{obs} vs pH for reanalysed data of Brown *et al.* 1970. (—) Fe(III)PPIX, (—) Fe(III)DP.

A pH-independent dimerisation equation can now be postulated :

$$2M \underset{}{\overset{K}{\rightleftharpoons}} D \qquad (9)$$

where log K is the pH-independent dimerisation constant of 6.9 ± 0.2 which compares favourably with the value of 7.2 ± 0.2 obtained using our data.

3.2.5. Spectral Evidence

That haematin dimerisation is pH-independent is further supported by the changes observed by Egan *et al.* in the Soret band of aqueous haematin with pH (Egan *et al.* 1994). At low pH (pH = 5.0), this peak remains broad and does not have the characteristic sharpness of monomeric haematin such as is observed in SDS solution and in the monomerising solvents methanol and DMSO.

Since formation of the haematin dimer does not involve deprotonation, this dimer must have a different structure to the μ-oxo dimer. This is supported by spectra of haematin in pure aqueous solution at pH 6.5 and pH 10.0 (Figure 3.29A) which are different to the spectrum of the synthesised μ-oxo dimer in benzene (Figure 3.29B) (O'Keeffe and Barlow 1975) or chloroform (Sadasivan *et al.* 1969). In the case of the aqueous haematin dimer, the band around 650nm shifts to about 610nm and increases in intensity with increased pH, whilst the band at 550nm decreases in intensity and is eventually obscured. This contrasts to the spectrum of the synthesised μ-oxo dimer which is characterised by a distinctive peaks around 567nm and a shoulder around 590nm (Figure 3.29B).

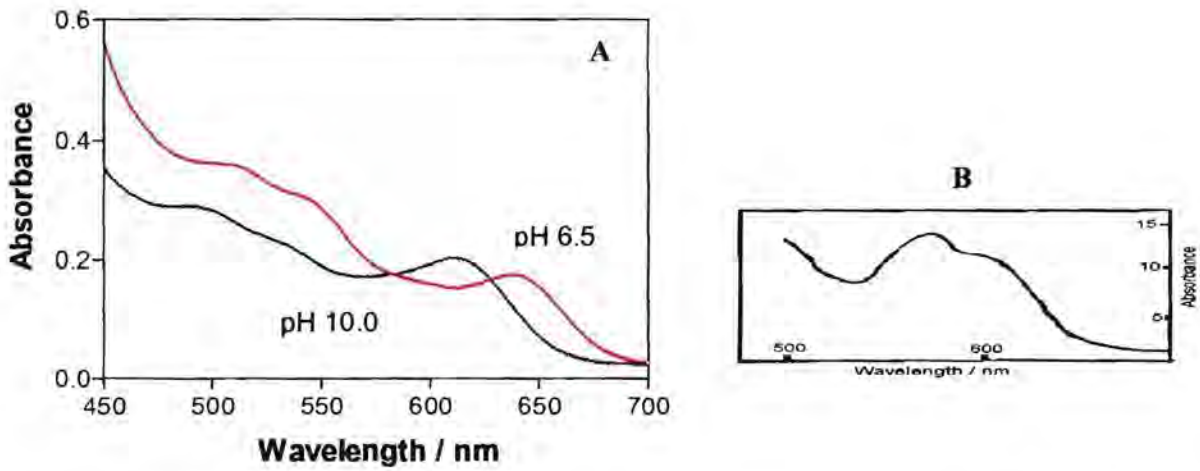

Figure 3.29. Uv-vis spectra of (A) haematin dimer in HEPES buffer at pH 6.5 (—) and in CHES buffer at pH 10.0 (—), (B) synthesised μ-oxo dimer of Fe(III)DP-DME in benzene (O'Keeffe and Barlow 1975).

Furthermore, a spectrum of the μ-oxo dimer can be obtained from the high pH spectrum of haematin in aqueous media if a small amount of pyridine is added (Figure 3.30C. and 3.30D.) which is in agreement with earlier studies (O'Keeffe and Barlow 1975, Gallagher and Elliot 1973). Alternatively, saturating sodium chloride or sodium perchlorate can induce μ-oxo dimer formation above but not below pH 7.4 (Figure 3.30A. and 3.30B.). Addition of

pyridine at or below pH 7.4 gives spectra of a bis pyridyl low spin complex (White 1978) implying that in this pH range, pyridine coordinates to the iron.

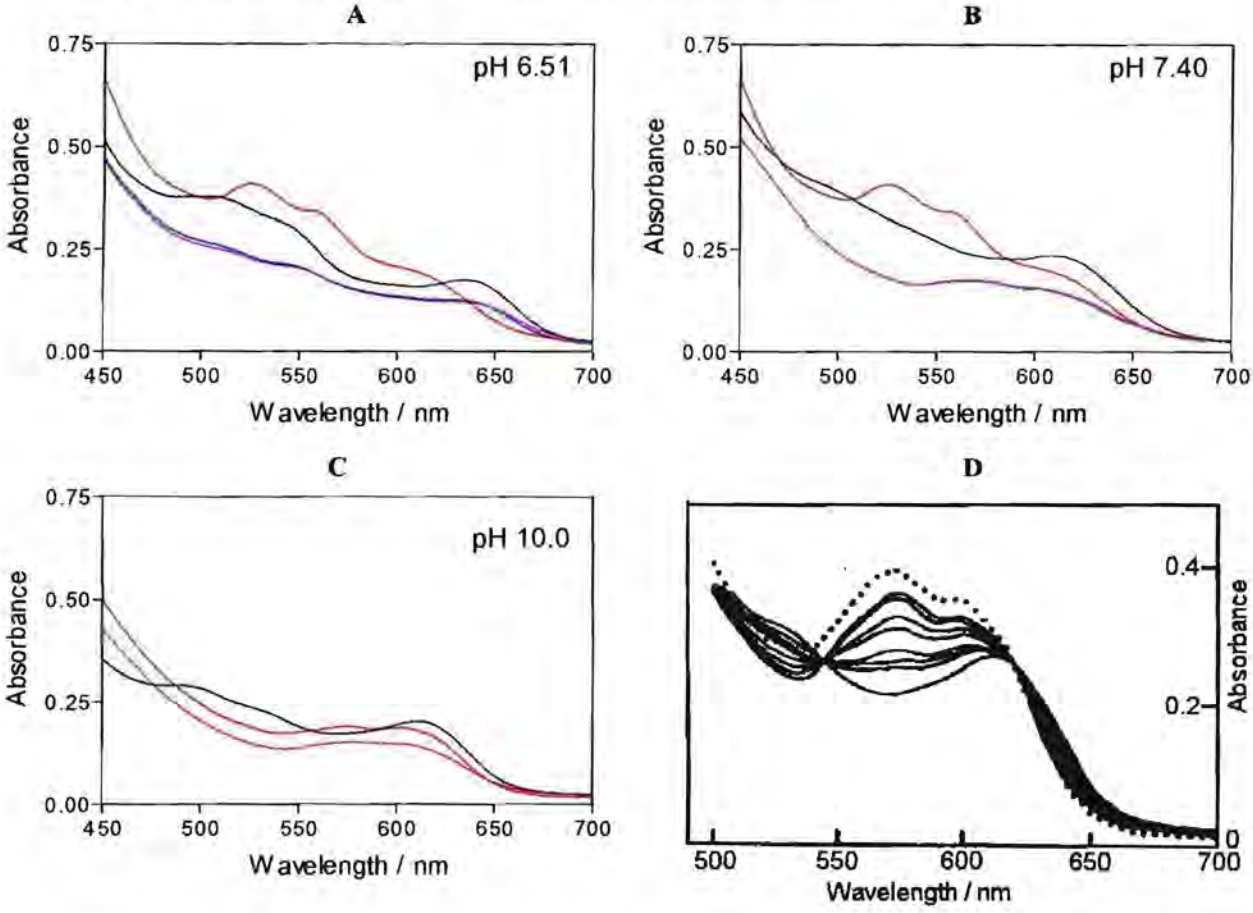

Figure 3.30. Spectra of haematin in HEPES buffer (—) at pH 6.51 (A) and 7.40 (B.) and in CHES buffer at pH 10.0 (C), haematin in the respective buffers with (—) 50μl pyridine, (—) saturating sodium chloride and (—) saturating sodium perchlorate. (D) Titration of 28μM haematin in 0.02M NaOH with pyridine (Gallagher and Elliot 1973).

Further work in our laboratories have shown that no isosbestic points exist in the haematin dimer spectrum as a function of pH implying that more than two dimer species are present in aqueous solution (Egan, unpublished results). This is contrary to what is reported by Silver and Lucas (Silver and Lucas 1983), although close inspection of their spectra show the absence of an isosbestic point at 500nm (Figure 3.8).

Given that the haematin dimer observed in aqueous solution is not a μ-oxo dimer, it is proposed that it is a coplanar π-π dimer in which the faces of the ferriporphyrins lacking axial ligands interact with each other (Scheme 3.1.). Interestingly, the proposed stoichiometry of the dimer is in accord with an early suggestion by Davies that the ferrimesoporphyrin and

ferrihematoporphyrin dimers appear to associate with one hydroxyl ion per iron atom in alkaline solution (Davies 1940). This dimeric structure is consistent with the lack of isosbestic points seen for the dimer in aqueous solution where presumably two pK_as give rise to the three dimeric species **93a**, **93b** and **93c**. Furthermore, this structure explains why in contrast to protoporohyrin IX, aggregates higher than dimers are not observed. In this case, the outwardly directed axial ligand would sterically hamper such aggregation (**93a – c** in Scheme 3.1), whereas there is no apparent reason why the μ-oxo dimer should not form higher aggregates (Scheme 3.2.).

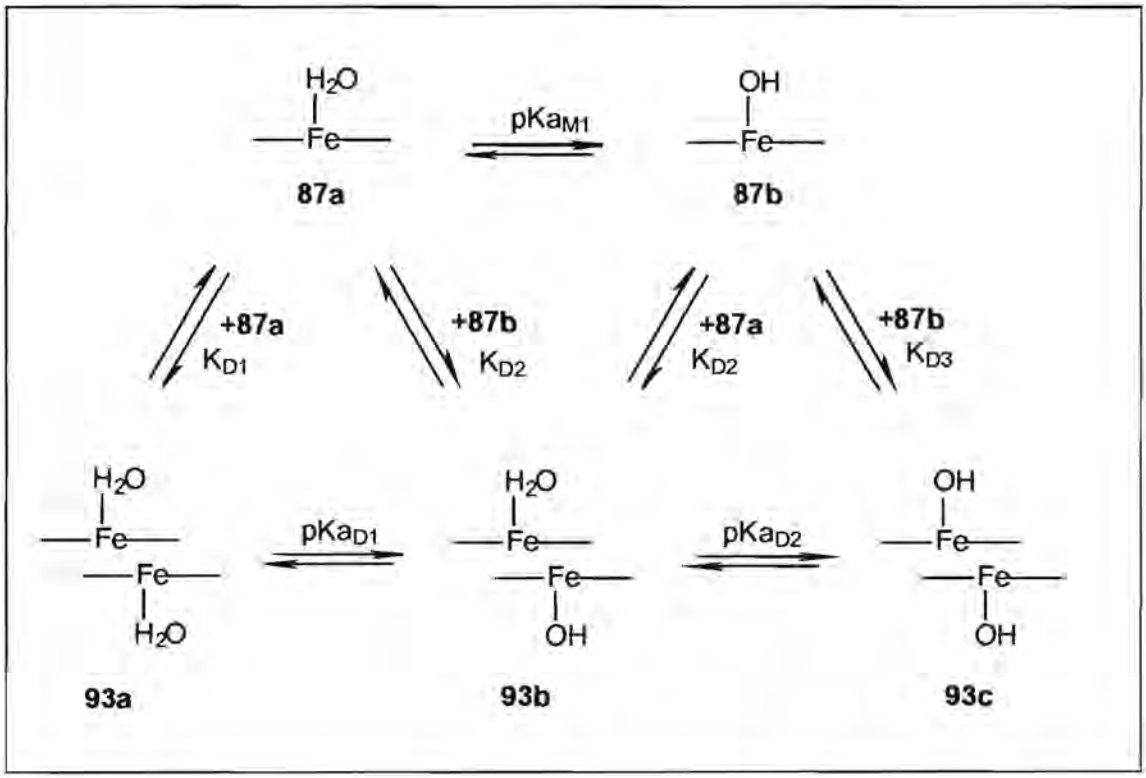

Scheme 3.1. Proposed structures of the haematin dimer 93a, 93b and 93c present in aqueous solution between pH 6.9 and 8.0 where K_D is the pH independent dimerisation constant, pK_{aM1} is the protonation constant of the axial ligand of the monomer and pK_{aD1} and pK_{aD2} are the protonation constants of the axial ligands of the dimer.

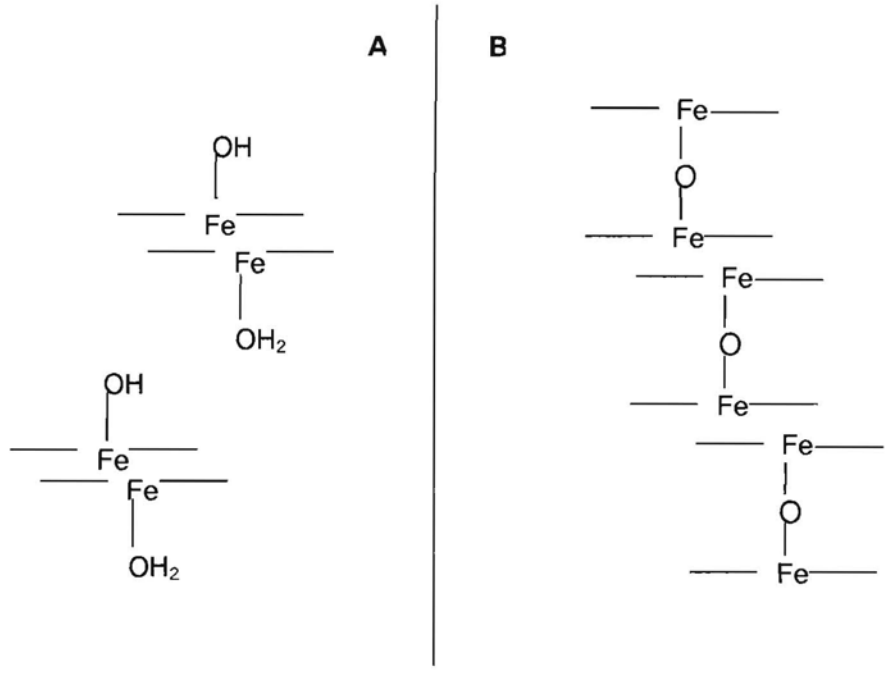

Scheme 3.2. Speculation on why aggregates higher than haematin dimers do not exist. If the haematin dimer is a μ-oxo dimer, the outwardly pointing face of the porphyrin ring would be expected to form aggregates higher than dimers in aqueous solution (**A**). On the contrary, aggregates higher than dimers would not be expected for the proposed π-π dimer (**B**) since the axial hydroxo- or aqua ligands are predicted to sterically hinder the outer porphyrin face.

3.3. CONCLUSIONS

Haematin in aqueous solution is extensively dimerised with a pH-independent equilibrium constant of log K_D = 7.2 ± 0.2 and the pK_a of the monomer equal to 7.56 ± 0.07. This dimer is not a μ-oxo dimer as proposed by Brown *et al.* but is likely to be a pH-dependent mixture of three π-π stacked dimers **93a**, **93b** and **93c**, it is presumably the low pH form that is the drug target of chloroquine and related antimalarial drugs.

STRUCTURE-ACTIVITY RELATIONSHIPS IN 4-AMINOQUINOLINES

4.1. BACKGROUND

As mentioned in the introduction, *CQ* has the ability to accumulate to mM concentrations in the food vacuole at therapeutic levels (nM). It is thought that some of this accumulation can be attributed to the weak base properties of *CQ*, whilst the majority has recently been attributed to saturable binding to the Fe(III)PPIX target (Bray *et al.* 1998). The resulting toxicitiy of this complex is still the subject of much debate. In this study, the hypothesis is investigated that the Fe(III)PPIX-quinoline complex inhibits haemozoin formation thereby causing a toxic build-up of Fe(III)PPIX or the Fe(III)PPIX-quinoline complex which ultimately leads to death of the parasite.

Although a wide range of quinoline antimalarials and antiplasmodials have been shown to bind to Fe(III)PPIX, little is known about the critical structural features on the quinoline nucleus required for complex formation. It was originally suggested that the similar inter-nitrogen ($N_{quinoline}$ – $N_{diethyl}$) atomic distance in the antimalarial drugs *AQ* (Yennawar and Viswamitra 1991, (Koh *et al.* 1994) and *CQ* may be important structural features for binding to a similar acceptor site on the Fe(III)PPIX receptor (O'Neill *et al.* 1997). No direct relationship was however found between the inter-nitrogen separation of isolated drug molecules and the antimalarial activity of *CQ*, **94** and a range of *AQ* analogues (Figure 4.1.) although the terminal amino group was suggested to be important for hydrogen bonding to the propionate groups of Fe(III)PPIX in the complex (O'Neill *et al.* 1997). That hydrogen bonding is important is questionable when considering the recent finding that *CQ* analogues with shortened (2-3C long) and lengthened (10-12C long) side chains retain full activity against *CQ*–resistant and *CQ*–sensitive malaria parasites (De *et al.* 1996). Furthermore, analogue **15** which lacks a side chain or a terminal amino group still forms a relatively strong complex with Fe(III)PPIX (Figure 1.4.) (Vippagunta *et al.* 1999). The authors propose that the 7-chloro group in *CQ* is the critical structural feature for complex formation as 6-chloro-chloroquine (**13**) failed to form a complex. Further support is shown by the inability of simple quinolines which lack a 7-chloro group to form a complex with Fe(III)PPIX (Figure 4.1.) (Egan *et al.* 1997, Mavuso PhD thesis 2001).

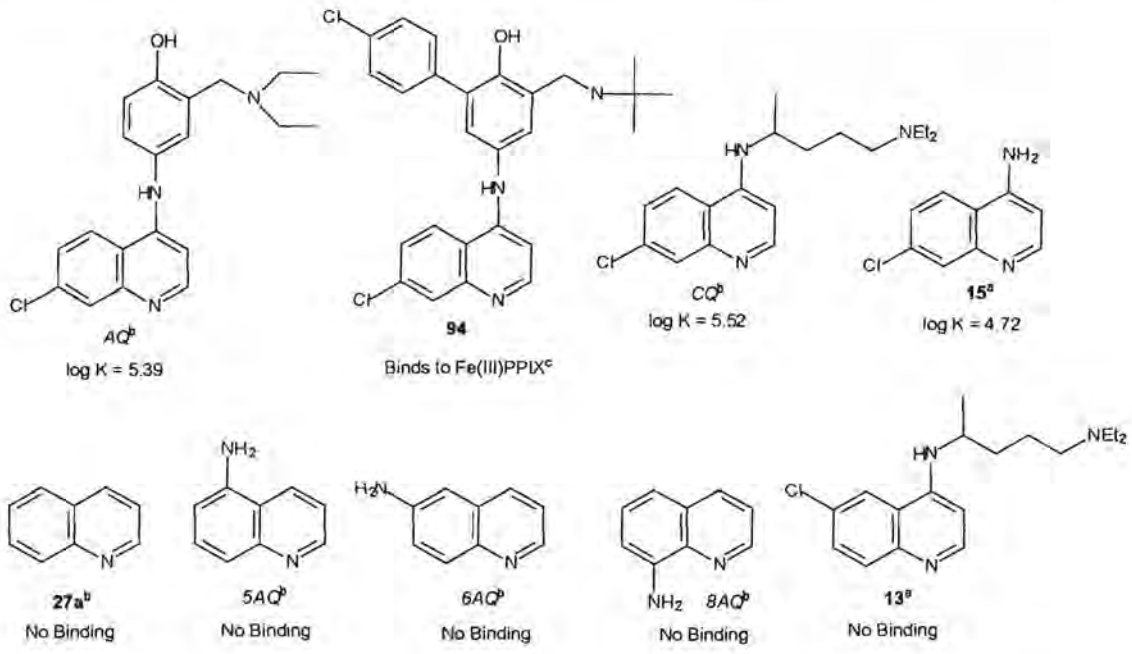

Figure 4.1. The relationship between some structural features on *AQ*, **94**, *CQ* and some simple aminoquinolines, and the ability to form a complex with Fe(III)PPIX. [a] Vippagunta *et al.* 1999, [b] Egan *et al.* 1997 and Mavuso PhD thesis 2001, [c] O'Neill *et al.* 1997.

Less is known about the structural features in *CQ* responsible for β-haematin inhibition although again, the group at the 7-postion appears to play a role. This is demonstrated by the 7-nitro and 7-bromo derivatives of *CQ* which retain β-haematin inhibitory activity, whereas the 7-amino and 7-hydro derivatives of *CQ* do not (Vippagunta *et al.* 1999).

In this chapter, the critical structural features in *CQ* responsible for complex formation with Fe(III)PPIX and β-haematin inhibition will be probed. It will be investigated if (i) there is a quantitative relationship between the strength of Fe(III)PPIX-quinoline association and antiplasmodial activity if (ii) the strength of Fe(III)PPIX-quinoline association is related to the ability to inhibit β-haematin formation, and (iii) if strong β-haematin inhibition is related to strong antiplasmodial activity.

The structural significance of the terminal amino group in the side chain will also be probed to ascertain if it plays a role in (i) stabilising the Fe(III)PPIX-quinoline complex, presumably through hydrogen bonding to the propionate groups in Fe(III)PPIX or (ii) contributing to enhanced accumulation in the food vacuole through pH trapping.

4.2. EXPERIMENTAL METHODS

4.2.1. Synthesis of the Chloroquine Analogues

Various simplified analogues of *CQ* were obtained commercially or synthesised according to the procedures outlined in Chapter 2. To ensure analytical purity of all the compounds, microanalysis were obtained for the solids and HRMS for the oils. Details of the experimental procedures used are reported in Section 7.1.2.

4.2.2. Spectrophotometric Titrations

It is not possible to determine quinoline-Fe(III)PPIX association constants spectrophotometrically in aqueous solution as the spectrum of the haematin dimer is broad (Figure 3.12.) and undergoes little change upon complex formation. The association constants were therefore obtained by the method of Egan *et al.* in aqueous 40% dimethylsulfoxide (DMSO) at pH 7.4 (Egan *et al.* 1997, Mavuso PhD thesis 2001) according to methods outlined in Section 7.2.3.

Association constants were determined spectrophotometrically at pH 7.4 and not at the pH of the food vacuole (5.2 and 5.5) as haematin has only 30% solubility in this lower pH range (see Figure 3.2.3). In 40% DMSO (aq) haematin is strictly monomeric (Collier *et al* 1979) with a coordinating DMSO molecule occupying the axial position (Brown and Lantzke 1969). Since the trends observed for the association constants in 40% DMSO are the same as those observed in pure aqueous media using titration calorimetry (Dorn *et al.* 1998a) it appears that the association constants measured in 40% DMSO at pH 7.4, provide a good reflection of the interactions occurring in the food vacuole. Furthermore, interpretation of the results is simplified under conditions where haematin is strictly monomeric and either one or two quinoline molecules associate with each haematin molecule (Egan *et al.* 1997) compared to large stoichiometries of between 1 and 19 haematin molecules per quinoline molecule obtained in a pure aqueous medium (Dorn *et al.* 1998a, Vippagunta *et al.* 1999).

From Figure 4.2A, it can be seen that no changes in the spectrum of Fe(III)PPIX in 40 % DMSO are observed in the presence of compounds unable to form complexes with Fe(III)PPIX (for example **27b**). Compounds that do however, form such complexes (for example **68**) cause a substantial decrease in intensity of the Soret band at 402nm with no shift in the peak maximum (Figure 4.2B.). At longer wavelengths, the Q band (494nm and 537nm) decreases in intensity and the charge transfer band at 620nm increases in intensity

and undergoes a substantial blue shift to 594nm. These changes are quite distinct from the spectrum of the haematin π-π dimer in pure aqueous solution (Figure 4.2C.) or the spectrum of the μ-oxo dimer (Figure 4.2D.). Where the resulting quinoline-Fe(III)PPIX complex involves 1:1 stoichiometry, excellent isosbestic points are observed (Figure 4.2B.).

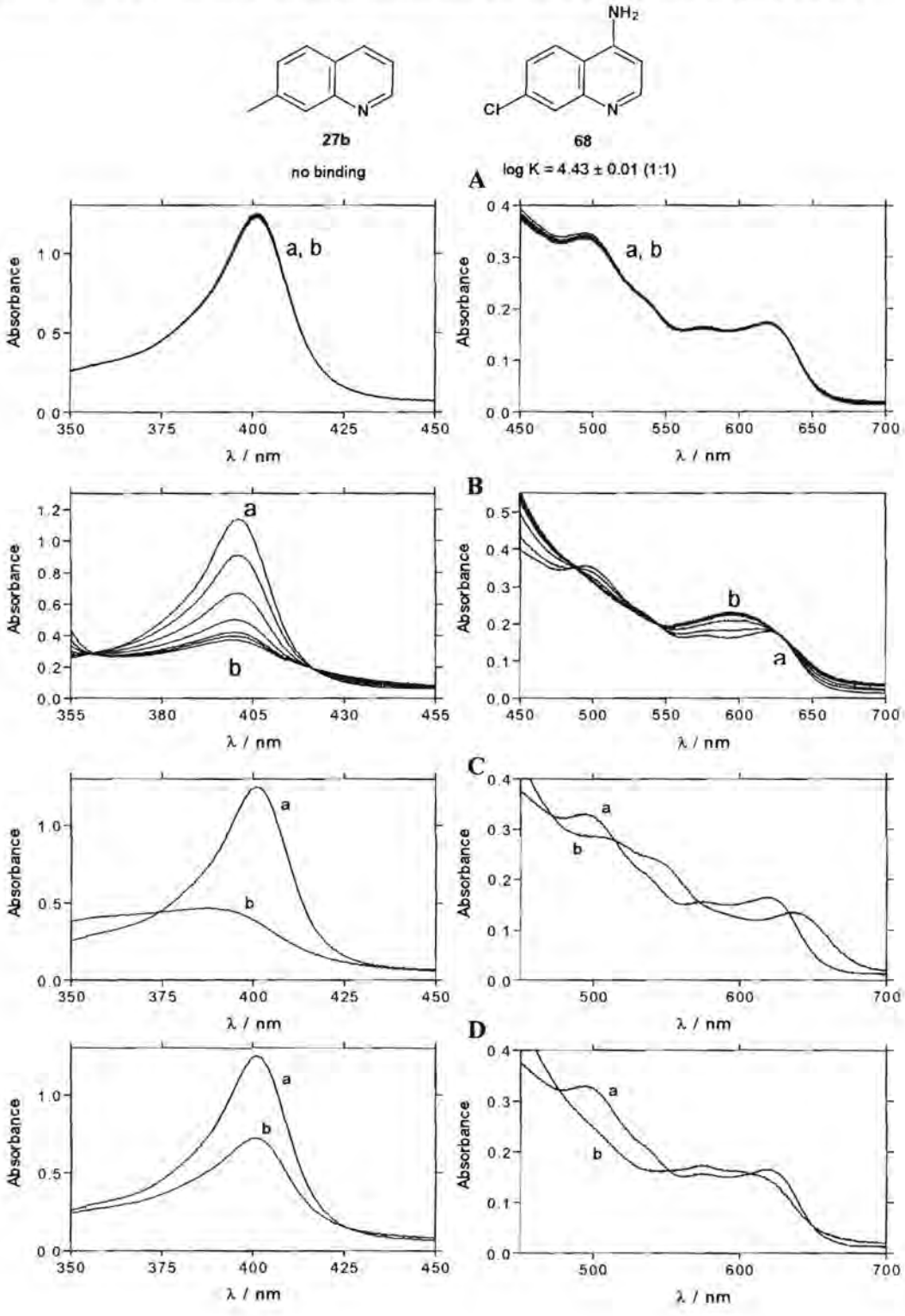

Figure 4.2. Visible spectra of Fe(III)PPIX in 40% DMSO, pH 7.5 (spectrum a) titrated with (A) a compound unable to form a complex with Fe(III)PPIX (**27b**) (spectrum b); (B) a compound that forms a complex with Fe(III)PPIX (**68**) (spectrum b). (C) Visible spectra of Fe(III)PPIX in 40% DMSO, pH 7.5 (spectrum a), and in water (spectrum b). (D) Visible spectra of Fe(III)PPIX in 40% DMSO, pH 7.5 (spectrum a), and under the same conditions but with the addition of saturating NaCl (spectrum b). The spectrum of the latter is identical to that of the μ-oxo dimer reported by O'Keeffe and Barlow (O'Keeffe and Barlow 1975). Concentrations of Fe(III)PPIX are 8×10^{-6}M (left panels) and 2.4×10^{-5}M (right panels). All spectra are corrected for dilution.

The absorbance of the Soret band at 402nm was recorded as a function of quinoline concentration according to the methods outlined in Chapter 7.2. In all cases, the corrected absorbance of the Soret band at 402nm as a function of quinoline concentration fitted a 1:1 or a 2:1 association model (quinoline:Fe(III)PPIX) (See Chapter 7.2 for the derivations). A typical example of an association curve is displayed in Figure 4.3 where the solid line represents a best fit of the data to the association model using non-linear least squares fitting procedures. The titration curves for all the other compounds are displayed in Appendix 2. In most cases where the quinolines formed 2:1 complexes with haematin, the second association constant was small with large relative errors and was therefore not reported. In all instances the values of the first association constant have acceptably small errors and the data is well fitted in the low quinoline concentration region where strong binding occurs. The association constants are all quoted as an average of three separated determinations and the error is reported as the standard error of the mean.

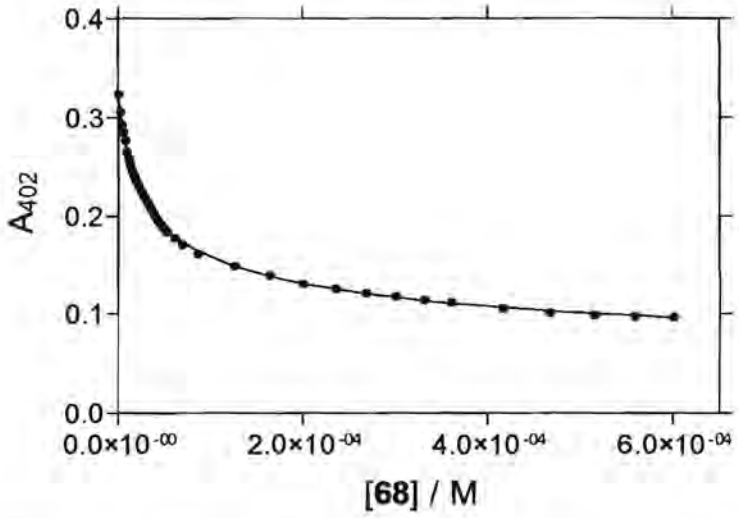

Figure 4.3. Typical spectrophotometric titration curve (in this case for **68**). The solid line is a best fit to the data of a 1:1 association model.

4.2.3. β-Haematin Inhibition

β-Haematin inhibition was determined by the infra-red method of Egan *et al.* 1994 which is outlined in Section 7.2.4. In this method, haematin is converted to β-haematin in 4.5M acetate, pH 4.5 at 60°C for 30mins. The infrared spectrum of β-haematin (Figure 4.4B.) has two characteristic peaks around 1660cm^{-1} and 1210cm^{-1} which are absent in haematin (Figure 4.4A). This method unequivocally distinguishes between inhibitory and non inhibitory compounds as is shown by the typical examples (Compounds **61** and **68** in Figure 4.4C and 4.4D respectively). These two characteristic peaks are absent in the product spectrum of an inhibitory compound (Figure 4.4C) and present in the product spectrum of a non inhibitory compound (Figure 4.4D). Since *CQ* inhibits β-haematin formation at 4eqivalents, all compounds were tested for inhibition at this mole ratio. A positive result therefore implies that the compound has comparable inhibitory activity to *CQ*, and a negative result implies that the compound is significantly less inhibitory than *CQ*.

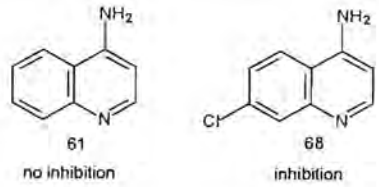

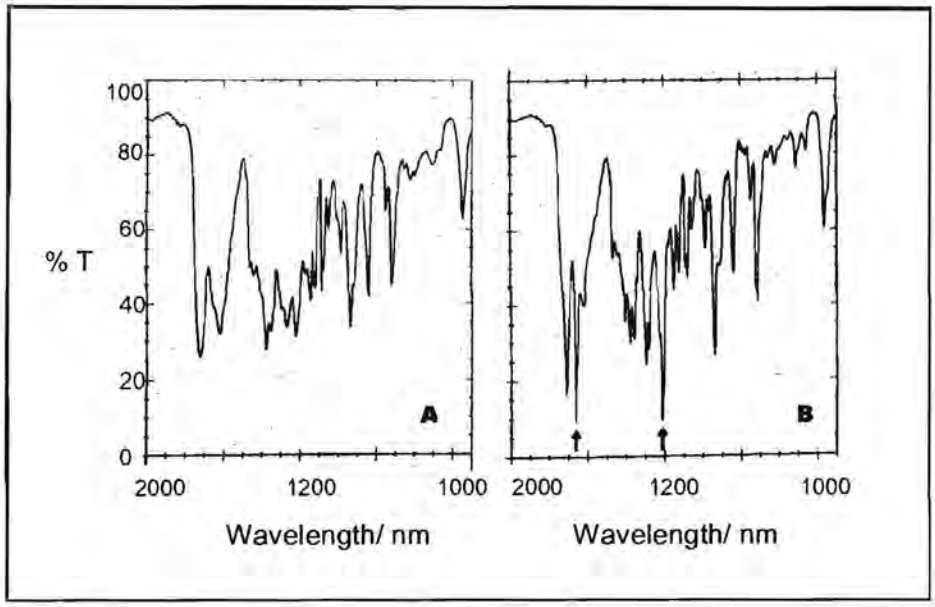

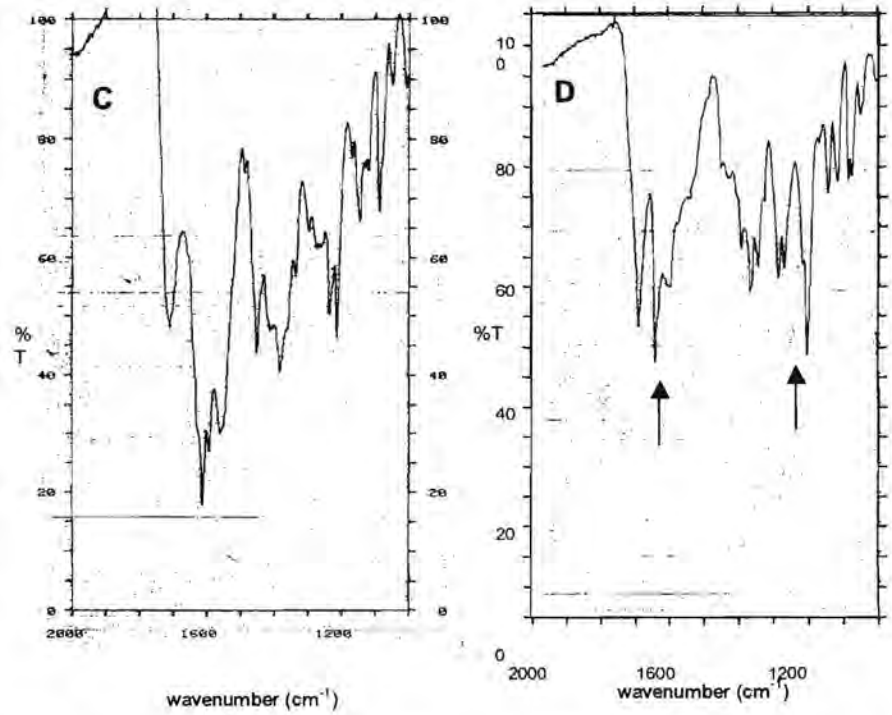

Figure 4.4. Infra red spectra of (A) haematin, (B) β-haematin, (C) the product of the β-haematin reaction in the presence of the inhibitory compound **68** and (D) the non inhibitory compound **61**. The arrows highlight the peaks at 1660cm^{-1} and 1210cm^{-1} which are present in the spectrum of β-haematin.

4.2.4. Antiplasmodial Testing

All compounds were sent away to Mr Jason Walden, Dept of Pharmacology, UCT for *in vitro* antiplasmodial testing using a cultured *CQ*-sensitive strain of *P. falciparum*, D10. No attempt was made to determine IC_{50} values in excess of 10μM as it has been observed that *CQ* exhibits several effects at μM and mM concentrations which probably play no role in its therapeutic activity (see Section 1.5.3.).

4.3. RESULTS

The results for all the quinolines tested for (i) association with Fe(III)PPIX, (ii) strong inhibition of β-haematin formation and (iii) *in vitro* antiplasmodial activity against the *CQ*-sensitive D10 strain are presented in Table 4.1.

Table 4.1. Results of quinolines tested for association with Fe(III)PPIX, inhibition of β-haematin formation and antiplasmodial activity.

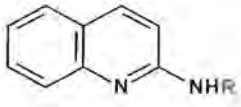

No.	R
58	H
59	CH_3
60	$CH_2CH_2NH_2$

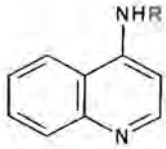

No.	R
61	H
62	CH_3
63	CH_2CH_2OH
81	$CH_2CH_2NHCOCH_3$
64	$CH_2CH_2NH_2$
65	$CH_2CH_2NEt_2$

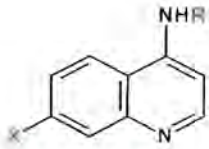

No.	X	R
66	CH_3	H
68	Cl	H
69	Cl	CH_3
70	Cl	$CH_2CH_2CH_3$
71	Cl	CH_2CH_2OH
72	Cl	$CH_2CH_2NH_2$
73	Cl	$CH_2CH_2NMe_2$
74	Cl	$CH_2CH_2NEt_2$

No.	log K ± SEM[a]	Stoichiometry[b]	β-Haematin Inhibition	IC_{50} (nM) ± SEM
58	4.23 ± 0.02	1:1	-	> 10 000
59	4.26 ± 0.03	1:1	-	> 10 000
60	4.34 ± 0.06	1:1	-	> 10 000
61	4.49 ± 0.01	2:1[c]	-	> 10 000
62	4.38 ± 0.03	1:1	-	> 10 000
63	4.18 ± 0.03	1:1	-	> 10 000
81	4.28 ± 0.06	2:1[c]	-	> 10 000
64	4.59 ± 0.04	1:1	-	4 700 ± 800
65	4.75 ± 0.03, (log K_2 = 3.2 ± 0.01)	2:1	-	799 ± 404
66	4.52 ± 0.01	1:1	-	> 10 000
68	4.43 ± 0.01	1:1	+	3 800 ± 500
69	4.48 ± 0.02	1:1	+	4 000 ± 2 200
70	4.43 ± 0.05	1:1	+	954 ± 28[d]
71	4.66 ± 0.02	2:1[c]	+	5 070 ± 80
72	4.928 ± 0.003	1:1	+	92 ± 12
73	4.96 ± 0.01	2:1[c]	+	81 ± 6
74	5.81 ± 0.01, (log K_2 = 4.47 ± 0.02)	2:1	+	49 ± 14
CQ	5.52 ± 0.03	1:1	+	38 ± 14

[a] Standard error of the mean, three determinations, [b] Quinoline:Fe(III)PPIX, [c] Fitted to a 2:1 model but meaningful value for log K_2 not obtained, [d] maximum error , two determinations

4.4. DISCUSSION

4.4.1. Structural Requirements for Haematin Binding

It was found that the quinolines in Figure 4.5A all associate strongly with Fe(III)PPIX and the quinolines in Figure 4.5B do not associate with Fe(III)PPIX.

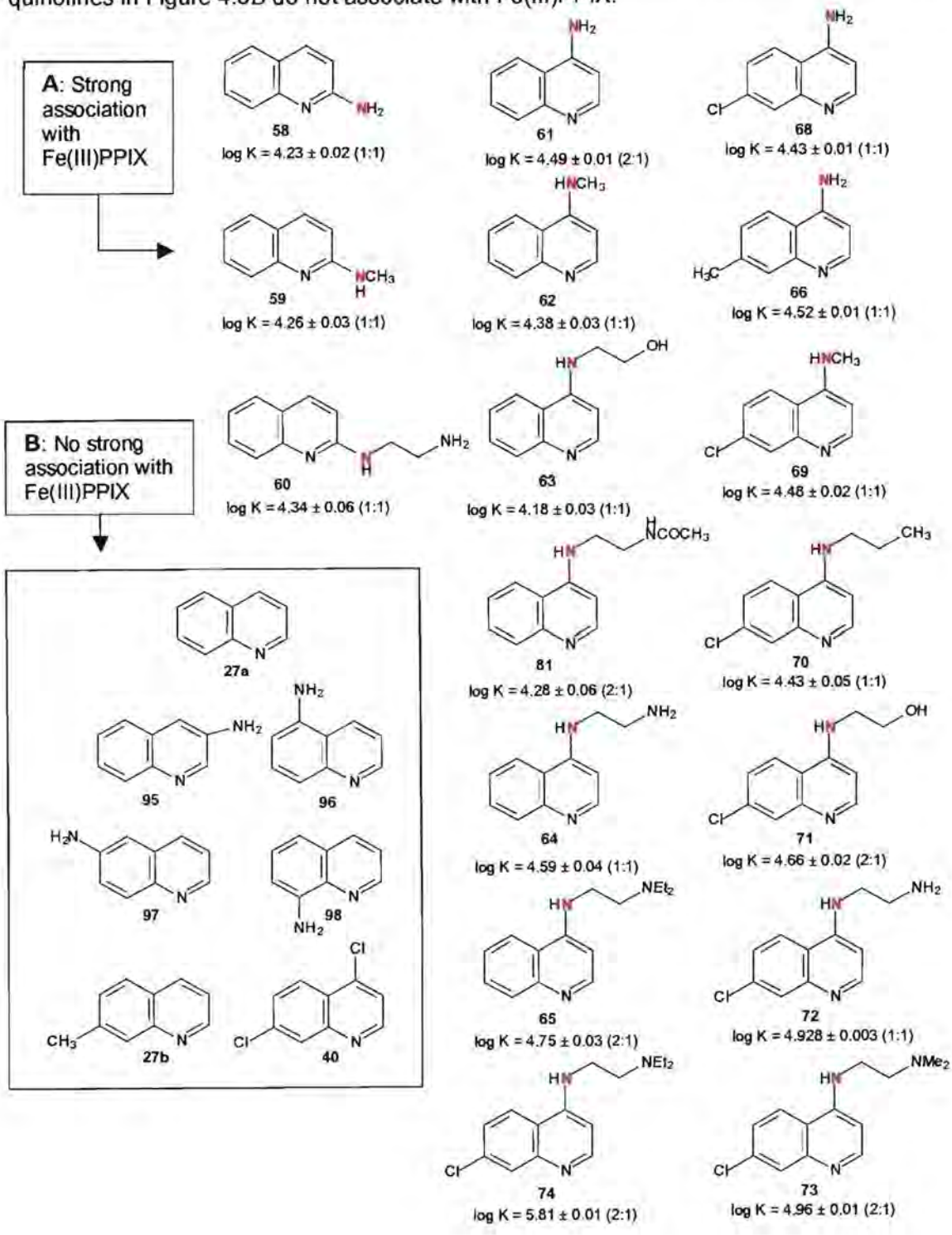

Figure 4.5. Quinolines and analogues of *CQ* that exhibit (A) a strong association with Fe(III)PPIX (log Ks between 4 and 5.5), and (B) no strong association with Fe(III)PPIX

It is immediatedly evident from Figure 4.5 that all quinolines with an amino-group at the 2-or 4-positions form strong complexes with Fe(III)PPIX. The ability of these compounds to form a complex with Fe(III)PPIX appears to be independent of the presence of a 7-chloro group as is elegantly demonstrated by comparing **40**, **61** and **68** (Figure 4.6). Here, **40** which has a 7-chloro group but lacks an amino group at the 4-position does not associate with Fe(III)PPIX, whereas **61** and **68** which both have 4-amino groups, associate equally strongly with Fe(III)PPIX.

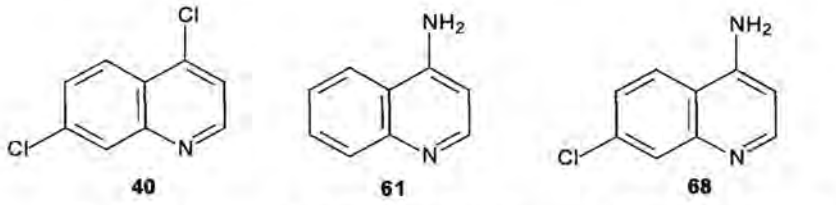

40 **61** **68**

No binding log K = 4.49 ± 0.01 (2:1) log K = 4.43 ± 0.01 (1:1)

Figure 4.6. Identification of the 4-aminoquinoline nucleus as critical for association with Fe(III)PPIX

Introduction of a short chain on the nitrogen atom at the 2- or 4-positions appears to also have little effect on the association constant although a combination of both the 7-chloro group and the terminal diethylamino group (*ie* **74** and *CQ*) increase the association constant significantly (around 7 fold). It has been recently found that the quinolines in Figure 4.5A do in fact, form complexes with Fe(III)PPIX but with association constants 300-10 000 fold weaker (log K ≈ 1.5) than those observed for the quinolines in Figure 4.5B (Smith, Egan and Marques, unpublished results). The 7-fold increase in the binding constant observed for **74** and *CQ* is therefore small in comparison to the association constants observed for those quinolines that do not bind strongly. Furthermore, the Fe(III)PPIX association constants obtained for all the quinolines used in this study are within the range of known antimalarials and antiplasmodials (Figure 4.7A). Since no significant correlation was found between the strength of Fe(III)PPIX association and antiplasmodial activity (Figure 4.7B), it appears that the strength of binding to the Fe(III)PPIX target is not a sufficient requirement for antiplasmodial activity.

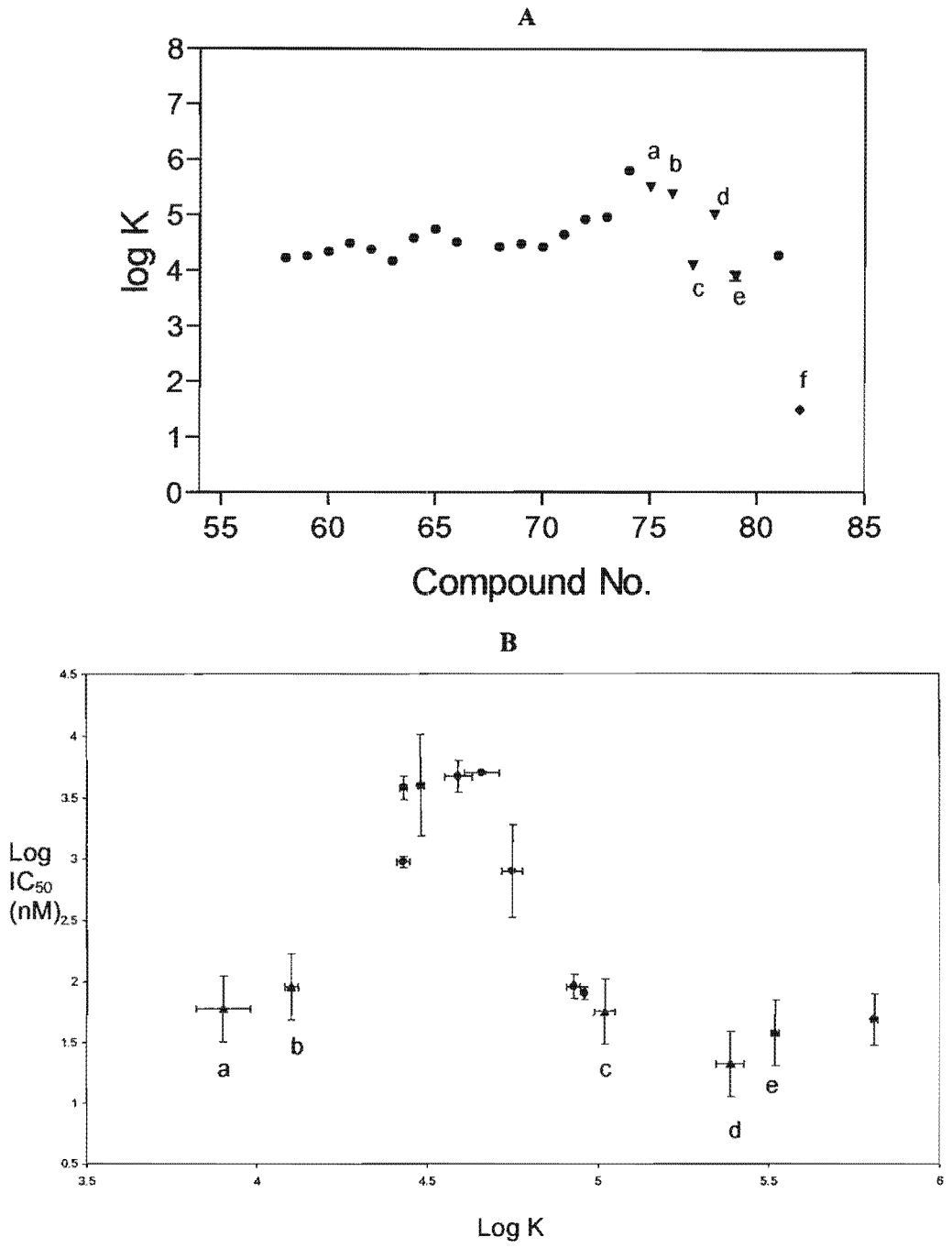

Figure 4.7. (A) Comparison of log K values for association between Fe(III)PPIX and the synthesised *CQ* analogues (**58 – 66, 68 - 74, 81**) (black circles). Triangles correspond to the log K values obtained for known antimalarial drugs and refer to (a) *CQ*, (b) amodiaquine, (c) quinacrine, (d) quinine and (e) quinidine. The weakly associating compound (**27b**) is shown for comparison (f). (B) Plot of log IC_{50} vs log K for the synthesised *CQ* analogues whose IC_{50} values are below 10 000nM (circles) and for the known antimalarial drugs (triangles) which refer to (a) mefloquine, (b) quinine, (c) quinidine, (d) amodiaquine, (e) chloroquine.

The molecular basis for the specific interaction of *2AQ* and *4AQ* with haematin is not clear. These two molecules have however substantially higher pK_as than the other aminoquinolines as a result of the unique resonance stabilised cations which retain the benzenoid structure of the carbocyclic ring (*2AQa* and *4AQa*, Scheme 4.1. and Table 4.2) (Barton and Ollis 1979). At the pH of the binding experiment (pH 7.4), *4AQ* is predominantly in the protonated form, whilst *2AQ* is 47% protonated. By contrast, the other quinolines are almost exclusively deprotonated which seems to suggest that complex formation may involve a π-cation interaction. The association constant of *4AQ* was however found to be pH–insensitive down to pH 5.5 (log K = 4.57 ± 0.02) and quinoline and *3AQ* still failed to form a complex with haematin at this lower pH where these molecules are 22% protonated. Presumably the ability to associate thus stems from the electronic distribution in these molecules, rather from their protonation state although the exact nature of these interactions is still unknown.

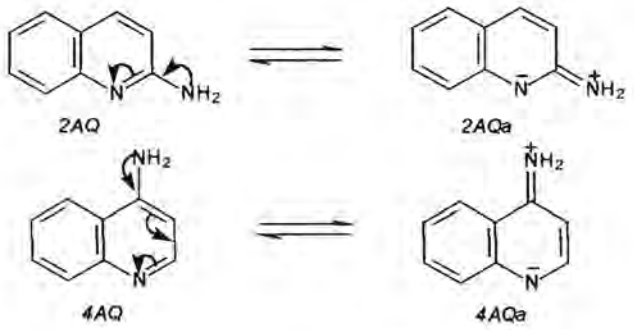

Scheme 4.1. Unique resonance forms of 2-and 4-aminoquinoline

Table 4.2 The pK_a values of the aminoquinolines (Barton and Ollis 1979 {262}).

Aminoquinoline	pK_a[a]
quinoline	4.94
2AQ	7.34
3AQ	4.95
4AQ	9.17
5AQ	5.51
6AQ	5.62
7AQ	6.65
8AQ	3.93

[a] Barton and Ollis 1979

4.4.2. Structural Requirements for β-Haematin Inhibition

It was found that the 4-aminoquinolines in Figure 4.8A do not strongly inhibit β-haematin formation and the quinolines in Figure 4.8B do strongly inhibit β-haematin formation.

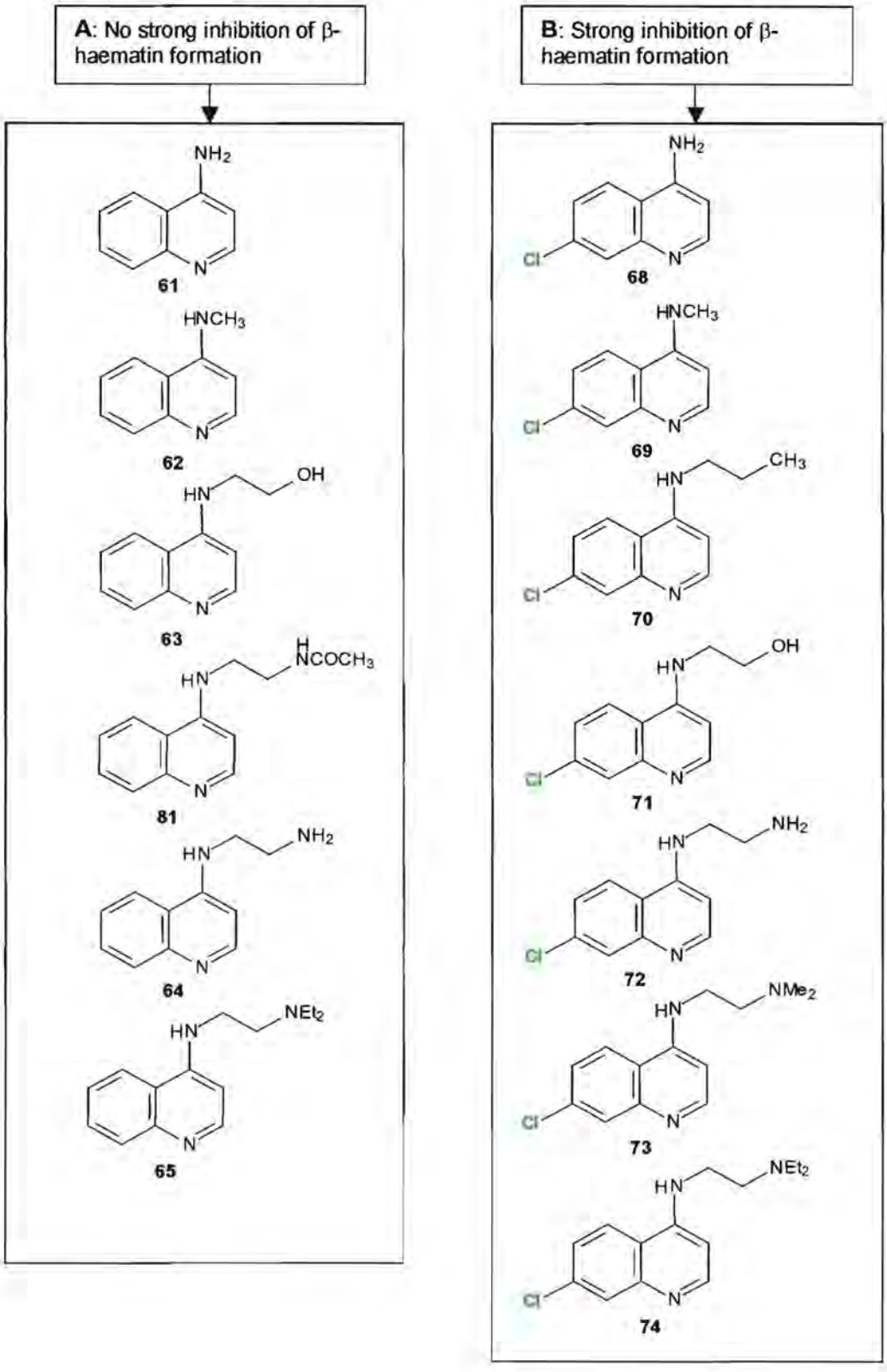

Figure 4.8. Structures of 4-aminoquinolines that all associate strongly with Fe(III)PPIX and (**A**) do not to strongly inhibit β-haematin formation and (**B**) strongly inhibit β-haematin formation.

It is immediately evident from Figure 4.8 that all the 4-aminoquinolines with a chloro-group at the 7-position, strongly inhibit β-haematin formation. This effect appears to be independent of the presence of a side chain or a terminal amino group. The ability to strongly inhibit β-haematin formation also appears to be independent of the strength of association with Fe(III)PPIX which is clearly demonstrated by **61**, **66** and **68** which all have virtually identical log K values yet only **68** which contains a chloro-group at the 7-position, strongly inhibits β-haematin formation (Figure 4.9.).

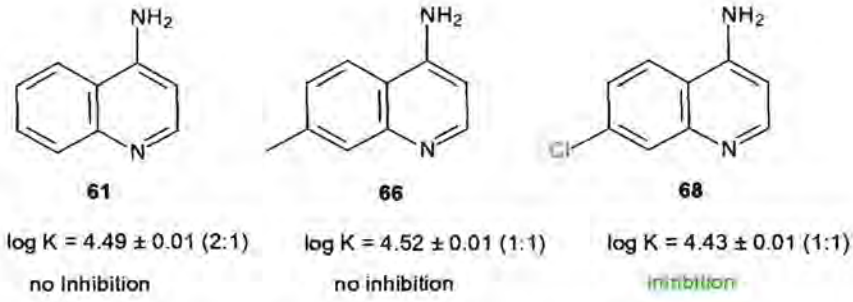

Figure 4.9. Critical structural feature in *CQ* responsible for β-haematin inhibition. The association model used is included in parenthesis.

Although the strength of association with Fe(III)PPIX does not distinguish between quinolines that do or do not inhibit β-haematin formation, it was found that all compounds that strongly inhibit β-haematin, also associate strongly with Fe(III)PPIX. Furthermore, not all quinolines that strongly inhibit β-haematin formation exhibit strong antiplasmodial activity although all strongly active antiplasmodials are able to strongly inhibit β-haematin formation.

4.4.3. Structural Requirements for Antiplasmodial Activity

All the 4-aminoquinolines can be divided into three catagories: those that are inactive (IC_{50} > 10 000nM) (Figure 4.10A), those that are weakly active (IC_{50} in or around the μM range) (Figure 4.10B) and those that are strongly active (IC_{50} < 100nM) (Figure 4.10C).

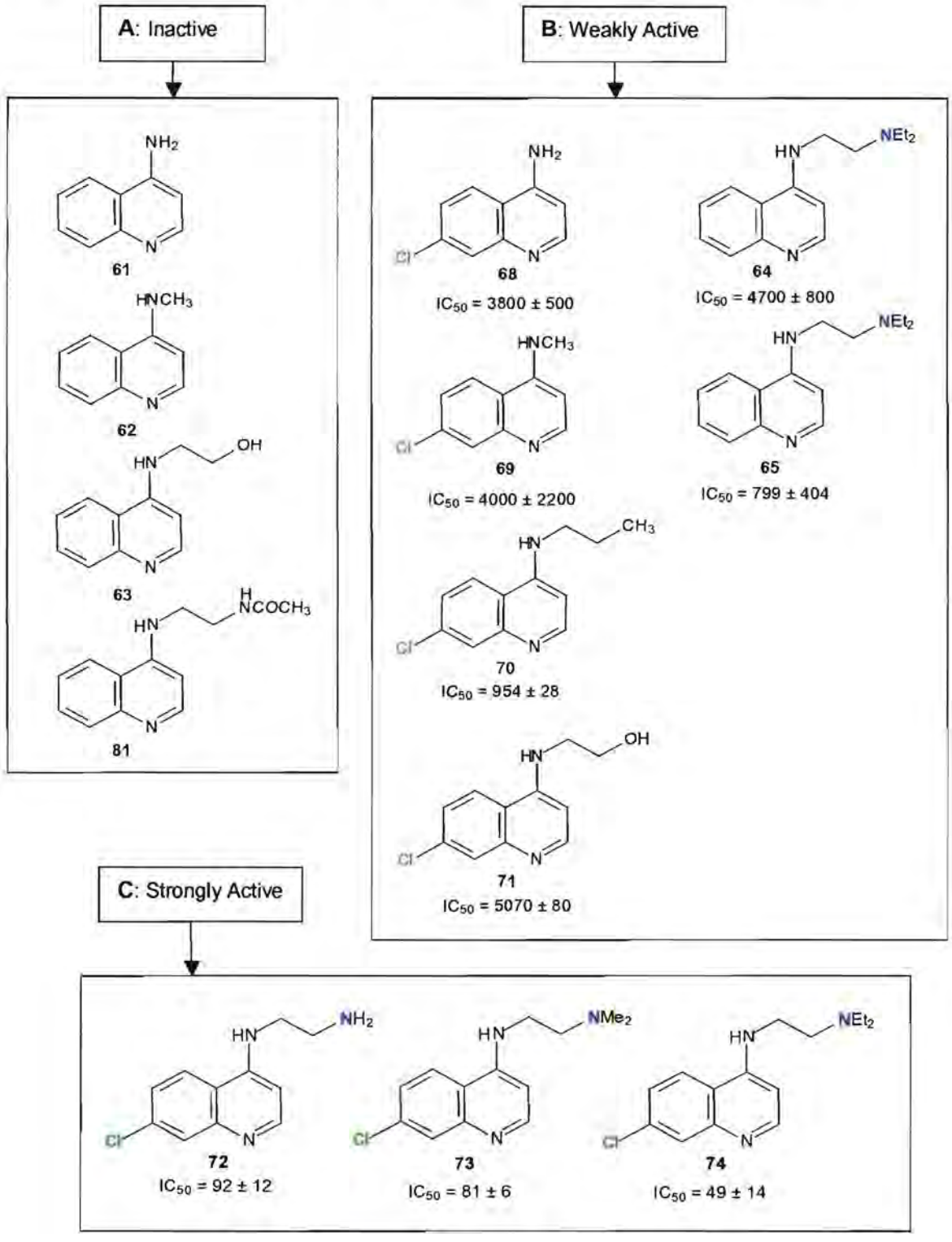

Figure 4.10. 4-Aminoquinolines that are (A) inactive (IC_{50} >10 000nM) , (B) weakly active and (C) strongly active (IC_{50} < 100nM) against the *CQ*-sensitive D10 strain of *P. falciparum*. Activities and standard deviations shown below each compound in nM.

It is immediately evident from Figure 4.10, that the strongly active 4-aminoquinolines (**72**, **73** **74** and *CQ*) are those that form strong complexes with Fe(III)PPIX, strongly inhibit β-haematin formation and contain a terminal amino side chain presumably for accumulation in the food vacuole via pH trapping. These observations are in line with our hypothesis that pH trapping of the diprotic base in the food vacuole contributes significantly towards the overall cellular accumulation (see section 1.5.3.3.2.), which in turn is important to drive formation of the quinoline-haematin complex through Le Chatelier's principle and to reach the concentrations required to inhibit β-haematin formation.

This hypothesis is further supported by the compounds (**68**, **69**, **70** and **71**) that strongly inhibit β-haematin formation but do not have a terminal amino group to bring about strong accumulation, and in turn exhibit only weak antiplasmodial activity (between 25 and 125 times less active than *CQ*)[a]. Compounds **64** and **65** exhibit limited antiplasmodial activity (4700nM and 800nM respectively) despite showing no evidence of strong β-haematin inhibition. This observation however is not contradictory to the SAR hypothesis as both compounds would be expected to accumulate to high concentrations in the food vacuole where they may act via an alternative mechanism. Furthermore, it is not known what effect replacement of the 7-chloro-group with hydro-group may have on the pK_a of the quinoline ring nitrogen. Since chloro is electron withdrawing, it is possible that this group may lower the pK_a of the quinoline ring nitrogen relative to hydro. The 7-hydro compounds may therefore accumulate more strongly in the food vacuole than the 7-chloro derivatives where at these higher concentrations they may inhibit β-haematin formation. These ideas are expanded further in Chapter 5.

Finally compounds which fail to inhibit β-haematin formation (**55 – 66**) and are not expected to accumulate more than 100 fold in the food vacuole (except for **60**) all show no significant antiplasmodial activity.

It has been found (Vippagunta *et al.* 1999), that the *CQ* analogue lacking a terminal amino group (**95**) still retains strong antiplasmodial activity (Figure 4.11). This result is however at odds with our SAR hypothesis and with a previous result that the *CQ* analogue with a

[a] The presence of the basic quinoline nitrogen will cause some accumulation, but in the absence of the terminal amino group this will be about 100 fold lower, accounting for the ~ 100 fold lower activity.

terminal hydroxy group (**96**) exhibits much reduced activity (Gasquet *et al.* 1987). The result of Vippagunta *et al.* is also at odds with the observed result that **70** has greatly reduced activity relative to **74** (Figure 4.11).

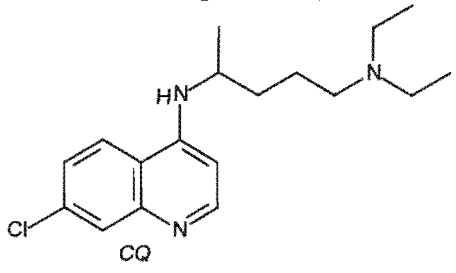

CQ

IC_{50} (nM) = 13 (NF54)[a]

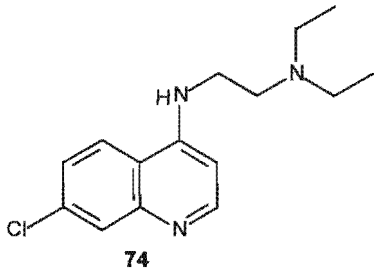

74

IC_{50} (nM) = 48 (D10)

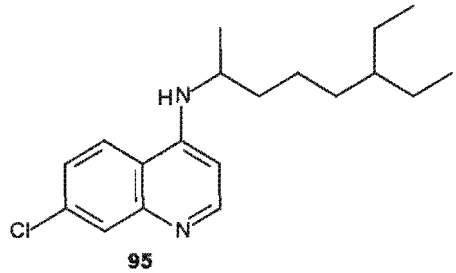

95

IC_{50} (nM) = 54 (NF54)[a]

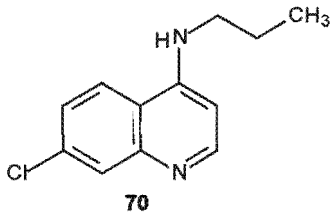

70

IC_{50} (nM) = 954 (D10)

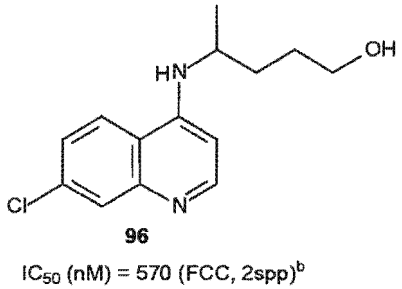

96

IC_{50} (nM) = 570 (FCC, 2spp)[b]

Figure 4.11. The quinoline analogue lacking a terminal amino group in the side chain **70** exhibits much reduced activity against the *CQ*- sensistive strain D10 relative to **74**. This result is at odds with the findings of Vippagunta *et al.* who found **95** had only 4-fold reduced activity relative to *CQ* against the *CQ*-sensitive strain NF54. [a] Vippagunta *et al.* 1999, [b] Gasquet *et al.* 1987. The IC_{50} has been normalised relative to the value obtained for *CQ* against the FCC strain and scaled for comparison with the NF54 strain

In line with the SAR hypothesis, all the 4-aminoquinolines used in this study can be classified into one of the four catagories presented in Table 4.3. 4-Aminoquinolines that do not strongly inhibit β-haematin formation and do not have a terminal amino-group for strong accumulation, have no activity against the malaria parasite (IC_{50} >10 000nM) (Category **A**). 4-Aminoquinolines that strongly inhibit β-haematin formation but do not have a terminal amino group are only weakly active (IC_{50} ~ μM) (Category **B**). Those 4-aminoquinolines that do not strongly inhibit β-haematin formation but can accumulate strongly in the food vacuole

exhibit weak activity (Category **C**) and fully active 4-aminoquinolines (Category **D**) are those that accumulate strongly in the food vacuole where they have the ability to strongly inhibit β-haematin formation.

Table 4.3. Classification of 4-aminoquinolines in into four catagories based on the SAR study in this chapter

Catagory	Examples of 4-Aminoquinolines in this Catagory	Strong β-Haematin Inhibition	Accumulation of Diprotic Weak Base	Activity
A	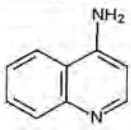	-	-	none
	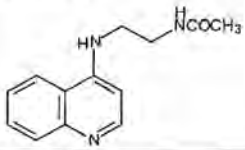	-	-	none
B	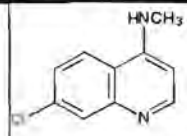	+	-	weak
	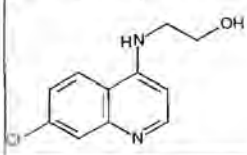	+	-	weak
C	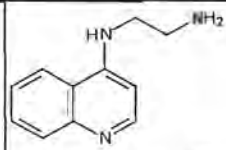	-	+	weak
	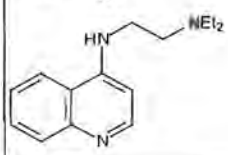	-	+	weak
D	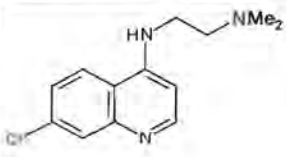	+	+	strong
	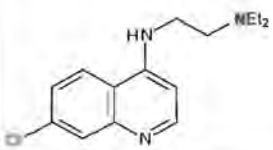	+	+	strong

These results are all in line with the hypothesis that *CQ* and related 4-aminoquinolines act by accumulating to therapeutic levels in the food vacuole, at least in part through pH trapping and that these high concentrations are required to drive the formation of a Fe(III)PPIX-quinoline complex which then inhibits haemozoin formation.

Since calculation of the predicted pH trapping of *CQ* in the food vacuole can only account for roughly 4 - 26% of the observed accumulation, and it has been recently suggested that the activity of *CQ* and *AQ* is solely dependent on saturable binding to haematin (Bray *et al.* 1998) it would appear that the saturable accumulation component is of far greater importance than the contribution from pH trapping. In this study however, the strength of association with Fe(III)PPIX was not found to be correlated to antiplasmodial activity. Fully active 4-aminoquinolines were only those that had a significant pH trapping component which suggests that the role of pH trapping in antiplasmodial activity is greater than recently suggested. That pH trapping is important is in line with the existence of a chemical equilibrium between free and the bound drug in the food vacuole of the malaria parasite. As outlined in the introduction (Section 1.5.3.3.2.), even though pH trapping may only account for roughly 4 - 26% of the observed accumulation, in its absence, the free drug concentration in the food vacuole will be significantly lowered. This will result in substantially less complex formation as predicted by Le Chateliers principle. This is supported by calculation of the cellular accumulation, in the absence of pH trapping, to be only around 8 fold (compared to 1700 fold in the presence of pH trapping).

4.5. CONCLUSIONS

This chapter brings together some useful data on 4-aminoquinolines from which the SAR profile of *CQ* in Figure 4.12. is proposed. It appears that the 4-aminoquinoline nucleus alone provides a template for complexing to Fe(III)PPIX and that complexation is not a sufficient requirement for β-haematin inhibition or antiplasmodial activity. The 7-chloro group is necessary for β-haematin inhibition and this group has little influence on the strength of association with Fe(III)PPIX. In addition, β-haematin inhibition is not a sufficient requirement for antiplasmodial activity in the absence of the terminal amino group which presumably allows the quinoline to accumulate in the food vacuole through pH trapping. A combination of the 7-chloro group and the terminal diethylamino group appears to further enhance the strength of association with Fe(III)PPIX although this effect does not appear to be critically related to antiplasmodial activity.

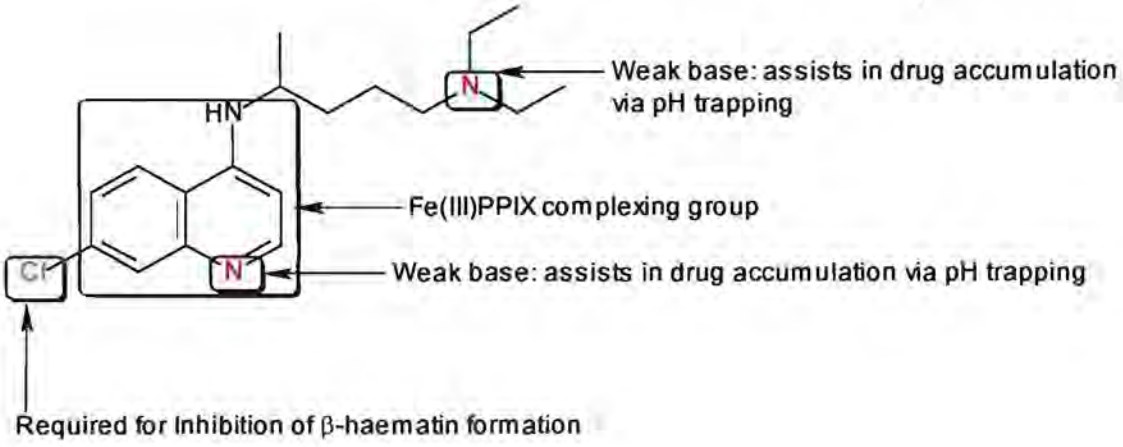

Figure 4.12. Proposed structure-activity relationships in *CQ*

The results from this study reconcile much evidence from the literature that structurally diverse analogues of *CQ* which retain the 4-amino-7-chloroquinoline nucleus but have very different side chains and contain a terminal amino group, retain strong activity against malaria parasites. This is shown in a wide range of 4-aminoquinolines (Figure 4.13) including *CQ* analogues with various straight or branched side chains (De *et al.* 1996, Ridley *et al.* 1996), analogues which have a bulky organometallic ferrocene moiety in the side chain (Biot *et al.* 1997, Chibale *et al.* 2000), numerous analogues of *AQ* which also contain a 4-amino-7-chloroquinoline nucleus and presumably act via the same mechanism (Hawley *et al.* 1996, O'Neill *et al.* 1997, Hawley *et al.* 1998), and a number a bis-quinolines (Chen 1991, Vennerstrom *et al.* 1992, Raynes *et al.* 1995, Ridley *et al.* 1997, Vennerstrom *et al.* 1998,

Raynes 1999) (Figure 4.14). Presumably these compounds are all fully active as they have a 4-aminoquinoline nucleus for association with Fe(III)PPIX, a 7-chloro group for strong inhibition of β-haematin formation, and contain a second weakly-basic quinoline ring nitrogen or basic piperazine nitrogen to assist with accumulation in the food vacuole.

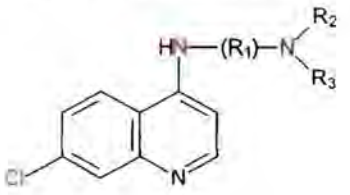

R_1	R_2	R_3	IC_{50} / nM	IC_{50} of *CQ* / nM
CH_2CH_2	CH_2CH_2	CH_2CH_2	7 (Haiti 135)[a]	8 (Haiti 135)[a]
$CH_2CH_2CH_2$	CH_2CH_2	CH_2CH_2	5 (Haiti 135)[a]	
$CH(CH_3)CH_2$	CH_2CH_2	CH_2CH_2	8 (Haiti 135)[a]	
$CH(CH_3)(CH_2)_3$	CH_2CH_2	CH_2CH_2	7 (Haiti 135)[a]	
$(CH_2)_{10}$	CH_2CH_2	CH_2CH_2	6 (Haiti 135)[a]	
$(CH_2)_{12}$	CH_2CH_2	CH_2CH_2	13 (Haiti 135)[a]	
$CH(CH_3)CH_2$	CH_3	CH_3	22 (NF54)[b]	16 (NF54)[b]

[a] De *et al.* 1996, [b] Ridley *et al.* 1996.

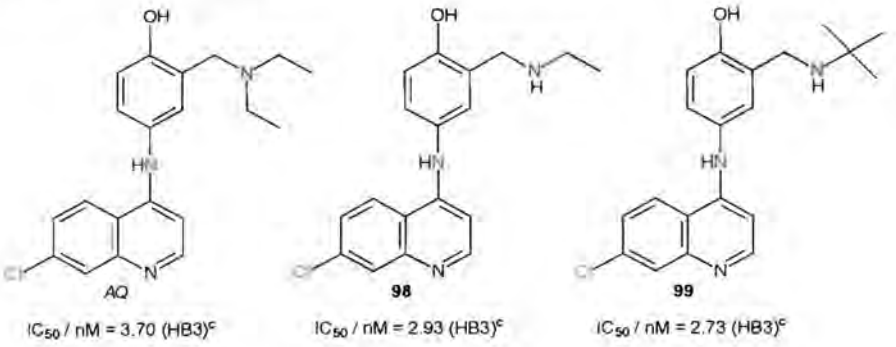

AQ

IC_{50} / nM = 3.70 (HB3)[c]

98

IC_{50} / nM = 2.93 (HB3)[c]

99

IC_{50} / nM = 2.73 (HB3)[c]

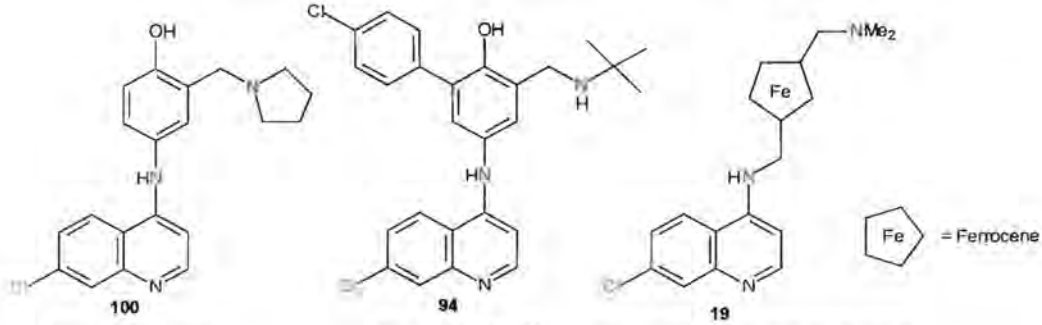

100

IC_{50} / nM = 1.74 (HB3)[c]

94

IC_{50} / nM = 0.9 (HB3)[d]

19

IC_{50} / mg/Kg^{-1} (**19**) = 75.5 (*P. Berghei*)[e]

IC_{50} / mg/Kg^{-1} (*CQ*) = 69.2 (*P. Berghei*)

= Ferrocene

Figure 4.13. 4-Aminoquinolines that have a chloro-group at the 7-position with varying side chains and a terminal amino group for accumulation all retain strong activity against malarial parasites. [a] De *et al.* 1996, [b] Ridley *et al.* 1996, [c] Hawley *et al.* 1996, [d] O' Neill *et al.* 1997, [e] Biot *et al.* 1997.

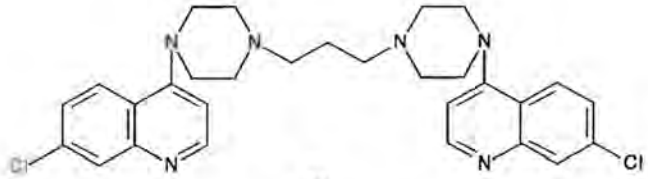

20

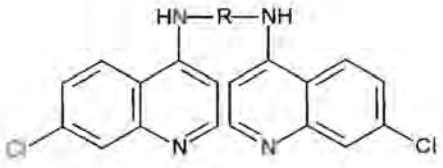

21

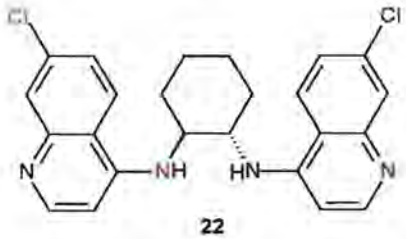

22

Figure 4.14. Some bis-quinolines that retain activity against malaria parasites are **20** (Chen 1991), **21** (Vennerstrom *et al.* 1992) and **22** (Ridley *et al.* 1997, Vennerstrom *et al.* 1998).

It is important to note that the SAR hypothesis proposed above only pertains to 4-aminoquinolines and does not include the quinoline methanols (ie mefloquine and quinine) or the 8-aminoquinolines (primaquine) which will likely have their own unique SAR profile.

QUANTITATIVE STRUCTURE-ACTIVITY RELATIONSHIPS IN 4-AMINOQUINOLINE ANTIPLASMODIALS

5.1 BACKGROUND

The current debate regarding the mode of action of *CQ*-related 4-aminoquinoline antimalarials is centred around whether these compounds exert a toxic effect solely through haemozoin inhibition or whether an alternative haem detoxification mechanism exists and that these compounds act by inhibition thereof (see Section 1.5.4.4). In Chapter 4, qualitative evidence was found in support of the hypothesis that *CQ*-related 4-aminoquinoline antimalarials and antiplasmodials act by accumulating to therapeutic levels in the food vacuole of the malaria parasite through a strong pH trapping component, where they exert a toxic effect by inhibiting haemozoin formation. In this study, the 7-chloro group on the 4-aminoquinoline nucleus alone was identified as the critical structural feature necessary for β-haematin inhibition. Further evidence that the substituent at the 7-position in 4-aminoquinoline antiplasmodials is of critical structural significance for β-haematin inhibition, and that β-haematin inhibition is directly related to the antiplasmodial activity is shown in a SAR study in which the 7-chloro group in *CQ* was replaced with nitro-, bromo-, hydro- and amino-groups (Vippagunta *et al.* 1999) (Table 5.1.). Here, the 7-nitro and 7-bromo analogues of *CQ* were found to strongly inhibit β-haematin formation and exhibit strong antiplasmodial activity against malaria parasites. Conversely, the 7-hydro and 7-amino analogues of *CQ* were found not to inhibit β-haematin formation and showed only weak activity against malaria parasites. In addition, De *et al.* showed that analogues of *CQ* in which the 7-chloro group had been replaced with iodo- or bromo- groups were fully active against malarial parasites whereas the 7-trifluoromethyl, 7-fluoro and 7-methoxy analogues were about 2 and 7 fold less active than *CQ* respectively (Table 5.1.). In support of the findings in Chapter 4, that the side chain in *CQ* and related 4-aminoquinolines serves only as a linker between the structurally significant features responsible for antiplasmodial activity, De *et al.* found that 7-substituted 4-aminoquinolines with a short, linear 2-C side chain or a short, isopropyl side chain had essentially the same antiplasmodial activity as the corresponding *CQ* analogues (De *et al.* 1998). Although none of these analogues were tested for β-haematin inhibitory activity, their antiplasmiodial activities appeared to depend solely on the group at the 7-position which has been identified as the structural feature responsible for β-haematin inhibition (Chapter 4). It can therefore be speculated that the

differences in antiplasmodial activities observed between these analogues may reflect their varying abilities to inhibit β-haematin formation.

Table 5.1. Apparent relationship between the group at the 7-position of *CQ* and two other short chain 4-aminoquinolines, and antiplasmodial activity

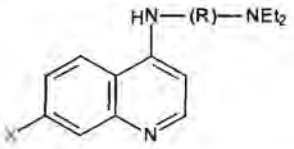

X	R	β-Haematin Inhibition IC_{50} / μM	IC_{50} / nM
***CQ* sensitive strain**			**NF54**[a]
Cl (*CQ*)	$CH(CH_3)(CH_2)_3$	15 ± 5	13
Br	$CH(CH_3)(CH_2)_3$	18 ± 2	93
NO_2	$CH(CH_3)(CH_2)_3$	100 ± 10	15
H	$CH(CH_3)(CH_2)_3$	>2500	350
NH_2	$CH(CH_3)(CH_2)_3$	>2500	2600
			Haiti 135[b, d]
Cl (*CQ*)	$CH(CH_3)(CH_2)_3$	Nd[c]	8[b]
	CH_2CH_2	Nd	7[d]
	$CH(CH_3)CH_2$	Nd	8[d]
I	$CHCH_3(CH_2)_3$	Nd	4[b]
	CH_2CH_2	Nd	6[b]
	$CH(CH_3)CH_2$	Nd	7[b]
Br	$CH(CH_3)(CH_2)_3$	Nd	5[b]
	CH_2CH_2	Nd	7[b]
	$CH(CH_3)CH_2$	Nd	11[b]
F	$CH(CH_3)(CH_2)_3$	Nd	20[b]
	CH_2CH_2	Nd	35[b]
	$CH(CH_3)CH_2$	Nd	30[b]
CF_3	$CH(CH_3)(CH_2)_3$	Nd	16[b]
	CH_2CH_2	Nd	30[b]
	$CH(CH_3)CH_2$	Nd	50[b]
OCH_3	$CH(CH_3)(CH_2)_3$	Nd	55[b]
	CH_2CH_2	Nd	48[b]
	$CH(CH_3)CH_2$	Nd	94[b]

[a] Vippagunta *et al.* 1999, [b] De *et al.* 1998, [c] not determined, [d] De *et al.* 1996.

Since the presence of the 7-chloro group on the 4-aminoquinoline nucleus appears to be directly responsible for β-haematin inhibition, it was decided to synthesise a series of 4-aminoquinolines which retain all of the structural features identified in Chapter 4 as required for strong antiplasmodial activity, and differ only with respect to the group at the 7-position. These 7-substituted analogues were then used as probes to ascertain if a quantitative relationship exists between β-haematin inhibition and antiplasmodial activity.

In this regard, it was decided to synthesise a series of quinolines (Figure 5.2.) with (i) an amino group at the 4-position to ensure strong association with Fe(III)PPIX, (ii) the simplest possible side chain with a terminal amino group to ensure strong accumulation at the site of action in the food vacuole and (iii) with variation in the substituent at the 7-position to test the hypothesis that β-haematin inhibition is directly responsible for antiplasmodial activity. Even though all these 4-aminoquinoline analogues contain a terminal amino group for strong accumulation, it is possible that variation of the group at the 7-position may influence the pK_a of the quinoline ring nitrogen and therefore the relative extent of accumulation between analogues. It was therefore decided to measure the pK_a's of the 4-aminoquinoline analogues in order to correct, if necessary, for this effect.

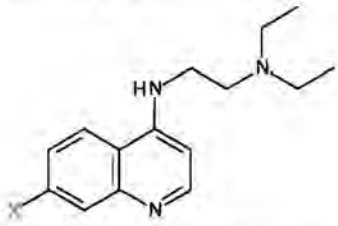

X	No.
NH_2	**83**
OH	**82**
OCH_3	**78**
H	**65**
CH_3	**67**
F	**75**
I	**77**
Br	**76**
Cl	**74**
CF_3	**80**
NO_2	**79**

Figure 5.2. N^2-(7-X-4-quinolinyl)-N^1,N^1-diethyl-1,2-ethanediamine analogues used in the study

5.2. EXPERIMENTAL METHODS

5.2.1. Synthesis of the N^2-(7-X-4-quinolinyl)-N^1,N^1-diethyl-1,2-ethanediamine Analogues

The N^2-(7-X-4-quinolinyl)-N^1,N^1-diethyl-1,2-ethanediamine analogues, where X = NH_2, OH, OCH_3, H, CH_3, F, I, Br, Cl, CF_3 and NO_2 were all synthesised according to the procedures outlined in Chapter 2 (see Section 7.1.2. for experimental details). To ensure analytical purity of all the compounds, microanalysis for all the solids and HRMS for the oils were obtained.

5.2.2. Spectrophotometric Titrations

The association constants between Fe(III)PPIX and the 4-aminoquinoline analogues were determined by spectrophotometric titration in aqueous 40% DMSO mixtures according to the procedures outlined in Section 4.2.2 (see section 7.2.3 for experimental details). The raw titration data and plots thereof fitted to either a 1:1 or 2:1 (quinoline:haematin) association model (derived in Chapter 7.2.3.5) appear in Appendix 1 and 2.

5.2.3. β-Haematin Inhibition

5.2.3.1. IR Method (Egan *et al.* 1994)

Qualitative data for β-haematin inhibition were obtained for the 4-aminoquinoline analogues by the infrared method of Egan *et al.* which is described in Section 4.2.3. (see Section 7.2.4. for experimental details and Appendix 3 for the infra red spectra). In short, this method unequivocally distinguishes between inhibitory and non-inhibitory compounds by examination of the infrared spectrum of the product formed in the β-haematin reaction. All compounds were tested at 4 equivalents relative to haematin, a mole ratio that is inhibitory in the case of *CQ*. A positive result therefore implies that the compound has comparable inhibitory activity to *CQ*, and a negative result implies that the compound is significantly less inhibitory than *CQ*.

5.2.3.1. BHIA Method (Parapini *et al.* 2000)

The 4-aminoquinoline analogues were sent to Prof. D. Taramelli (Institute of Microbiology, University of Milan) for testing using the BHIA (beta-haematin inhibitory activity) assay

(Parapini *et al.* 2001) in order to obtain quantitative β-haematin inhibitory results. This method is based on the differential solubilisation of the starting material (haematin) and the product (β-haematin) in DMSO and NaOH solution respectively. In this method, the $BHIA_{50}$ value corresponds to the number of equivalents of 4-aminoquinoline required to obtain 50% percent inhibition of β-haematin formation relative to a control experiment under the same experimental conditions.

5.2.4. pK_a Determinations

The pK_a's of the 4-aminoquinolines were determined by glass electrode potentiometric titration according to the methods of Jackson *et al.* 1996 (see Section 7.2 for experimental details) and the data were analysed by Thembalani E Nomkoko (Department of Chemistry, University of Cape Town) using the program ESTA (May *et al.* 1985, May *et al.* 1988). In each case two pK_a values were obtained.

5.2.5. Antiplasmodial Testing

All the 4-aminoquinolines were sent to Prof. D. Taramelli (Institute of Microbiology, University of Milan) for antiplasmodial testing against the *CQ*-sensitive D10 strain of malaria parasite. No attempt was made to investigate the activities against a *CQ*-resistant strain as in these systems, the reduced uptake or enhanced efflux mechanism is likely to mask the inherent mechanism of action of the 4-aminoquinoline antiplasmodials.

5.2.6. Statistical Correlations

The statistical correlations were performed using the computer programs EXCEL and GPAPHPAD PRISM 3.0. In all cases where the p value was < 0.05, the correlations were considered to be significant.

5.3. RESULTS

All the physical constants and biological results obtained for the 4-aminoquinoline analogues are presented in Table 5.2. These include: association constants between Fe(III)PPIX and the 4-aminoquinoline, β-haematin inhibitory activities from the infrared assay and the BHIA assay, two pK_a's obtained for each compound and the antiplasmodial activity against the *CQ*-sensitive D10 strain of malaria parasite. Also listed in Table 5.3 are the meta- and para-Hammett constants (σ_m and σ_p respectively) and lipophilicity constants (π) for the substituents (-X) (Hansch 1979). The meta- and para-Hammettt constants give a relative empirical measure of the meta and para π-electron withdrawing abilities of the substituent on an aromatic ring. Positive values of σ indicate electron withdrawal from the aromatic system and negative σ values indicate electron release into the aromatic system. The lipophilicity values give an indication of the relative affinity of the group towards organic-like or aqueous-like phases. Positive values indicate that the group is lipophilic (partitions preferably into an organic phase) and a negative value indicates that the group is hydrophilic (partitions preferably into an aqueous phase).

Table 5.2. Experimentally determined Fe(III)PPIX-quinoline association constants, acid dissociation constants, β-haematin inhibitory activity using the infrared and BHIA methods and antiplasmodial activity[a]

No.	-X	pK_{a1}[b]	pK_{a2}[b]	log K[c]	βHI[d]	$BHIA_{50}$[e]	IC_{50} / nM[f]
83	NH_2	8.36 ± 0.02	10.02 ± 0.01	4.35 ± 0.02	-	>20	>5000
82	OH	6.82 ± 0.01	8.953 ± 0.007	4.48 ± 0.02	-	>20	3071 ± 112
78	OCH_3	8.094 ± 0.002	9.495 ± 0.002	4.83 ± 0.01	-	>20	448 ± 40
65	H	7.964 ± 0.003	9.422 ± 0.002	4.75 ± 0.03	-	>20	1060 ± 103
67	CH_3	8.118 ± 0.006	9.508 ± 0.004	4.86 ± 0.01	-	17 ± 4	82 ± 6
75	F	7.62 ± 0.01	9.241 ± 0.009	4.60 ± 0.02	-	9.7 ± 0.8	138 ± 26
77	I	7.48 ± 0.02	7.79 ± 0.06	5.02 ± 0.02	+	2.8 ± 0.2	35 ± 3
76	Br	7.93 ± 0.02	7.97 ± 0.04	4.99 ± 0.01	+	4.4 ± 0.7	36 ± 1
74	Cl	7.56 ± 0.02	8.83 ± 0.01	5.81 ± 0.01	+	2.2 ± 0.2	37 ± 3
80	CF_3	7.50 ± 0.02	7.65 ± 0.03	4.67 ± 0.02	+	8 ± 2	99 ± 29
79	NO_2	6.28 ± 0.03	8.80 ± 0.02	4.65 ± 0.02	+	3.1 ± 0.6	325 ± 170
CQ		8.55 ± 0.05	9.81 ± 0.04	5.52 ± 0.02	+	1.7 ± 0.8[g]	30 ± 1

[a] All data represents an average of three independent determinations, errors represent one SD for pK_a determinations and one SEM for the remaining data, [b] at 25°C, 0.15M NaCl background electrolyte, [c] at 25°C, pH

7.5, 20mM HEPES buffer, 40% DMSO (aq). Data fitted to a 1:1 association model, [d] Positive (+) or negative (-) result obtained for β-haematin inhibition assayed by the infrared method at 4eq of 4-aminoquinoline relative to haematin, [e] β-haematin inhibitory activity in equivalents of 4-aminoquinoline relative to haematin causing 50% inhibition, [f] Concentration required to kill 50% of the *CQ*-sensitive D10 strain of malaria parasite, [9] Parapini *et al.* 2001.

Table 5.3. The para- and meta-Hammett constants and the lipophilicity constants

-X	σ_p [a]	σ_m [b]	π [c]
NH_2	-0.66	-0.16	-1.23
OH	-0.37	0.12	-0.67
OCH_3	-0.27	0.12	-0.02
H	0	0	0
CH_3	-0.17	-0.07	0.56
F	0.06	0.34	0.14
I	0.18	0.35	1.12
Br	0.23	0.39	0.86
Cl	0.23	0.37	0.71
CF_3	0.54	0.43	0.88
NO_2	0.78	0.71	-0.28

[a] para Hammett constant , [b] meta Hammett constant, [c] lipophilicity constant from Hansch and Leo 1979.

5.4. DISCUSSION

5.4.1. Effect of the group at the 7-Position on pK_{a1} and pK_{a2}

As seen from Table 5.2, the pK_a of the quinoline ring nitrogen (pK_{a1}) is strongly dependent on the nature of the group at the 7-position. This value varies over a range of 2 log units with the 7-nitro analogue having the lowest value (6.28 ± 0.03) and the 7-amino analogue having the highest value (8.36 ± 0.02). These findings suggest that good π-electron donors (eg. NH_2) raise the pK_a of the quinoline ring nitrogen whereas strong π-electron withdrawing groups (eg. NO_2) decrease the pK_a of the quinoline ring nitrogen. With the exception of the OH derivative, this is supported by the existence of good statistical correlations between pK_{a1} and the meta- or para- Hammett constants (σ_m or σ_p respectively in Table 5.3) (Figure 5.3). The apparently anomalous behaviour of the OH derivative may be an indication that the pK_a of this derivative could correspond to deprotonation of the OH group rather than deprotonation of the quinolinium nitrogen.

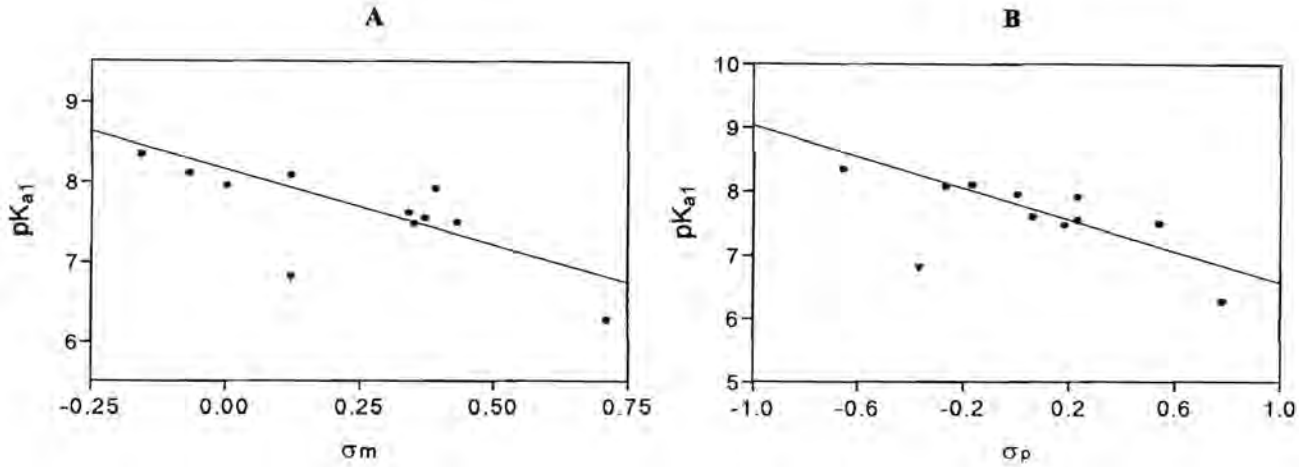

Statistical Variables	A	B
r^2	0.77	0.75
p	0.0009	0.001
Derivation from Zero	Significant	Significant
Equation Describing pK_{a1}	$-1.70\sigma_m + 8.01$	$-1.23\sigma_p + 7.80$

Figure 5.3. Statistical correlations between the quinoline ring nitrogen pK_a (pK_{a1}) and the meta- (A) and (B) para-Hammett constants (σ_m and σ_p respectively) of the group at the 7-position on the quinoline ring. (•) experimental data points (excluding the 7-OH derivative (▾)). The straight line represents the best fit of the data to a linear equation. Error bars represent one standard deviation of the mean and are smaller than the plotted symbols.

That a relationship exists between the electronic characteristics of the group at the 7-position and the pK_a of the quinoline ring nitrogen is to be expected when considering their resonance relationship through the π quinoline ring system (Figure 5.4). It is somewhat surprising however, that the group at the 7-position has a large effect on the pK_a of the terminal amino group (pK_{a2}) (Table 5.2). The values of pK_{a2} for the 7-substituted 4-aminoquinolines ranges over 2.4 log units with the 7-NH_2 analogue having the highest value (10.02 ± 0.01) and the 7-CF_3 analogue having the lowest value (7.65 ± 0.03). Again a relationship exists between both the meta- and para-Hammettt constants of the group at the 7-position and the value of pK_{a2} (Figure 5.5) although in both cases it is far poorer than that exhibited for pK_{a1}.

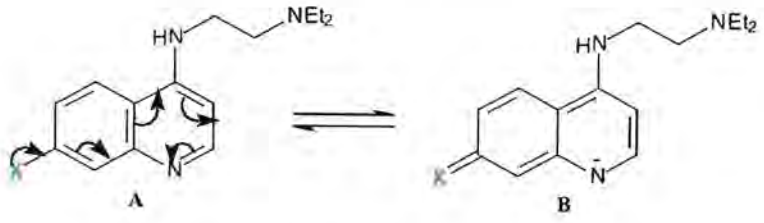

Figure 5.4. Resonance relationship between the group at the 7-position and the quinoline ring nitrogen

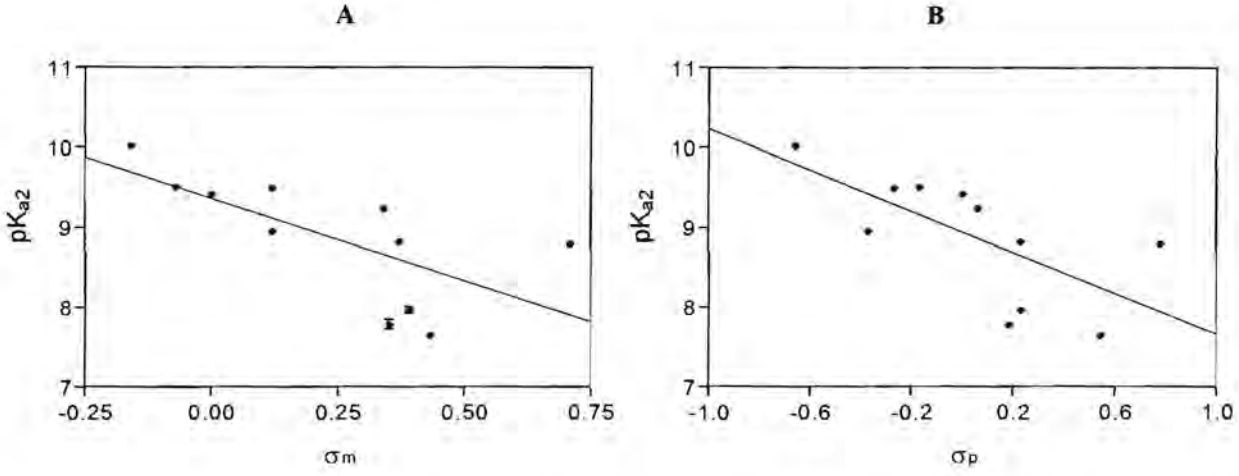

Statistical Variables	A	B
r^2	0.46	0.46
p	0.02	0.02
Derivation from Zero	Significant	Significant
Equation Describing pK_{a1}	$-2.06\sigma_m + 9.37$	$-1.29\sigma_p + 8.94$

Figure 5.5. Statistical correlations between the terminal amino group pK_a (pK_{a2}) and the meta- (A) or para-(B) Hammett constants (σ_m or σ_p respectively) of the group at the 7-position on the quinoline ring. The straight line represents the best fit of the data to a linear equation based on σ_m (for A) and σ_p (for B), Error bars represent one standard deviation of the mean and are smaller than the plotted symbols in most cases.

The more substituted, lengthened side chain in *CQ* appears to increase both pK_{a1} and pK_{a2} relative to the 2-C side chain in the 7-chloro derivative (**74**) (Table 5.4.). This is presumably due to the enhanced σ-electron donating ability of the more substituted side chain in *CQ* onto the quinoline ring nitrogen and the terminal-amino nitrogen. It is possible that this through-space interaction between the group at the 7-position and the terminal amino group in the 7-substituted 4-aminoquinolines would be lessened in an analogous family of 7-substituted *CQ* analogues. It is therefore possible, that the pK_{a2} values in a corresponding

set of *CQ* analogues would be similar to that of *CQ*, and that the pK_{a1} values would be slightly higher than the analogous values for the 7-substuituted analogues used in this study.

Table 5.4. Comparison between pKa_1 and pK_{a2} obtained for *CQ* and **74**.

	pK_{a1}	pK_{a2}
CQ	8.55 ± 0.05	9.81 ± 0.04
74	7.56 ± 0.02	8.83 ± 0.01

5.4.2. Relationship Between β-Haematin Inhibition and Antiplasmodial Activity

In agreement with the findings in Chapter 4, no quantitative relationship was found between the strength of Fe(III)PPIX association and antiplasmodial activity for the 7-substituted 4-aminoquinoline analogues (Figure 5.6A). Furthermore, no significant correlation was found between the strength of β-haematin inhibition and antiplasmodial activity (Figure 5.6B).

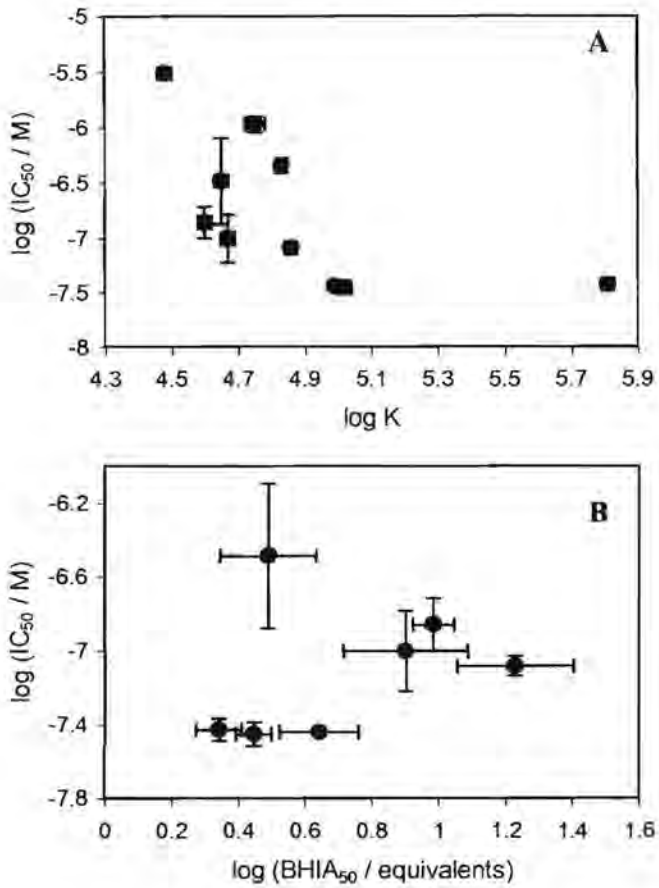

Variables	r^2	P value	Deviation from zero
log IC_{50} vs log K	0.39	0.053	Not significant
log IC_{50} vs $BHIA_{50}$	0.08	0.55	Not significant

Figure 5.6. Graphs and statistical variables demonstrating the lack of significant correlation between antiplasmidial activity and (**A**) log K and (**B**) log $BHIA_{50}$. The straight line represents the best fit of the data to a linear equation. Error bars represent one standard error of the mean.

The lack of any apparent correlation between antiplasmodial activity and β-haematin inhibititory activity is in line with the structure-activity hypothesis that pH trapping in addition to β-haematin inhibition is important for strong antiplasmodial activity. Since there is a substantial variation between the pK_a's of the 7-substituted 4-aminoquinoline analogues they would be expected to accumulate in the food vacuole to different extents. From knowledge of the pK_a's, the accumulation ratio (concentration of quinoline in the food vacuole relative to the medium) of each analogue from the medium (pH 7.4) into the vacuole (pH 5.5) could be calculated using Equation **1** (Box 1, See Chapter 7.2 for derivation) and the values are presented in Table 5.5.

The assumptions made in Equation **1** are that the vacuolar membrane is totally impermeable to the mono- and diprotonated 4-aminoquinoline species and that equilibrium concentrations of the neutral species is reached between external medium and vacuole. It is likely that these assumptions are not entirely correct although the predicted accumulation ratios based on Equation **1** probably give a good indication of the relative accumulation ratios between the different derivatives.

$$\frac{[Q]_v}{[Q]_e} = \left\{ \frac{1 + \frac{[H^+]_v}{K_{a2}} + \frac{[H^+]_v^2}{K_{a1}K_{a2}}}{1 + \frac{[H^+]_e}{K_{a2}} + \frac{[H^+]_e^2}{K_{a1}Ka2}} \right\} \qquad (1)$$

Here $[Q]_v$ refers to the total vacuolar concentration of the 4-aminoquinoline and $[Q]_e$ refers to its total extravacuolar concentration. The terms $[H^+]_v$ and $[H^+]_e$ refer to the vacuolar and extravacuolar hydrogen ion concentrations respectively and K_{a1} and K_{a2} refer to the first and second acid dissociation constants respectively.

Box 1. Equation **1** derived from the Hendelson-Hesselbach equation in Section 7.2.3. that was used to calculate the concentration of the quinoline in the food vacuole relative to the medium.

If the accumulation ratio for each 7-substituted analogue is normalised relative to *CQ* (α in Table 5.5), it is evident that the extent of pH trapping between the analogues varies substantially (between 9% for the 7-nitro analogue, and 97% for the 7-amino analogue relative to *CQ*). Since different vacuolar concentrations of the analogues may mask their inherent ability to exert their toxic effect, the IC_{50}'s were normalised to give an IC_{50} value that was independent of the pH trapping effect ($IC_{50} \times \alpha$) (Table 5.5).

Table 5.5. Accumulation ratios calculated from Equation 1, normalised accumulation ratios (α) and normalised IC_{50} values ($IC_{50} \times \alpha$)

No.	X	Acc. Ratio[a]	α[b]	$IC_{50} \times \alpha$ / nM[c]
83	NH_2	5693	0.966	>4830
82	OH	1347	0.228	700 ± 26
78	OCH_3	5254	0.891	399 ± 32
65	H	4963	0.842	893 ± 87
67	CH_3	5302	0.899	74 ± 6
75	F	3946	0.669	92 ± 17
77	I	2937	0.498	17 ± 1
76	Br	4607	0.781	28 ± 1
74	Cl	3706	0.628	23 ± 2
80	CF_3	2844	0.482	48 ± 14
79	NO_2	500	0.085	28 ± 15
CQ		5896	1.000	32 ± 2

[a] Vacuolar accumulation ratio calculated using Equation 1, [b] normalised vacuolar accumulation ratio relative to *CQ*, [c] normalised IC_{50}.

No significant correlation was found between the strength of Fe(III)PPIX-quinoline association and antiplasmodial activity, normalised for pH trapping, for the 7-substituted 4-aminoquinoline analogues (Figure 5.7A). An impressive correlation ($r^2 = 0.83$, $p = 0.004$) was however found between β-haematin inhibition for the analogues that had measurable $BHIA_{50}$ values (< 20 equivalents) and antiplasmodial activity normalised for pH trapping (Figure 5.7B). Furthermore, the four compounds that had $BHIA_{50}$ values above the measurable limit of the experiment, all had normalised antiplasmodial activities higher than any of the other compounds.

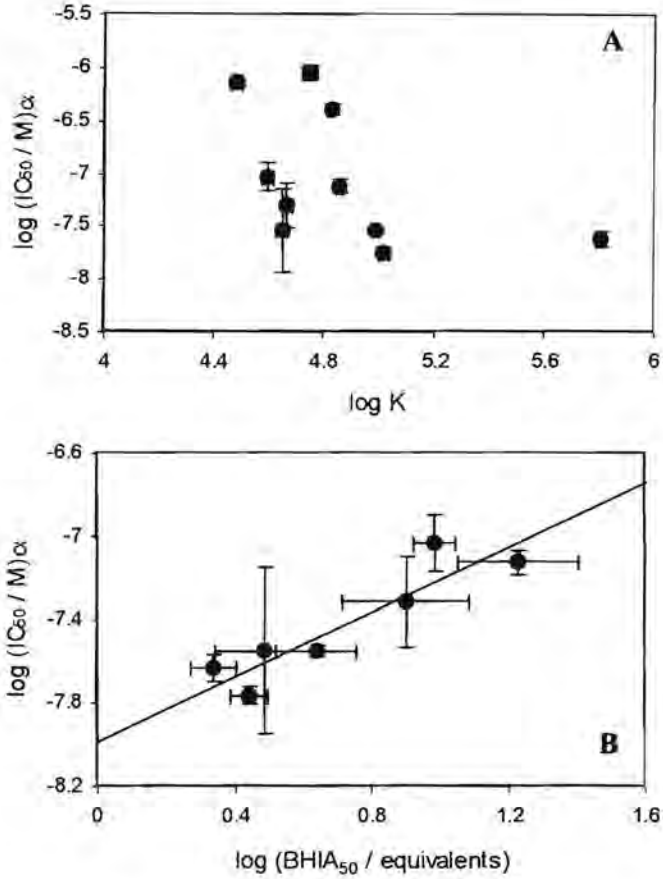

Variables	r^2	P value	Deviation from zero	Equation describing log IC_{50}
log $IC_{50} \times \alpha$ vs log K	0.24	0.15	Not significant	
log $IC_{50} \times \alpha$ vs $BHIA_{50}$	0.83	0.004	significant	$0.76(\log BHIA_{50}) - 7.98$

Figure 5.7. Graphs and statistical variables demonstrating (**A**) the lack of any significant correlation between normalised antiplasmodial activity (log $IC_{50} \times \alpha$) and log K, and (**B**) the significant correlation obtained between log $IC_{50} \times \alpha$ and log $BHIA_{50}$. The straight line represents the best fit of the data to a linear equation. Error bars represent one standard error of the mean.

In support of the findings in Figure 5.7B, Hawley *et al.* found a good correlation ($r^2 = 0.81$, $p = 0.026$) between antiplasmodial activity for *AQ*, *CQ* and a series of *AQ* analogues and β-haematin inhibition, only when the former was corrected for accumulation into a malaria infected red cell (Hawley *et al* 1998) which had been measured *in vitro* by the innoculum effect. Dorn *et al.* also observed a good correlation ($r^2 = 0.91$, $p = 0.002$) between antiplasmodial activity, uncorrected for accumulation, and β-haematin inhibition for a range of structurally diverse known antimalarial drugs (Dorn *et al.* 1998). This correlation is questionable when considering the broad spectrum of drugs that the authors included in their study of which quinine (and possibly the other quinoline methanols, mefloquine and

halofantrine) is thought to form a complex with Fe(III)PPIX via a different mechanism to the 4-aminoquinolines (see Section 1.5.3.4.). Vippagunta *et al.* also observed a modest correlation (r^2 = 0.61, p = 0.046) for a series of *CQ* analogues, between antiplasmodial activity and β-haematin inhibition, only when the former was normalised for Fe(III)PPIX binding (Vippagunta *et al.* 1999). We find no such correlation with our data (r^2 = 0.32, p = 0.19) and indeed, upon closer scrutiny of their data, it appears that the correlation may be strongly weighted by a single outlying point.

5.4.3. Insights into the Molecular Basis of Complex Formation and β-Haematin Inhibition

Evidence from this study suggests that active antiplasmodials all form strong complexes with Fe(III)PPIX, and inhibit β-haematin formation. Complex formation appears to play an indirect role in antiplasmodial activity as not all compounds that associate strongly with Fe(III)PPIX exhibit antiplasmodial activity. Also no direct relationship has been found between the strength of Fe(III)PPIX-quinoline association and antiplasmodial activity. Since complex formation appears to be a prerequisite for antiplasmodial activity it would appear that it indirectly facilitates β-haematin inhibition.

Since the structures of the Fe(III)PPIX-quinoline complexes are unknown, it is not possible to gauge what effect the 7-substituent on the 4-aminoquinoline nucleus has in influencing any particular orientation within the complex that may result in β-haematin inhibition. In order to gain some insight into the origin of these interactions, correlations were sought between the association constant and β-haematin inhibitory activity for the 7-substituted 4-aminoquinolines and tabulated empirical substituent constants (Table 5.3) using multiple correlation analysis.

It was found that a reasonable correlation exists between the association constant and the lipophilicity of the group at the 7-position (Figure 5.8A). In agreement with the findings in Chapter 4, that the 7-chloro group and the terminal amino-group appear to have a synergistic effect on increasing the strength of the association constant relative to other 4-aminoquinolines, the 7-chloro analogue (**74**) appeared to be an outlier from the other data points. Its omission renders the correlation even better (Figure 5.8B). The apparent dependence of log K on the lipophilicity is in agreement with previous observations that the π-π complex arises from hydrophobic interactions between the quinoline and Fe(III)PPIX as demonstrated by the solvent dependence of these interactions (see section 1.5.3.4.).

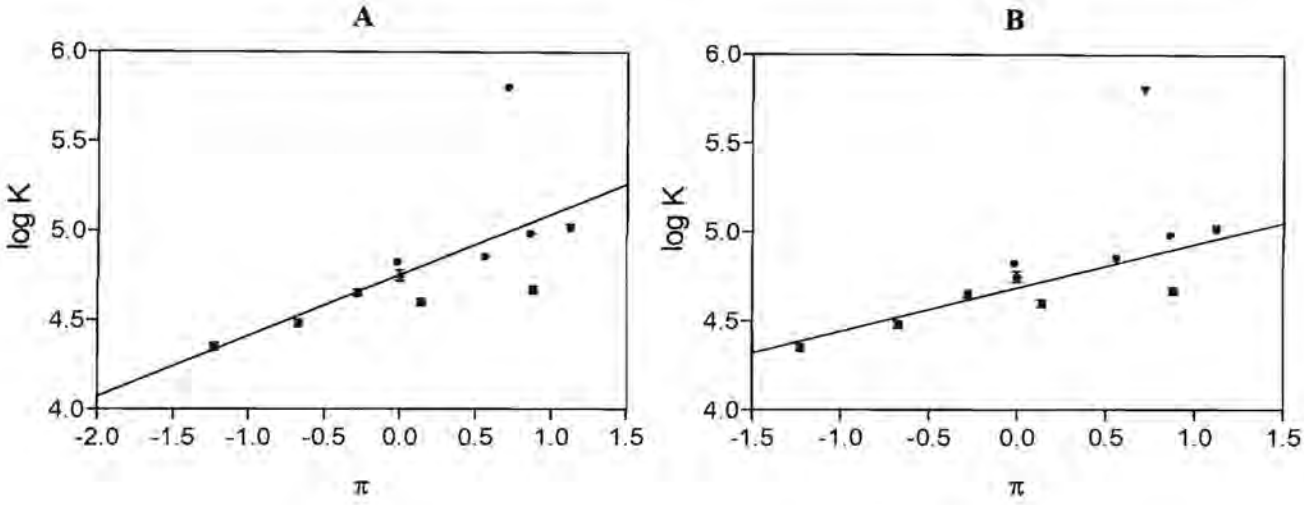

	log K vs π	log K vs π (excl. Cl)
r^2	0.41	0.73
P value	0.035	0.002
Deviation from zero	Significant	Significant
Equation describing log K	0.34π + 4.76	0.25π + 4.69

Figure 5.8. Graphs and statistical variables demonstrating the dependence of the association constant on the lipophilicity of the group at the 7-position when (A) all 11 derivatives are correlated and (B) when all the derivatives excluding the 7-chloro analogue (▾) are correlated. The straight line in both cases represents the best fit to the data using a linear equation. Error bars represent one standard error of the mean.

The extent of β-haematin inhibition is significantly correlated with both the strength of Fe(III)PPIX-quinoline association and σ_m or σ_p (Figure 5.9B). The dependence of β-haematin inhibition on the strength of the Fe(III)PPIX-quinoline complex supports the hypothesis that complex formation is indirectly related to antiplasmodial activity through β-haematin inhibition. The finding that β-haematin inhibition is dependent on the electron withdrawing capacity of the group at the 7-position most likely highlights the electronic requirements in the quinoline ring responsible for adoption of a particular conformational alignment in the complex which is important for β-haematin inhibition. The magnitude of the coefficients in the correlation equation for σ_m and log K indicate that the electronic effects in the quinoline are more important than the strength of association with Fe(III)PPIX in promoting β-haematin inhibition. This suggests that the conformational alignment of the compound in the complex is of greater importance in β-haematin inhibition than the strength of association with Fe(III)PPIX.

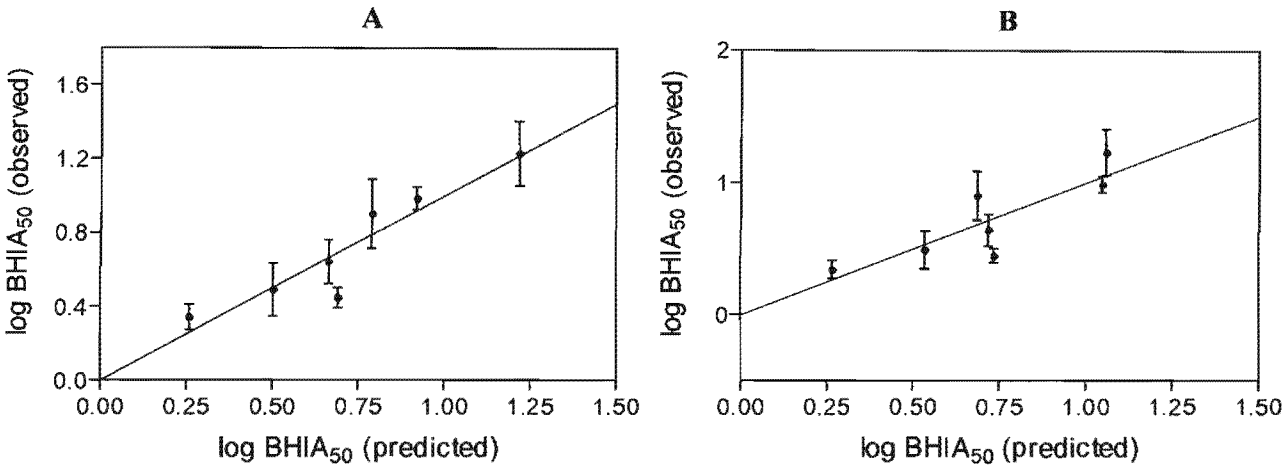

	log $BHIA_{50}$ vs log K and σ_m	log $BHIA_{50}$ vs log K and σ_p
r^2	0.87	0.72
P value	0.002	0.015
Deviation from zero	Significant	Significant
Equation describing log $BHIA_{50}$	$-1.06\sigma_m$-0.52logK +3.67	$-0.68\sigma_p$-0.55logK +3.62

Figure 5.9. Graphs and statistical variables demonstrating the dependence of β-haematin inhibitory activity on the association constant and σ_m (A) or σ_p (B) of the group at the 7-position. The straight line represents the best fit of a linear equation to the data. Error bars represent one standard error from the mean.

5.5. CONCLUSIONS

Evidence from this study supports the hypothesis that 4-aminoquinoline antiplasmodials act by accumulating to therapeutic levels in the food vacuole of the malaria parasite through an important pH trapping component, and that here they exert their antimalarial effect by inhibiting β-haematin formation. In support of previous observations (Hunter and Sanders 1991, Egan *et al.* 1997, Mavuso, PhD thesis 2001), the Fe(III)PPIX-quinoline complex stability appears to be governed by hydrophobic interactions. Antiplasmodial activity was found to depend indirectly on Fe(III)PPIX-quinoline association through β-haematin inhibition. The electron withdrawing ability of the substituent at the 7-position was found to be of greater importance in promoting β-haematin inhibition than the strength of association with Fe(III)PPIX. This is presumably related to the ability of the complex to adopt a particular conformation which is required for β-haematin inhibition.

The results from this study partly explain why *CQ* is a particularly good antimalarial. The chloro-group at the 7-position is sufficiently lipophilic to promote strong Fe(III)PPIX-quinoline association, and sufficiently electron withdrawing to promote strong β-haematin inhibition. This group is however not too electron withdrawing so as not to lower the pK_a's of the quinoline ring nitrogen and the terminal amino nitrogen to too large an extent, This would lower the extent of pH trapping into the food vacuole.

These results are also consistent with reported antiplasmodial activities for families of 4-aminoquinolines with varying side-chains (De *et al.* 1998). All these compounds exhibited strong antiplasmodial activity when the substituent at the 7-position was chloro, bromo or iodo. This is presumably because chloro, bromo and iodo are sufficiently lipophilic (π = 0.71 - 1.12) to interact strongly with Fe(III)PPIX, and are moderately electron withdrawing (σ_m = 0.35 - 0.37) to inhibit β-haematin formation but not lowering the pK_a's too much.

CONCLUSIONS AND FUTURE WORK

6.1. CONCLUSIONS

In this project, the nature of the ferriprotoporphyrin IX (Fe(III)PPIX) drug target was investigated. The critical structural features on *CQ*-related 4-aminoquinolines responsible for Fe(III)PPIX-quinoline complexation, β-haematin inhibition and pH trapping were also probed to investigate the mechanism of action of this class of compounds.

It was found that haematin in aqueous solution is extensively dimerised and that aggregates higher than dimers do not exist. The structure of the haematin dimer is not a μ-oxo dimer as previously thought (Brown *et al.* 1970) but is a proposed π-π dimer in which an axial water ligand points outwards from each of the iron centres. This was evidenced by the apparent pH-independence of the dimerisation constant which was found to have a log K_D of 7.2 ± 0.2, and the apparent differences in the charge transfer region of the uv-vis spectrum of the aqueous haematin dimer and the μ-oxo dimer. It is also supported by observation of pH-dependent differences in the charge transfer spectrum of the aqueous dimer that would not occur in the μ-oxo dimer.

The proposed structure of the haematin π-π dimer can likely explain why association constants obtained between antimalarial drugs in pure aqueous media and 40% DMSO (aq) (in which haematin is reported to be strictly monomeric) are very similar (Egan *et al.* 1997, Mavuso PhD Thesis 2001) and follow the same trends (Dorn *et al.* 1998). This is presumably because both the structures of the aqueous haematin dimer and the haematin monomer in DMSO are similar with an axial oxygen ligand occupying the fifth coordination site (Figure 6.1.).

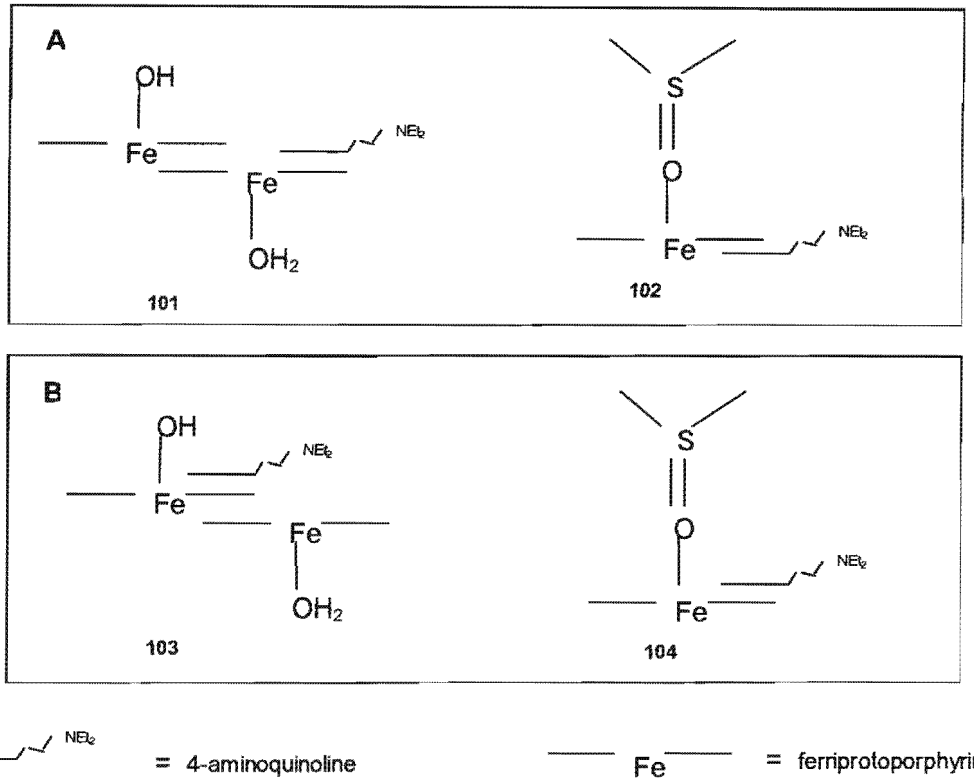

Figure 6.1. Possible structures of the predominant haematin-quinoline complex at pH 7.4 (**101** and **103**). Here the 4-aminoquinoline interacts with the porphyrin ring of the stacked π-π dimer on either the top face (**103**) or in between the two monomer units of the dimer (**101**). For comparison, the proposed structures of the haematin-quinoline complex in 40% DMSO at pH 7.4 (**102** and **104**) where the fifth coordination site is occupied by the oxygen atom of a DMSO molecule (Brown and Lantzke 1969). Again the 4-aminoquinoline is proposed to interact with the porphyrin ring on either the top (**104**) or the bottom (**102**) face of the porphyrin ring. The proposed structure of the π-π dimer likely explains why association constants obtained in 40% DMSO and in pure aqueous solution are similar as both haematin species have oxygen as an axial ligand.

In this study, interactions between the aminoquinolines and the haematin-DMSO monomer *in vitro* were used to model interactions that occur between aminoquinolines and the π-π dimer *in vivo*. It was found that the 4-aminoquinoline nucleus is the critical structural feature in *CQ* and related quinolines responsible for Fe(III)PPIX-quinoline complexation. The 7-chloro group and the terminal amino group were found to have relatively little effect on the strength of Fe(III)PPIX association although a combination of these two structural features increased the association constant significantly relative to 4-aminoquinoline. In a series of 7-substituted 4-aminoquinolines, the association constant was found to depend on the lipophilicity of the substituent at the 7-position which is in agreement with previous reports that the Fe(III)PPIX-quinoline complexes are held together by hydrophobic interactions.

In support of previous observations encompassing a wide range of quinoline antimalarial (Dorn *et al.* 1998) and antiplasmodials (Vippagunta *et al.* 1999), no direct relationship was found between the strength of Fe(III)PPIX association and antiplasmodial activity. This supports the view that formation of a strong complex with the heamatin target is not sufficient for antiplasmodial activity.

It was found that the 7-chloro group in *CQ* is the critical structural feature responsible for β-haematin inhibition. In the series of 7-substituted 4-aminoquinolines studied, a direct relationship was found between antiplasmodial activity and β-haematin inhibition only when the latter was corrected for pH trapping (r^2 = 0.83, p = 0.004). This result strongly implies that 4-aminoquinoline antiplasmodials act by directy inhibiting β-haematin formation. In turn, the strength of β-haematin inhibition was found to depend on both the association constant and the electron withdrawing capacity of the group at the 7-position which highlights the indirect role that complex formation plays in antiplasmodial activity. A recent study has found that saturable *CQ* uptake is due solely to binding to haematin (Bray *et al.* 1999). Whilst binding to the haematin target is important in overall drug accumulation, the results from this study highlight the significant contribution that pH-trapping plays in overall accumulation and hence antiplasmodial activity.

There have been various hypotheses proposed for the resulting toxicity of the haematin-quinoline complex. These hypothesies are based on the premise that additional haematin detoxification mechanisms to haemozoin formation exist in the food vacuole (Loria *et al.* 1999) or in the cytosol (Ginsburg *et al.* 1998) and that *CQ* and related aminoquinolines act by inhibiting these pathways through Fe(III)PPIX-quinoline complexation. There is a possibility that β-haematin inhibitory activity is quantitatively correlated to one or both of these putative haematin detoxification pathways thereby masking the true basis of antiplasmodial activity and giving rise to the observed correlation between β-haematin formation and antiplasmodial activity. No direct correlation between β-haematin formation and the other two haematin detoxification mechanisms have however been shown to exist. In addition, strong evidence that all the haemoglobin-derived haematin is not converted to haemozoin has yet to be provided. The most obvious interpretation of the observed correlation is that the 4-aminoquinoline antiplasmodials act by directly inhibiting β-haematin formation

Based on these observations the following hypothesis on the mechanism of action of *N, N*-diethyl-N^2-(7X-4-quinolinyl)1,2-ethanediamine antiplasmodials can be proposed (Figure 6.2.):

The 4-aminoquinoline antiplasmodials enter the food vacuole via passive diffusion of the free base accross the vacuole membrane. Once inside the food vacuole a substantial proportion of the 4-aminoquinoline becomes mono- and diprotonated, and binds to the π-π haematin dimer. These chemical processes result in more free base diffusing across the membrane by Le Chateliers principle until the equilibrium concentrations of free base on both sides of the membrane are equal. It is proposed that these two processes account in total for the observed 1700 fold accumulation of *CQ* into the parasitised cell. In turn, these vacuolar concentrations are required to inhibit haemozoin formation which results in a build-up of non-haemozoin haem. This free haem is proposed to cause a toxic effect, possibly by partitioning into the membranes and causing loss of membrane order and cell lysis.

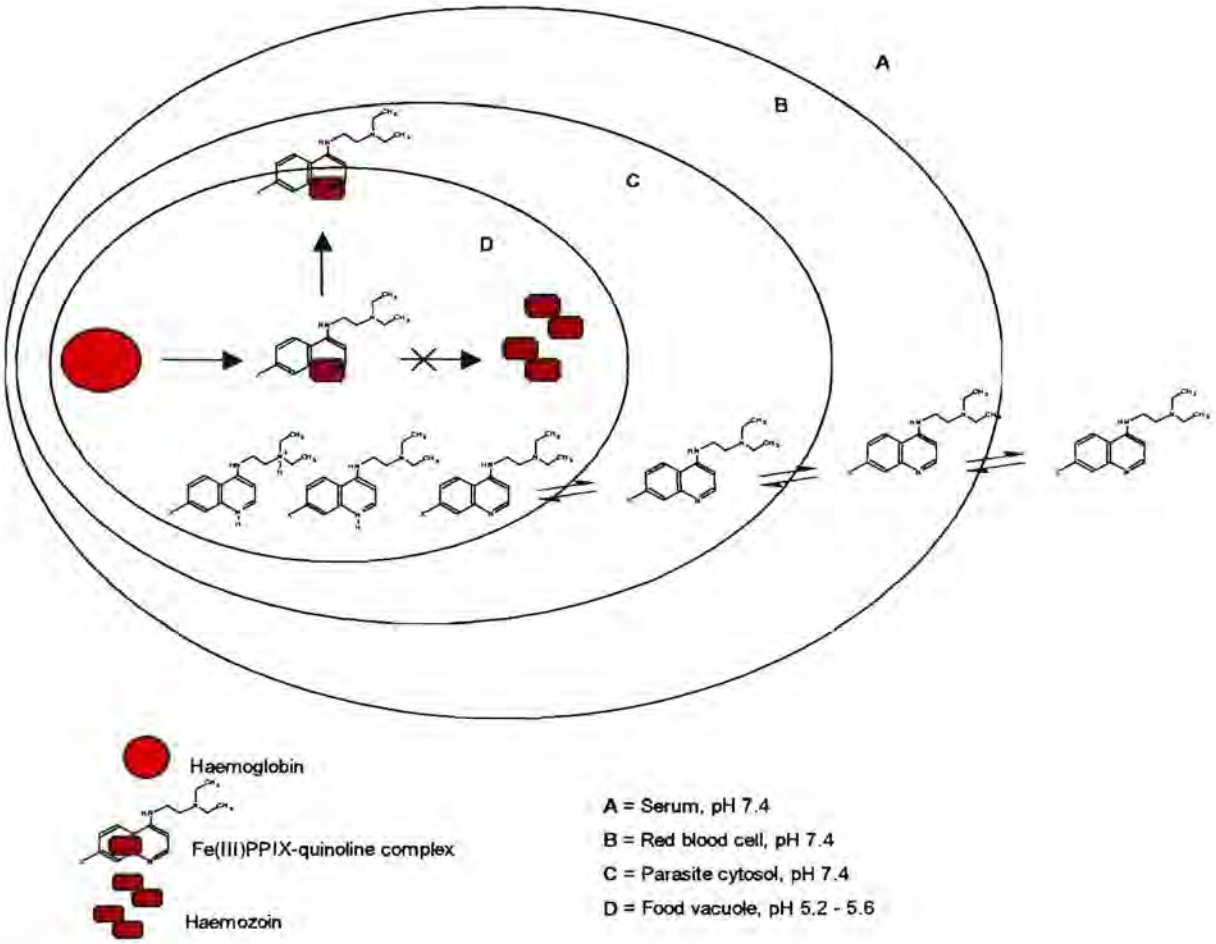

Figure 6.2. Proposed model for the mechanism of action of *N*, *N*-diethyl-N^2-(7X-4-quinolinyl)1,2-ethanediamine antiplasmodials. The aminoquinolines are proposed to accumulate to the therapeutically required levels through a combination of pH trapping and saturable binding to a haematin target in the acidic food vacuole of the intraerythrocytic malaria parasite. Heamatin binding is essential for the aminoquinolines to extert their toxic effect by inhibiting the haematin detoxification pathway (haemozoin formation). This results in a build up of free haematin which likely becomes associated with the membranes where it exerts a toxic effect.

Since close analogues of *CQ* maintain activity against *CQ* resistant parasites, it appears that the resistance mechanism does not involve any change to the haematin target but rather involves a compound specific resistance. Insights gained from this study further enhance our understanding of the structural-function relationships in *CQ* and allow for the rational design novel antimalarials based on the *CQ* template (Figure 6.3).

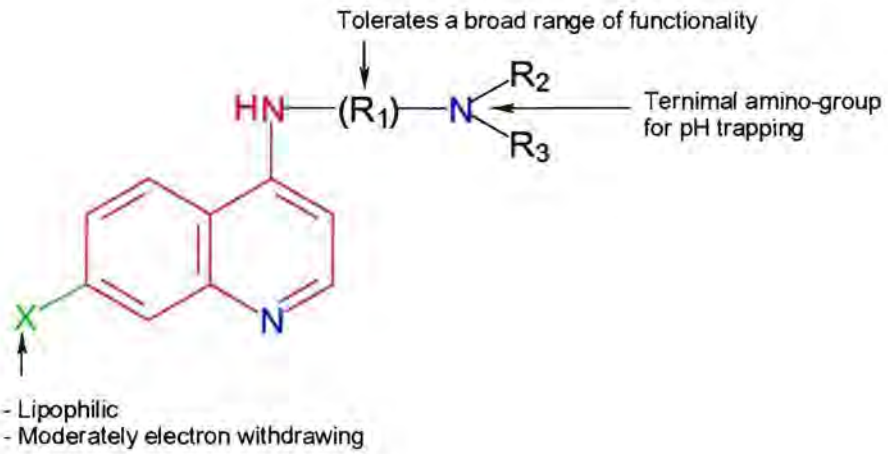

Figure 6.3. Proposed structural and electronic requirements for antiplasmodial activity based on the 4-aminoquinoline template. Key: (—) group at the 7-position required for β-haematin inhibition, (—) 4-aminoquinoline template required for strong association with Fe(III)PPIX, (—) amino-groups required for pH trapping.

The 4-aminoquinoline template is required for strong association with Fe(III)PPIX and this in turn is further influenced by the lipophilicity of the group at the 7-position. The group at the 7-position must also be moderately electron withdrawing to promote β-haematin inhibition, but not too electron withdrawing so as to lower the pK_a's of the quinoline and terminal amino nitrogens and therby lower the extent of pH trapping into the food vacuole. A wide variety of functionality can be tolerated in the lateral side chain which must contain a terminal amino group for pH-trapping. Literature evidence suggests that this is the key structural feature for cross resistance with *CQ*. Thus sufficient alteration of this group should result in compounds active against resistant parasites.

6.2. FUTURE WORK

Using the statistical equations obtained in Chapter 5, it is now possible to rationally design novel N^1-(4-aminoquinolinyl)-N^2,N^2-diethylenediamine antimalarials. Choice of the lipophilic and moderately electron withdrawing OCF_3 and SCF_3 substituents at the 7-position on the 4-

aminoquinoline template are predicted to have the strong association constants, good β-haematin inhibitory activities and strongly active antiplasmodial activities presented in Table 6.1.

Table 6.1. (top) Meta-Hammett constant and lipophilicity constants for OCF_3 and SCF_3 groups. (bottom) Predicted pK_a's , log K's , $BHIA_{60}$s and IC_{50}s against the D10 strain of malaria parasites

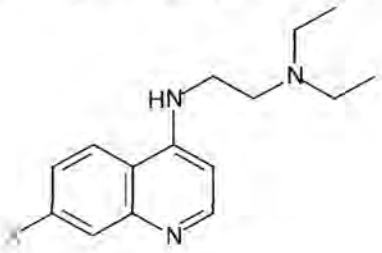

X	σ_m[a]	π[a]
OCF_3	0.38	1.04
SCF_3	0.40	1.44

X	pK_{a1}	pK_{a2}	log K	$BHIA_{50}$	$IC_{50}\alpha$	α	IC_{50} / nM
OCF_3	7.36	8.59	4.95	4.9	35	0.499	70
SCF_3	7.33	8.55	5.05	4.2	31	0.489	63

[a] Hansch and Leo 1979

Since 2-aminoquinoline associates strongly with Fe(III)PPIX, it is possible that introduction of chlorine or another moderately electron withdrawing group at the 7-position will cause the resulting 2-amino-7-chloroquinoline to inhibit β-haematin formation. If so, it may be possible to synthesise 2-aminoquinoline antiplasmodials based on this template (for example **101** in Figure 6.4). In addition, it has not been established if 2,4-diaminoquinoline has the ability to form a strong complex with Fe(III)PPIX and if 2,4-diamino-7-chloroquinoline has the ability to inhibit β-haematin formation. If both the answers to these questions are positive, then a disubstituted analogue like **102** may have useful antiplasmodial properties. Since thiophene is an isostere for benzene (King 1994), it may be possible that the pyridinethiophene ring system (eg in **103**) may behave in a similar a manner to quinoline which may provide a new template on which to base rationally designed antiplasmodials.

In order to rationally design antimalarials other than 4-aminoquinolines it will be necessary in the future to determine what structural conformations in the complex lead to β-haematin

inhibition. In this regard, it will be necessary to study the molecular interactions in the complex using computational methods, taking into account the molecular orbitals and solvent interactions.

Although evidence from this study supports the hypothesis that *CQ*-related 4-aminoquinolines act by inhibiting haemozoin formation, proof for this hypothesis has not been provided *in vivo*. In order to unequivocally establish the validity of this hypothesis, it would have to be shown that *CQ* and related 4-aminoquinolines are capable of blocking haemozoin formation *in vivo*, and that this effect is dose dependent. This would presumably have to be investigated using a physical technique (eg Mössbauer spectroscopy) which is capable of distinguishing unequivocally between haematin iron, haemozoin iron and iron in the Fe(III)PPIX-quinoline complex.

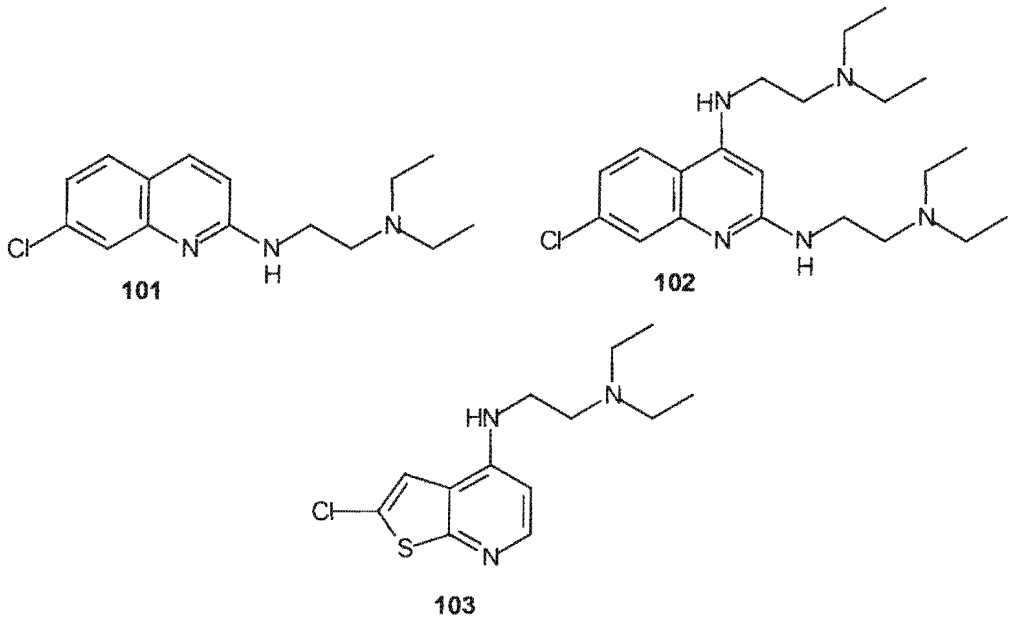

Figure 6.4. Proposed compounds that may exhibit antiplasmodial activity

Since the *CQ*-resistance mechanism appears to be compound specific rather than target specific, compounds that act by interacting with the Fe(III)PPIX target and inhibiting β-haematin formation may still find utility in malaria chemotherapy. Since the 4-aminoquinoline class of compounds acts via this mechanism, it may be possible to rationally design novel 4-aminoquinoline antimalarials based on the findings in this project.

EXPERIMENTAL

7.1. SYNTHETIC METHODS

7.1.1. General Procedures

Reactions were monitored by thin layer chromatography using Merck F_{254} aluminium-backed precoated silica gel plates and were visualised with a combination of ultraviolet light and iodine vapour. Silica gel column chromatography was performed using Merck kieselgel 60: 70 – 230 mesh for gravity columns and 230 – 400 mesh for flash chromaography. Neutral alumina chromatography was performed using 70 – 230 mesh (activity 1). Melting points were determined either using a Reichert-Jung Thermovar hot stage microscope or using Differential Scanning Calorimetry (DSC). Infrared spectra were recorded as DMSO or chloroform solutions or as KBr discs using a Perkin Elmer Paragon 1000 FT-IR spectrophotometer or a Perkin Elmer 983 IR spectrophotometer in the range 3600 – 800cm^{-1}. ^{1}H and ^{13}C nmr were recorded on a Varian VXR-200 spectrometer at 200MHz, Varian Mercury spectrometer at 300MHz or a Varian Unity spectrometer at 400MHz. All spectra were recorded in deuterochloroform or deuterodimethylsulfoxide using internal standards for ^{1}H nmr of δ_H = 7.26ppm and respectively and for ^{13}C nmr of δ_C = 54.39ppm and 40.35ppm respectively. All chemical shifts are reported in ppm. Elemental analyses were performed using a Fison's Instruments Elemental Analyser EA1108. Mass spectra were recorded on a VG micromass 16F spectrometer operating at 70eV with an accelerating voltage of 4kV and a variable temperature source. Accurate mass determinations were performed on a Kratos Limited MS9/50 spectrometer. All mass spectra were performed using electron impact techniques.

Commercially available chemicals used in the synthetic work were obtained from the suppliers in Table 7.1.

Table 7.1. Commercially available chemicals used in the synthetic work

Chemical	**Supplier**
3-Aminophenol	Sigma
m-Anisidine	Sigma
4-Amino-1-diethylaminopentane	Sigma
4-Chloro-7-(trifluoromethyl)quinoline	Sigma
4,7-Dichloroquinoline	Sigma
N,N-Diethylenediamine	Sigma
Diethyl ethoxymethylenemalonate	Sigma
Diphenylether	ACROS Organics
3-Fluoroaniline	Sigma
2-Hydroxyquinoline	Sigma
30% Hydrogen peroxide	Protea Chemicals
3-Iodoaniline	Sigma
7-Methylquinoline	Sigma
3-Nitroaniline	Merck
Phosphorus oxychloride	Protea Chemicals
Phosphorus trichloride	Protea Chemicals
Propylamine	Sigma
Silver nitrate	Labchem (Pty) Ltd

7.1.2. Synthesis, Purification and Characterisation of Compounds

2-Chloroquinoline (24)

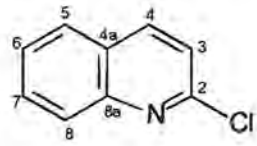

Method A

A solution of phosphorus oxychloride (5ml, 54mmol) and 2-hydroxyquinoline (**25**) (0.49g, 3.4mmol) was heated in a tube, sealed under N_2 at 100°C for 2h. The reaction mixture was then cooled and $NaHCO_3$ (aq) added until pH 8 was obtained. The resulting solid was then extracted into ethyl acetate (four times), dried over anhydrous $MgSO_4$ and the solvent removed under reduced pressure to give, after drying, **1** (0.44g, 79%), mp 32 - 34°C (lit. Aldrich Catalogue 2000, 34 - 37°C); (Found MS (EI) *m/z*% 163 (M^+, 100). Requires for C_9H_6NCl: M^+, 163).

Method B

To a cooled solution of phosphorus oxychloride (30ml), under N_2, quinoline 1-oxide (**27a**) (3.8g, 23mmol) was added slowly over 45mins and then refluxed at 65°C for 1h. The reaction mixture was then poured onto ice (150g) and 25% ammonia (aq) added until the solution was alkaline. Extraction of the products into ethyl acetate (three times), followed by drying over anhydrous $MgSO_4$ and evaporation under reduced pressure gave a mixture of products which were chromatographed on silica gel using mixtures of ethyl acetate : petroleum ether (0:100) to (20:80) as the eluent to give **24** (2.6g, 69%) and 4-chloroquinoline (**30a**) (0.79g, 21%). MS for **24** identical to that found for the product in Method A. ^1H NMR of **30a** identical to that found for the product synthesised via the N-oxide route.

Quinoline-1-oxide (28a)

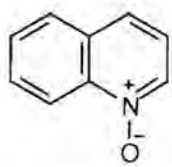

To a stirred solution of quinoline (5.0cm^3, 42mmol) in glacial acetic acid (13.1cm^3, 228mmol) at 65°C was added 30% H_2O_2 (7.2 cm^3, 64mmol). After 6h, a further quantity of 30% H_2O_2 (7.2cm^3, 64mmol) was added and the reaction mixture heated at 65°C for a further 20h. The mixture was then concentrated in vacuo and basified with saturated Na_2CO_3 (aq). The

products were extracted into chloroform (three times), dried over anhydrous $MgSO_4$ and the extracts concentrated again. On standing, the residue solidified to give **28a** (5.46g, 89%). The crude extract was then used directly; (Found MS (EI) *m/z*% 145 (M^+, 100). Requires for C_9H_7NO: M^+, 145).

7-Methylquinoline-1-oxide (28b)

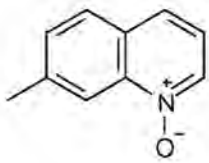

To a stirred solution of 7-methylquinoline (0.40g, 2.8mmol) in glacial acetic acid (0.90cm^3, 16mmol) at 70°C was added 30% H_2O_2 (0.33cm^3, 2.9mmol). After 20h, a further quantity of 30% H_2O_2 (0.47cm^3, 4.1mmol) was added and the reaction allowed to proceed at 70°C for a further 20h. The reaction mixture was then concentrated in vacuo and basified to pH 8 with portions of saturated $NaHCO_3$ (aq). The mixture was extracted into chloroform (four times), dried over anhydrous Na_2CO_3 and the extracts concentrated again to yield a beige solid **28b** (0.414g, 93%). The crude extract was then used directly.

4-Nitroquinoline-1-oxide (29a)

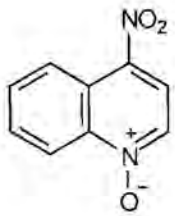

To a stirred solution of **28a** (2.7g, 19mmol) in trifluoroacetic acid (60cm^3, 78mmol) at 60°C, was added 5.7g (56mmol) of KNO_3 in a single addition. After 1hr at this temperature, the reaction mixture was poured onto iced water (400cm^3). The solution was basified with cold saturated K_2CO_3 (aq) and the products extracted into dichloromethane (four times). The solvent was then removed under reduced pressure and brine (100ml) added to the residue. The organic products were extracted into dichloromethane (four times), dried over anhydrous K_2CO_3 and evaporated under reduced pressure to give two products which were separated by silica gel chromatography (60g) using mixtures of acetonitrile : dichloromethane (20:80) to (50:50) as the eluent. The major product **29a** (2.7g, 77%) was crystallised from acetone to give fine yellow needles, mp 157°C (DSC) (lit. Yokoyama *et al.* 1997, 157°C; Ochiai 1953, 153 - 154°C); ν_{max}/cm^{-1} (CH_2Cl_2) 1522, 1345 (Ar-NO_2); δ_H (400MHz, $CDCl_3$) 7.88 (2H, m), 8.20 (1H, d, *J* 6.8Hz), 8.52 (1H, d, *J* 6.8Hz), 8.76 (1H, m),

8.84 (1H, m); (Found: MS (EI) *m/z*% 190 (M^+, 100). Requires: M^+, 190); (Found: C, 56.8; H, 3.1; N, 14.8%. Requires for $C_9H_6N_2O_3$: C, 56.8; H, 3.2; N, 14.7%).

7-Methyl-4-nitroquinoline-1-oxide 29b

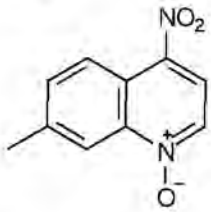

To a stirred solution of **28b** (0.41g, 2.6mmol) in trifluoroacetic acid (20cm^3, 26mmol) at 65°C, was added KNO_3 (0.8g, 7.9mmol) in a single addition. After 1hr at this temperature, the reaction mixture was poured onto ice. The solution was basified with cold saturated K_2CO_3 and the products extracted into dichloromethane (four times). The combined organic layers were evaporated under reduced pressure, washed with brine and the organic products reextracted into dichloromethane (four times), dried over anhydrous K_2CO_3 and evaporated under reduced pressure. The solid residue was crystallised from acetone to give **29b** (0.42g, 79%), mp 165 - 168°C (lit. Takahashi *et al.* 1983, 165°C); ν_{max}/cm^{-1} (KBr) 1515, 1328, 1289, 1153, 823; δ_H (400MHz, $CDCl_3$) 2.63 (3H, s, CH_3), 7.69 (1H, dd, *J* 8.9, 1.7, H-6), 8.11 (1H, d, *J* 6.8, H-2), 8.47 (1H, d, *J* 6.8, H-3), 8.56 (1H, m, H-8), 8.72 (1H, d, *J* 8.9, H-5); (Found: MS (EI) *m/z*% 204 (M^+, 57), 30 (100). Requires: M^+, 204); (Found: C, 59.1; H, 3.9; N, 13.8%. Requires for $C_{10}H_8N_2O_3$: C, 58.8; H, 4.0; N, 13.7%).

4-Chloroquinoline 30a

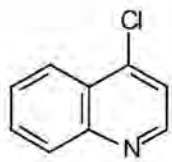

To a stirred room temperature solution of **29a** (0.98g, 5.2mmol) in dry dichloromethane (7cm^3), was added phosphorus trichloride (5.0cm^3, 57mmol) under nitrogen, dropwise. After 6h at room temperature, a further quantity of phosphorus trichloride (1.0cm^3, 11mmol) was added and the mixture refluxed under nitrogen at 60°C for a further 50h. The reaction mixture was then poured onto ice (100g) and basified with cold saturated $NaHCO_3$ (aq) followed by saturated KOH (aq). Brine was added to the aqueous phase to facilitate extraction of the products into ethyl acetate (four times). The combined organic layers were dried over anhydrous $MgSO_4$ and evaporated under reduced pressure. The mixture was then adsorbed onto silica gel (50g) and chromatographed using mixtures of ethyl acetate :

hexane (1:99) to (10:90) as the eluent to give **30a** (0.66g, 78%) as the major product in the form of a pale yellow oil, (lit. mp Aldrich Calatague 2000, 29 - 32°C). δ_H (400MHz, $CDCl_3$) 7.50 (1H, d, *J* 4.8, H-3), 7.67 (1H, td, *J* 7.6, 1.2, H-6 or H-7), 7.80 (1H, td, *J* 7.6, 1.2, H-6 or H-7), 8.18 (1H, dd, *J* 8.6, 1.2, H-5 or H-8) 8.26 (1H, dd, *J* 8.6, 1.2, H-5 or H-8), 8.80 (1H, d, *J* 4.8, H-2); (Found: MS (EI) *m/z%* 163 (M^+, 100). Requires for C_9H_6NCl: M^+, 163).

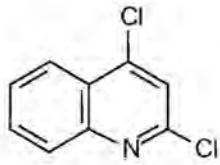

A minor product of lower polarity, 2,4-dichloroquinoline (**32**) was isolated (80mg, 6.6%) and crystallised from petroleum ether, mp 62 - 64°C (lit. Beak *et al.* 1972, 64.5 - 65.5°C; Shah *et al.* 1960, 66 - 67°C); δ_H (200MHz, $CDCl_3$) 7.52 (1H, s, H-3), 7.66 (1H, td, *J* 7.7, 1.2), 7.80 (1H, td, 7.7, 1.2), 8.04 (1H, d, *J* 8.4), 8.20 (1H, dd, *J* 8.4, 1.2); δ_C (50.3MHz, $CDCl_3$) 121.9, 124.2, 125.2, 127.9, 129.0, 131.5, 144.3, 148.1, 149.8; (Found: MS (EI) *m/z%* 197 (M^+, 100). Requires: M^+, 197); (Found: C, 54.5; H, 2.5; N, 7.3%. Requires for $C_9H_5NCl_2$: C, 54.6; H, 2.5; N, 7.1%).

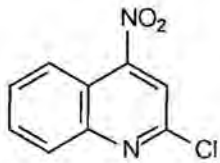

A slightly less polar product than **30a**, 2-chloro-4-nitroquinoline (**33**) (40mg, 3.1%) was also isolated from the reaction and crystallised from petroleum ether, mp 82 - 84°C (lit. Belli 1963, 81 - 81.5°C); ν_{max} /cm^{-1} (KBr) 1523, 1341 (Ar- NO_2); δ_H (400MHz, $CDCl_3$) 7.78 (1H, td, *J* 7.8, 1.2), 7.90 (1H, td, *J* 7.8, 1.2), 7.95 (1H, s, H-3), 8.17 (1H, dq, *J* 8.6, 1.2, 0.6), 8.37 (1H, dq, *J* 8.6, 1.2, 0.6); δ_C (100.6MHz, $CDCl_3$) 117.0, 117.7, 123.0, 129.4, 130.0, 132.2, 149.8, 150.6, 153.8; (Found: MS (EI) *m/z%* 208 (M^+, 91), 150 (100). Requires: M^+, 208); (Found: C, 51.9; H, 2.5; N, 13.4%. Requires for $C_9H_5N_2O_2Cl$: C, 51.8; H, 2.4; N, 13.4%).

7-Methyl-4-chloroquinoline (30b)

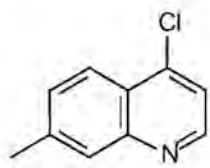

To a stirred room temperature solution of **29b** (0.16g, 0.79mmol) in dry dichloromethane ($3cm^3$), was added phosphorus trichloride ($0.90cm^3$, 10mmol) under N_2, dropwise. After 20h

at room temperature, a further quantity of phosphorus trichloride (0.3cm^3, 3.4mmol) was added and the mixture refluxed under nitrogen at 55°C for a further 40h. The reaction mixture was then poured into iced water (20ml), basified with cold $NaHCO_3$ (aq) followed by KOH (aq). The products were extracted into ethyl acetate (four times), dried over anhydrous $MgSO_4$ and evaporated under reduced pressure. The residue was chromatographed on silica gel (15g) using elution mixtures of ethyl acetate : petroleum ether (1:99) to (9:91) to give the major product **30b** (0.11g, 75%) as an oil, (lit. mp Breslow *et al.* 1946, 28°C); (Found: MS (EI) *m/z%* 177 (M^+, 100). Requires for $C_{10}H_8NCl$: M^+, 177).

Ethyl 2-ethoxycarbonyl-3-(3-fluoroanilino)propenoate (51a)

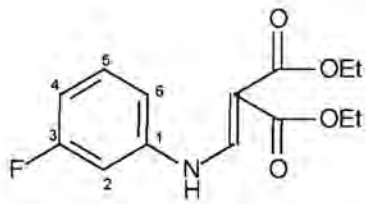

A mixture of 3-fluoroaniline (8.7ml, 90mmol) and diethyl ethoxymethylenemalonate (18.2ml, 90.0mmol) was stirred in an open flask at room temperature for 0.5hr. The reaction mixture was then heated for 2h at 70°C on the rotary evaporator. Upon standing at room temperature overnight, **51a** precipitated out of solution. Collection of the solid by filtration followed by recrystallisation from ethanol yielded a hard pale yellow solid (21g, 83%), mp 44.7 - 45.9°C (lit. Shah and Coats 1977, 47 - 48°C); δ_H (300MHz, $CDCl_3$) 1.32 (3H, t, *J* 7.2, CH_3), 1.37 (3H, t, *J* 7.2, CH_3), 4.25 (2H, q, *J* 7.2, CH_2), 4.30 (2H, q, *J* 7.2, CH_2), 6.85 (3H, m, Ar-H), 7.31 (1H, m, H-5), 8.44 (1H, d, *J* 13.5, vinylic H), 10.97 (1H, bd, *J* 13.5, NH); δ_C (75.5MHz, $CDCl_3$) 14.2 (CH_3), 14.4 (CH_3), 60.2 (CH_2), 60.5 (CH_2), 94.6 (C=CH), 104.3 ($J_{C\text{-}F}$ 26, C-2 or C-4), 111.5 ($J_{C\text{-}F}$ 21, C-2 or C-4), 112.8 ($J_{C\text{-}F}$ 3, C-6), 131.2 ($J_{C\text{-}F}$ 10, C-5), 141.0, ($J_{C\text{-}F}$ 10, C-1), 151.3 (C=CH), 163.6 (*J* 248, C-3), 165.4 (C=O), 168.9 (C=O); (Found: MS (EI) *m/z%* 281 (M^+, 100). Requires: M^+, 281); (Found: C, 59.5; H, 5.7; N, 4.9%. Requires for $C_{14}H_{17}NO_4F$: C, 59.8; H, 5.7; N, 5.0%).

Ethyl 3-(3-bromoanilino)-2-ethoxycarbonylpropenoate (51b)

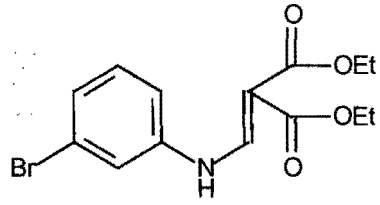

A mixture of 3-bromoaniline (10g, 58mmol) and diethyl ethoxymethylenemalonate (13g, 60mmol) was stirred at room temperature for 0.5h and then heated under reduced pressure at 60°C for 2h. Initially a lot of bubbling was observed as the ethanol produced was liberated. Upon cooling, a red/rust solid came out of solution. This was crystallised twice from ethanol to yield **51b** (18g, 88%), mp 70 - 72°C (lit. Conroy *et al* 1949, 70 - 71°C); δ_H (300MHz, $CDCl_3$) 1.33 (3H, t, *J* 7.2, CH_3), 1.37 (3H, t, *J* 7.2, CH_3), 4.22 – 4.34 (4H, m, *J* 7.2, 2 × CH_2), 7.05 (1H, dt, *J* 7.5, 2.0, 2.0, Ar-H), 7.20 – 7.30 (3H, m, 3 × Ar-H), 8.44 (1H, d, *J* 13.4, vinylic H), 11.0 (1H, bd, *J* 13.4, NH); δ_C (75.5MHz, $CDCl_3$) 14.2 (CH_3), 14.4 (CH_3), 60.3 (CH_2), 60.6 (CH_2), 94.7 (C=CH), 115.8 (Ar-CH), 120.1 (Ar-CH), 123.5 (C-3), 127.7(Ar-CH), 131.1 (Ar-CH), 140.6 (C-1), 151.2 (C=CH), 165.5 (C=O), 168.9 (C=O); (Found: MS (EI) *m/z%* 343 ($(M+2)^+$, 88), 341 (M^+, 89), 297 (89), 295 (87), 29 (100). Requires: $(M+2)^+$, 343; M^+, 341); (Found: C, 49.3; H, 4.5; N, 4.0%. Requires for $C_{14}H_{16}NO_4Br$: C, 49.1; H, 4.7; N, 4.1%).

Ethyl 2-ethoxycarbonyl-3-(3-iodoanilino)-3-propenoate (51c)

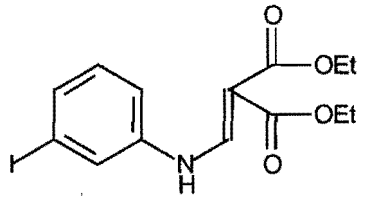

A mixture of 3-iodoaniline (10g, 46mmol) and diethyl ethoxymethylenemalonate (11g, 50mmol) was stirred at room temperature for 0.5h and then under reduced pressure for 10mins. Initially a lot of bubbling was observed as the ethanol produced was liberated, The resulting solid was crystallised from ethanol to give **51c** (15, 83%), mp 90 - 92°C (lit. Conroy *et al* 1949, 92 - 93°C; Counsell *et al* 1967, 88 - 89°C); δ_H (400MHz, $CDCl_3$) 1.33 (3H, t, *J* 7.2, CH_3), 1.37 (3H, t, *J* 7.2, CH_3), 4.25 (2H, q, *J* 7.2, CH_2), 4.30 (2H, q, *J* 7.2, CH_2), 7.08 (2H, m, 2 × Ar-H), 7.47 (2H, m, 2 × Ar-H), 8.42 (1H, d, *J* 13.8, vinylic H), 10.93 (1H, bd, *J* 13.8, NH); δ_C (100.6MHz, $CDCl_3$) 14.2 (CH_3), 14.4 (CH_3), 60.3 (CH_2), 60.5 (CH_2), 94.8 (C=CH), 94.9 (C-3), 116.4 (Ar-CH), 126.0 (Ar-CH), 131.2 (Ar-CH), 133.7 (Ar-CH), 140.5 (C-1), 151.2 (C=CH),

165.5 (C=O), 168.9 (C=O); (Found: MS (EI) *m/z%* 389 (M^+, 100). Requires: M^+, 389); (Found: C, 43.5; H, 3.9; N, 4.0%. Requires for $C_{14}H_{16}INO_4$: C, 43.2; H, 4.1; N, 3.6%).

Ethyl 2-ethoxycarbonyl-3-(3-nitroanilino)-3-propenoate (51d)

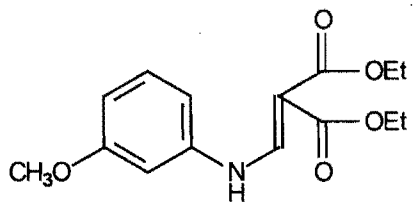

A mixture of 3-methoxyaniline (10g, 81mmol) and diethyl ethoxymethylenemalonate (17ml, 83mmol) was heated in an open flask at 105°C for 1h. Petroleum ether was added to the warm reaction mixture and the insoluble starting material filtered off. The residue was evaporated under reduced pressure and dried to give **51d** (23g, 91%), mp 39 - 41°C; δ_H (400MHz, $CDCl_3$) 1.30 (3H, t, *J* 7.2, CH_3), 1.36 (3H, t, *J* 7.2, CH_3), 3.80 (3H, s, OCH_3), 4.22 (2H, q, *J* 7.2, CH_2), 4.29 (2H, q, *J* 7.2, CH_2), 6.63 (1H, t, *J* 2.4, H-2), 6.67 (1H, ddd, *J* 8.2, 2.4, 0.8, Ar-H), 6.71 (1H, dd, *J* 8.2, 2.4, Ar-H), 7.24 (1H, t, *J* 8.2, H-5), 8.48 (1H, d, *J* 14, C=CH), 10.93 (1H, d, *J* 14, NH); δ_C (100.6MHz, $CDCl_3$) 14.3 (CH_3), 14.4 (CH_3), 55.4 (OCH_3), 60.1 (CH_2), 60.4 (CH_2), 93.7 (C=CH), 103.3 (C-2), 109.4 (Ar-CH), 110.3 (Ar-CH), 130.7 (C-5), 140.5 (C-1), 151.8 (HC=C), 160.9 (C-3), 165.7 (C=O), 169.0 (C=O); (Found: MS (EI) *m/z%* 293 (M^+, 87), 247 (100). Requires: M^+, 293); (Found: C, 61.7; H, 6.7; N, 4.8%. Requires for $C_{15}H_{19}NO_5$: C, 61.4; H, 6.5; N, 4.8%).

Ethyl 2-ethoxycarbonyl-3-(3-nitroanilino)-3-propenoate (51e)

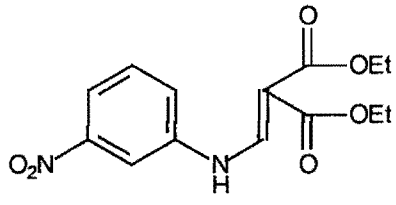

A solution of 3-nitroaniline (50g, 0.36mol) and diethyl ethoxymethylenemalonate (80g, 0.37mol) was stirred in an open flask at 110°C for 1hr. The mixture was then cooled slightly and hot ethanol (400ml) added. Upon cooling, canary-yellow crystals of **51e** were obtained (106g, 95.3%), mp 82 - 83°C (lit. Vippagunta *et al.* 1999, 81 - 82°C); δ_H (300MHz, d_6 DMSO) 1.26 (6H, t, *J* 7.2, 2 × CH_3), 4.18 (4H, bs, 2 × CH_2), 7.65 (1H, t, *J* 8.2, H-5), 7.85 (1H, ddd, *J* 8.2, 2.1, 0.9, Ar-H), 7.95 (1H, ddd, *J* 8.2, 2.1, 0.9, Ar-H), 8.27 (1H, t, *J* 2.1, H-2), 8.40 (1H, s,

C=CH), 10.71 (1H, s, NH); (Found: MS (EI) *m/z*% 308 (M^+, 82), 206 (100). Requires: M^+, 308); (Found: C, 54.8; H, 5.6; N, 9.2%. Requires for $C_{14}H_{16}N_2O_6$: C, 54.6; H, 5.2; N, 9.1%).

Ethyl 2-ethoxycarbonyl-3-(3-hydroxyanilino)-3-propenoate (51f)

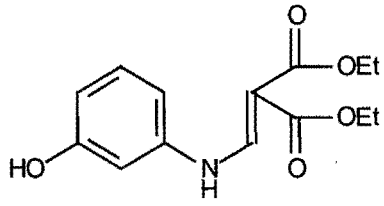

A vigorously stirred mixture of 3-hydroxyaniline (20.1g, 184mmol), diethyl ethoxymethylenemalonate (38.0ml, 188mmol) and methanol (20ml) was refluxed at 80°C for 0.5h. During this time, the insoluble white flakey starting material changed to a powdery white solid. This solid was crystallised from methanol and ethanol directly from the reaction flask. Collection of the crystals by filtration followed by drying gave **51f** (48g, 91%), mp 151 - 153°C; ν_{max}/cm^{-1} (KBr) 3337, 1691, 1648, 1593, 1320, 1256, 1216, 1159, 1089, 1080; δ_H (300MHz, d_6 DMSO) 1.25 (6H, m, 2 × CH_3), 4.12 (2H, q, *J* 9.6, CH_2), 4.20 (2H, q, *J* 9.6, CH_2), 6.58 (1H, ddd, *J* 10.9, 2.9, 1.1, Ar-H), 6.70 (1H, t, *J* 2.9, H-2), 6.75 (1H, ddd, *J* 10.9, 2.9, 1.1 Ar-H), 7.17 (1H, t, *J* 10.9, H-5), 8.34 (1H, d, *J* 13.8, C=CH), 9.68 (1H, bs, OH), 10.57 (1H, d, *J* 13.8, NH); δ_C (75.5MHz, d_6 DMSO) 14.1 (CH_3), 14.2 (CH_3), 59.4 (CH_2), 59.6 (CH_2), 92.9 (C=CH), 104.1 (C-2), 108.2 (Ar-CH), 111.9 (Ar-CH), 130.5 (C-5), 140.4 (C-1), 150.8 (C=CH), 158.5 (C-3), 164.8 (C=O), 167.3 (C=O); (Found: MS (EI) *m/z*% 279 (M^+, 55), 187 (100). Requires: M^+, 279); (Found: C, 60.5; H, 6.4 N, 5.0%. Requires for $C_{14}H_{17}NO_5$: C, 60.2; H, 6.1; N, 5.0%).

7-Fluoro-4-hydroxyquinoline-3-carboxylic acid ethyl ester (52a)[a]

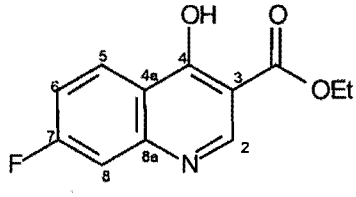

To a refluxing solution of diphenyl ether (60ml) at 260°C, crushed **51a** (10g, 36mmol) was

[a] 4-hydroxyquinoline exists in tautomeric equilibrium with 4-quinolone. For simplicity, the quinoline tautomer has been shown throughout the thesis but in some cases the protons assigned as OH in the ^1H NMR spectrum may likely be NH protons from the quinolone tautomer.

added slowly over 20 mins. Whilst performing the addition, the water in the condenser was switched off to allow the ethanol formed to escape. Thereafter the mixture was refluxed for a further 20mins. Once the solution had cooled to room temperature, hexane (20ml) was added, and the solid white precipitate was collected by filtration, washed with hexane and dried in vacuo over P_2O_5. Any remaining diphenyl ether was removed in the next step; (Found: MS (EI) *m/z*% 235 (M^+, 48), 189 (100). Requires for $C_{12}H_{10}NO_3F$: M^+, 235).

7-Bromo-4-hydroxyquinoline-3-carboxylic acid ethyl ester (52b)

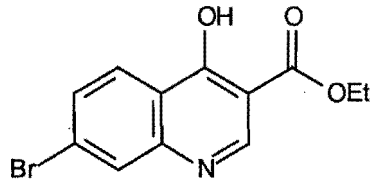

Over a period of 20mins, **51b** (10g, 29mmol) was added to refluxing diphenyl ether (50ml) and then refluxed for a further 25mins. After cooling to room temperature, petroleum ether (15ml) was added and the powdery, white precipitate collected by filtration and washed with large volumes of petroleum ether to give **52b** (1.7g, 20%), mp 285 - 288°C (lit. Conroy *et al.* 1949, 307 - 309°C); (Found: MS (EI) *m/z*% 297 ($(M+2)^+$, 42), 295 (M^+, 43), 251 (97), 249 (100). Requires: $(M+2)^+$, 297; M^+, 295); (Found: C, 49.0; H, 3.1; N, 4.6%. Requires for $C_{12}H_{10}NO_3Br$: C, 48.7; H, 3.4; N, 4.7%).

4-Hydroxy-7-iodoquinoline-3-carboxylic acid ethyl ester (52c)

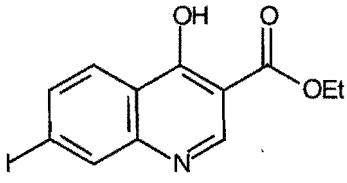

To a boiling solution of diphenyl ether (60ml), crushed 51c (6.1g, 16mmol) was added over 10mins. During this time, the condenser was switched off to allow the ethanol formed to escape. Thereafter the mixture was refluxed for a further 40mins. Once the solution had cooled to room temperature the resulting white precipite was filtered and washed extensively with methanol to remove all the diphenyl ether to give, after drying, **52c** (4.2g, 77%), mp 287 - 295°C (lit. Conroy *et al.* 1949, 302 - 304°C; Counsell *et al.* 1967, 255°C); (Found: MS (EI) *m/z*% 343 (M^+, 75), 297 (100). Requires for M^+, 343); (Found: C, 42.0; H, 2.7; N, 4.0%. Requires for $C_{12}H_{10}NO_3I$: C, 42.0; H, 2.9 N, 4.1%).

4-Hydroxy-7-methoxyquinoline-3-carboxylic acid ethyl ester (52d)

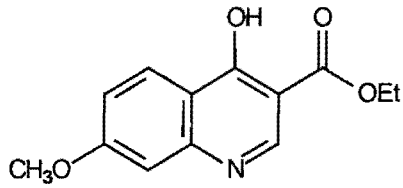

To a stirred, refluxing solution of diphenyl ether (60ml), was added 51d (10g, 34mmol) and the resulting mixture refluxed for 0.5hr. After cooling to room temperature, the precipitate was filtered, washed extensively with cold dichloromethane and dried to give **52d** (4.5g, 54%) in the form of a pale beige-pink solid, mp 269 - 273°C (lit. Lauer *et al.* 1946, 275°C dec.); δ_H (400MHz, d_6 DMSO) 1.26 (3H, t, *J* 7.2, CH_3), 3.85 (3H, s, OCH_3), 4.18 (2H, q, *J* 7.2, CH_2), 6.98 (2H, m, H-6 and H-8), 8.04 (1H, d, *J* 7.6, H-5), 8.45 (1H, s, H-2), 12.02 (1H, s, Ar-OH); δ_H (300MHz, C_6D_6 / d_6 DMSO) 1.08 (3H, t, *J* 7.2, CH_3), 3.60 (3H, s, OCH_3), 4.08 (2H, q, *J* 7.2, CH_2), 6.83 (1H, dd, *J* 8.3, 2.5, H-6), 6.94 (1H, d, *J* 2.5, H-8), 8.16 (1H, d, *J* 8.3, 1.0, H-5), 8.42 (1H, s, H-2); (Found: MS (EI) *m/z%* 247 (M^+, 38), 201 (100). Requires for $C_{13}H_{13}NO_4$: M^+, 247).

4-Hydroxy-5-nitroquinoline-3-carboxylic acid ethyl ester (52e), and 4-hydroxy-7-nitroquinoline-3-carboxylic acid ethyl ester (52e)

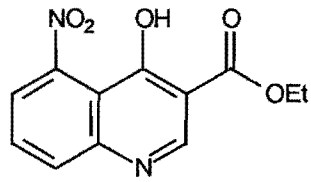

51e (25g, 81mmol) was added over 10mins to vigorously stirred, refluxing diphenyl ether (160ml) at 265°C, and then refluxed for 5hr. Upon cooling to room temperature, petroleum ether was added (150ml) and the powdery yellow product filtered and washed extensively with cold acetone (important) and petroleum ether to remove any unreacted starting material and diphenyl ether. Treatment of the dried product with boiling methanol selectively solubilised the 5-nitro isomer **52e**, which was collected as a filtrate, by filtration. Evaporation of the filtrate under reduced pressure followed by crystallisation from methanol yielded **52e** (2.1g, 11%), mp 267 - 272°C; ν_{max}/cm^{-1} (KBr) 3082, 1684, 1624, 1588, 1529, 1465, 1357, 1206; δ_H (300MHz, d_6 DMSO) 1.27 (3H, t, *J* 7.0, CH_3), 4.22 (2H, q, *J* 7.0, CH_2), 7.62 (1H, t, *J* 4.2, H-7), 7.84 (2H, m, *J* 4.2, H-6 and H-8), 8.63 (1H, s, H-2); δ_C (75.5MHz, d_6 DMSO) 14.2 (CH_3), 59.8 (CH_2), 111.0, 117.5, 118.7 (C-7), 121.9 (Ar-CH), 132.5 (Ar-CH), 140.3, 145.5 (C-

2), 148.4, 164.2 (C=O), 170.4 (Ar-OH); (Found: MS (HRMS) *m/z*% 262.05826. Requires: 262.05897); (Found: C, 55.3; H, 3.8; N, 10.6%. Requires for $C_{12}H_{10}N_2O_5$: C, 55.0; H, 3.8; N, 10.7%).

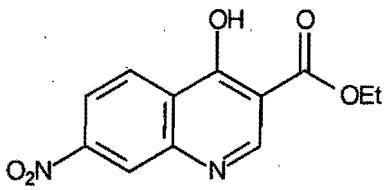

The remaining yellow solid was crystallised from a large volume of DMSO and washed extensively with water and methanol to afford **53e** (5.0g, 23%), mp 293 - 295°C (lit. Vippagunta *et al.* 1999, 290 -296°C); δ_H (400MHz, d_6 DMSO) 1.28 (3H, t, *J* 7.0, CH_3), 4.23 (2H, q, *J* 7.0, CH_2), 8.11 (1H, dd, *J* 8.6, 2.3, H-6), 8.35 (1H, d, *J* 8.6, H-5), 8.48 (1H, d, *J* 2.3, H-8), 8.70 (1H, s, H-2), 14.83 (1H, bs, OH); (Found MS (HRMS) *m/z*% 262.05782. Requires: 262.05897; (Found: C, 55.2; H, 3.6; N, 10.7%. Requires for $C_{12}H_{10}N_2O_5$: C, 55.0; H, 3.8; N, 10.7%).

7-Fluoro-4-hydroxyquinoline-3-carboxylic acid (54a)

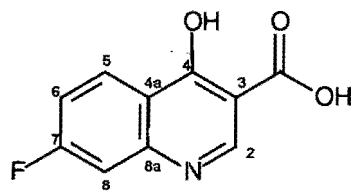

The crude ester **52a** (8.0g, 34mmol) and 10% NaOH (60ml) was heated at 110°C for 2hr and subsequently stirred at room temperature overnight. Any remaining diphenyl ether was then extracted into hexane (three times) after which dropwise addition of 10% HCl to the aqueous phase resulted in precipitation of the white powdery acid **54a**. This product was collected by filtration and dried in vacuo over P_2O_5. The product obtained (6.5g, 88% yield) was recrystallised from methanol to give a white, feathery solid, mp 259 - 260°C (lit. Shah and Coats 1977, 267 - 268°C), δ_H (400MHz, d_6 DMSO) 7.45 (1H, ddd, *J* 8.9, 8.8, 2.4, H-6), 7.55 (1H, dd, *J* 9.6, 2.4, H-8), 8.33 (1H, dd, *J* 8.9, 6.4, H-5), 8.90 (1H, s, H-2), 13.32 (1H, bs, RCOO<u>H</u>), 15.09 (1H, s, Ar-O<u>H</u>); δ_C (100.6MHz, d_6 DMSO) 105.8 ($J_{C\text{-}F}$ 25, C-8), 108.6 (C-3), 115.9 ($J_{C\text{-}F}$ 24, C-6), 122.2 ($J_{C\text{-}F}$ 2, C4a), 129.3 ($J_{C\text{-}F}$ 11, C-5), 141.8 ($J_{C\text{-}F}$ 13, C-8a), 146.8 (C-2), 165.4 ($J_{C\text{-}F}$ 253, C-7), 166.8 (C=O), 178.5 (Ar-OH); (Found MS (EI) *m/z*% 207 (M^+, 29), 189 (52), 163 (100), 135 (38). Requires: M^+, 207); (Found: C, 57.3; H, 3.0; N, 6.6%. Requires for $C_{10}H_6NFO_3$: C, 58.0; H, 2.9; N, 6.8%).

Vippagunta *et al.* 1999, 274 - 275°C); δ_H (300MHz, d_6 DMSO) 8.26 (1H, dd, *J* 9.2, 2.3, H-6), 8.50 (1H, d, *J* 9.2, H-5), 8.81 (1H, d, *J* 2.3, H-8), 8.94 (1H, s, H-2), 14.49 (1H, bs, Ar-OH); δ_C (75.5MHz, d_6 DMSO) 109.0 (C-3), 115.7 (C-8), 119.5 (C-6), 127.5 (C-5), 128.0 (C-4a), 139.4 (C-8a), 146.8 (C-2), 149.9 (C-7), 165.7 (C=O), 177.5 (Ar-OH); (Found MS (EI) *m/z%* 234 (M^+, 16), 216 (43), 190 (100), 144 (56), 53 (71). Requires: M^+, 234); (Found: C, 51.3; H, 2.5; N, 11.8%. Requires for $C_{10}H_6N_2O_5$: C, 51.3; H, 2.6; N, 12.0%).

7-Fluoro-4-hydroxyquinoline (56a)

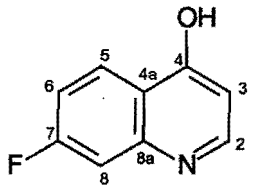

To refluxing diphenyl ether (264°C), was added **54a** (1.3g, 6.1mmol) and the mixture refluxed for 50mins. The reaction could be monitored by solubilisation of the product in the biphenyl ether. Upon cooling to room temperature, petroleum ether (12ml) was added and the subsequent beige solid filtered, washed with cold ethyl acetate : petroleum ether (2:1) and dried to give **56a** (0.81g, 81%). This product was crystallised from water, mp 247 - 248°C (lit. Shah and Coats 1977, 247 - 249°C); δ_H (400MHz, d_6 DMSO) 6.01 (1H, d, *J* 7.4, H-3), 7.14 (1H, ddd, *J* 8.9, 8.8, 2.4, H-6), 7.26 (1H, dd, *J* 10.4, 2.4, H-8), 7.88 (1H, d, *J* 7.4, H-2), 8.12 (1H, dd, *J* 8.9, 6.4, H-5), 11.71 (1H, bs, OH); δ_C (100.6MHz, d_6 DMSO) 104.0 (J_{C-F} 25, C-8), 109.7 (C-3), 112.6 (J_{C-F} 24, C-6), 123.5 (C-4a), 129.0 (J_{C-F} 11, C-5), 140.6 (C-2), 142.1 (J_{C-F} 13, C-8a), 164.4 (J_{C-F} 248, C-7), 177.0 (Ar-OH); (Found MS (EI) *m/z%* 163 (M^+, 100). Requires for C_9H_6NOF: M^+, 163).

7-Bromo-4-hydroxyquinoline (56b)

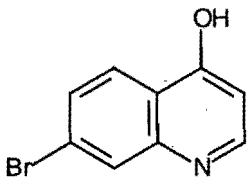

A vigorously stirred mixture of **54b** (1.2g, 4.5mmol) and diphenyl ether (10ml) was heated to 260°C over 40mins, and then refluxed at this temperature for a further 30mins. After cooling this mixture to room temperature, petroleum ether was added, and the light brown, powdery precipitate was collected by filtration and washed extensively (important) with cold petroleum ether. After drying in vacuo, **56b** was obtained (0.99g, 99%). This product was crystallised from ethanol, mp 288 - 292°C (lit. Surrey and Hammer 1946, 279 – 281°C, Conroy *et al.*

1949, 289 - 291°C); δ_H (400MHz, d_6 DMSO) 6.03 (1H, d, *J* 7.0, H-3), 7.42 (1H, dd, *J* 8.5, 1.8, H-6), 7.78 (1H, s, H-8), 7.87 (1H, d, *J* 7.0, H-2), 7.99 (1H, d, *J* 8.5, H-5), 11.9 (1H, bs, Ar-OH); δ_C (100.6MHz, d_6 DMSO) 109.3 (C-3), 120.4 (C-8), 124.7, 124.9, 126.0 (C-6), 127.3 (C-5), 139.7 (C-2), 141.0 (C-8a), 176.4 (Ar-OH); (Found: MS (EI) *m/z%* 225 ($(M+2)^+$, 98), 223 (M^+, 100). Requires: $(M+2)^+$, 225; M^+, 223); (Found: C, 48.3; H, 2.6; N, 6.2%. Requires for C_9H_6NOBr: C, 48.2; H, 2.7; N, 6.3%).

4-Hydroxy-7-iodoquinoline (56c)

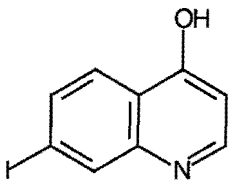

54c (2.8g, 9.0mmol) and diphenyl ether (15ml) were heated to 264°C over 45mins and then refluxed at this temperature for a further 30mins. After cooling to room temperature, the resulting precipitate was filtered and washed thoroughly with petroleum ether to give, after drying, **56c** (2.4g, 97%). This product was crystallised from water and methanol, mp >315°C (lit. Conroy *et al.* 1949, 306 - 308°C; Surrey and Hammer 1946, 346 - 348°C); (Found: MS (EI) *m/z%* 271 (M^+, 100). Requires for C_9H_6NOI: M^+, 271).

4-Hydroxy-7-methoxyquinoline (56d)

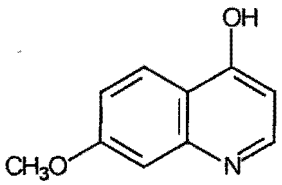

The crushed HCl salt of **54d** (3.9g, 15mmol) was added slowly to refluxing diphenyl ether (40ml) resulting in effervescence. After 10 mins at this temperature, the insoluble starting material had been converted to soluble product. The reaction was stopped after 0.5h and allowed to cool to room temperature. Petroleum ether (40ml) was then added and the white precipitate washed extensively with ethyl acetate:petroleum ether (2:1) to remove the diphenyl ether and then dried to give **56d** (2.2g, 82%), mp 210 - 215°C (lit. Lauer *et al.* 1946, 215°C); δ_H (300MHz, d_6 DMSO) 3.84 (3H, s, OCH_3), 5.92 (1H, d, *J* 7.3, H-3), 6.89 (1H, dd, *J* 9.2, 2.4, H-6), 7.02 (1H, d, *J* 2.4, H-8), 7.78 (1H, d, *J* 7.3, H-2), 7.97 (1H, d, *J* 9.2, H-5), 11.9 (1H, bs, Ar-OH); δ_C (75.5MHz, d_6 DMSO) 55.3 (OCH_3), 99.1 (C-8), 108.4 (C-3), 113.0 (C-6), 120.1 (C-4a), 126.7 (C-5), 138.9 (C-2), 141.8 (C-8a), 161.6 (C-7), 176.4 (Ar-OH); (Found: MS (EI) *m/z%* 175 (M^+, 100). Requires for $C_{10}H_9NO_2$: M^+, 175).

4-Hydroxy-7-nitroquinoline (56e)

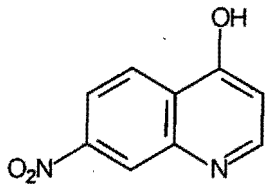

54e was decarboxylated according to the method of Baker *et al.* 1946 {187} by way of its silver salt. This was prepared by addition of 25% NH_3 (aq) (0.64ml, 9.4mmol) to a slurry of **54e** (2.1, 8.9mmol) in deionised water (25ml) at 100°C, followed by addition of a saturated solution of $AgNO_3$ (1.5g, 9.1mmol). The reaction mixture was then refluxed and vigorously stirred (important) at 100°C for 16hr. The mixture was then cooled on ice and the beige, powdery solid precipitate filtered, washed with water and dried in vacuo over P_2O_5 to yield the silver salt of **54e** (2.7g, 90%); δ_H (300MHz, d_6 DMSO) 8.15 (1H, dd, *J* 8.9, 2.3, H-6), 8.47 (1H, d, *J* 8.9, H-5), 8.79 (1H, d, *J* 2.3, H-8), 9.04 (1H, s, H-2), 16.33 (1H, s, Ar-OH); δ_C (100.6MHz, d_6 DMSO) 109.4, 117.2 (C-6), 123.8 (C-8), 127.1 (C-5), 130.1, 149.3, 149.9, 154.8 (C-2), 169.8, 174.9. This solid was added slowly to refluxing diphenyl ether (260°C), as effervescence upon addition was observed. The mixture was refluxed for 45mins, cooled to room temperature and the resulting grey solid washed thoroughly with ethyl acetate : petroleum ether (2:1). This product was then refluxed in ethanol (100ml) at 90°C for 5hr. Hot filtration of the resulting mixture followed by removal of the ethanol under reduced pressure yielded a yellow, powdery solid **56e** (0.38g, 13%), mp 312 - 317°C dec. (lit. Ellis *et al.* 1973, 317 - 320°C; Vippagunta *et al.* 1999, 314 - 317°C dec.); δ_H (200MHz, d_6 DMSO) 6.18 (1H, d, *J* 7.5, H-3), 8.04 (1H, dd, *J* 8.9, 2.1, H-6), 8.11 (1H, d, *J* 7.5, H-2), 8.29 (1H, d, *J* 8.9, H-5), 8.44 (1H, d, *J* 2.1, H-8); (Found: MS (EI) *m/z*% 190 (M^+, 100). Requires for $C_9H_6N_2O_3$: M^+, 190).

4-Chloro-7-fluoroquinoline (57a)

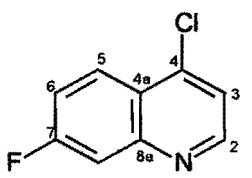

56a (0.73g, 4.5mmol) was treated with phosphorus oxychloride (7.0ml, 74mmol) and the mixture refluxed under N_2 at 115°C for 1hr. The reaction mixture was then poured onto ice followed by neutralisation with 10% NaOH (aq). The white precipitate was extracted into ethyl acetate, dried over $MgSO_4$ and evaporated to dryness under reduced pressure to give a crystalline solid (0.74g, 91%) of **57a** which was crystallised from hexane, mp 71 - 72°C (lit.

Snyder *et al.* 1947, 73.5 - 74°C); δ_H (300MHz, d_6 DMSO) 7.70 (1H, ddd, *J* 9.3, 8.5, 2.4, H-6), 7.76 (1H, d, *J* 4.5, H-3), 7.87 (1H, dd, *J* 9.9, 2.4, H-8), 8.29 (1H, dd, *J* 9.3, 5.7, H-5), 8.87 (1H, d, *J* 4.5, H-2); δ_C (75.5MHz, d_6 DMSO) 113.0 (J_{C-F} 21, C-8), 118.3 (J_{C-F} 25, C-6), 121.1 (C-3), 122.8 (C-4a) 126.6 (J_{C-F} 10, C-5), 141.3 (C-4), 149.5 (J_{C-F} 13, C-8a), 151.8 (C-2), 162.8 (J_{C-F} 250, C-7); (Found: MS (EI) *m/z%* 181 (M^+, 100). Requires: M^+, 181); (Found: C, 59.3; H, 2.7; N, 7.6%. Requires for C_9H_5NClF: C, 59.5; H, 2.8; N, 7.7%).

7-Bromo-4-chloroquinoline (57b)

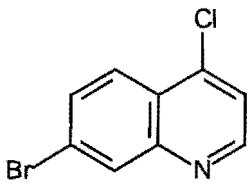

To a stirred mixture of phosphorus oxychloride (4.5ml, 48mmol) and phosphorus pentachloride (0.93g, 4.2mmol) under N_2, **56b** (0.93g, 4.2mmol) was added and the mixture refluxed at 120°C for 0.5hr. The reaction mixture was then poured onto ice followed by neutralisation with cold 10% NaOH (aq). The cream white precipitate was collected by filtration, washed with water and dried in vacuo over P_2O_5. The dried material was then dissolved in benzene and unreacted **56b** removed by filtration to give **57b** (0.74g, 73%) which was crystallised from hexane, mp 100 - 105°C (lit. Surrey and Hammer 1946, 100.5 – 101.5°C, Conroy *et al.* 1949, 105 - 106°C); δ_H (300MHz, $CDCl_3$) 7.50 (1H, d, *J* .4.8, H-3), 7.73 (1H, dd, *J* 9.0, 1.8, H-6), 8.10 (1H, d, *J* 9.0, H-5), 8.31 (1H, d, *J* 1.8, H-8), 8.77 (1H, d, *J* 4.8, H-2); δ_C (75.5MHz, $CDCl_3$) 121.5, 124.8, 125.3, 125.6, 131.2, 132.1, 142.8, 149.7, 150.9; (Found: MS (EI) *m/z%* 243 ($(M+2)^+$, 100), 241 (M^+, 80). Requires: $(M+2)^+$, 243; M^+, 241); (Found: C, 44.7; H, 1.8; N, 5.8%. Requires for C_9H_5NBrCl: C, 44.6; H, 2.0; N, 5.8%).

4-Chloro-7-iodoquinoline (57c)

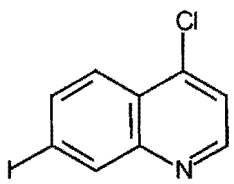

A mixture of **56c** (1.8g, 6.6mmol), phosphorus oxychloride (5ml, 53mmol) and phosphorus pentachloride (1.7g, 7.9mmol) was refluxed under N_2 at 120°C for 0.5hr. The reaction mixture was then poured onto ice followed by neutralisation with 10% NaOH (aq). The yellow precipitate was then filtered, washed with water and dried in vacuo over P_2O_5. The product was dissolved in benzene and insoluble impurities filtered off to give a solid which

was crystallised from heptane and benzene to give **57c** (1.2g, 62%), mp 97 - 101°C (lit. Conroy *et al.* 1949, 101 - 102°C; Surrey and Hammer 1946, 95.5 - 97°C; Counsell *et al.* 1967, 97 - 98°C); δ_H (300MHz, $CDCl_3$) 7.49 (1H, d, *J* 4.8, H-3), 7.91 (2H, m, H-5 and H-6), 8.55 (1H, d, *J* 1.2, H-8), 8.76 (1H, d, *J* 4.8, H-2); δ_C (75.5MHz, $CDCl_3$) 96.8 (C-7), 121.7 (C-3), 125.4 (C-5), 125.7 (C-4a), 136.4 (C-6), 138.8 (C-8), 142.8 (C-4), 149.7 (C-8a), 150.6 (C-2); (Found: MS (EI) *m/z*% 289 (M^+, 100). Requires: M^+, 289); (Found: C, 37.7; H, 1.4; N, 4.7%. Requires for C_9H_5NCII: C, 37.3; H, 1.7; N, 4.8%).

4-Chloro-7-methoxyquinoline (57d)

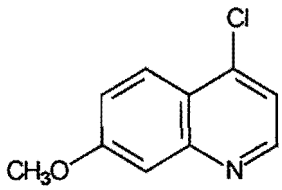

56d (2.0g, 12mmol) was treated with phosphorus oxychloride (14ml) and the mixture was refluxed under N_2 at 110°C for 20mins. The reaction mixture was then poured onto ice and neutralised with 10% NaOH (aq). The white-powdery precipitate was then extracted into dichloromethane (four times), dried ($MgSO_4$), and evaporated to dryness under reduced pressure to give the HCl salt of **57d** (2.2g, 80%). Crystallisation from ethyl acetate yielded the HCl salt of **57d** (1.3g, 49%), mp 180 - 186°C; δ_H (300MHz, d_6 DMSO) 4.00 (3H, s, OCH_3), 5.06 (1H, bs, NH), 7.59 (1H, dd, *J* 9.3, 2.6, H-6), 7.75 (1H, d, *J* 2.6, H-8), 7.94 (1H, d, *J* 5.4, H-3), 8.26 (1H, d, *J* 9.3, H-5), 9.03 (1H, d, *J* 5.4, H-2); δ_C (75.5MHz, d_6 DMSO) 56.3 (OCH_3), 102.7 (C-8), 119.9 (C-3), 121.5 (C-4a), 122.6 (C-6), 126.1 (C-5), 144.2 (C-4), 146.5 (C-2), 147.4 (C-8a), 163.1 (C-7). Extraction of this product from water (pH 7) into ethyl acetate gave the free base of **57d**, mp 84 - 85°C (Lauer *et al.* 1946, 82 - 83°C), δ_H (400MHz, DMSO) 3.94 (3H, s, OCH_3), 7.39 (1H, dd, *J* 9.2, 2.6, H-6), 7.46 (1H, d, *J* 2.6, H-8), 7.56 (1H, d, *J* 4.6, H-3), 8.08 (1H, d, *J* 9.2, H-5), 8.74 (1H, d, *J* 4.6, H-2); δ_C (100.6MHz, d_6 DMSO) 56.4 (OCH_3), 108.6 (C-8), 120.1 (C-3), 121.0 (C-4a), 121.4 (C-6), 125.6 (C-5), 141.6 (C-4), 151.5 (C-2), 153.5 (C-8a), 161.7 (C-7); (Found: MS (EI) *m/z*% 193 (M^+, 100). Requires: M^+, 193); (Found: C, 61.9; H, 4.4; N, 7.1%. Requires for $C_{10}H_8NOCl$: C, 62.0; H, 4.2; N, 7.2%).

4-Chloro-7-nitroquinoline (57e)

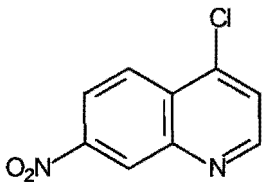

A mixture of **56e** (0.36g, 1.9mmol) and phosphorus oxychloride (3.0ml) was refluxed under N_2 at 115°C for 0.5hr. The reaction mixture was then poured onto ice followed by neutralisation with 10% NaOH (aq). The peach coloured precipitate was extracted into ethyl acetate, dried over $MgSO_4$ and evaporated under reduced pressure. The residue was chromatographed on silica gel (70:1) using dichloromethane as the eluent. Subsequent crystallisation from heptane and toluene yielded **57e** (0.30g, 76%), mp 169 - 172°C (lit. Ellis *et al.* 1973, 171 - 173°C; Vippagunta et al. 1999, 156 -160°C); δ_H (300MHz, $CDCl_3$) 7.67 (1H, d, *J* 4.7, H-3), 8.41 (2H, m, 2 × Ar-H), 8.95 (1H, d, *J* 4.7, H-2), 9.02 (1H, m, Ar-H); δ_C (100.6MHz, $CDCl_3$) 121.0 (Ar-CH), 123.8 (C-3), 126.1 (Ar-CH), 126.3 (Ar-CH), 129.7, 142.9, 148.3, 148.7, 152.2 (C-2); (Found: MS (EI) *m/z*% 208 (M^+, 100). Requires for $C_9H_5N_2O_2Cl$: M^+, 208).

2-Aminoquinoline (58)

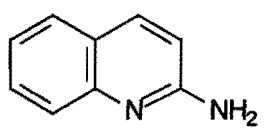

A mixture of **24** (0.44g, 2.7mmol), 25% NH_3 (aq) (10ml) and a catalytic amount of $ZnCl_2$ were placed in a sealed glass tube and heated at 140°C for 65h. The product was then extracted into ethyl acetate (four times), dried over anhydrous $MgSO_4$ and concentrated under reduced pressure to give a white crystalline residue which was crystallised from benzene to give **58** (0.30g, 78%), mp 129°C (DSC) (lit. Brown and Plasz 1970, 128 - 129°C); ν_{max}/cm^{-1} (KBr) 3402 and 3336 (Ar-NH_2); δ_H (400MHz, $CDCl_3$) 4.68 (2H, bs, NH_2), 6.61 (1H, d, *J* 8.9, H-3), 7.15 (1H, td, *J* 7.6, 1.3), 7.45 (1H, td, 7.6, 1.3), 7.53 (1H, dd, *J* 8.2, 1.3), 7.58 (1H, dd, *J* 8.2, 1.3), 7.78 (1H, d, *J* 8.9, H-4); δ_C (100.6MHz, $CDCl_3$) 111.6 (C-3), 122.7 (C-6), 123.6 (C-4a or C-8a), 126.0 (C-8), 127.5 (C-5), 129.7 (C-7), 138.0 (C-4), 147.7 (C-4a or C-8a), 156.9 (C-2); (Found MS (HRMS) *m/z*% 144.0690. Requires: 144.0687); (Found: C, 75.3; H, 5.6; N, 19.5%. Requires for $C_9H_8N_2$: C, 75.0; H, 5.6; N, 19.4%).

2-Methylaminoquinoline (59)

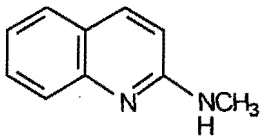

A mixture of **24** (0.50g, 3.1mmol) and 33% methylamine : methanol (33:66) (4ml) was placed in a sealed tube and the mixture heated at 120°C for 20h. The methylamine was then removed under reduced pressure and Na_2CO_3 (aq) added. The products were extracted into ethyl acetate (three times), dried over anhydrous $MgSO_4$ and the solvent removed under reduced pressure. The residue was chromatographed on silica gel using triethylamine : ethyl acetate : petroleum ether (10:30:60) as the eluent to give **59** (0.39g, 81%) which was then crystallised from benzene and petroleum ether, mp 70 - 72°C (lit. Watanabe *et al.* 1980, 69 - 71°C); δ_H (200MHz, $CDCl_3$) 3.09 (3H, d, *J* 5.1, NCH_3), 4.78 (1H, bs, NH), 6.63 (1H, d, *J* 9.0, H-3), 7.21 (1H, td, 7.7, 1.4, Ar-H), 7.51 (1H, td, *J* 7.7, 1.4, Ar-H), 7.58 (1H, d, Ar-H), 7.71 (1H, d, *J* 8.3, Ar-H), 7.81 (1H, d, *J* 9.0, H-4); δ_C (50.3MHz, $CDCl_3$) 28.7 (CH_3), 111.1 (C-3), 121.9 (C-6), 123.3 (C-4a or C-8a), 126.1 (C-8), 127.4 (C-5), 129.5 (C-7), 137.2 (C-4), 148.1 (C-4a or C-8a), 157.6 (C-2); (Found: MS (EI) *m/z*% 159 (M^+, 100). Requires: M^+, 159); (Found; C, 76.1; H, 6.5; N, 17.4%. Requires for $C_{10}H_{10}N_2$: C, 75.9; H, 6.4; N, 17.7%).

***N*-(2-Quinolinyl)-1,2-ethanediamine monohydrochloride (60)**

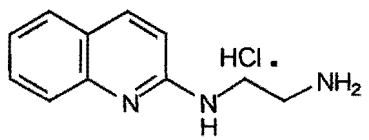

A mixture of **24** (2.7g, 16mmol) and excess 90% ethylenediamine (aq) (10ml) were heated in a 25ml sealed tube at 105°C for 19h. The reaction mixture was then concentrated under reduced pressure and the residue chromatographed on silica gel (40:1). The unreacted starting material was first eluted with petroleum ether followed by product elution using 25% NH_3 (aq) : methanol (1:99) to afford **60** as a hydrochloride salt (3.0g, 82%) which was crystallised from ethanol to give white needles, mp 174 - 178°C;. ν_{max}/cm^{-1} (KBr) 3259, 3132, 3051, 2954, 2892, 2076, 1625, 1540, 1148, 813; δ_H (400MHz, d_6 DMSO) 3.06 (2H, t, *J* 6.2, CH_2-α), 3.61 (2H, m, CH_2-β), 6.80 (1H, dd, *J* 9.0, 1.2, H-3), 7.16 (1H, dt, H-6), 7.44 (1H, bs, NH), 7.48 (1H, dt, H-7), 7.56 (1H, dd, *J* 8.0, 1.0, H-8), 7.63 (1H, dd, *J* 8.0, 1.0, H-5), 7.88 (1H, d, *J* 9.0, H-4), 8.15 – 8.25 (2H, bs, NH_2) ; δ_C(100.6MHz, d_6 DMSO) 39.0 (CH_2-α), 39.1 (CH_2-β), 113.7 (C-3), 122.0 (C-6), 123.4 (C-4a or C-8a), 125.9 (C-8), 127.9 (C-5), 129.6 (C-7), 136.9 (C-4), 147.8 (C-4a or C-8a), 157.2 (C-2); (Found: MS (EI) *m/z*% 187 (M^+, 9), 158

(41), 157 (100), 145 (46), 144 (50), 129 (50), 128 (66). Requires: M^+ (free base), 187); (Found: C, 59.0; H, 6.3; N, 18.8%. Requires for $C_{11}H_{13}N_3.HCl$: C, 59.1; H, 6.3; N, 18.8%).

4-Aminoquinoline (61)

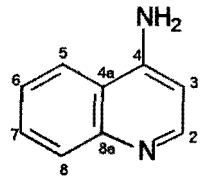

Method A

To a solution of dry, distilled liquid ammonia (50ml) and freshly prepared potassium amide (1.1g, 19mmol) in a sealed tube at -40°C, quinoline (1.0g, 7.7mmol) was added. The clear yellow solution that resulted upon quinoline addition changed to opaque dark green upon warming to room temperature. After 1hr at room temperature, the tube was recooled to -40°C, opened and the contents transferred to a wide-necked conical flask in a bath at -40°C. Potassium permanganate was then added (4.3g, 27mmol) slowly, with stirring. After 15mins the reaction temperature was raised very slowly to 0°C during which time the ammonia slowly evaporated off. The mixture was then quenched dropwise with cold $(NH_4)_2SO_4$ (aq), filtered through celite, extracted into ethyl acetate (four times), dried over anhydrous $MgSO_4$ and evaporated under reduced pressure. The residue was chromatographed on silica gel using mixtures of triethylamine : ethyl acetate (0:100) to (10:90) as the eluent and crystallised from benzene to afford **61** (0.26mg, 26%), mp 151 - 153°C (lit. Den Hertog *et al.* 1967, 151 - 152°C; Tondys *et al.* 1985, 149 - 150°C); ν_{max}/cm^{-1} (KBr) 3402 and 3336 (Ar-NH_2); δ_H (200MHz, $CDCl_3$) 5.02 (2H, bs, NH_2), 6.56 (1H, d, *J* 5.1, H-3), 7.41 (1H, td, H-6), 7.62 (1H, td, H-7), 7.78 (1H, dd, *J* 8.4, 0.8, H-8), 7.95 (1H, dd, *J* 8.5, 0.7, H-5), 8.51 (1H, d, *J* 5.1, H-2), δ_C (50.3MHz, $CDCl_3$) 103.6 (C-3), 118.8, 120.3 (C-5), 124.7 (C-6), 129.3 (C-7), 129.7 (C-8), 148.8 (C-4 or C-8a), 149.8 (C-4 or C-8a), 150.6 (C-2); (Found: MS (EI) *m/z*% 144 (M^+, 100). Requires: M^+, 144); (Found: C, 74.8; H, 5.7; N, 19.6%. Requires for $C_9H_8N_2$: C, 75.0; H, 5.6; N, 19.4%).

Method B

A mixture of **30a** (0.11g, 0.66mmol), 25% NH_3 (aq) (3ml) and a catalytic amount of $ZnCl_2$ were placed in a sealed glass tube. After 35h at 150°C, the product was extracted into ethyl acetate (three times), dried over anhydrous $MgSO_4$ and evaporated under reduced pressure. The product was chromatographed on silica gel (5g) using mixtures of triethylamine : ethyl acetate (0:100) to (10:90) as the eluent and crystallised from benzene to give **61** (57mg, 60%), mp 149 - 152°C; ^1H NMR ($CDCl_3$) identical to that found with the reference compound (Method A); (Found: MS (EI) *m/z*% 144 (M^+, 100). Requires for $C_9H_8N_2$: M^+, 144).

Method C

A mixture of **29a** (0.95g, 5.0mmol), 10% Pd-C (2.7g, 2.6mmol), glacial acetic acid (7ml), acetic anhydride (1.5ml) and ethanol (5ml) was placed in a three-necked round bottomed flask. Hydrogen was bubbled through the reaction mixture at room temperature for 7.5h. The mixture was then filtered through Celite and a solution of potassium hydroxide in ethanol added to the filtrate until an alkaline solution was obtained. The organic phase were then removed under reduced pressure and the products extracted into ethyl acetate (three times), dried over anhydrous $MgSO_4$ and the extracts concentrated again. The products were adsorbed onto a silica gel column (60g) and eluted using mixtures of triethylamine : ethyl acetate (0:100) to (10:90) to obtain **61** (0.50g, 69%) which was crystallised from benzene, mp 152 - 155°C. ^1H NMR ($CDCl_3$) identical to that found with the reference compound (Method A); (Found: MS (EI) *m/z%* 144 (M^+, 100). Requires for $C_9H_8N_2$: M^+, 144).

4-Methylaminoquinoline (62)

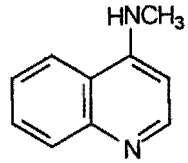

A solution of **30a** (0.53g, 3.2mmol) and excess methylamine : methanol (1:2) (4ml) was heated in a sealed tube at 154°C for 20h. The reaction mixture was then concentrated under reduced pressure and the residue chromatographed using flash column chromatography (80:1). Any unreacted starting material was first eluted using triethylamine : methanol : ethyl acetate (1:1:98), followed by product elution using mixtures of triethylamine : methanol : ethyl acetate (2:5:93) to (10:10:80) to afford **62** (0.48g, 94%) which was crystallised from ethyl acetate and ethanol, mp 233°C (DSC) (lit. Luthy *et al.* 1949, 227 - 227.5°C; Watanabe *et al.* 1980, 231 - 232°C; ν_{max}/cm^{-1} (d_6 DMSO) 3484, 3432, 1662, 1586, 1545, 1343, 1152; δ_H (400MHz, d_6 DMSO) 2.87 (3H, d, *J* 4.5, CH_3), 6.35 (1H, d, *J* 5.3, H-3), 7.25 (1H, bd, *J* 4.5, NH), 7.40 (1H, ddd, *J* 8.0, 7.5, 0.9, H-6), 7.56 (1H, ddd, *J* 8.0, 7.5, 0.9, H-7), 7.75 (1H, d, *J* 8.0, H-8), 8.10 (1H, d, *J* 8.0, H-5), 8.40 (1H, d, *J* 5.3, H-2); δ_C (100.6MHz, d_6 DMSO) 29.7 (CH_3), 98.3 (C-3), 119.2 (C-4a), 121.8 (C-5), 124.2 (C-6), 129.1 (C-7), 129.4 (C-8), 148.5 (C-8a or C-4), 151.2 (C-2), 151.2 (C-8a or C-4); (Found: MS (EI) *m/z%* 158 (M^+, 100). Requires: M^+, 158); (Found; C, 75.8; H, 6.6; N, 17.9%. Requires for $C_{10}H_{10}N_2$: C, 75.9; H, 6.4; N, 17.7%).

2-(4-Quinolinyl)-aminoethanol (63)

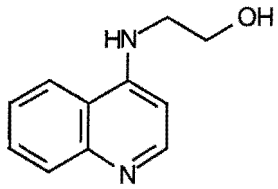

A solution of **30a** (0.20g, 1.2mmol) and ethanolamine (3ml) was heated in a sealed tube at 120°C for 4.5h. The product was then extracted into ethyl acetate (three times) from Na_2CO_3 (aq), dried over anhydrous $MgSO_4$ and evaporated under reduced pressure. Crystallisation from ethyl acetate and methanol followed by drying in vacuo over P_2O_5 afforded **63** (86mg, 37%), mp 139°C (DSC); ν_{max}/cm^{-1} (KBr) 3322, 1585, 1546, 1340, 1070; δ_H (400MHz, d_6 DMSO) 3.35 (2H, m, CH_2), 3.65 (2H, m, CH_2), 4.82 (1H, bs, OH), 6.45 (1H, d, *J* 5.4, H-3), 7.05 (1H, t, *J* 5.5, NH), 7.39 (1H, td, H-6), 7.58 (1H, td, H-7), 7.75 (1H, dd, *J* 8.3, 0.9, H-8), 8.18 (1H, dd, *J* 8.5, 1.1, H-5), 8.36 (1H, d, *J* 5.4, H-2); δ_C (100.6MHz, d_6 DMSO) 45.5 (CH_2), 59.2 (CH_2), 98.6 (C-3), 119.2 (C-4a), 122.0 (C-5), 124.2 (C-6), 129.1 (C-7), 129.4 (C-8), 148.7 (C-8a or C-4), 150.5 (C-8a or C-4), 151.1 (C-2); (Found: MS (EI) *m/z*% 188 (M^+, 48), 157 (100). Requires: M^+, 188); (Found: C, 69.6; H, 6.7; N, 14.0%. Requires for $C_{11}H_{12}N_2O$: C, 70.2; H, 6.4; N, 14.9%).

***N*-(4-Quinolinyl)-1,2-ethanediamine monohydrochloride (64)**

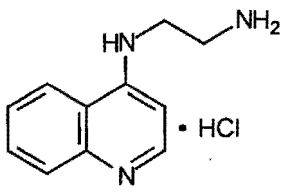

A solution of **30a** (0.57g, 3.5mmol) in excess 90% ethylenediamine (aq) was heated in a sealed tube at 120°C for 5h. The reaction mixture was then concentrated under reduced pressure and the residue chromatographed on silica gel (60:1) using mixtures of 25% NH_3 (aq) : methanol (0.5:95.5) to (3.5:96.5) as the eluent to yield **64** as the hydrochloride salt. This was crystallised from ethyl acetate and methanol to afford **64** as a powdery beige solid (0.60g, 92%), mp 211 - 212°C; ν_{max}/cm^{-1} (d_6 DMSO) 3482, 3314, 2971, 1663, 1583, 1543, 1342; δ_H (400MHz, d_6 DMSO) 3.10 (2H, t, *J* 6.3, CH_2-β), 3.56 (2H, t, *J* 6.3, CH_2-α), 3.2 - 4.2 (3H, bs, NH_2 and NH), 6.56 (1H, d, *J* 5.4, H-3), 7.44 (1H, td, H-6), 7.63 (1H, td, H-7), 7.80 (1H, dd, *J* 8.4, 0.6, H-8), 8.33 (1H, d, *J* 8.5, H-5), 8.43 (1H, d, *J* 5.4, H-2); δ_C (100.6MHz, d_6 DMSO) 38.3 (CH_2-β), 41.2 (CH_2-α), 99.2 (C-3), 119.7 (C-4a), 123.0 (C-5), 124.8 (C-6), 129.4 (C-8), 129.9 (C-7), 148.7 and 150.7 (C-8a and C-4), 151.2 (C-2); (Found MS (HRMS) *m/z*%

187.1116. Requires: 187.1109 (free base)); (Found: C, 59.0; H, 6.5; N, 18.6%. Requires for $C_{11}H_{13}N_3$.HCl: C, 59.1; H, 6.3; N, 18.8%).

N^2-(4-Quinolinyl)-N^1,N^1-diethyl-1,2-ethanediamine (65)

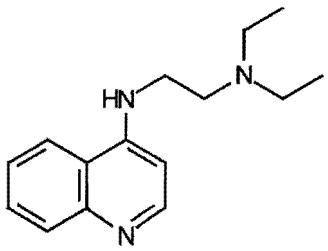

A mixture of **30a** (0.40g, 2.5mmol) in excess *N,N*-diethylethylenediamine (1.5ml) was heated in a sealed tube at 150°C for 8h. The reaction mixture was then concentrated under reduced pressure and the residue extracted into dichloromethane (four times) from K_2CO_3 (aq), evaporated under reduced pressure, dried over anhydrous $MgSO_4$ and chromatographed on silica gel (60:1) using mixtures of triethylamine : ethyl acetate (0:100) to (2.5:97.5) to elute **65** as a brown solid (0.46g, 77%), mp 82°C; ν_{max}/cm^{-1} (KBr) 3202, 2965, 1581, 1550, 1167, 1092, 809; δ_H (400MHz,$CDCl_3$) 1.08 (6H, t, *J* 7.1, 2×CH_3), 2.61 (4H, q, *J* 7.1, 2×CH_2), 2.83 (2H, t, *J* 6.0, CH_2-β), 3.27 (2H, m, CH_2-α), 6.07 (1H, bs, NH), 6.38 (1H, d, *J* 5.4, H-3), 7.43 (1H, td, H-6), 7.62 (1H, td, H-7), 7.74 (1H, dd, *J* 8.3, 1.1, H-8), 7.97 (1H, dd, *J* 8.5, 0.7, H-5), 8.55 (1H, d, *J* 5.4, H-2); δ_C(100.6MHz, $CDCl_3$) 12.1 (2 × CH_3), 39.8 (CH_2-α), 46.6 (2 × CH_2), 50.8 (CH_2-β), 99.0 (C-3), 119.1 (C-5),119.6 (C-4a), 124.5 (C-6), 128.9 (C-7), 129.8 (C-8), 148.4 (C-8a or C-4), 149.9 (C-8a or C-4), 151.1 (C-2); (Found MS (HRMS) *m/z*% 243.1731. Requires: 243.1735); (Found: C, 74.0; H, 8.8; N, 17.2%. Requires for $C_{15}H_{21}N_3$: C, 74.0; H, 8.7; N, 17.3%).

4-Amino-7-methylquinoline (66)

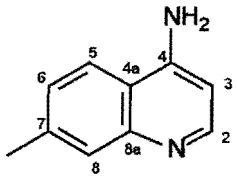

A solution of **30b** (0.14g, 0.79mmol) in 25% ammonia (aq) (3ml) and a catalytic amount of $ZnCl_2$ was heated in a sealed tube at 145°C for 18h, followed by a further 24h at 160°C. The products were then extracted into ethyl acetate (four times), dried over anhydrous $MgSO_4$ and the solvent evaporated under reduced pressure. The residue was chromatographed on silica gel (15g) using mixtures of triethylamine : ethyl acetate (0:100) to (1:99) as the eluent. The solid residue was crystallised from benzene to give **66** (80mg, 64%), mp 164 - 165°C;

ν_{max}/cm^{-1} (KBr) 3428, 3315, 3160-2970, 1652, 1582, 1511, 1455, 1332, 1291, 1224; δ_H (400MHz, $CDCl_3$) 2.52 (3H, s, CH_3), 4.76 (2H, s, NH_2), 6.53 (1H, d, *J* 5.1, H-3), 7.27 (1H, dd, *J* 8.6, 1.7, H-6), 7.65 (1H, d, *J* 8.6, H-5), 7.77 (1H, m, H-8,), 8.47 (1H, d, *J* 5.1, H-2); δ_C (100.6MHz, $CDCl_3$) 21.6 (CH_3), 103.2 (C-3), 116.7 (C-4a), 119.9 (C-5), 127.0 (C-6), 128.9 (C-8), 139.5 (C-7), 149.1 (C-8a or C-4), 149.4 (C-8a or C-4), 150.7 (C-2); (Found: MS (EI) *m/z%* 158 (M^+, 100). Requires: M^+, 158); (Found: C, 75.7; H, 6.5; N, 17.7%. Requires for $C_{10}H_{10}N_2$: C, 75.9; H, 6.4; N, 17.7%).

N^1,N^1-Diethyl -N^2-(7-methyl-4-quinolinyl)-1,2-ethanediamine (67)

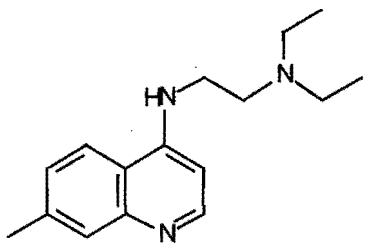

A solution of **30b** (0.14g, 0.79mmol) and excess N,N-diethylethylenediamine (3ml) was heated in a sealed tube at 130°C for 18h followed by a further 6h at 150°C. The reaction mixture was then concentrated under reduced pressure. The products were extracted into dichloromethane (four times) from aqueous K_2CO_3, dried over anhydrous $MgSO_4$ and the solvent evaporated under reduced pressure. The residue was chromatographed on silica gel (15g) using mixtures of triethylamine : ethyl acetate (0:100) to (2:98) as the eluent to give a solid that was crystallised from hexane to give white crystals of **67** (0.16g, 78%), mp 102 - 105°C (lit. Patent US2940974 1960, 99 - 103.6°C); ν_{max}/cm^{-1} (KBr) 3195, 2964, 1591, 1580, 1552, 1455, 1380, 1230, 1165, 809; δ_H (400MHz, $CDCl_3$) 1.07 (6H, t, *J* 7.2, 2 × CH_3), 2.51 (3H, s, CH_3), 2.60 (4H, q, *J* 7.2, 2 × CH_2), 2.82 (2H, t, CH_2-β), 3.26 (2H, m, CH_2-α), 6.02 (1H, s, NH), 6.33 (1H, d, *J* 5.3, H-3), 7.26 (1H, dd, *J* 8.6, 1.7, H-6), 7.63 (1H, d, *J* 8.6, H-5), 7.75 (1H, m, H-8,), 8.50 (1H, d, *J* 5.3, H-2); δ_C (100.6MHz, $CDCl_3$) 12.1 (2 × CH_3), 21.6 (CH_3), 39.8 (CH_2-α), 46.5 (2 × CH_2), 50.8 (CH_2-β), 98.5 (C-3), 116.9 (C-4a), 119.3 (C-5), 126.6 (C-6), 128.9 (C-8), 139.0 (C-7), 148.6 (C-8a or C-4), 149.9 (C-8a or C-4), 151.1 (C-2); (Found: MS (EI) *m/z%* 257 (M^+, 13), 171 (14), 115 (19), 86 (100), 58 (38), 30 (58). Requires: M^+, 257); (Found: C, 74.6; H, 9.4; N, 16.3%. Requires for $C_{16}H_{23}N_3$: C, 74.7; H, 9.0; N, 16.3%).

4-Amino-7-chloroquinoline (68)

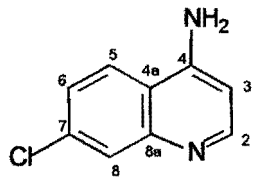

68 was prepared via reaction of 4,7-dichloroquinoline with aqueous ammonia and $ZnCl_2$. The material was then crystallised from benzene and ethanol to give **68**, mp 134°C (lit. Price *et al.* 1946, 105 - 110°C; Roseman *et al.* 1970, 152 - 154.4°C; Lin and Loo 1978, 146 - 147°C); ν_{max}/cm^{-1} (KBr) 3460, 3358, 3242, 3428, 1643, 1613, 1578, 1510, 1284, 878; δ_H (200MHz, d_6 Acetone) 6.35 (2H, bs, NH_2), 6.67 (1H, d, *J* 5.1, H-3), 7.36 (1H, dd, *J* 9.0, 2.1, H-6), 7.85 (1H, d, *J* 2.1, H-8), 8.14 (1H, d, *J* 9.0, H-5), 8.38 (1H, d, *J* 5.1, H-2); δ_C(100.6MHz, d_6 DMSO) 103.1 (C-3), 117.5 (C-4a), 124.2 (C-6), 125.1 (C-5), 127.7 (C-8), 133.9 (C-7), 149.9 (C-8a or C-4), 151.9 (C-2), 152.1 (C-8a or C-4); (Found: MS (EI) *m/z*% 178 (M^+, 100). Requires for $C_9H_7N_2Cl$: M^+, 178).

7-Chloro-4-methylaminoquinoline (69)

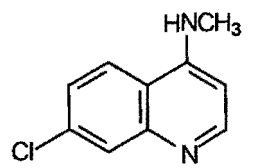

69 was prepared via 4-substitution of 4,7-dichloroquinoline with methylamine : methanol (1:2) and then crystallised from ethyl acetate and ethanol to give **69**, mp 245°C (lit. Craig and Pearson 1968, 245 - 246°C); ν_{max}/cm^{-1} (KBr) 3201, 3060, 1580. 1436, 1369, 1280, 1203, 1146, 1080. 867; δ_H (400MHz, d_6 DMSO) 2.86 (3H, d, *J* 4.8, CH_3), 6.38 (1H, d, *J* 5.4, H-3), 7.42 (2H, m, H-6 and NH), 7.77 (1H, d, *J* 2.4, H-8), 8.16 (1H, d, *J* 9.0, H-5), 8.40 (1H, d, *J* 5.4, H-2); δ_C (100.6MHz, d_6 DMSO) 29.7 (CH_3), 98.8 (C-3), 117.8 (C-4a), 124.2 (C-6), 124.5 (C-5), 127.9 (C-8), 133.7 (C-7), 149.3 (C-8a or C-4), 151.3 (C-8a or C-4), 152.4 (C-2); (Found: MS (EI) *m/z*% 192 (M^+, 100). Requires: M^+, 192); (Found: C, 62.2; H, 4.6; N, 14.5%. Requires for $C_{10}H_9N_2Cl$: C, 62.3; H, 4.7; N, 14.5%).

N-(7-Chloro-4-quinolinyl)-aminopropane (70)

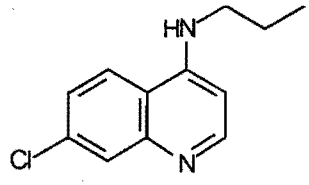

A mixture of 4,7-dichloroquinoline (2.0g, 10mmol) and propylamine (15ml) were heated in a tube, sealed under N_2 at 95°C for 20h. After cooling to room temperature, the tube was reopened and the propylamine evaporated off under reduced pressure. 0.95M potassium hydroxide (40ml) was added and the white solid residue collected by filtration and washed with cold ether. The crude solid was dried in vacuo over P_2O_5, and then crystallised from ethanol and ethyl acetate to give **70** (0.91g, 37%), mp 146 - 148°C; δ_H (300MHz, d_6 DMSO) 0.96 (3H, t, *J* 7.3, CH_3), 1.67 (2H, sext, *J* 7.3, 4.8, CH_2-β), 3.21 (2H, m, CH_2-α), 6.45 (1H, d, *J* 5.1, H-3), 7.29 (1H, t, *J* 5.3, NH), 7.43 (1H, dd, *J* 8.9, 2.3, H-6), 7.78 (1H, d, *J* 2.3, H-8), 8.28 (1H, d, *J* 8.9, H-5), 8.38 (1H, d, *J* 5.1, H-2); δ_C (75.5MHz, d_6 DMSO) 11.5 (CH_3), 21.0 (CH_2-β), 44.1 (CH_2-α), 98.6 (C-3), 117.4 (C-4a), 123.9 (C-6), 124.1 (C-5), 127.4 (C-8), 133.3 (C-7), 149.1 (C-8a or C-4), 150.1 (C-8a or C-4), 151.8 (C-2); (Found MS (HRMS) *m/z%* 220.07708. Requires: 220.07673); (Found: C, 65.5; H, 6.1 N, 12.5%. Requires for $C_{12}H_{13}N_2Cl$: C, 65.3; H, 5.9; N, 12.7%).

2-(7-Chloro-4-quinolinyl)-aminoethanol (71)

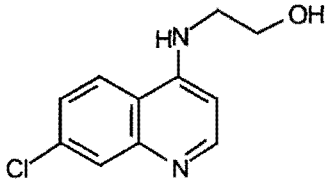

71 was obtained via 4-substitution of 4,7-dichloroquinoline with ethanolamine (aq) and subsequent crystallisation from ethanol to give **71**, mp 217 - 218°C (lit. Elderfield *et al.* 1946, 214°C); ν_{max}/cm^{-1} (KBr) 3311, 3100-2845, 1583, 1453, 1344, 1081, 803; δ_H (400MHz, d_6 DMSO) 3.35 (2H, t, CH_2-β), 3.65 (2H, m, CH_2-α), 4.84 (1H, bs, OH), 6.49 (1H, d, *J* 5.5, H-3), 7.25 (1H, bt, *J* 5.3, NH), 7.43 (1H, dd, *J* 9.0, 2.2, H-6), 7.77 (1H, d, *J* 2.2, H-8), 8.25 (1H, d, *J* 9.0, H-5), 8.38 (1H, d, *J* 5.5, H-2); δ_C (100.6MHz, d_6 DMSO) 45.5 (CH_2-β), 59.1 (CH_2-α), 99.1 (C-3), 117.8 (C-4a), 2 × 124.4 (C-5 and C-6), 127.9 (C-8), 133.7 (C-7), 149.5 (C-8a or C-4), 150.6 (C-8a or C-4), 152.3 (C-2); (Found: MS (EI) *m/z%* 222 (M^+, 60), 191 (100), 156 (70). Requires: M^+, 222); (Found: C, 59.2; H, 5.0; N, 12.5%. Requires for $C_{11}H_{11}N_2OCl$: C, 59.3; H, 5.0; N, 12.6%).

N-(7-Chloro-4-quinolinyl)-1,2-ethanediamine (72)

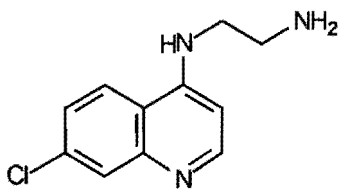

72 was prepared via 4-substitution of 4,7-dichloroquinoline with 90% ethylenediamine (aq). The material was then crystallised from acetonitrile and methanol to give **72** mp 137 - 139°C (lit. Peck *et al* 1959, 137 - 139°C); ν_{max}/cm^{-1} (d_6 DMSO) 3490, 1660, 1580, 1450, 1366, 1280; δ_H (400MHz, d_6 DMSO) 2.80 (2H, t, *J* 6.5, CH_2-β), 3.23 (2H, m, CH_2-α), 3.30 (2H, bs, NH_2), 6.47 (1H, d, *J* 5.4, H-3), 7.21 (1H, bs, NH), 7.41 (1H, dd, *J* 9.0, 2.1, H-6), 7.76 (1H, d, *J* 2.1, H-8), 8.26 (1H, d, *J* 9.0, H-5), 8.36 (1H, d, *J* 5.4, H-2); δ_C (100.6MHz, d_6 DMSO) 40.5 (CH_2-β), 46.5 (CH_2-α), 99.1 (C-3), 117.9 (C-4a), 124.4 (C-5), 124.5 (C-6), 127.9 (C-8), 133.8 (C-7), 149.5 (C-8a or C-4), 150.7 (C-8a or C-4), 152.3 (C-2); (Found: MS (EI) *m/z%* 221 (M^+, 46), 191 (77), 163 (23), 156 (37), 30 (100). Requires: M^+, 221); (Found: C, 59.6; H, 5.6; N, 18.9%. Requires for $C_{11}H_{12}N_3Cl$: C, 59.6; H, 5.5; N, 19.0%).

N^2-(7-Chloro-4-quinolinyl)-N^1,N^1-dimethyl-1,2-ethanediamine (73)

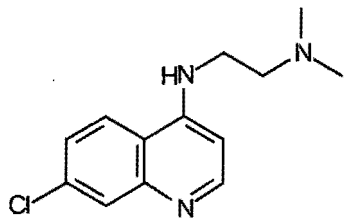

A solution of 4,7-dichloroquinoline (0.53g, 2.7mmol) and excess *N,N*-dimethylenediamine (5ml) was heated in a sealed tube at 140°C for 3.5h. The reaction mixture was then concentrated under reduced pressure to give a solid residue, which was crystallised from benzene to afford colourless crystals of **73** (0.36g, 54%), mp 122 - 124°C (lit. Surrey *et al.* 1959, 121 - 122.8°C); δ_H (400MHz, d_6 DMSO) 2.20 (6H, s, 2 × CH_3), 2.49 (2H, m, CH_2-β), 3.36 (2H, m, CH_2-α), 6.47 (1H, d, *J* 5.3, H-3), 7.14 (1H, bt, NH), 7.42 (2H, dd, *J* 9.1, 2.3, H-6), 7.77 (1H, d, *J* 2.3, H-8), 8.20 (1H, d, *J* 9.1, H-5), 8.38 (1H, d, *J* 5.3, H-2); δ_C (100.6MHz, d_6 DMSO) 41.2 (CH_2), 45.9 (2 × CH_3), 57.6 (CH_2), 99.4 (C-3), 118.1 (C-4a), 124.6 (C-5), 124.8 (C-6), 128.2 (C-8), 134.1 (C-7), 149.7 (C-8a or C-4), 150.7 (C-8a or C-4), 152.6 (C-2); (Found: MS (EI) *m/z%* 249 (M^+, 33), 59 (100), 42 (88), 30 (70). Requires: M^+, 249); (Found: C, 61.7; H, 6.6; N, 16.4%. Requires for $C_{13}H_{16}N_3Cl$: C, 62.5; H, 6.5; N, 16.8%).

N^2-(7-Chloro-4-quinolinyl)-N^1,N^1-diethyl-1,2-ethanediamine (74)

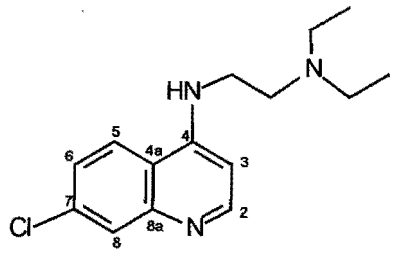

A solution of 2,4-dichloroquinoline (2.1g, 10mmol) and excess *N,N*-diethylethylenediamine (6ml) was heated in a sealed tube at 150°C for 5h. The reaction mixture was then concentrated under reduced pressure and the solid residue crystallised from petroleum ether and ethyl acetate to give glassy-like colourless crystals of **74** (0.94g, 33%), mp 106 - 108°C (lit. De *et al.* 1997, 92°C); δ_H (400MHz, $CDCl_3$) 1.07 (6H, t, *J* 7.1, 2 × CH_3), 2.60 (4H, q, *J* 7.1, 2 × CH_2), 2.82 (2H, t, *J* 6.0, CH_2-β), 3.25 (2H, m, CH_2-α), 6.10 (1H, bs, NH), 6.36 (1H, d, *J* 5.4, H-3), 7.36 (1H, dd, *J* 8.9, 2.2, H-6), 7.65 (1H, d, *J* 8.9, H-5), 7.94 (1H, d, *J* 2.2, H-8,), 8.52 (1H, d, *J* 5.4, H-2); δ_C (100.6MHz, $CDCl_3$) 12.0 (2 × CH_3), 39.7 (CH_2-α), 46.5 (2 × CH_2), 50.6 (CH_2-β), 99.3 (C-3), 117.4 (C-4a), 121.1 (C-5), 125.2 (C-6), 128.7 (C-8), 134.7 (C-7), 149.1 (C-8a or C-4), 149.8 (C-8a or C-4), 152.1 (C-2); (Found: MS (EI) *m/z*% 277 (M^+, 1), 86 (100), 58 (6), 30 (12). Requires: M^+, 277); (Found: C, 64.7; H, 7.3; N, 15.1%. Requires for $C_{15}H_{20}N_3Cl$: C, 64.9; H, 7.3; N, 15.1%).

N^1,N^1-Diethyl-N^2-(7-fluoro-4-quinolinyl)-1,2-ethanediamine (75)

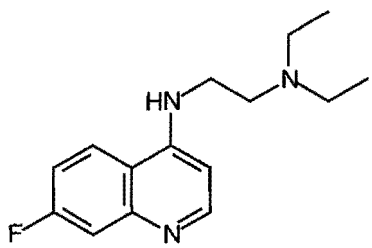

32a (0.43g, 2.4mmol) and N,N-diethylethylenediamine (4ml) were heated under N_2 in a sealed tube at 160°C for 6hr. Excess reagent was then removed under reduced pressure to give a brown oil. This oil was then treated with Na_2CO_3 (aq) and the product extracted into ethyl acetate (four times), dried ($MgSO_4$) and evaporated to dryness under reduced pressure. This crude material was chromatographed on silica gel (60:1) using triethylamine : ethyl acetate (2:98) as the eluent. The residue was crystallised from heptane to give **75** (0.39g, 62%), mp 81 - 82°C (lit. De *et al* 1998, 72 - 73°C); δ_H (300MHz, $CDCl_3$) 1.07 (6H, t, *J* 7.2, 2 × CH_3), 2.59 (4H, q, *J* 7.2, 2 × CH_2), 2.81 (2H, t, *J* 6.3, CH_2-β), 3.25 (2H, m, CH_2-α), 6.09 (1H, bs, NH), 6.33 (1H, d, *J* 5.4, H-3), 7.17 (1H, td, *J* 8.4, 2.7, H-6), 7.57 (1H, dd, 10.5,

2.7, H-8), 7.71 (1H, dd, *J* 9.3, 6.0, H-5), 8.51 (1H, d, *J* 5.4, H-2); δ_C (75.5MHz, $CDCl_3$) 12.1 (2 × CH_3), 39.7 (CH_2-α), 46.5 (2 × CH_2), 50.7 (CH_2-β), 98.7 (C-3), 113.3 ($J_{C\text{-}F}$ 20, C-8), 114.3 ($J_{C\text{-}F}$ 25, C-6), 115.9 (C-4a), 121.8 ($J_{C\text{-}F}$ 10, C-5), 149.9 ($J_{C\text{-}F}$ 12, C-8a), 150.0 (C-4), 152.2 (C-2), 162.9 ($J_{C\text{-}F}$ 249, C-7); (Found: MS (EI) *m/z*% 261 (M^+, 2), 86 (100), 58 (7), 30 (12). Requires: M^+, 261); (Found: C, 69.1; H, 7.8; N, 16.2%. Requires for $C_{15}H_{20}N_3F$: C, 68.9; H, 7.7; N, 16.1%).

N^2-(7-Bromo-4-quinolinyl)-N^1,N^1-diethyl-1,2-ethanediamine (76)

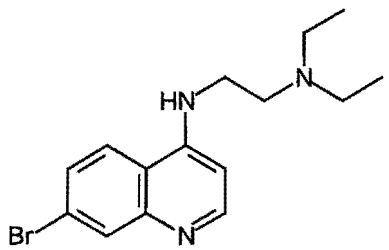

57b (0.69g, 2.8mmol) and N,N-diethylethylenediamine (7ml) were heated in a sealed tube at 135°C for 6hr. The excess reagent was then removed under reduced pressure and 10% NaOH added. The product was extracted into dichloromethane (three times), dried ($MgSO_4$) and evaporated under reduced pressure. The solid residue was crystallised from ethyl acetate to give glassy-like, flat, white, transparent crystals of **76** (0.52g, 57%), mp 120 - 121°C (lit. De *et al.* 1998, 111 - 112°C); δ_H (300MHz, $CDCl_3$) 1.07 (6H, t, *J* 7.1, 2 × CH_3), 2.60 (4H, q, *J* 7.2, 2 × CH_2), 2.82 (2H, t, *J* 5.9, CH_2-α), 3.25 (2H, m, CH_2-β), 6.07 (1H, bs, NH), 6.38 (1H, d, *J* 5.4, H-3), 7.49 (1H, dd, *J* 8.9, 2.0, H-6), 7.58 (1H, d, *J* 8.9, H-5), 8.13 (1H, d, *J* 2.0, H-8), 8.52 (1H, d, *J* 5.4, H-2); δ_C (75.5MHz, $CDCl_3$) 12.1 (2 × CH_3), 39.8 (CH_2-α), 46.5 (2 × CH_2), 50.7 (CH_2-β), 99.4 (C-3), 117.8 (C-4a), 121.2 (C-5), 123.0 (C-7), 127.8 (C-6), 132.1 (C-8), 149.4 (C-8a or C-4), 149.9 (C-8a or C-4), 152.1 (C-2); (Found: MS (EI) *m/z*% 323 ($(M+2)^+$, 1), 321 (M^+, 1), 155 (3), 86 (100), 58 (9), 30 (15). Requires: $(M+2)^+$, 323; M^+, 321); (Found: C, 56.0; H, 6.3; N, 13.0%. Requires for $C_{15}H_{20}N_3Br$: C, 55.9; H, 6.3; N, 13.0%).

N^1,N^1-Diethyl-N^2-(7-iodo-4-quinolinyl)-1,2-ethanediamine (77)

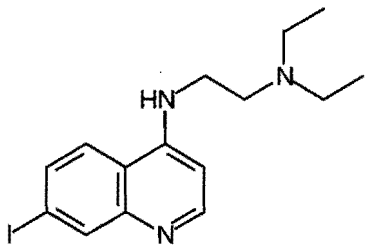

57c (0.97g, 3.4mmol) and N,N-diethylethylenediamine (8ml) were heated in a tube, sealed under N_2, at 120°C for 8hr. The excess reagent was then removed under reduced pressure and 10% NaOH added to the residue. The resulting precipitate was extracted into dichloromethane (three times), dried ($MgSO_4$) and the solvent removed under reduced pressure. The solid was crystallised from ethyl acetate to give 77 (0.83g, 67%), mp 133 - 136°C (lit. 131 - 132°C, De *et al* 1998); δ_H (300MHz, $CDCl_3$) 1.07 (6H, t, *J* 7.1, 2 × CH_3), 2.60 (4H, q, *J* 7.1, 2 × CH_2), 2.81 (2H, t, *J* 6.3, CH_2-β), 3.25 (2H, m, CH_2-α), 6.07 (1H, bs, NH), 6.37 (1H, d, *J* 5.3, H-3), 7.43 (1H, d, *J* 8.8, H-5), 7.68 (1H, dd, 8.8, 1.8, H-6), 8.37 (1H, d, *J* 1.8, H-8), 8.50 (1H, d, *J* 5.3, H-2); δ_C (75.5MHz, $CDCl_3$) 12.1 (2 × CH_3), 39.8 (CH_2-α), 46.5 (2 × CH_2), 50.7 (CH_2-β), 94.8 (C-7), 99.5 (C-3), 118.2 (C-4a), 121.1 (C-5), 133.0 (C-6), 138.7 (C-8), 149.5 (C-8a or C-4), 150.0 (C-8a or C-4), 151.8 (C-2); (Found: MS (EI) *m/z*% 369 (M^+, 1), 155 (2), 86 (100), 58 (6), 30 (10). Requires: M^+, 369); (Found: C, 48.8; H, 5.7; N, 11.4%. Requires for $C_{15}H_{20}N_3I$: C, 48.8; H, 5.5; N, 11.4%).

N^1,N^1-Diethyl-N^2-(7-methoxy-4-quinolinyl)-1,2-ethanediamine (78)

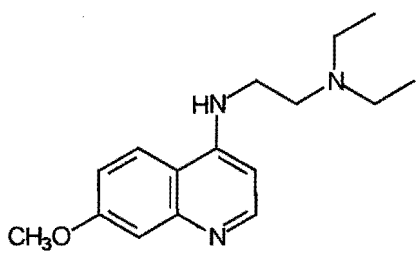

57d (1.2g, 5.3mmol) and N, N-diethylethylenediamine (6ml) were heated in a tube, sealed under N_2, at 140°C for 5h. The reagent was then removed under reduced pressure to give a thick, yellow oil, to which 10% NaOH (aq) was added. The product was extracted into dichloromethane (four times), dried ($MgSO_4$) and evaporated under reduced pressure. The resulting solid was crystallised from heptane to give **78** as a white solid (1.1g, 75%), mp 98 - 99°C (lit. De *et al* 1998, 94 - 95°C), δ_H (400MHz,$CDCl_3$) 1.08 (6H, t, 2 × CH_3), 2.60 (4H, q, *J* 7.2, 2 × CH_2), 2.81 (2H, t, *J* 6.0, CH_2-β), 3.26 (2H, m, CH_2-α), 3.93 (3H, s, OCH_3), 5.97 (1H, bs, NH), 6.30 (1H, d, *J* 5.2, H-3), 7.07 (1H, dd, *J* 9.2, 2.6, H-6), 7.33 (1H, d, *J* 2.6, H-8), 7.62 (1H, d, *J* 9.2, H-5), 8.47 (1H, d, *J* 5.2, H-2); δ_C (100.6MHz, $CDCl_3$) 12.1 (2 × CH_3), 39.8 (CH_2-

α), 46.6 (2 × CH_2), 50.8 (CH_2-β), 55.4 (OCH_3), 98.1 (C-3), 108.1 (C-8), 113.5 (C-4a), 116.9 (C-6), 120.9 (C-5), 150.1 (C-8a or C-4), 150.2 (C-8a or C-4), 151.3 (C-2), 160.3 (C-7); (Found: MS (EI) *m/z*% 273 (M^+, 5), 86 (100), 58 (9), 30 (15). Requires: M^+, 273); (Found; C, 70.4; H, 8.8; N, 15.2.%. Requires for $C_{16}H_{23}N_3O$: C, 70.3; H, 8.5; N, 15.4%).

N^1,N^1-Diethyl-N^2-(7-nitro-4-quinolinyl)-1,2-ethanediamine (79)

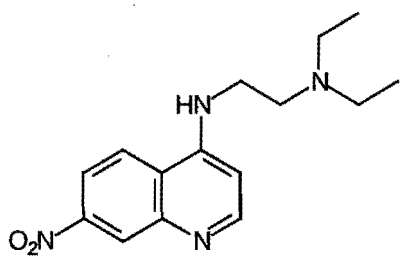

A mixture of 57e (0.16g, 0.77mmol) and N,N-diethylethylenediamine (7ml) were heated at 85°C, under N_2, for 5h. The reaction mixture was then cooled to room temperature and Na_2CO_3 (aq) added. The organic material was extracted into ethyl acetate (three times), dried over $MgSO_4$, and the solvent removed under reduced pressure. The residue was chromatographed firstly on silica gel (150:1) using ethyl acetate as the eluent to remove the excess reagent and then on silica gel (200:1) using mixtures of triethylamine : ethyl acetate (0.5:99.5) to (3:97) as the eluent to isolate **79** (0.14g, 63%), mp 110 - 113°C; ν_{max}/cm^{-1} ($CDCl_3$) 3018, 2972, 1754, 1590, 1546, 1479, 1374, 1352; δ_H (300MHz, $CDCl_3$) 1.09 (6H, t, *J* 7.2, 2 × CH_3), 2.63 (4H, q, *J* 7.2, 2 × CH_2), 2.85 (2H, t, *J* 5.9, CH_2-β), 3.28 (2H, m, CH_2-α), 6.28 (1H, s, NH), 6.49 (1H, d, *J* 5.4, H-3), 7.85 (1H, d, *J* 9.0, H-5), 8.17 (1H, dd, *J* 9.0, 2.3, H-6), 8.65 (1H, d, *J* 5.4, H-2), 8.84 (1H, d, *J* 2.3, H-8); δ_C (75.5MHz, $CDCl_3$) 12.1 (2 × CH_3), 39.8 (CH_2-α), 46.5 (2 × CH_2), 50.5 (CH_2-β), 101.1 (C-3), 117.7 (C-6), 121.5 (C-5), 122.5 (C-4a), 125.9 (C-8), 147.9, 147.9, 149.7, 153.2 (C-2); (Found: MS (EI) *m/z*% 288 (M^+, 1), 155 (3), 86 (100), 58 (21), 30 (29). Requires: M^+, 288); (Found: C, 62.8; H, 6.7; N, 19.1.%. Requires for $C_{15}H_{20}N_4O_2$: C, 62.5; H, 7.0; N, 19.4%).

N^1,N^1-Diethyl-N^2-(7-trifluoromethyl-4-quinolinyl)-1,2-ethanediamine (80)

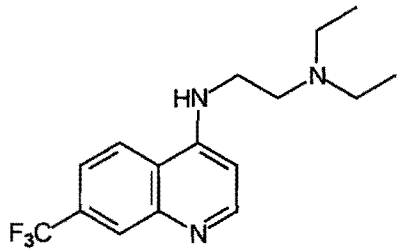

A mixture of 4-chloro-7-trifluoromethylquinoline (0.29g, 1.3mmol) and N,N-diethyl-ethylenediamine (7ml) were heated in a tube, sealed under N_2, at 145°C for 7h. Most of the excess reagent was then removed under reduced pressure and the product selectively dissolved in hot petroleum ether. This was then decanted and evaporated under reduced pressure to afford **80** after crystallisation from heptane (0.22g, 56%), mp 121 - 123°C (lit. De *et al* 1998, 122 - 123°C); δ_H (400MHz, $CDCl_3$) 1.07 (6H, t, *J* 7.2, 2 × CH_3), 2.61 (4H, q, *J* 7.2, 2 × CH_2), 2.83 (2H, t, *J* 6.0, CH_2-β), 3.27 (2H, m, CH_2-α), 6.20 (1H, s, NH), 6.43 (1H, d, *J* 5.2, H-3), 7.58 (1H, dd, *J* 9.0, 1.5, H-6), 7.84 (1H, d, *J* 9.0, H-5), 8.24 (1H, d, *J* 1.5, H-8), 8.59 (1H, d, *J* 5.2, H-2); δ_C (100.6MHz, $CDCl_3$) 12.1 (2 × CH_3), 39.8 (CH_2-α), 46.6 (2 × CH_2), 50.6 (CH_2-β), 100.3 (C-3), 120.1 (C-6), 120.1 (C-4a), 121.0 (C-5), 127.6 (C-8), 127.6 (C-7), 147.7 (C-8a or C-4), 149.7 (C-8a or C-4), 152.3 (C-2); (Found: MS (EI) *m/z*% 311 (M^+, 1), 86 (100), 58 (11), 30 (20). Requires: M^+, 311); (Found: C, 61.9; H, 6.4; N, 13.4%. Requires for $C_{16}H_{20}N_3F_3$: C, 61.7; H, 6.5; N, 13.5%).

***N*-2-(4-Quinolinyl)-aminoethylethanamide (81)**

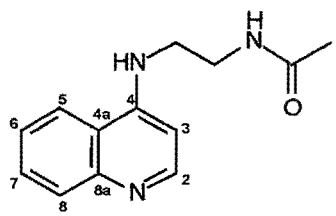

To a stirred solution under N_2 at 0°C of **64** (0.17g, 0.92mmol) in THF (0.5ml) was added triethylamine (0.17ml, 1.2mmol) and acetic anhydride (0.11g, 1.1mmol) and the resulting solution was stirred at this temperature for 1hr, followed by 2.5hr at ambient temperature. The reaction mixture was then extracted into ethyl acetate (three times) from Na_2CO_3 (aq), dried over anhydrous $MgSO_4$ and evaporated under reduced pressure. The residue (0.16g, 78%) was crystallised from ethyl acetate and ethanol to give **81**, mp 200 - 202°C; ν_{max}/cm^{-1} (d_6 DMSO) 3463, 3300, 3062, 1666, 1583, 1542, 1285; δ_H (400MHz, d_6 DMSO) 1.82 (3H, s, CH_3), 3.30 - 3.37 (4H, m, 2 × CH_2), 6.49 (1H, d, *J* 5.3, H-3), 7.22 (1H, bt, NH), 7.40 (1H, dt, H-6), 7.59 (1H, dt, H-7), 7.76 (1H, d, *J* 8.4, H-8), 8.10 (2H, m, CONH and H-5), 8.38 (1H, d, *J*

5.3, H-2); δ_C (100.6MHz, d_6 DMSO) 23.0 (CH_3), 37.8 (CH_2), 42.9 (CH_2), 98.5 (C-3), 119.2 (C-4a), 121.8 (C-5), 124.3 (C-6), 129.1 (C-7), 129.4 (C-8), 148.7 (C-8a or C-4), 150.2 (C-8a or C-4), 151.1 (C-2), 170.5 (C=O); (Found: MS (EI) *m/z%* 229 (M^+, 39), 170 (28), 157 (100). Requires: M^+, 229); (Found: C, 67.9; H, 6.6; N, 18.3%. Requires for $C_{13}H_{15}N_3O$: C, 68.1; H, 6.6; N, 18.3%).

***N*^{1},*N*^{1}-Diethyl-*N*^{2}-(7-hydroxy-4-quinolinyl)-1,2-ethanediamine (82)**

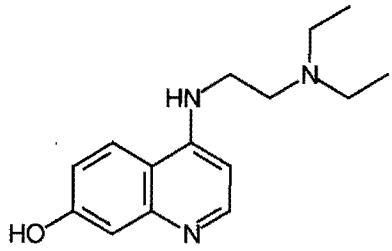

A solution of 78 (1.1g, 4.0mmol) in dry dichloromethane (15ml) was cooled under N_2, to -78°C. BBr_3 (4.0g, 16mmol) was added to this solution and the mixture stirred at -78°C for 1hr. The reaction mixture was then placed in the freezer at -13°C for 40h. Work-up involved recooling the mixture to -78°C and basification by dropwise addition of K_2CO_3 (aq). Upon heating to room temperature, a white solid precipitate formed This was filtered, washed with water and dried in vacuo over P_2O_5. The dried organic material was extracted into methanol and the insoluble material filtered off. The product was then chromatographed on silica gel (three times) (20:1) using ethyl acetate to pack the column and methanol to load the material. Elution using triethylamine : methanol : ethyl acetate (2:20:78) afforded mono-aqua **82** (0.685g, 61.6%) as a luminous, yellow-green, thick oil, ν_{max}/cm^{-1} (DMSO) 3257, 1617, 1584, 1545, 1458, 1346, 1301, 1235; δ_H (400MHz, d_6 DMSO) 0.95 (6H, t, *J* 7.2, 2 × CH_3), 2.53 (4H, q, *J* 7.0, 2 × CH_2), 2.66 (2H, t, *J* 7.0, CH_2-β), 3.35 (2H, t, CH_2-α), 6.38 (1H, d, *J* 6.2, H-3), 6.99 (1H, dd, *J* 9.1, 2.5, H-6), 7.04 (1H, d, *J* 2.5, H-8), 7.10 (1H, bs, NH), 8.02 (1H, d, *J* 9.1, H-5), 8.25 (1H, d, *J* 6.2, H-2); δ_C (100.6MHz, d_6 DMSO) 12.5 (2 × CH_3), 41.5 (CH_2-α), 47.4 (2 × CH_2), 51.4 (CH_2-β), 97.3 (C-3), 108.5 (C-8), 112.3 (C-4a), 117.3 (C-6), 124.0 (C-5), 147.6 (C-8a or C-4), 148.5 (C-2), 152.3 (C-8a or C-4), 159.9 (C-7); (Found MS (HRMS) *m/z%* 259.16770. Requires: 259.16846).

N^2-(7-Amino-4-quinolinyl)-N^1,N^1-diethyl-1,2-ethanediamine (83)

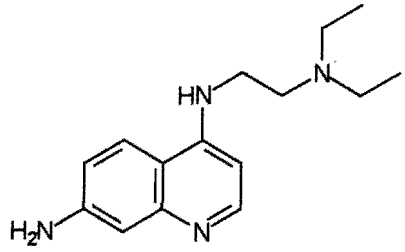

A mixture of **79** (0.11g, 0.38mmol) and 10% Pd-C (12mg, 0.011mmol) in ethanol (15ml) was stirred under H_2 for 22h. The mixture was then filtered through Celite and washed with large volumes of ethanol. The filtrate was evaporated under reduced pressure and the residue adsorbed onto silica gel (80:1) and eluted using mixtures of methanol : triethylamine : ethyl acetate (0.5:10:89.5) to (1.5:10:88.5). Purification was achieved by neutral alumina chromatography (70:1) eluting firstly with large volumes of ethyl acetate and then methanol : 25% NH_3 (aq) : ethyl acetate (10:2:88) to obtain **83** (76mg, 78%) in the form of a brown oil; ν_{max}/cm^{-1} ($CDCl_3$) 3402, 3382, 3020, 1631, 1586, 1538, 1471, 1329, 1224; δ_H (400MHz, $CDCl_3$) 1.06 (6H, t, *J* 7.2, 2 × CH_3), 2.58 (4H, q, *J* 7.2, 2 × CH_2), 2.78 (2H, t, *J* 6.0, CH_2-β), 3.23 (2H, m, CH_2-α), 3.96 (2H, bs, NH_2), 5.86 (1H, s, NH), 6.20 (1H, d, *J* 5.2, H-3), 6.84 (1H, dd *J* 9.0, 2.4, H-6), 7.11 (1H, d, *J* 2.4, H-8), 7.54 (1H, d, *J* 9.0, H-5), 8.40 (1H, d, *J* 5.2, H-2); δ_C (100.6MHz, $CDCl_3$) 12.0 (2 × CH_3), 39.8 (CH_2-α), 46.5 (2 × CH_2), 50.9 (CH_2-β), 97.1 (C-3), 110.4 (C-8), 112.3 (C-4a), 116.0 (C-6), 120.9 (C-5), 147.2 (C-7), 150.0 (C-8a or C-4), 150.0 (C-8a or C-4), 151.3 (C-2); (Found MS (HRMS) *m/z*% 258.18425. Requires for $C_{15}H_{22}N_4$: 258.18445).

7.2. PHYSICAL METHODS

7.2.1. Commercially Available Chemicals Used

The chemicals used were all of analytical grade and were obtained from the following suppliers:

Chemical	Supplier
3-Aminoquinoline	Sigma
5-Aminoquinoline	Sigma
6-Aminoquinoline	Sigma
8-Aminoquinoline	Sigma
Dimethyl Sulphoxide (DMSO)	BDH Laboratory Supplies
Haematin	Sigma
Haemin	Sigma
Hydrochloric Acid (HCl)	BDH Laboratory Supplies
2-[N-Morpholino]ethanesulfonic acid (MES acid)	Sigma
2-[N-Morpholino]ethanesulfonic sodium salt (MES salt)	Sigma
N-[2-Hydroxyethyl]piperazine-N'-2-ethanesulfonic acid] (HEPES acid)	Sigma
N-[2-Hydroxyethyl]piperazine-N'-2-ethanesulfonic sodium salt] (HEPES salt)	Sigma
Sodium Hydrogen Phthalate (KHP)	Merck
2-[N-Cyclohexylamino]ethanesulfonic acid (CHES acid)	Sigma
Methanol for HPLC	Riedel-de Haen
Sodium Perchlorate	Hopkin and Williams LTD
Potassium bromide	Merck
Sodium Chloride	Saarchem-Holpro Analytic (PTY) LTD
Sodium Hydroxide	Orion Chemicals
Sodium Dodecyl Sulphate (SDS)	BDH Chemicals
Polyoxoethylene (10) Isooctylpentyl Ether (TRITON X-100)	DH Chemicals
Polyoxoethylene Sorbitan Monolaurate (TWEEN-20)	Merck

7.2.2. Haematin Dimerisation Methods

7.2.2.1. Instrumentation and General Methods

The pH measurements were carried out using a Crison MicropH 2000 pH meter. Standard phosphate buffer solutions, from BDH laboratory supplies, at pH 4.00 ± 0.02 and 7.00 ± 0.02 were used to calibrate the meter prior to use. Samples were mixed on a Snijders Magnetic Stirrer 34521, vortexed using a press-to-mix Snijders Analyser 34524 and centrifuged using a Centrifuge 5410 for Eppendorf. Volumes were delivered using combinations of Gilson's Pipetman and Hamilton syringes. Uv-vis readings for haematin dimerisation titrations were done on a CARY 3E using 10cm quartz cuvettes with temperature control using a thermostated Haoke waterbath. Uv-vis readings for spectra collected between 700 and 450nm were obtained on a Beckman DU-68 spectrophotometer using 1cm quartz cuvettes with temperature control using a circulating YIH DER BL-710 thermostated waterbath.

Methanol was dried over 4Å molecular sieves in a tightly sealed, parafilmed bottle for one week prior to use. Water was purified by glass distillation and pyridine was distilled and stored over KOH. Cuvettes and volumetric flasks used in the work were prepared by washing with detergent followed by rinsing with 30% nitric acid and drying in an oven overnight. Sample vials used for storage of solutions were used only once, as new, and then discarded.

7.2.2.2. Methods for Determination of K_{obs}, α and β

7.2.2.2.1. Preparation of HEPES Buffers

The 50mM HEPES Buffers were prepared by dissolving HEPES acid (2.98g, 12.5mmol) and sodium perchlorate (see Table 7.2) in less than 250ml of distilled water in a beaker. The pH was then adjusted using concentrated sodium hydroxide and the solution transferred carefully to a volumetric flask, taking care to transfer all the dissolved material with distilled water. The final volume was then adjusted to the mark with distilled water.

7.2.2.2.2. Calculation of Ionic Strength

Since only the HEPES base contributes to the ionic strength, the equilibrium proportions of HEPES acid (BH) and HEPES base (B^-) were calculated at the five different pHs (Table 3.1.)

using the derivation below, the ionic strength was then adjusted to the desired value with sodium perchlorate (Table 7.2.).

$$BH \rightleftharpoons B^- + H^+ \qquad (7)$$

$$K_a = \frac{[B^-][H^+]}{[BH]} \qquad (8)$$

But $[B_T]=[B^-]+[BH]$

Therefore $[BH]=[B_T]-[B^-]$ (9)

Substitute (9) into (8)

$K_a[B_T]-K_a[B^-]=[B^-][H^+]$

$K_a[B_T]=[B^-]([H^+]+K_a)$

$$[B^-] = \frac{K_a[B_T]}{[H^+]+K_a} \qquad (10)$$

Since $[B_T]$ = 50mM and $K_a = 10^{-7.5} = 3.16\times10^{-8}$M

$$[B^-] = \frac{(3.16\times10^{-8}M)\{50\times10^{-3}M)}{[H^+]+(3.16\times10^{-8}M)}$$

$[B^-]$ can be calculated at the five different pH's (Table 3.1.).

Table 7.2. Concentrations of B^- calculated at the five different pHs.

pH	$[H^+]$ / M	[B] / mM
6.9	1.3×10^{-7}	10.0
7.2	6.3×10^{-8}	16.7
7.4	4.0×10^{-8}	22.1
7.7	2.0×10^{-8}	30.7
8.0	1.0×10^{-8}	38.0

The ionic strength, μ, is defined as $\mu = \frac{1}{2}\Sigma m_i z_i^2$, where m_i is the molarity of species (i) and z_i is the charge on species (i). Therefore, at pH 6.9, the contribution to the ionic strength from B^-:

$\mu = \frac{1}{2}\{m_{B^-}.(-1)^2 + m_{Na^+}.(+1)^2\}$

$= \frac{1}{2}\{(10.0mM \times 1) + (10.0mM \times 1)\}$

$= 10.0mM$

ie. the contribution to μ from B^- = $[B^-]$

To obtain μ_{Total} = 154mM; $[NaClO_4.H_2O]$ added = 154mM – $[B^-]$ (Table 7.3).

Table 7.3. Amounts of $NaClO_4.H_2O$ added to adjust the ionic strength of the 50mM HEPES solutions (V = 250ml) to 154mM.

pH	$[B^-]$ / mM	$NaClO_4.H_2O$ / g	$[NaClO_4.H_2O]$ / mM	μ_{Total} / mM
6.9	10.0	5.065	144.2	154.2
7.2	16.7	4.832	137.6	154.3
7.4	22.1	4.635	132.0	154.1
7.7	30.7	4.333	123.4	154.1
8.0	38.0	4.075	116.0	154.0

7.2.2.2.3. Preparation of Haematin Solutions

A 0.1M NaOH solution was prepared by dissolving NaOH (405.2mg, 10.13mol) in distilled water (100ml) in a volumetric flask. This solution was flushed with argon (20mins) and then used to prepare the haematin stock solutions **C1**, **C2** and **C3**.

C1 2.68×10^{-3}M: Haematin (17.0mg, 2.68×10^{-5}mol) was dissolved in 0.1M NaOH (10ml) in a volumetric flask. This solution had to be shaken vigorously and was left to stand in the dark for 0.5h before further use as the large haematin crystals were slow in dissolving in 0.1M NaOH.

C2 5.79×10^{-4}M: An aliquot of **C1** (2.160ml) was diluted to 10ml with 0.1M NaOH in a volumetric flask.

C3 9.92×10^{-5}M: An aliquot of **C2** (1.713ml) was diluted to 10ml with 0.1M NaOH in a volumetric flask.

The stock solutions **C1**, **C2** and **C3** were then transferred to 10ml sample vials that had been wrapped in aluminium foil, stoppered with septums and deoxygenated with argon for 10mins. These solutions were used within a few hours and then discarded.

7.2.2.2.4. Collection of Titration Data

Titrations were performed in 50mM HEPES buffer, μ = 154mM at pHs 6.92, 7.19, 7.39, 7.69 and 7.99 in a haematin concentration range 2×10^{-7}M – 4.2×10^{-6}M. Typically, the buffer solution (20ml) was placed in duplicate into two 10cm, quartz cuvettes. Parafilm was placed over the top of the cuvettes and argon bubbled through the solutions for 10mins. Thereafter the cuvettes were placed in the spectrophotometer at 25°C and the compartment continually flushed with a strong argon flow. The buffer solutions were allowed to equilibrate under these conditions for 10mins before the titrations were commenced. The titrations were performed by adding 160μl of **C3** in 2-10μl aliquots followed by 120μl of **C2** in 5-20μl aliquots to give a final haematin concentration of 4.2×10^{-6}M. After each addition, the same volume of 0.1M NaOH was dispensed into the reference cuvette and both solutions were stirred about 10 times each in a back and forth motion with a spatula. The data was fitted to a dimerisation model (derived in 7.2.2.2.5. below) using non-linear-least squares fitting procedures with the program FIT.

7.2.2.2.5. Derivation of the Haematin Dimerisation Model

7.2.2.2.5.1. Methods for Determination of K_{obs}, α and β

Brown *et al.* proposed the following relationship for haematin dimerisation (Brown *et al.* 1970):

$$2M \underset{}{\overset{K}{\rightleftharpoons}} M_2 + nH^+ \qquad (11)$$

where M is the haematin monomer, M_2 is the haematin dimer, K is the equilibrium constant and n is an integer or zero corresponding to the number of protons released in the dimerisation process.

The equilibrium constant for Equation (**11**) can be written as follows:

$$K = \frac{[M_2][H^+]^n}{[M]^2} \qquad (12)$$

At a fixed pH, a conditional equilibrium constant K_{obs} is defined such that:

$$K_{obs} = \frac{K}{[H^+]^n} = \frac{[M_2]}{[M]^2} \qquad (13)$$

The total haematin concentration, M_T, can be written in terms of M and M_2:

$$[M_T] = [M] + 2[M_2], \text{ therefore } [M] = [M_T] - 2[M_2] \quad \textbf{(14)}$$

Substituting **(14)** into **(13)** where M_T, M and M_2 all refer to concentrations:

$$K_{obs} = \frac{M_2}{(M_T - 2M_2)^2}$$

$$K_{obs} = \frac{M_2}{M_T^2 - 4M_T M_2 + 4M_2^2}$$

$$K_{obs}M_T^2 - 4K_{obs}M_T M_2 + 4K_{obs}M_2^2 = M_2$$

$$K_{obs}M_T^2 - 4K_{obs}M_T M_2 + 4K_{obs}M_2^2 - M_2 = 0$$

$$K_{obs}M_T^2 - M_2(4K_{obs}M_T + 1) + 4K_{obs}M_2^2 = 0$$

$$(4K_{obs})M_2^2 - (4K_{obs}M_T + 1)M_2 + K_{obs}M_T^2 = 0$$

Solving for M_2

$$x = \frac{-b \pm \sqrt{b^2 - 4ac}}{2a}$$

where $a=4K_{obs}$, $b=-(4K_{obs}M_T+1)$, $c=K_{obs}M_T^2$

$$M_2 = \frac{(4K_{obs}M_T + 1 \pm \sqrt{(-4K_{obs}M_T - 1)^2 - 4(4K_{obs})(K_{obs}M_T^2)}}{2(4K_{obs})}$$

$$M_2 = \frac{(4K_{obs}M_T + 1) \pm \sqrt{(4K_{obs}M_T + 1)^2 - 16K_{obs}^2 M_T^2}}{8K_{obs}} \quad \textbf{(15)}$$

We now have an expression for M_2 in terms of K_{obs} and M_T (Equation **15**) and an expression for M in terms of M_2 and M_T (Equation **14**).

The absorbance ratio at any particular haematin concentration is a weighted average of the absorbance ratio due to the fraction of haematin in the monomer (f_M) and the absorbance ratio due to the fraction of haematin in the dimer (f_{M2}) (Equation **16**):

$$\left(\frac{A_{395}}{A_{361}}\right)_T = f_M\left(\frac{A_{395}}{A_{361}}\right)_M + f_{M_2}\left(\frac{A_{395}}{A_{361}}\right)_{M_2} \quad (16)$$

Where the fraction of haematin in the form of the monomer is:

$$f_M = \frac{M}{M_T}$$

and the fraction of haematin in the form of the dimer is:

$$f_{M_2} = \frac{2M_2}{M_T}$$

Let the observed absorbance ratio be R_{abs} where:

$$R_{abs} = \left(\frac{A_{395}}{A_{361}}\right)_T$$

Let the absorbance ratio of the pure monomer be α, such that:

$$\alpha = \left(\frac{A_{395}}{A_{361}}\right)_M$$

Let the absorbance ratio of the pure dimer be β, such that:

$$\beta = \left(\frac{A_{395}}{A_{361}}\right)_{M_2}$$

Therefore:

$$R_{abs} = \frac{M}{M_T}\alpha + 2\frac{M_2}{M_T}\beta \quad (17)$$

Using Equation **17** it is now possible to calculate α, β and K_{obs} using non-linear least squares fitting procedures where: A_{395}/A_{361} is the experimentally determined absorbance ratio, M_T is the total haematin concentration,

$$M = M_T - 2M_2$$

$$M_2 = \frac{(4K_{obs}M_T + 1) \pm \sqrt{(4K_{obs}M_T + 1)^2 - 16K_{obs}{}^2M_T^2}}{8K_{obs}}$$

In solving for M_2, only the negative root was used as the positive root gave negative values for α and β.

7.2.2.2.5.2. Methods for Determination of K and n

K and n were determined by the method of Brown *et al.* where K_{obs} is defined as:

$$K_{obs} = \frac{K}{[H^+]^n} = \frac{[M_2]}{[M]^2}$$

Taking logs of both sides gives a linear relationship between log K_{obs} and pH:

$$\boxed{log\ K_{obs} = log\ K + npH}$$

Hence a plot of log K_{obs} against pH should give a straight line with slope equal to the number of protons involved in dimerisation and the y-intercept equal to log K.

7.2.2.3. Derivation of the Model for Single Deprotonation

An equilibrium expression for single deprotonation can be written as follows:

$$AH \underset{}{\overset{K_a}{\rightleftharpoons}} A^- + H^+ \qquad \textbf{(18)}$$

Where AH is the protonated species and A^- is the deprotonated species. The equilibrium constant for Equation **18** can then be written:

$$K_a = \frac{[A^-][H^+]}{[AH]} \qquad \textbf{(19)}$$

The total concentration of A (A_T) can be written as in Equation **20** where A_T, A^- and AH all refer to concentrations:

$$A_T = AH + A^-, \text{ therefore } AH = A_T - A^- \qquad \textbf{(20)}$$

An expression for A^- can now be formulated in terms of A_T, H^+ and K_a by substituting Equation **20** into Equation **19**.

$$K_a = \frac{A^-.H^+}{A_T - A^-}$$

$$K_a(A_T - A^-) = A^-.H^+$$

$$K_aA_T - K_aA^- = A^-.H^+$$

$$K_aA_T = A^-.H^+ + K_aA^-$$

$$A_T = \frac{A^-(H^+ + K_a)}{K_a}$$

$$A_T = A^-\left(\frac{H^+}{K_a} + 1\right)$$

$$A^- = \frac{A_T}{\left(\frac{H^+}{K_a} + 1\right)} \qquad \textbf{(21)}$$

An expression for AH can also be formulated (Equation **22**) in terms of A_T, H^+ and K_a by substituting Equation **21** into Equation **20**.

$$AH = A_T - \frac{A_T}{\left(\frac{H^+}{K_a} + 1\right)} \qquad \textbf{(22)}$$

The absorbance ratio A_{395}/A_{361} at any particular concentration of A (α_{obs}) is a weighted average of the absorbance ratio due to the fraction of A in the form of AH (f_{AH}) and the absorbance ratio due to the fraction of A in the form of A^- (f_{M2}) (Equation 23):

$$\alpha_{obs} = \left(\frac{A_{395}}{A_{361}}\right)_{AH}.f_{AH} + \left(\frac{A_{395}}{A_{361}}\right)_{A^-}.f_{A^-} \qquad \textbf{(23)}$$

Where f_{AH} is the fraction of A in the form of AH:

$$f_{AH} = \frac{AH}{A_T} = 1 - \frac{1}{\left(\frac{H^+}{K_a} + 1\right)} \qquad \textbf{(24)}$$

and f_{A^-} is the fraction of A in the form of A^-:

$$f_{A^-} = \frac{A^-}{A_T} = \frac{1}{\left(\frac{H^+}{K_a} + 1\right)} \quad (25)$$

Let the absorbance ratio of pure AH be α_{AH} such that:

$$\alpha_{AH} = \left(\frac{A_{395}}{A_{361}}\right)_{AH} \quad (26)$$

Let the absorbance ratio of pure A^- be α_{A^-} such that:

$$\alpha_{A^-} = \left(\frac{A_{395}}{A_{361}}\right)_{A^-} \quad (27)$$

Substituting Equations **24, 25, 26** and **27** into Equation **23** gives Equation **28** which can be used to calculate values of α_{AH}, α_{A^-} and K_a using non-linear least squares fitting procedures.

$$\alpha_{obs} = \alpha_{AH}\left(1 - \frac{1}{\frac{H^+}{K_a} + 1}\right) + \alpha_{A^-}\left(\frac{1}{\frac{H^+}{K_a} + 1}\right) \quad (28)$$

7.2.2.4. Methods for Determination of α in Detergent and Methanol Solutions

7.2.2.4.1. Preparation of Buffer Solutions

7.2.2.4.1.1. Preparation of SDS Solution

Solutions of 0.25 - 3% SDS in 50mM HEPES buffer with an ionic strength corrected to 154μM using $NaClO_4.H_2O$ were prepared using the quantities in Table 7.4. below.

Table 7.4. Quantities of SDS, HEPES and $NaClO_4.H_2O$ used to make the SDS Detergent Solutions

% SDS	SDS / g	pH	HEPES / g	[HEPES] / mM	$NaClO_4.H_2O$ / g	μ / mM	V_{Total} / ml
2.0	2.002	7.24	1.192	50.0	0.955	154.0	100
2.0	2.002	8.00	1.193	50.0	0.655	154.2	100
2.0	1.001	10.13	0.592	49.7	0.592	153.7	50
0.25	0.249	8.01	1.192	50.0	1.509	154.0	100
0.5	0.501	8.01	1.192	50.0	1.382	153.8	100
1.0	1.001	8.00	1.192	50.0	1.141	153.9	100
2.5	1.251	8.02	0.596	50.0	0.208	154.4	50
3.0	3.003	8.01	1.193	50.1	0.169	154.1	100

7.2.2.4.1.2. Preparation of TRITON X-100 and TWEEN 20 Solutions

Solutions of 3% TRITON X-100 and 2% TWEEN 20 were prepared by dissolving TRITON X-IOO (1.5g) or TWEEN-20 (1g) with HEPES acid (1.19g, 5.00mmol) and $NaClO_4.H_2O$ (see Table 7.5.) in less than 100ml deionised water and the pH was adjusted using concentrated NaOH. The total volume was then adjusted to 100ml using distilled water (Table 7.5.).

Table 7.5. Preparation of 100ml of 3% TRITON X-100 and 2% TWEEN-20 Solutions

pH	$NaClO_4.H_2O$ / g	μ / mM
	3% TRITON X-100	
7.18	1.893	150.8
8.01	1.571	150.9
	2% TWEEN-20	
7.19	1.894	150.8
7.99	1.570	150.9

7.2.2.4.1.3. Preparation of MES, HEPES and CHES Solutions

The 50mM buffer solutions were prepared by dissolving MES acid, HEPES acid or CHES acid and $NaClO_4.H_2O$ in less than the total volume of distilled water in a beaker. The pH was then adjusted with concentrated NaOH and the total volume adjusted with distilled water (Table 7.6.).

Table 7.6. Preparation of 50mM Buffers, μ = 154mM from pH 5.99 to 10.03

pH	$NaClO_4.H_2O$ / g	V_{Total} / ml	μ / mM
	MES acid (0.976g, 5.00mmol)		
5.99	1.855	100	154.2
6.51	1.659	100	153.9
	HEPES acid (2.98g, 12.5mmol)		
6.89	5.056	250	154.0
7.19	4.816	250	153.9
7.41	4.632	250	154.0
7.73	4.332	250	153.9
8.00	4.074	250	154.0
	CHES acid (0.518g, 2.50mmol)		
9.22	0.963	50	159.8
10.03	0.516	50	154.0

The buffered water-methanol mixtures were prepared by pipetting the required amount of 50mM HEPES, MES or CHES solution into a 10ml volumetric flask and adjusting to the mark with dry methanol.

7.2.2.4.2. Preparation of Haematin Stock Solutions and Water-Methanol Solutions

Haematin stock solution for determination of α in the detergent solutions (**H1**): haematin (8.6mg, 1.36×10^{-5}mol) was dissolved in 0.1M NaOH in a volumetric flask. This solution was then transferred to a 10ml sample vial and covered with aluminium foil.
Haematin stock solution for determination of α in the water-methanol solutions (**H2**): a saturated solution of haematin in dry methanol (2ml) was centrifuged at 10rpm for 10mins. The supernatent was then removed and used.

7.2.2.4.3. Collection of Spectra

Determination of α in the detergent solution and water-methanol solutions: the relevant buffer solution (2ml) was placed in a 1cm cuvette and a baseline between 700 and 450nm recorded. To this solution, H1 (45ml) or H2 (75ml) was added and the resulting solution was stirred with a spatula. The spectrum then rescanned between 700 and 450nm to obtain the individual absorbances at 395 and 361nm and α was collected from the ratio.

7.2.2.5. Determination of Haematin Solubility in Aqueous Solution

7.2.2.5.1. Preparation of KHP, MES and HEPES Buffers

The 50mM buffer solutions were prepared using either KHP, MES salt or HEPES salt and sodium chloride was used to adjust the ionic strength. For buffers at pH 5.06, 5.27 and 5.38, KHP (2.55g, 12.5mmol) was dissolved in less than the total volume of distilled water. The pH was then adjusted with concentrated NaOH (aq) from which the equilibrium concentrations of the monodeprotonated (B^-) and dideprotonated (B^{2-}) KHP species were calculated (Table 7.7.). The ionic strength was then corrected to 154mM using NaCl and the final volume adjusted to 250ml in a volumetric flask.

Table 7.7. Preparation of 50mM KHP Buffers, μ = 154mM from pH 5.06 to 8.01

pH	$[B^-]$ / mM	$[B^{2-}]$ / mM	NaCl / g	[NaCl] / mM	V_{Total}	μ / mM
5.06	35	15	1.053	72.1	250	152
5.27	29	21	0.920	63.0	250	155
5.38	26	24	0.789	54.0	250	152

MES salt was used to make buffers at pH 5.54, 5.60, 5.94, 6.24 and 6.55 by dissolving MES salt (2.72g, 12.5mmol) and NaCl (1.52g, 26.0mmol) in less than 250ml of distilled water. The pH was then adjusted using concentrated HCl and the total volume adjusted to 250ml in a volumetric flask.

HEPES acid was used to make buffers at pH 6.85, 7.11 and 7.97 by dissolving HEPES acid (3.26g, 12.5mmol) and NaCl (1.52g, 26.0mmol) in less than 250ml of distilled water. The pH was then adjusted using concentrated HCl and the total volume adjusted to 250ml in a volumetric flask.

7.2.2.5.2. Preparation of Haematin Stock Solution and Collection of Spectra

The haematin stock solution (**H3**: 1.94×10^{-3}M) was prepared by dissolving haemin (12.3mg, 18.9mmol) in DMSO (10ml) in a volumetric flask. The haematin solutions (**H4**: 1.01×10^{-6}M) were then prepared by dissolving **H3** (26μl) in the relevant buffer solution (50ml) in a volumetric flask. The solution was stirred in the dark for 0.5h and then centrifuged. The supernatent was removed and the absorbance at 395nm recorded.

7.2.2.6. Spectra of Haematin Solutions Between 700nm and 450nm

7.2.2.6.1. Spectra of Haematin in HEPES Buffer with Pyridine, NaCl or $NaClO_4$

The relevant HEPES buffer solution (2ml) was placed in a 1cm cuvette and the background absorbance scanned. **H2** (75μl) was then added to the buffer, the mixture stirred with a spatula and the resulting spectrum scanned between 700 to 450nm. Thereafter, either pyridine (50μl), saturating NaCl or saturating $NaClO_4$ was added to the cuvette mixture and the resulting spectrum recorded again in the same absorbance range.

7.2.2.6.2. Spectra of Haematin in 20% HEPES-Methanol Mixtures

A 50mM HEPES buffer that had not been pH adjusted was prepared by dissolving HEPES acid (0.596g, 2.50mmol) in distilled water (50ml). This solution was used to make a 20% water-methanol mixture by pipetting the 50mM HEPES buffer (2ml) into a 10ml volumetric flask and filling to the mark with dry methanol. The initial pH of this mixture was measured. This solution (2ml) was then placed in a 1cm cuvette and the background absorption between 700 and 450nm recorded. **H2** (70μl) was then added, the mixture stirred with a spatula, and the absorption spectrum recorded again. Thereafter 1M NaOH (20μl) was added in 2μl aliquots and the spectrum recorded after each addition. At the end, the final pH was recorded again.

7.2.3. Methods for Determination of Haematin-Quinoline Association Constants

7.2.3.1. Instrumentation Used

The pH measurements were carried out using a Crison MicropH 2000 pH meter. Standard buffer solutions from BDH laboratory supplies, at pH 4.00 ± 0.02 and 7.00 ± 0.02 were used

to calibrate the meter prior to use. Spectrophotometric titration data for compounds **58**, **61-63** were collected on a Hewlet-Packard 8450A diode array spectrophotometer and the remaining compounds were collected on a on a Beckman DU-68 spectrophotometer. The latter uv-vis spectrophotometer was used to record all spectra. Cuvettes for spectroscopic titrations were connected to a thermostated YIH DER BL-710 waterbath. Volumes were delivered using combinations of Gilson's Pipetman and Hamilton syringes and compounds were weighed on a E. Mettler or Sartorius balance.

7.2.3.2. Preparation of Buffers

The 0.2M HEPES and MES buffers were made by dissolving HEPES acid (4.77g, 20mmol) or MES salt (4.34g, 20mmol) in less than 100ml of distilled water. To this solution concentrated NaOH was added until the desired pH was obtained. The mixture was then transferred to a 100ml volumetric flask taking care to transfer all the dissolved material with distilled water and the total volume was adjusted with distilled water.

7.2.3.3. Preparation of Stock Solutions

It has been found that scrupiously clean glassware can help to stabilise the haematin solutions in the 40% DMSO (aq). This was done by washing the 10ml volumetric flasks and cuvettes in concentrated NaOH, followed by concentrated nitric acid then rinsing with acetone and drying in an oven overnight.

S1 (1.23×10^{-3}M): Haematin (8.0mg, 1.23×10^{-5}mol) was dissolved in DMSO (10ml). This solution was stored in the dark and could be used for up to a week.
S2 (1.97×10^{-6}M): DMSO (4ml), and 0.2M HEPES or MES buffers (1ml) were mixed together in a 10ml volumetric flask. To this solution **S1** (16μl) was added and the resulting solution was mixed again. The volume was then adjusted to 10ml with distilled water. **S2** was then stored in a new, unused vial (important for maintaining stability of the solution) which had been wrapped in aluminium foil and was used within a few hours.

B1: The blank solution was prepared by mixing DMSO (4ml) and 0.2M HEPES or MES buffers (1ml) in a 10ml volumetric flask. The volume was then adjusted to 10ml with distilled water.
D1: The quinoline solution was prepared by dissolving the quinoline (2.0×10^{-5} mol) in DMSO (4ml) in a 10ml volumetric flask. 0.2M HEPES or MES (1ml) was then added and the volume

adjusted with distilled water. The solution was then stored in a sample vial and after use and kept in the fridge.

7.2.3.4. Collection of Spectra

The blank solution **B1** (2ml) was placed in a 1cm thermostated cuvette at 25°C in the uv-vis spectrophotometer. After 5mins at this temperature, a baseline was recorded between the appropriate wavelengths. This solution was then discarded and **S2** (2ml) placed in the cuvette. The spectrum was then recorded between the same wavelengths as **B1** after an equilibration period of 5mins. **D1** was then added in microlitre aliquots up to a total volume of 1ml and resulting spectrum was recorded after each addition.

7.2.3.5. Spectrophotometric Titrations

The blank solution **B1** (2ml) was placed in a 1cm thermostated cuvette at 25°C in the uv-vis spectrophotometer. After 5mins at this temperature, the instrument was zeroed at 402nm. This solution was then discarded and **S2** (2ml) was placed in the cuvette. In general, the absorbance at 402nm dropped slightly over 10 mins but was stable thereafter. In the case where the absorbance at 402nm continued to drop, the **S2** solution was discarded and a fresh stock solution was made. To the stable **S2** solution, **D1** was added in microlitre aliquots over about 37 additions until a total of 1ml had been added. After each addition the resulting solution was stirred with a spatula in a back and forth motion and the stabilised absorbance at 402nm recorded (see Appendix for raw titration data).

The absorbance data at 402nm was corrected for dilution. Where the compound exhibited significant absorbance at 402nm, a blank titration was preformed and the absorbance of the compound subtracted from the titration data. The resulting data was fitted to either 1:1 association model (Equation **30**) or a stepwise 2:1 model (quinoline:haematin) (Equation **33**) using non-linear least squares fitting methods. For the derivation of these equations see Mavuso (Mavuso PhD thesis 2001).

7.2.3.5.1. The 1:1 (quinoline:haematin) Association Model (Model 1)

The equation representing 1:1 (quinoline:haematin) association can be written as follows:

$$Q + M \underset{}{\overset{K}{\rightleftharpoons}} QM \qquad \textbf{(29)}$$

Where Q represents the quinoline, M represents haematin and QM represents the haematin-quinoline complex. The equation to describe model 1 is:

$$A = \frac{A_0 + A_\infty K[Q]_{free}}{1 + K[Q]_{free}} \quad (30)$$

Where A is the corrected absorbance at 402nm, A_0 is the absorbance of the haematin before the quinoline is added, $A\infty$ is the corrected absorbance at the end of the titration, K is the association constant for the process and $[Q]_{free}$ is the concentration of the uncomplexed quinoline.

7.2.3.5.2. The 2:1 (quinoline:haematin) Association Model (Model 2)

The equation representing 2:1 (quinoline:haematin) stepwise association can be written as follows:

$$Q + M \underset{}{\overset{K_1}{\rightleftharpoons}} QM \quad (31)$$

$$QM + M \underset{}{\overset{K_2}{\rightleftharpoons}} QM_2 \quad (32)$$

where K_1 is the first association constant and K_2 is the second association constant. The equation to describe model 2 is:

$$A = A_0 f_H + A_1 f_{HD} + A_\infty f_{HD2} \quad (33)$$

where $f_H = \frac{[H]}{[H]_T}$, $f_{HD} = \frac{[HD]}{[H]_T}$, $f_{HD2} = \frac{[HD_2]}{[H]_T}$

and: $[HD_2] = [H]_T - [HD] - [H]$

$$[H] = \frac{[H]_T}{1 + K_1[Q]_{free} + K_1K_2[Q]_{free}^{\ 2}}$$

$$[HD] = \frac{[H]_T}{\left(\frac{1}{K_1[Q]_{free}}\right) + 1 + K_2[Q]_{free}}$$

7.2.3. Derivation of the Equation for Vacuolar Accumulation Ratio

The equations representing deprotonation of a diprotic base (H_2A) can be written as follows:

$$H_2A \rightleftharpoons HA + H^+ \quad \textbf{(34)}$$

$$HA \rightleftharpoons A + H^+ \quad \textbf{(35)}$$

Where HA represents the singly deprotonated species of H_2A and A represents the doubly deprotonated species H_2A. The equilibrium constant for Equations **34** and **35** can then be written:

$$K_{a1} = \frac{[HA][H^+]}{[H_2A]} \quad therefore \quad [H_2A] = \frac{[HA][H^+]}{K_{a1}} \quad \textbf{(36)}$$

$$K_{a2} = \frac{[H^+][A]}{[HA]} \quad therefore \quad [HA] = \frac{[H^+][A]}{K_{a2}} \quad \textbf{(37)}$$

The total concentration of A (A_{tot}) can be written as in Equation **38** where A_{tot}, A, H_2A and HA all refer to concentrations:

$$A_{tot} = H_2A + HA + A \quad \textbf{(38)}$$

Substituting Equations **36** and **37** into Equation **38**, it is possible to obtain an expression in terms of A_{tot} (Equation **39**)

$$A_{tot} = \frac{HA.H^+}{K_{a1}} + \frac{H^+.A}{K_{a2}} + A \quad \textbf{(39)}$$

$$A_{tot} = \frac{\left\{\frac{H^+.A}{K_{a2}}\right\}.H^+}{K_{a1}} + \frac{H^+.A}{K_{a2}} + A$$

$$A_{tot} = \frac{\left(H^+\right)^2.A}{K_{a2}.K_{a1}} + \frac{H^+A}{K_{a2}} = A$$

$$A_{tot} = A\left\{\frac{H^{+2}}{K_{a1}K_{a2}} + \frac{H}{K_{a2}} + 1\right\} \quad \textbf{(40)}$$

If $(A_{tot})_v$ is the total vacuolar concentration of A and $(A_{tot})_e$ is the total extravacuolar concentration of A then from Equation **40**:

$$\frac{(A_{tot})_v}{(A_{tot})_e} = \frac{A}{A}\frac{\left\{\frac{H_v^{+2}}{K_{a1}K_{a2}} + \frac{H_v^{+}}{K_{a2}} + 1\right\}}{\left\{\frac{H_e^{+2}}{K_{a1}K_{a2}} + \frac{H_e^{+}}{K_{a2}} + 1\right\}}$$

therefore $$\frac{(A_{tot})_v}{(A_{tot})_e} = \frac{\left\{\frac{H_v^{+2}}{K_{a1}K_{a2}} + \frac{H_v^{+}}{K_{a2}} + 1\right\}}{\left\{\frac{H_e^{+2}}{K_{a1}K_{a2}} + \frac{H_e^{+}}{K_{a2}} + 1\right\}} \quad \textbf{(41)}$$

7.2.4. β-Haematin Inhibition

7.2.4.1. IR Method (Egan *et al.* 1994)

7.2.4.1.1. Instrumentation and General Methods

The β-haematin reaction was carried out in a glass titration cell connected to a GRANT Y6 thermostated water bath set at 60°C. Compounds were weighed on a E. Mettler or Sartorius balance and volumes of solutions were delivered using a Gilson's Pipetman. Infrared disks of the product were pressed on a 30 Ton Press and the spectrum was recorded using a Perkin-Elmer 983 infrared spectrophotometer.

7.2.4.1.2. Assay

The inhibition experiments for the compounds were always done in duplicate and compared to a single control experiment in every case.

Control: β-Haematin was prepared by dissolving haemin (6mg, 9.2×10^{-6}mol) in 0.1M NaOH (1.2ml) and the resulting solution stirred in a glass titration cell connected to a thermostated water bath at 60°C for 5mins. 1.0M HCl (0.120ml) was then added followed by 12.9M acetate (0.707ml), which had been preincubated at the same temperature, to give a final acetate concentration in the mixture of 4.5M. After 30mins at this temperature, the reaction was stopped by cooling on ice and diluting with cold water. The solid was collected by

filtration on a cellulose nitrate disc (0.22μm), washed extensively with water and dried over phosphorous pentoxide for two days.

Compounds: The same procedure was followed as for the control except that the compound (4eq, 3.68×10^{-5}mol) was added to the haematin-NaOH solution and the resulting mixture allowed to stir for 10mins before addition of the 1.0M HCl.
The infrared sample was prepared by grinding the dried product (1.5mg) with KBr (250mg) to form a homogeneous mixture which was subsequently pressed into a pellet under 15 tons for 1min. Two peaks around 1660 and 1210cm^{-1} in the infrared spectrum of the product characterise the β-haematin product. Therefore, the absence of these two peaks in the product spectrum indicates that the compound is inhibitory.

7.2.4.2. BHIA Method (Parapini *et al.* 2000)

The compounds were sent away to the laboratory of Prof. D. Taramelli, University of Milan, Italy to test for β-haematin inhibition using the BHIA method.

7.2.5. pK_a Determinations

Two pK_a's were determined the 4-aminoquinoline analogues **65, 67, 74-80, 82-83**. Solutions for potentiometry were prepared in glass-distilled, deionised water which had been boiled to remove CO_2. Solutions of NaOH were prepared form Merck Titisol ampoules and stored under an atmosphere of N_2 (g) in high-densisty polyethylene bottles. These solutions were standardised againsed recrystallised potassium hydrogenphthalate and used within one week of preparation or discarded. The HCl solutions were also prepared from ampoules and standardised againsat recrystallised sodium tetrabarate and the previously standerdised NaOH. The titration procedure followed has been described previously (Jackson and Kelley 1989, Jackson *et al.* 1996) except that the 4-aminoquinolines were weighed directly into the titration vessel (2.0-4.0 mM) and the electrode system was callibrated *in situ*. To measure the potential, a 6.0133.100 glass electrode and a 6.0726.100 reference electrode was used. Protonation constants were determined under stirring, at 25°C and at an ionic strength of 0.15M NaCl. Three independent titrations were measured in each case and between 100 and 120 data points were collected per titration. The data was then analysed by Mr Thembalani E Nomkoko using the programme ESTA (Murray and May 1984, May *et al.* 1985, May *et al.* 1988).

7.2.6. Antiplasmodial Testing

All compounds were tested for antiplasmodial activity against the *CQ*-sensitive D10 strain of *P. falciparum*. Compounds **58-62**, **63-74** and **81** were tested by Jason Waldon, Dept of Pharmacology, UCT and compounds **65** and **74** were retested along with compounds **67**, **75-80**, **82-83** in the laboratory of Prof. D. Taramelli, University of Milan, Italy. In both laboratories, the compounds were cultured continuously according to the method of Trager and Jensen (Trager and Jensen 1976). Chloroquine diphosphate was dissolved in water and all other compounds were dissolved in methanol and then diluted with medium to obtain the required concentrations (final concentrations all contained less than 1% methanol which was found to be non toxic to the parasites). Antiplasmodial activity was assessed by measuring the activity of the parasite lactate dehydrogenase enzyme, according to a modified method of the method of Makler *et al.* (Makler *et al.* 1993). All antiplasmodial testing was performed at 1% hematocrit and 2% parasitemia. Compounds were added at the late trophozoite stage for a period of 48h before LDH measurement. Each IC_{50} measurement is the result of at least three separate experiments performed in duplicate.

APPENDIX 1

1.1. Spectroscopic Titration Curves

Titration curves for compounds **58 – 83** fitted to a 1:1 association model for **58 – 60, 62 – 70, 72, 75 – 80, 82, 83** and a 2:1 association model (quinoline:Fe(III)PPIX) for **61, 65, 71, 73 – 74, 81**. The solid line represents a best fit to the association model.

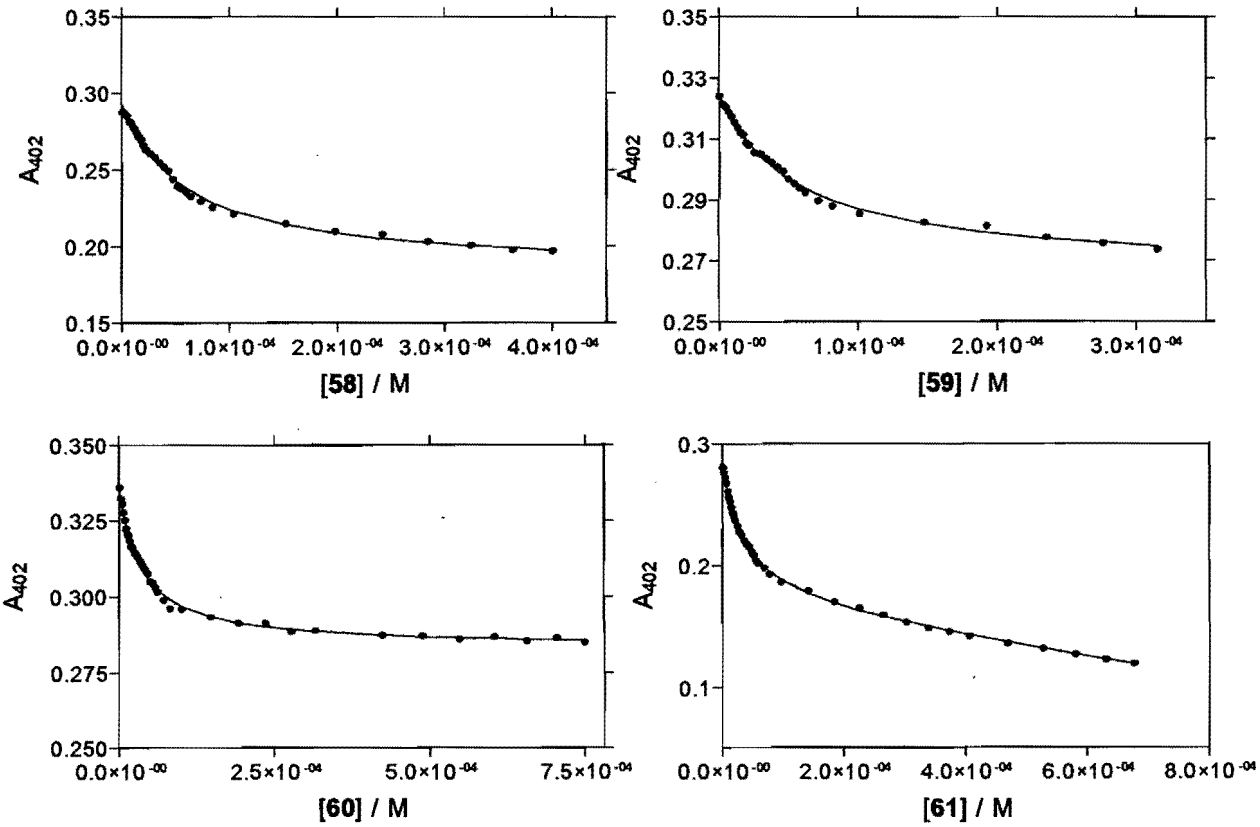

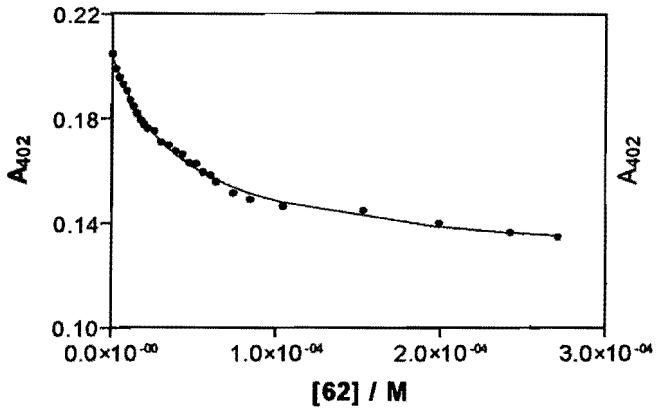
A402
0.22
0.18
0.14
0.10
0.0×10-00
1.0×10-04
2.0×10-04
3.0×10-04
[62] / M

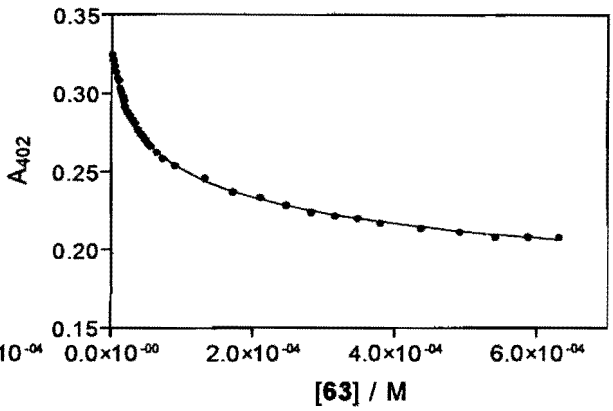
A402
0.35
0.30
0.25
0.20
0.15
0.0×10-00
2.0×10-04
4.0×10-04
6.0×10-04
[63] / M

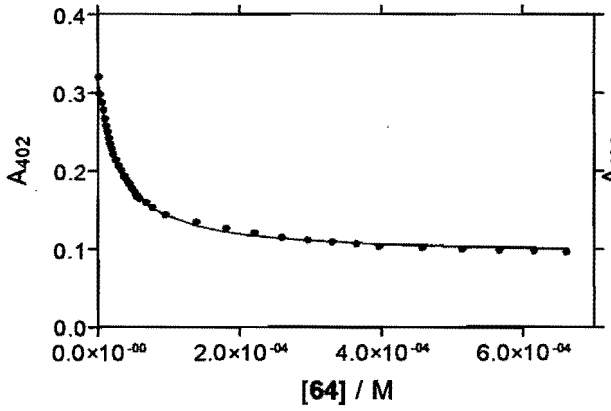
A402
0.4
0.3
0.2
0.1
0.0
0.0×10-00
2.0×10-04
4.0×10-04
6.0×10-04
[64] / M

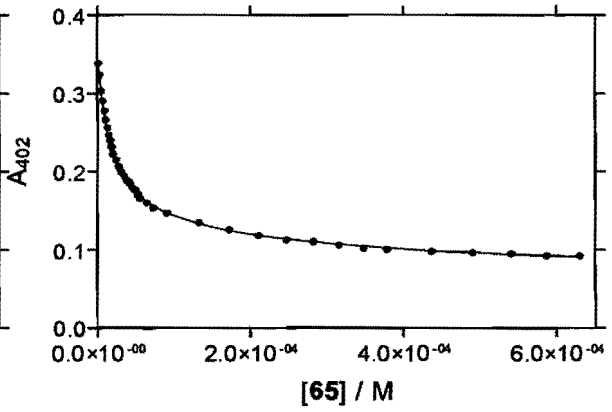
A402
0.4
0.3
0.2
0.1
0.0
0.0×10-00
2.0×10-04
4.0×10-04
6.0×10-04
[65] / M

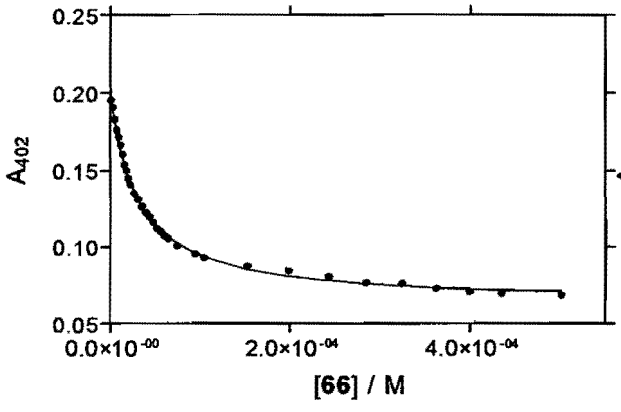
A402
0.25
0.20
0.15
0.10
0.05
0.0×10-00
2.0×10-04
4.0×10-04
[66] / M

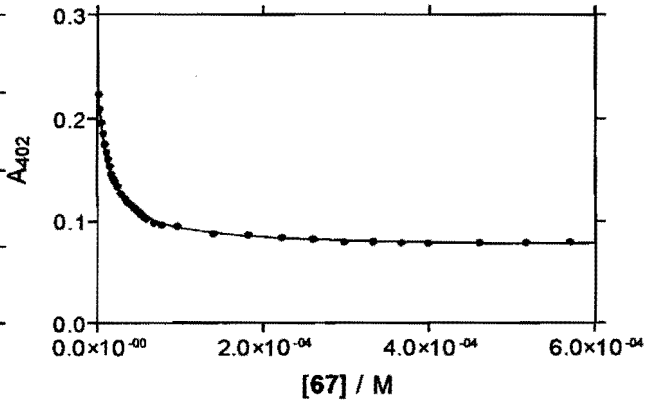
A402
0.3
0.2
0.1
0.0
0.0×10-00
2.0×10-04
4.0×10-04
6.0×10-04
[67] / M

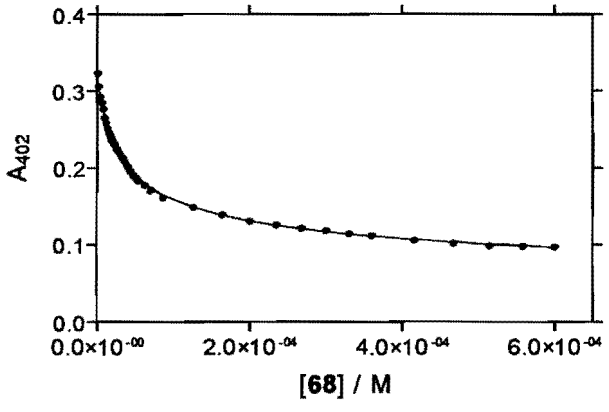
A402
0.4
0.3
0.2
0.1
0.0
0.0×10-00
2.0×10-04
4.0×10-04
6.0×10-04
[68] / M

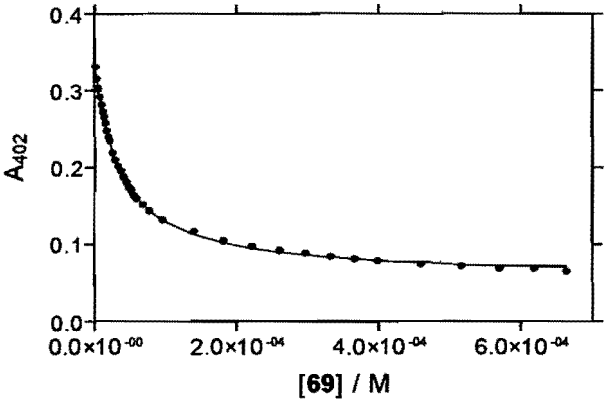
A402
0.4
0.3
0.2
0.1
0.0
0.0×10-00
2.0×10-04
4.0×10-04
6.0×10-04
[69] / M

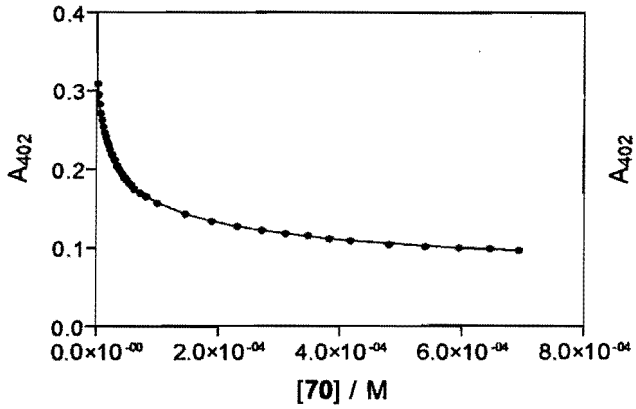
0.4
0.3
0.2
0.1
0.0
A_{402}
0.0×10⁻⁰⁰ 2.0×10⁻⁰⁴ 4.0×10⁻⁰⁴ 6.0×10⁻⁰⁴ 8.0×10⁻⁰⁴
[70] / M

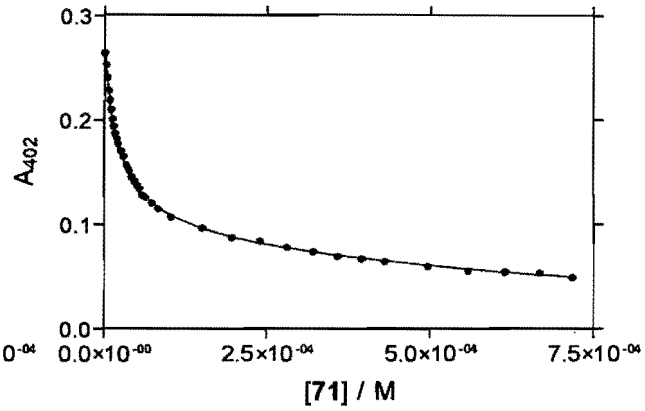
0.3
0.2
0.1
0.0
A_{402}
0.0×10⁻⁰⁰ 2.5×10⁻⁰⁴ 5.0×10⁻⁰⁴ 7.5×10⁻⁰⁴
[71] / M

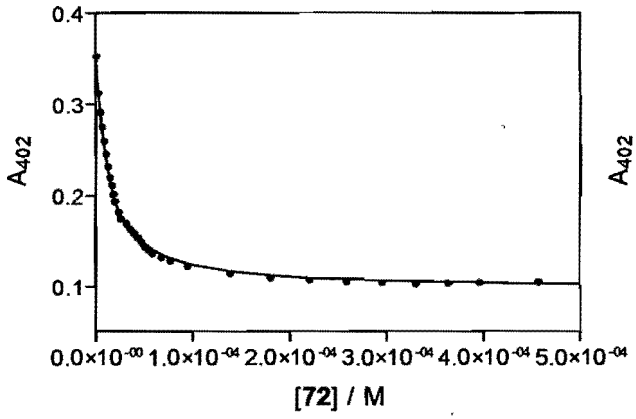
0.4
0.3
0.2
0.1
A_{402}
0.0×10⁻⁰⁰ 1.0×10⁻⁰⁴ 2.0×10⁻⁰⁴ 3.0×10⁻⁰⁴ 4.0×10⁻⁰⁴ 5.0×10⁻⁰⁴
[72] / M

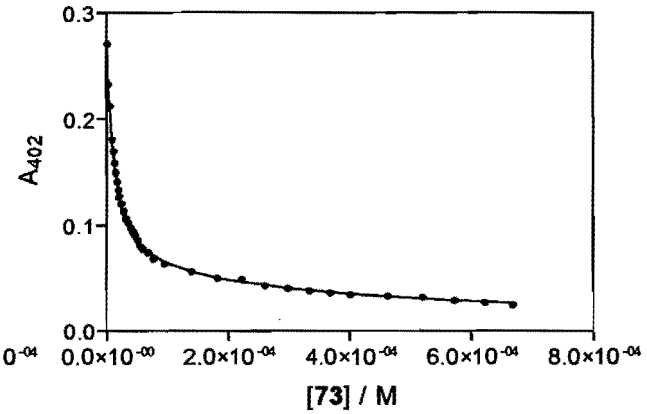
0.3
0.2
0.1
0.0
A_{402}
0.0×10⁻⁰⁰ 2.0×10⁻⁰⁴ 4.0×10⁻⁰⁴ 6.0×10⁻⁰⁴ 8.0×10⁻⁰⁴
[73] / M

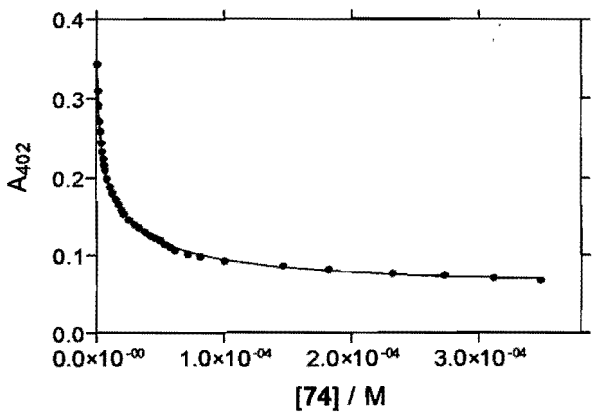
0.4
0.3
0.2
0.1
0.0
A_{402}
0.0×10⁻⁰⁰ 1.0×10⁻⁰⁴ 2.0×10⁻⁰⁴ 3.0×10⁻⁰⁴
[74] / M

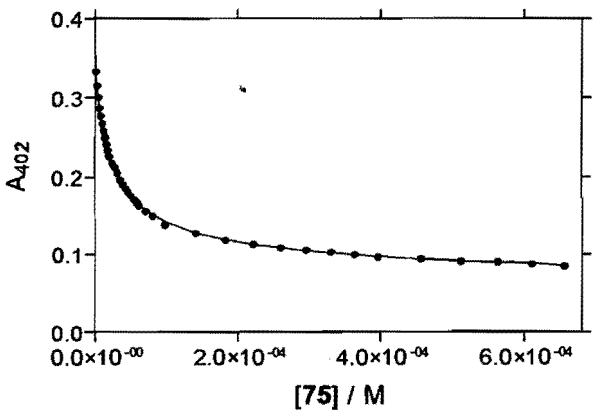
0.4
0.3
0.2
0.1
0.0
A_{402}
0.0×10⁻⁰⁰ 2.0×10⁻⁰⁴ 4.0×10⁻⁰⁴ 6.0×10⁻⁰⁴
[75] / M

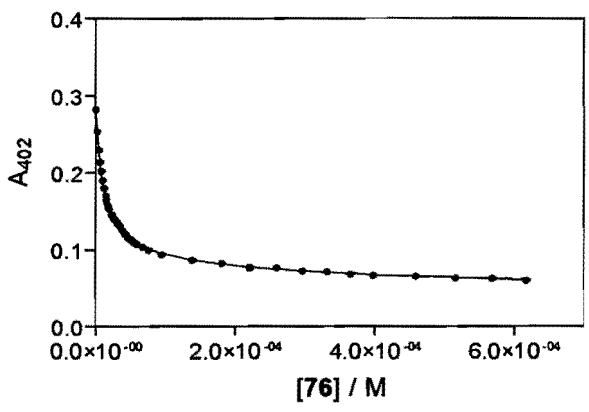
0.4
0.3
0.2
0.1
0.0
A_{402}
0.0×10⁻⁰⁰ 2.0×10⁻⁰⁴ 4.0×10⁻⁰⁴ 6.0×10⁻⁰⁴
[76] / M

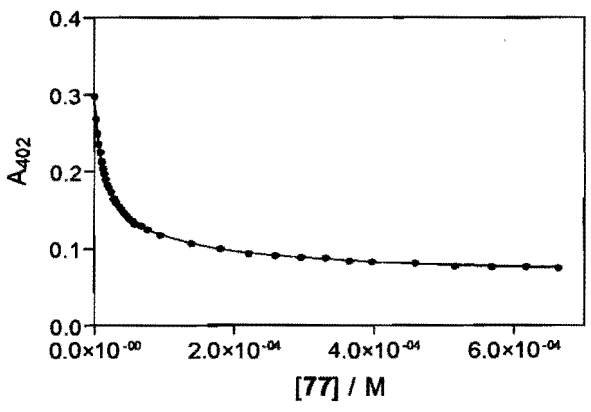
0.4
0.3
0.2
0.1
0.0
A_{402}
0.0×10⁻⁰⁰ 2.0×10⁻⁰⁴ 4.0×10⁻⁰⁴ 6.0×10⁻⁰⁴
[77] / M

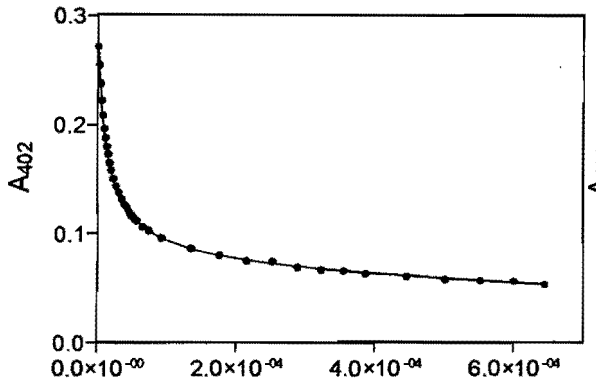

[78] / M

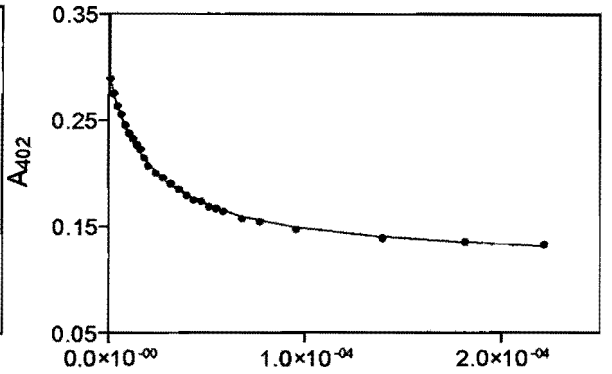

[79] / M

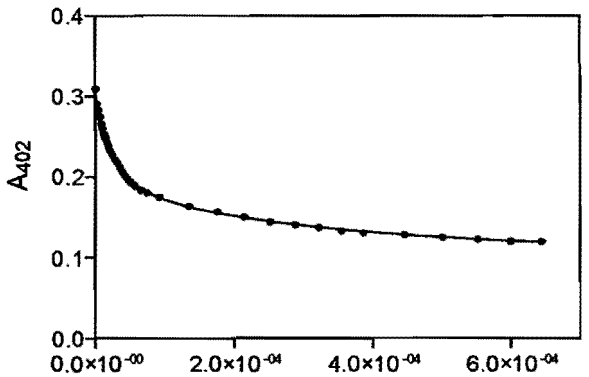

[80] / M

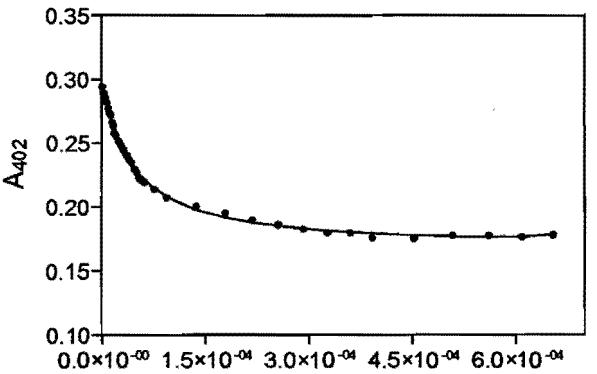

[81] / M

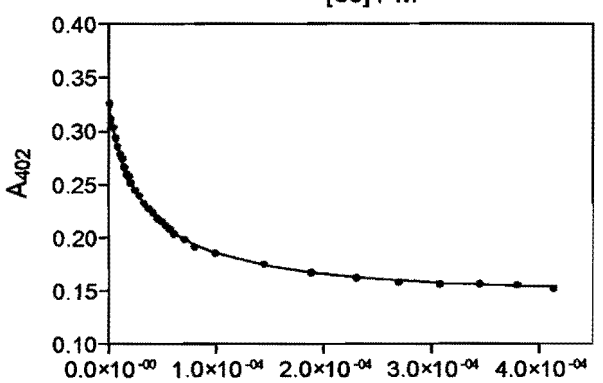

[82] / M

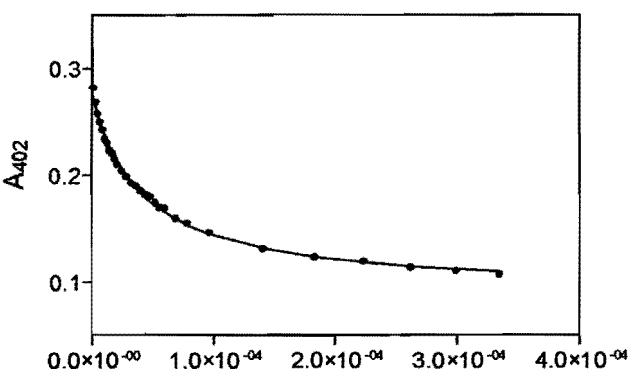

[83] / M

APPENDIX 2

Infrared spectra of the preducts of all the compounds in the project tested for β-Haematin inhibitory activity by the IR method of Egan *et al.* (Egan *et al.* 1994).

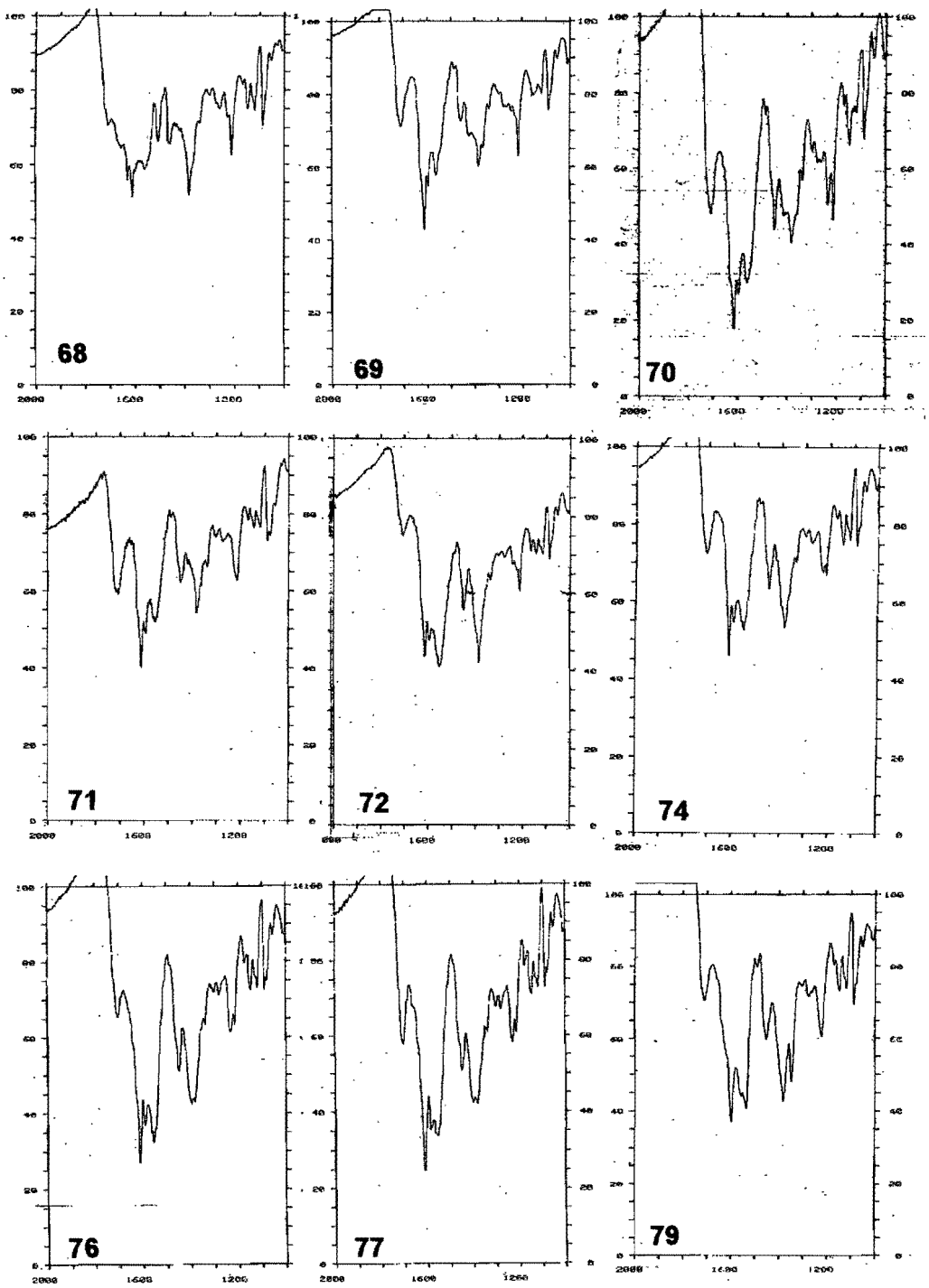

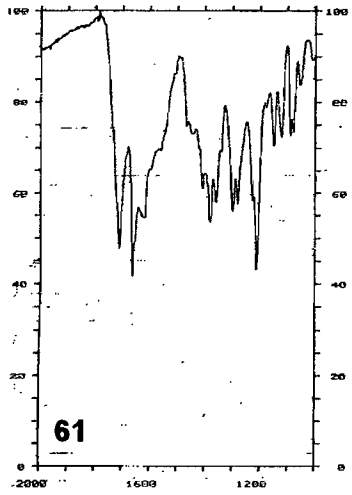
61

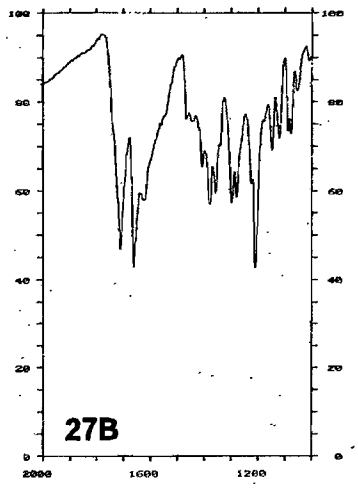
27B

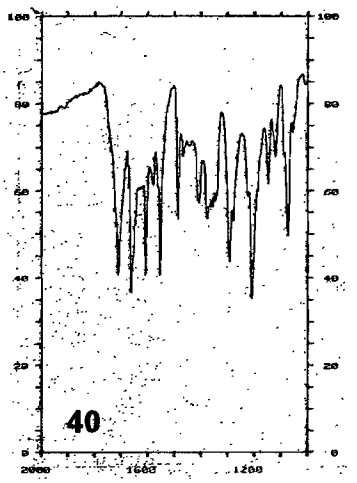
40

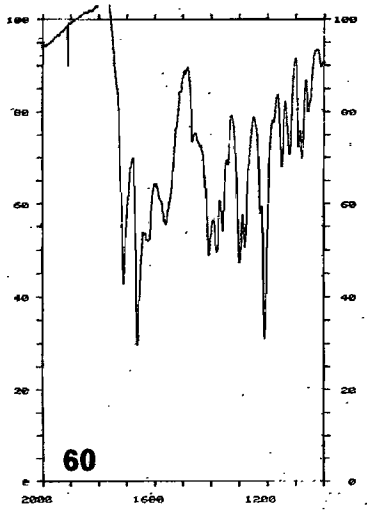
60

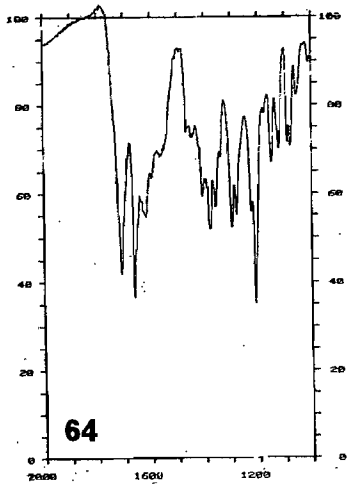
64

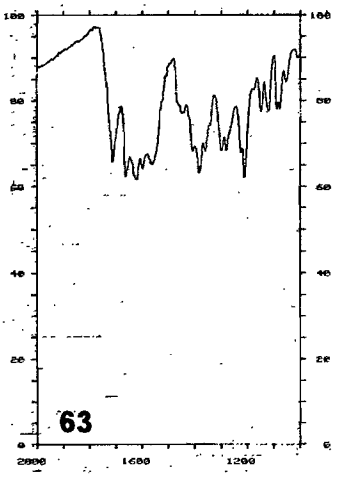
63

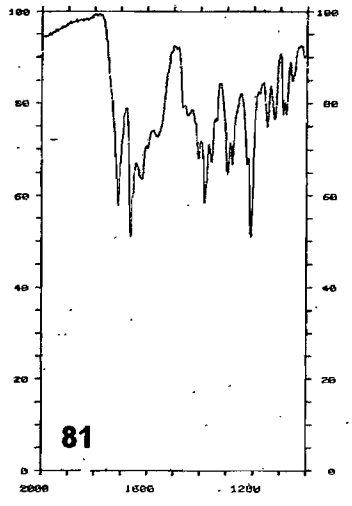
81

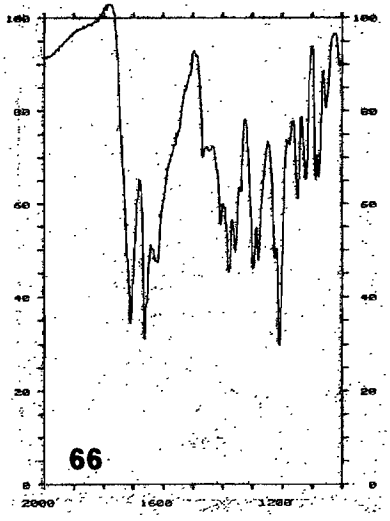
66

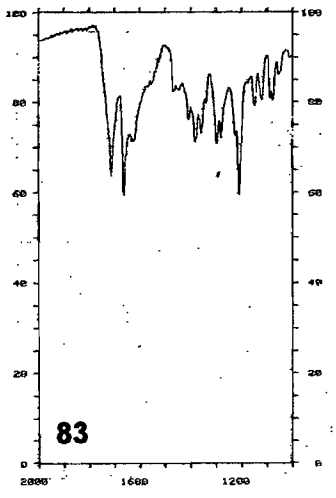
83

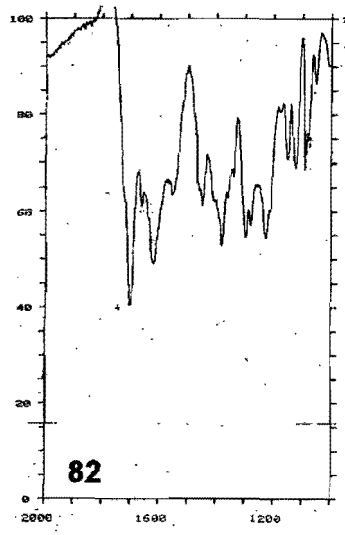
82

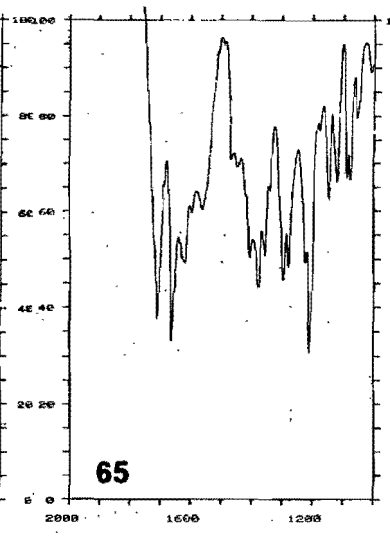
65

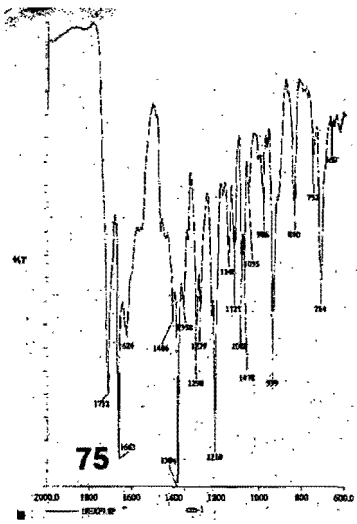
75

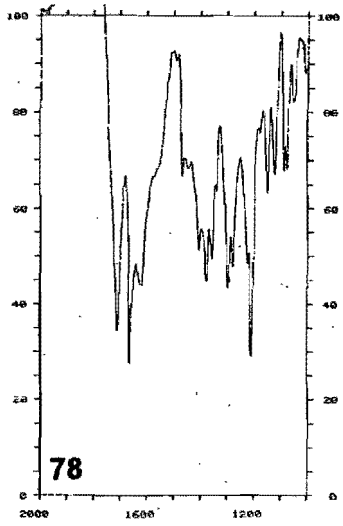
78

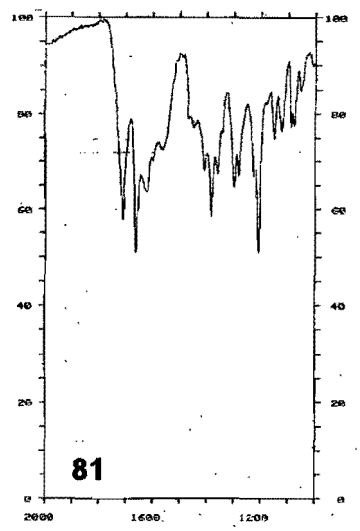
81

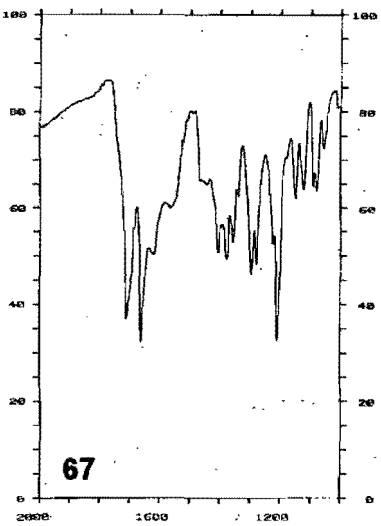
67

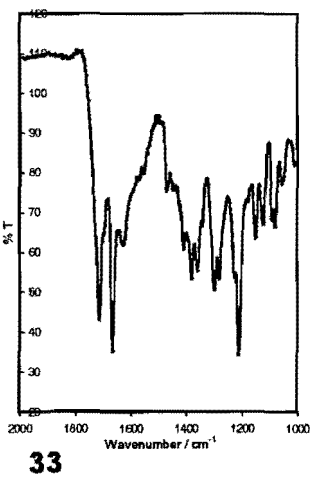
% T
Wavenumber / cm-1
33

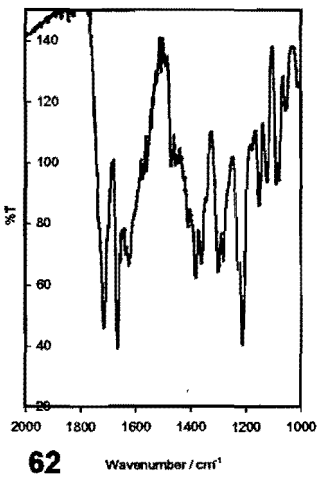
%T
62
Wavenumber / cm-1

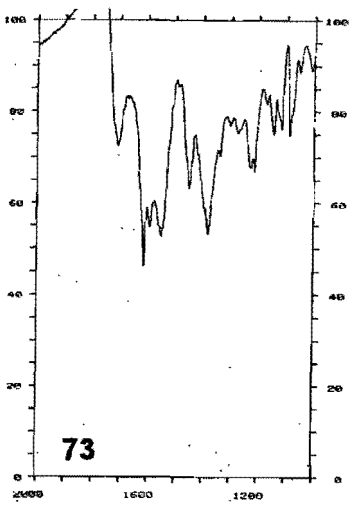
73

BIBLIOGRAPHY

Aldrich, C7,050-9, 2000.

Adams, P.A., Berman, P.A.M., Egan, T.J., Marsh, P.J., Silver, J. The iron environment in heme and heme-antimalarial complexes of pharmacological interest. *J. Inorg. Biochem.* **1996**a, 63, 69- 77.

Adams, P.A., Egan, T.J., Ross, D.C., Silver, J., Marsh, P.J. The chemical mechanism of *B*-haematin formation studied by Mössbauer spectroscopy. *Biochem. J.* **1996**b, 318, 25- 27.

Aikawa, M. High resolution autoradiography of malaria parasites treated with ^{3}H-chloroquine. *Am. J. Pathol.* **1972**, 67(2), 277- 280.

Ajay and Murcko, M.A. Computational methods to predict binding free energy in ligand-receptor complexes. *J. Med. Chem.* **1995**, 38(26), 4953- 4967.

Alben, J.O., Fuchsman, W.H., Beaudreau, C.A., Caughey, W.S. Substituted deuteroporphyrins. III. Iron (II) derivatives. Reactions with oxygen and preparations from chloro- and methoxohemins. *Biochemistry.* **1968**, 7(2), 624- 635.

Angerman, N.S., Danyluk, S.S., Victor,T.A. A direct determination of the spatial geometry of molecules in solution. 1. Conformation of chloroquine, an antimalarial.

Asawamahasakda, W., Ittarat, I., Chang, C., McElroy, P., Meshnick, S. R. Effects of antimalarials and protease inhibitors on plasmodial haemozoin production. *Mol. Biochem. Parasitol.* **1994**, 67, 183-191.

Atamna, H. and Ginsburg, H. Heme degradation in the presence of glutathione. *J. Biol. Chem.* **1995**, 270(42), 24876- 24883.

Bachhawat, K., Thomas, C.J., Surolina, N., Surolina, A. Interaction of chloroquine and its analogues with heme: an isothermal titration calorimetric study. *Biochem. Biophys. Res. Commun.* **2000**, 276, 1075- 1079.

Bachman, G.B. and Cooper, D.E. Quinoline derivatives from 2- and 4-chloroquinolines. *J. Am. Chem. Soc.* **1944**, 302- 309.

Badger, G. M. The Chemistry of the Heterocyclic Compounds. Academic press, 1961.

Baker, R.H., Lappin, G.R., Albisetti, C.J., Riegel, B. The decarboxylation of nitro-substituted 3-carboxy-4-quinolinols by pyrolysis of their silver salts. *J. Am. Chem. Soc.* **1946**, 68, 1267.

Balasubramanian, D., Mohan Rao, C., Panijpan, B. The malarial parasite monitored by photoacoustic spectroscopy. *Science.* **1984**, 223, 828- 830.

Baldwin, D.A., Marques, H.M., Pratt, J.M. Hemes and hemeproteins, 2: The pH-dependent equilibria of microperoxidase-8 and characterization of the coordination sphere of Fe(III). *J. Inorg. Biochem.* **1986**, 27(4), 245- 254.

Banerjee, R., Liu, J., Beatty, W., Pelosof, L., Klemba, M., Goldberg, D.E. Four plasmepsins are active in the *Plasmodium falciparum* food vacuole, including a protease with an active-site histidine. *Proc. Natl. Acad. Sci. USA.* **2002**, 99(2), 990- 995.

Barton, D. and Ollis, D. W. Comprehensive organic chemistry. Pergamon Press Ltd, 1979, 16.4, Quinolines. p. 155-203.

Beak, P., Woods, T.S., Mueller, D.S. Equilibrium studies: substituent effects on methoxypyridine-1-methylpyridone equilibria. *Tetrahedron.* **1972**, 28, 5507- 5519.

Belli *Ric. Sci.* **1963**, 3, 530

Bendrat, K., Berger, B.J., Cerami, A. Haem polymerization in malaria. *Nature.* **1995**, 378, 138

Biot, C., Glorian, G., Maciejewski, L.A., Brocard, J.S. Synthesis and antimalarial activity in vitro and in vivo of a new ferrocene-chloroquine analogue. *J. Med. Chem.* **1997**, 40(23), 3715- 3718.

Bitonti, A.J., Sjoerdsma, A., McCann, P.P., Kyle, D.E., Oduola, A.M.J., Rossan, R.N., Milhous, W.K., Davidson, D.E., Jr. Reversal of chloroquine resistance in malaria parasite *plasmodium falciparum* by desipramine. *Science.* **1988**, 242, 1301- 1303.

Blauer, G. Interaction of ferriprotoporphyrin IX with the antimalarials amodiaquine and halofantrine. *Biochem. Int.* **1988**, 17(4), 729- 734.

Blauer, G., Akkawi, M., Bauminger, E.R. Further evidence for the interaction of the antimalarial drug amodiaquine with ferriprotoporphyrin IX. *Biochem. Pharmacol.* **1993**, 46(9), 1573- 1576.

Bray, P.G., Howells, R.E., Ritchie, G.Y., Ward, S.A. Rapid chloroquine efflux phenotype in both chloroquine-sensitive and chloroquine resistant *P. falciparum. Biochem. Pharmacol.* **1992**a, 44(7), 1317- 1324.

Bray, P.G., Howells, R.E., Ward, S.A. Vacuolar acidification and chloroquine sensitivity in *Plasmodium falciparum. Biochem. Pharmacol.* **1992**b, 43(6), 1219- 1227.

Bray, P.G. and Ward, S.A. Malaria chemotherapy: resistance to quinoline containing drugs in *P. falciparum. FEMS Microbiol. Lett.* **1993**, 113, 1- 8.

Bray, P.G., Hawley, S.R., Mungthin, M., Ward, S.A. Physicochemical properties correlated with drug resistance and the reversal of drug resistance in *P. falciparum. Mol. Pharmacol.* **1996**, 50, 1559- 1566.

Bray, P.G., Mungthin, M., Ridley, R.G., Ward, S.A. Access to hematin: The basis of chloroquine resistance. *Mol. Pharmacol.* **1998**, 54, 170- 179.

Bray, P.G., Janneh, O., Raynes, K.J., Mungthin, M., Ginsburg, H., Ward, S.A. Cellular uptake of chloroquine is dependent on binding to ferriprotoporphyrin IX and is Independent of NHE activity in *pasmodium falciparum.. J. Cell Biol.* **1999**, 145(2), 363- 376.

Bray, P.G., Saliba, K.J., Davies, J.D., Spiller, D.G., White, M.R.H., Kirk, K., Ward, S.A. Distribution of actidine orange fluorescence in *P. falciparum*-infected erythrocytes and its implications for the evaluation of digestive vacuole pH. *Mol. Biochem. Parasitol.* **2002**a, 119, 301- 304.

Bray, P.G., Saliba, K.J., Davies, J.D., Spiller, D.G., White, M.R.H., Kirk, K., Ward, S.A. Further comments on the distribution of acridine orange fluorescence in *P. falciparum*-infected erythrocytes. *Mol. Biochem. Parasitol.* **2002**b, 119, 311- 313.

Breslow, D.S., Bloom, M.S., Shivers, J.C., Adams, J.T., Weiss, M.J., Yost, R.S., Hauser, C.R. Synthesis of antimalarials. V. The synthesis of certain 4-aminoquinoline derivatives. *J. Am. Chem. Soc.* **1946**, 68, 1232- 1238.

Brown, E.V. and Plasz, A.C. Spectroscopic determination of the second dissociation constants of the aminoquinolines. *J. Heterocycl. Chem.* **1970**a, 7, 335- 338.

Brown, S.B., Jones, P., Suggett, A. Reactions between haemin and hydrogen peroxide. *Trans. Faraday. Soc.* **1968**, 64, 986- 993.

Brown, S.B., Jones, P., Lantzke, I.R. Infrared evidence for an oxo-bridged (Fe-O-Fe) haemin dimer. *Nature.* **1969**a, 223, 960- 961.

Brown, S.B. and Lantzke, I.R. Solution structures of ferrihaem in some dipolar aprotic solvents and their binary aqueous mixtures. *Biochem. J.* **1969**b, 115, 279- 285.

Brown, S.B., Dean, T.C., Jones, P. Aggregation of Ferrihaems: Dimerization and protolytic equilibria of protoferrihaem and deuteroferrihaem in aqueous solution. *Biochem. J.* **1970b**, 117, 733- 739.

Brown, S.B. and Shillcock, M. Equilibrium and kinetic studies of the aggregation of porphyrins in aqueous solution. *Biochem. J.* **1976**, 153, 279- 285.

Bruce-Chwatt, L.J, Chemotherapy of malaria. 2nd ed. Geneva, World health organisation, **1981**.

Bruce-Chwatt, L.J, Essential malariology. 2nd ed. London, William Heineman Medical Books Ltd, **1985**.

Buchler, J.W. Hemoglobin-an inspiration for research in coordination chemistry. *Angew. Chem. Int. Ed. Engl.* **1978**, 17, 407- 423.

Campbell, Biochemistry. Saunders college publishing, **1991**.

Cannon, J.B., Kuo, F., Pasternack, R.F., Wong, N.M., Muller-Eberhard, U. Kinetics of the interaction of hemin liposomes with heme binding proteins. *Biochemistry.* **1984**, 23, 3715- 3721.

Chen, L. Recent studies on antimalarial efficacy of piperaquine and hydroxypiperaquine. *Chin. Med. J.* **1991**, 104, 161- 163.

Chen, M.M., Shi, L., Sullivan, D.J. *Haemoproteins* and *Schistosoma* synthesise heme polymers similar to *Plasmodium* hemozoin and β-hematin. *Mol. Biochem. Parasitol.* **2001**, 113, 1- 8.

Chibale, K., Moss, J.R., Blackie, M., van Schalkwyk, D., Smith, P.J. New amine and urea analogues of ferrochloroquine: synthesis, antimalarial activity in vitro and electrochemical studies. *Tet. Lett.* **2000**, 41, 6231- 6235.

Choi, C.Y.H., Cerda, J.F., Chu, H., Babcock, G.T., Marletta, M.A. Spectroscopic characterisation of the heme-binding sites in *plasmodium falciparum* histidine-rich protein 2. *Biochemistry.* **1999**, 38, 16916- 16924.

Chou, A.C., Chevli, R., Fitch, C.D. Ferriprotoporphyrin IX fulfills the criteria for identification as the chloroquine receptor of malaria parasites. *Biochemistry.* **1980**, 19, 1543- 1549.

Chou, A.C. and Fitch, C.D. Mechanism of hemolysis induced by ferriprotoporphyrin IX. *J. Clin. Invest.* **1981**, 68, 672- 677.

Clarke, W.M. and Perkins, M.E. Metalloporphyrins V. A spectroscopic study of pyridine coproporphyrin I. *J. Biol. Chem.* **1940**, 135, 643- 657.

Coatney, R.G. Pitfalls in the discovery of chloroquine. *Am. J. Trop. Med. Hyg.* **1963**, 12, 121- 128.

Cohen, I.A. The dimeric nature of hemin hydroxides. *J. Am. Chem. Soc.* **1969**, 91(8), 1980- 1983.

Cohen, S.N., Phifer, K.O., Yielding, K.L. Complex formation between chloroquine and ferrihaemic acid *in vitro*, and its effect on the antimalarial action of chloroquine. *nature.* **1964**, 202(4934), 805- 806.

Collier, G.S., Pratt, J.M., De Wet, C.R., Tshabalala, C.F. Studies in haemin in dimethyl sulphoxide/water mixtures. *Biochem. J.* **1979**, 179, 281- 289.

Comins *et al.*, ; Katritzky AR, Rees CW, Scriven EFV, editors.Comprehensive Hetreocyclic Chemistry II. II ed. Elsevier Science Ltd, 1996; 5.02, Pyridines and their Benzo Derivatives: Reactivity at the Ring. p. 37-90.

Conroy, A.E., Mosher, H.S., Whitmore, F.C. Heterocyclic basic compounds XII. 7-Bromo- and 7-iodo-quinolines. *J. Am. Chem. Soc.* **1946**, 71, 3236- 3237.

Constantinidis, I. and Satterlee, J.D. UV-Visible and carbon NMR studies of quinine binding to urohemin I chloride and uroporphyrin I in aqueous solution. *J. Am. Chem. Soc.* **1988a**, 110, 927- 932.

Constantinidis, I. and Satterlee, J.D. UV-Visible and carbon NMR studies of chloroquine binding to urohemin I chloride and uroporphyrin I in aqueous solutions. *J. Am. Chem. Soc.* **1988b**, 110, 4391-4395.

Counsell, R.E., Pocha, P., Morales, J.O., Beierwalters, W.H. Tumor localising agents III. Radioiodinated quinoline derivatives. *J. Pharm. Sci.* **1967**, 56(8), 1042- 1044.

Cowgill, R.W. and Clarke, W.M. Metalloporphyrins VII. Coordination of imidazoles with ferrimesoporphyrin. *J. Biol. Chem.* **1952**, 33- 61.

Cowman, A.F., Galatis, D., Thompson, J.K. Selection for mefloquine resistance in *P. falciparum* is not linked to amplification of the *pfmdr1* gene and cross resistance to halofantrine and quinine. *Proc. Natl. Acad. Sci. USA.* **1994**, 91, 1143- 1147.

Craig, J.C. and Pearson, D.E. NMR proof of the structure of 4-aminoquinolines and pyridines. *J. Heterocyclic. Chem.* **1968**, 5, 631- 637.

Dahle, L.K., Hill, E.G., Holman, R.T. The thiobarbituric acid reaction and the autoxidations of polyunsaturated fatty acid methyl esters. *Arch. Biochem. Biophys.* **1962**, 98, 253- 261.

Davidson, M.W., Griggs, B.G., Boykin, D.W., Wilson, D.W. Mefloquine, a clinically useful quinolinemethanol antimalarial which does not significantly bind to DNA. *Nature.* **1975**, 254, 632- 634.

Davies, T.H. Metalloporphyrins III. Coordination of Nitrogenous bases with Iron Meso-, Proto-, and Hematoporphyrins. *J. Biol. Chem.* **1940**, 135, 597- 622.

De Almeida Ribeiro, M.C., Augusto, O., da Costa Ferreira, A.M. Inhibitory effect of chloroquine on the peroxiase activity of ferriprotoporphyrin IX. *J. Chem. Soc. Dalton Trans.* **1995**, 3759- 3766.

De Almeida Ribeiro, M.C., Augusto, O., da Costa Ferreira, A.M. Influence of quinoline-containing antimalarials in the catalase activity of ferriprotoporphyrin IX. *J. Inorg. Biochem.* **1997**, 65, 15- 23.

De, D., Krogstad, F.M., Cogswell, F.B., Krogstad, D.J. Aminoquinolines that circumvent resistance in *plasmodium falciparum* in vitro. *Am. J. Trop. Med. Hyg.* **1996**, 55(6), 579- 583.

De, D., Byers, L.D., Krogstad, D.J. Antimalarials: synthesis of 4-aminoqinolines that circumvent drug resistance in malaria parasites [1]. *J. Heterocyclic Chem.* **1997**, 34, 315- 320.

De, D., Krogstad, F.M., Byers, L.D, Krogstad, D. J. Structure-function relationships for antiplasmodial activity among 7-substsuted 4-aminoquinolines. *J .Med. Chem.* **1998**, 41 (25), 4918- 4926.

Den Hertog, H.J. and Buurman, D.J. Action of potassium amide on 2-, 3- and 4-bromoquinolines in liquid ammonia. *Rec. Trav. Chim.* **1967**, 86, 187- 192.

Dibyendu, D., Krogstad, F.M., Byers, L.D., Krogstad, D.J. Structure-activity relationships for antiplasmodial activity among 7-substituted 4-aminoquinolines. *J. Med. Chem.* **1998**, 41, 4918- 4926.

Dorn, A., Stoffel, R., Matile, H., Bubendorf, A., Ridley, R.G. Malaria haemozoin/β-haematin supports haem polymerisation in the absence of protein. *Nature.* **1995**, 374, 269- 271.

Dorn, A., Vippagunta, S.R., Matile, H., Bubendorf, A., Vennerstroom, J.L., Ridley, R.G. A comparison and analysis of several ways to promote haematin (haem) polymerisation and an assessment of its initiation *In vitro*. *Biochem. Pharmacol.* **1998a**, 55, 737- 747.

Dorn, A., Vippagunta, S.R., Matile, H., Jaquet, C., Vennerstroom, J.L., Ridley, R.G. An assessment of drug-haematin binding as a mechanism for inhibition of haematin polymerisation by quinoline antimalarials. *Biochem. Pharmacol.* **1998b**, 55, 727- 736.

Dzekunov, S.M., Ursos, L.M.B., Roepe, P.D. Digestive vacuolar pH of intact intraerythrocytic *P. falciparum* either sensitive or resistant to chloroquine. *Mol. Biochem. Parasitol.* **2000**, 110, 107- 124.

Dzekunov, S.M., Ursos, L.M.B., Roepe, P.D. Response to Bray *et al.* "Distribution of acridine orange fluorescence in *P. falciparum*-infected erythrocytes and its implications for the evaluation of digestive vacuole pH". *Mol. Biochem. Parasitol.* **2002**, 119, 307- 309.

Egan, T.J., Ross, D.C., Adams, P.A. Quinoline anti-malarial drugs inhibit the spontaneous formation of β-haematin (malaria pigment). *FEBS Lett.* **1994**, 352, 54- 57.

Egan, T.J., Mavuso, W.W., Ross, D., C., Marques, H.M. Thermodynamic factors controlling the interaction of quinoline antimalarial drugs with ferriprotoporphyrin IX. *J. Inorg. Biochem.* **1997**, 68, 137- 145.

Egan, T.J., Hempelmann, E., Mavuso, W.W. Characterisation of synthetic β-haematin and effects of the antimalarial drugs quinidine, halofantrine, desbutylhalofantrine and mefloquine on its formation. *J. Inorg. Biochem.* **1999**a, 73, 101- 107.

Egan, T.J. and Marques, H.M. The role of haem in the activity of chloroquine and related antimalarial drugs. *Coord. Chem. Rev.* **1999**b, 190-192, 493- 517.

Egan, T.J. Structure-function relationships in chloroquine and related 4-aminoquinoline antimalarials. *Mini Revs. Med. Chem.* **2001**a, 1, 113- 123.

Egan, T.J. Quinoline antimalarials. *Exp. Opin. Ther. Patents.* **2001**b.

Egan, T.J., Mavuso, W.W., Ncokazi, K.K. The mechanism of β-hematin formation in acetate solution. Parallels between hemozoin formation and biomineralization. *Biochemistry.* **2001**c, 40, 204- 213.

Eggleson, K.K., Duffin, K.L., Goldberg, D.E. Identification and characterisation of falcilysin, a metallopeptidase involved in hemoglobin catabolism within the malaria parasite *P. falciparum*. *J. Biol. Chem.* **1999**, 274(45), 32411- 32417.

Elderfield, R.C., Gensler, W.J., Birsten, O., Kreysa, F.J., Maynard, J.T., Galbreath, J. Synthesis of certain simple 4-aminoquinoline derivatives. *J. Am. Chem. Soc.* **1946**, 68, 1250- 1251.

Ellis, J., Gellert, E., Robson, J. Synthesis of some new iodoquinolines. *Aust. J. Chem.* **1973**, 26, 907- 911.

Ferrari, V. and Cutler, D.J. Simulation of kinetic data on the influx and efflux of chloroquine by erythrocytes infected with *Plasmodium falciparum*. *Biochem. Pharmacol.* **1991**, 42, 5167- 5179.

Fidock, D.A., Nomura, T., Cooper, R.A., Su, X., Talley, A.K., Wellems, T.E. Allelic modifications of the *cg2* and *cg1* genes do not alter the chloroquine response of drug-resistant *P. falciparum*. *Mol. Biochem. Parasitol.* **2000**a, 110, 1- 10.

Fidock, D. A., Nomura, T., Talley, A. K., Cooper, R. A., Dzekunov, S. M., Ferdig, M. T., Ursos, L. M., Sidhu, A. B., Naude, B., Deitsch, K. W., Su, X. Z., Wootton, J. C., Roepe, P. D., Wellems, T. E. Mutations in the P. falciparum digestive vacuole transmembrane protein PfCRT and evidence for their role in chloroquine resistance. *Molecular Cell.* **2000**b, 6(4), 861-871

Fitch, C.D. Plasmodium falciparum in owl monkeys: drug resistance and chloroquine binding capacity. *Science.* **1970**, 169, 289- 290.

Fitch, C.D., Chevli, R., Gonzalez, Y. Chloroquine accumulation by erythrocytes: a latent capability. *Life Sci.* **1974**a, 14, 2441- 2446.

Fitch, C.D., Yunis, N.G., Chevli, R., Gonzalez, Y. High affinity accumulation of chloroquine by mouse erythrocytes infected with *Plasmodium berghei*. *J. Clin. Invest.* **1974**b, 54, 24- 33.

Fitch, C.D., Chevli, R., Banyal, H.S., Phillips, G., Pfaller, M.A., Krogstad, D.J. Lysis of *plasmodium falciparum* by ferriprotoporphyrin IX and a chloroquine-ferriprotoporphyrin IX complex. *Antimicrob. Agents Chemother.* **1982**, 21(5), 819- 822.

Fitch, C.D. and Chou, A.C. Heat-labile and heat-stimulable heme polymerase activities in *P. berghei*. *Mol. Biochem. Parasitol.* **1996**, 82, 261- 264.

Fitch, C.D. and Chou, A.C. Regulation of heme polymerising activity and the antimalarial action of chloroquine. *Antimicrob. Agents Chemother.* **1997**, 41(11), 2461- 2465.

Fitch, C.D., Cai, G., Chen, Y., Shoemaker, J.D. Involvement of lipids in ferriprotoporphyrin IX polymerisation in malaria. *Biochim. Biophys. Acta.* **1999**, 1454, 31- 37.

Fitch, C.D., Cai, G., Shoemaker, J.D. A role for linoleic acid in erythrocytes infected with plasmodium berghei. *Biochim. Biophys. Acta.* **2000**, 1535, 45- 49.

Fleischer, E.B. and Srivastsva, T.S. The structure and properties of μ-oxo-bis(tetraphenylporphineiron(III)). *J. Am. Chem. Soc.* **1969**, 91(9), 2403- 2405.

Fleischer, E. B., Palmer, J. M., Srivastava, T. S., Chatterjee, A. Thermodynamic and kinetic properties of an iron-porphyrin system. *J. Am. Chem. Soc.* **1971**, 93 (13), 3162- 3167.

Foley, M. and Tilley, L. Quinoline antimalarials: Mechanism of action and resistance. *Int. J. Parasitol.* **1997**, 27(2), 231- 240.

Foote, S.J., Kyle, D.E., Martin, R.K., Oduola, A.M.J., Forsyth, K., Kemp, D.J., Cowman, A.F. Several alleles of the multidrug-resistance gene are closely linked to chloroquine resistance in *P. falciparum*. *Nature.* **1990**, 345, 255- 258.

Foote, S.J. and Cowman, A.F. The mode of action and the mechanism of resistance to antimalarilal drugs. *Acta Trop.* **1994**, 56, 157- 171.

Fuhrhop, J. The reactivity of the porphyrin ligand. *Angew. Chem. Internat. Edit.* **1974**, 13(5), 321- 335.

Futch, C.D. Chloroquine resistance in malaria: a deficiency of chloroquine binding. *Proc. Natl. Acad. Sci. USA.* **1969**, 64, 1181- 1187.

Gallagher, W.A. and Elliot, W.B. Ligand-binding in porphyrin systems. *An. N. Y. Acad. Sci.* **1973**, 206, 463- 482.

Gasquet, M., Atouk, A., Samat, A., Timon-David, P., Viala, A. *In vitro* chemosensitivity of *P. falciparum* to four chloroquine derivatives. *Ann. Trop. Med. Parasitol.* **1987**, 81(4), 355- 358.

Geary, T.G., Jensen, J.B., Ginsburg, H. Uptake of [^{3}H] chloroquine by drug-sensitive and -resistant strains of the human malaria parasite *Plasmodium falciparum*. *Biochem. Pharmacol.* **1986**, 35(21), 3805- 3812.

Ginsburg, H. and Demel, R.A. The effect of ferriprotoporphyrin IX and chloroquine on phospholipid monolayers and the possible implications to antimalarial activity. *Biochim. Biophys. Acta.* **1983**, 732, 316- 319.

Ginsburg, H. and Geary, T.G. Current concepts and new ideas on the mechanism of action of quinoline-containing antimalarials. *Biochem. Pharmacol.* **1987**, 36(10), 1567- 1576.

Ginsburg, H. and Stein, W.D. Kinetic modelling of chloroquine uptake by malaria-infected erythrocytes. *Biochem. Pharmacol.* **1991**, 41, 1463- 1470.

Ginsburg, H. and Krugliak, M. Quinoline-containing antimalarials-mode of action, drug resistance and its reversal. *Biochem. Pharmacol.* **1992**, 43(1), 63- 70.

Ginsburg, H., Famin, O., Zhang, J., Krugliak, M. Inhibition of glutathione-dependent degradaion of heme by chloroquine and amodiaquine as a possible basis for their antimalarial mode of action. *Biochem. Pharmacol.* **1998**, 56, 1305- 1313.

Gladwell, M. The mosquito killer. *The New Yorker.* **2001**, 42- 51.

Gleghorn, J.T., Moodie, R.B., Qureshi, E.A., Schofield, K. Heteroaromatic reactivity. Part IV. The kinetics of nitration of cinnoline 2-oxide and quinoline 1-oxide in sulphuric acid. The mechanism of nitration of *N*-heteroaromatic oxides, with special reference to 2,6-lutidine 1-oxide. *J. Chem. Soc.* **1968**, Part B, 316- 323.

Gluzman, I.Y., Francis, S.E., Oksman, A., Smith, C.E., Duffin, K.L., Goldberg, D.E. Order and specificity of the *Plasmodium falciparum* hemoglobin degradation pathway. *J. Clin. Invest.* **1994**, 93, 1602- 1608.

Goldberg, D.E., Slater, A.F.G., Cerami, A., Henderson, G.B. Hemoglobin degradation in the malaria parasite *plasmodium falciparum*: an ordered process in a unique organelle. *Proc. Natl. Acad. Sci. USA.* **1990**, 87(Biochemistry), 2931- 2935.

Goldberg, D.E., Slater, A.F.G., Beavis, R. Hemoglobin degradation in the human malaria pathogen *plasmodium falciparum*: a catabolic pathway initiated by a specific aspartic protease. *J. Exp. Med.* **1991**, 173, 961- 969.

Goldberg, D.E. and Slater, A.F.G. The pathway of hemoglobin degradation in malaria parasites. *Parasitol. Today.* **1992**, 8(8), 280- 283.

Gutteridge, J.M.C. Iron and oxygen: A biologically damaging mixture. *Acta Poediatr. Scand. Suppl.* **1989**, 361, 78- 85.

Hansch, C., and Leo, A. Substituent constants for correlation analysis in chemistry and biology. New York: John Wiley and Sons Inc, **1979**.

Hawley, S.R., Bray, P.G., O'Neill, P.M., Naisbitt, D.J., Park, B.K., Ward, S.A. Manipulation of the *N*-alkyl substituent in amodiaquine to overcome the verapamil-sensitive chloroquine resistance component. *Antimicrob. Agents Chemother.* **1996a**, 40(10), 2345- 2349.

Hawley, S.R., Bray, P.G., O'Neill, P.M., Park, B.K., Ward, S.A. The role of drug accumulation in 4-aminoquinoline antimalarial potency. *Biochem. Pharmacol.* **1996b**, 52, 723- 733.

Hawley, S.R., Bray, P.G., Park, B.K., Ward, S.A. Amodiaquine accumulation in *plasmodium falciparum* as a possible explanation for its superior antimalarial activity over chloroquine. *Mol. Biochem. Parasitol.* **1996c**, 80, 15- 25.

Hawley, S.R., Bray, P.G., Mungthin, M., Atkinson, J.D., O'Neill, P.M., Ward, S.A. Relationship between antimalarial drug activity, accumulation, and inhibition of heme polymerization in *Plasmodium falciparum* in vitro. *Antimicrob. Agents Chemother.* **1998**, 42(3), 682- 686.

Hoard, J.L., Hamor, M.J., Hamor, T.A., Caughey, W.S. The crystal structure and molecular stereochemistry of methoxyiron(III) mesoporphyrin IX dimethyl ester. *J. Am. Chem. Soc.* **1965**, 87(11), 2312- 2319.

Hoard, J.L. Stereochemistry of hemes and other metalloporphyrins. *Science.* **1971**, 174, 1295- 1302.

Hoffman, A.B., Collins, D.M., Day, V.W., Fleischer, E.B., Srivastava, T.S., Hoard, J.L. The crystal structure and molecular stereochemistry of u-Oxo-bis[a,b,g,d-tetraphenylporphinatoiron (III)]. *J. Am. Chem. Soc.* **1972**, 94(10), 3620- 3626.

Homewood, C.A., Warhurst, D.C., Peters, W., Baggaley, V.C. Lysosomes, pH and the antimalarial action of chloroquine. *Nature.* **1972**, 235, 50- 52.

Hunter, C.A. and Sanders, J.K.M. The nature of π-π interactions. *J. Am. Chem. Soc.* **1990**, 112, 5525- 2234.

Inada, Y. and Shibata, K. The soret band of monomeric hematin and its changes on polymerization. *Biochemical and biophysical research communications.* **1962**, 9(4), 323- 327.

Inoue, Y. and Wada, T. Advances in Supramolecular Chemistry. JAI Press Inc, **1997**, Molecular recognition in chemistry and biology as viewed from enthalpy-entropy compensation effect: global understanding of supramolecular interactions. 55-96.

Irvin, J.L. and Irvin, E.M. Spectrophotometric and potentiometric evaluation of apparent acid dissociation exponents of various 4-aminoquinolines. *J. Am. Chem. Soc.* **1947**, 69, 1091- 1099.

Jackson, G.E., Linder, P.W., Voye, A. A potentiometric and spectroscopic study of copper(II)diamidodiamino complexes. *J. Chem. Soc. Dalton Trans.* **1996**, 4605- 4612.

Jackson, G. E and Kelley, M. J. *J. Chem. Soc., Dalton Trans.*, **1989**, 2429

Jacobs, G.H., Oduola, A.M.J., Kyle, D.E., Milhous, W.K., Martin, S.K., AiKawa, M. Ultrastructural study of the effects of chloroquine and verapamil on *P. falciparum*. *Am. J. Trop. Med. Hyg.* **1988**, 39(1), 15- 20.

Johnson, W.S. and Buell, B.G. A new synthesis of chloroquine. *J. Am. Chem. Soc.* **1952**, 74, 4513- 4516.

Katritzky, A. R., and Lagowski, J. M. Chemistry of the heterocyclic *n*-oxides, London and New York, Academic press, **1971**.

Katritzky A. R., Rees, C. W., Scriven, E. F. V., Comprehensive heterocyclic chemistry II. II ed. Elsevier Sciences Ltd, **1996**; 5.03, Pyridines and their Benzo Derivatives: Reactivity of Substituents. 91-134.

Kenyon, R.L. Chloroquine manufacture. *Ind. Chem. Eng.* **1949**, 41(4), 654- 662.

King, F. D., Medicinal Chemistry: principles and practice. 1 ed, The royal society of chemistry, **1994**, Camebridge.

Koenig, D.F. The structure of □-chlorohemin. *Acta Cryst.* **1965**, 18, 663- 673.

Koh, H.L., Go, M.L., Ngiam, T.L., Mak, J.W. Conformational and structural features determining *in vitro* antimalarial activity in some Indolo[3,2-a]quinolines, anilinoquinolines and tertrahydroindolo[3,2-d]benzazepeines. *Eur. J. Med. Chem.* **1994**, 29, 107- 113.

Konigk, E., Mirtsch, S., Putfarken, B., Abdel-Rasoul, S. Plasmodium chabaudi-infection of mice: effects of chloroquine and mefloquine. Inhibition of ornithine decarboxylase activity. *Tropenmed. Parasitol.* **1981**, 32(2), 73- 76.

Krogstad, D.J., Schlesinger, P.H., Gluzman, I.Y. Antimalarials increase vesicle pH in *plasmodium falciparum*. *J. Cell Biol.* **1985**, 101, 2303- 2309.

Krogstad, D.J., Gluzman, I.Y., Kyle, D.E., Oduola, A.M.J., Martin, S.K., Milhous, W.K., Schlesinger, P.H. Efflux of chloroquine from *plasmodium falciparum*: mechanism of chloroquine resistance. *Science.* **1987**, 238, 1283- 1285.

Krogstad, D.J., Schlesinger, P.H., Herwaldt, B.L. Antimalarial agents: mechanism of chloroquine resistance. *Antimicrob. Agents Chemother.* **1988**, 32(6), 799- 801.

Krogstad, D.J., Gluzman, I.Y., Herwaldt, B.L., Schlesinger, P.H., Wellems, T.E. Energy dependence of chloroquine accumulation and chloroquine efflux in *Plasmodium falciparum*. *Biochem. Pharmacol.* **1992**, 43(1), 57- 62.

Kuzelova, K., Mrhalova, M., Hrkal, Z. Kinetics of heme interaction with heme-binding proteins: the effect of heme aggregation state. *Biochim. Biophys. Acta.* **1997**, 1336, 497- 501.

Langreth, S.G., Nguyen-Dinh, P., Trager, W. *Plasmodium falciparum*: Merezoite invasion *in vitro* in the presence of chloroquine. *Exper. Parasitol.* **1978**, 46, 235- 238.

Lauer, W.M., Arnold, R.T., Tiffany, B., Tinker, J. The synthesis of some chloromethoxyquinolines. *J. Am. Chem. Soc.* **1946**, 68, 1268- 1272.

Le Bras, J., Deloron, P., Ricour, A., Andrieu, B., Savel, J., Coulaud, J.P. *P. falciparum*: drug sensitivity *in vitro* of isolates before and after adaptation to continuous culture. *Exper. Parasitol.* **1983**, 56, 9- 14.

Lin, A.J. and Loo, T.J. Synthesis and antitumor activity of halogen substituted 4-(3,3-dimethyl-1-triazeno)quinolines. *J. Med. Chem.* **1978**(21), 268- 272.

Loria, P., Miller, S., Foley, M., Tilley, L. Inhibition of the peroxidative degradation of heme as the basis of action of chloroquine and other quinoline antimalarials. *Biochem. J.* **1999**, 339, 363- 370.

Lucas, B., Miller, J.R., Silver, J., Wilson, M.T. Studies on copper-protoporphyrin-iron(III) complexes. A possible model for cytochrone *c* oxidase. *J. Chem. Soc. Dalton Trans.* **1982**, 1035- 1040.

Lucas, B. and Silver, J. Studies on metal-protoporphyrin-iron(III) complexes. *Inorg. Chim. Acta.* **1983**, 78, 205- 210.

Luthy, N.G., Bergstroom, F.W., Mosher, H.S. Introduction of alkylamino and dialkylamino groups into the quinoline nucleus. *J. Am. Chem. Soc.* **1949**, 71, 1109- 1110.

Lynn, A., Chandra, S., Malhotra, P., Chauhan, V.S. Heme binding and polymerization by *plasmodium falciparum* histadine rich protein II: influence of pH on activity and conformation. *FEBS Lett.* **1999**, 459, 267- 271.

Macintyre, A.C. and Cutler, D.J. Kinetics of chloroquine uptake into isolated rat hepatocytes. *J. Pharm. Sci.* **1993**, 82(6), 592- 600.

Macomber, P.B. and Sprinz, H. Morphological effects of chloroquine on *Plasmodium berghei* in mice. *Nature.* **1967**, 214, 937- 939.

Makler, M.T., Ries, J.M., Williams, J.A., Bancroft, J.E., Piper, R.C., Gibbins, B.L., Hinrichs, D.J. Parasite lactate dehydrogenase as an assay for *P. falciparum* drug sensitivity. *Am. J. Trop. Med. Hyg.* **1993**, 48, 739- 741.

Marques, H.M., Munro, O.Q., Crawcour, M.L. Coordination of N-donor ligands by hematohemin. *Inorg. Chim. Acta.* **1992**, 196, 221- 229.

Marques, H.M., Voster, K., Egan, T.J. The interaction of the haem-octapeptide, N-acetylmicroperoxidase-8 with antimalarial drugs: solution studies and modeling by molecular mechanics methods. *J. Inorg. Biochem.* **1996**, 64, 7- 23.

Martin, S.K., Oduola, A.M.J., Milhous, W.K. Reversal of chloroquine resistance in *plasmodium falciparum* by verapamil. *Science.* **1987**, 235, 899- 901.

Martiney, J.A., Cerami, A., Slater, A.F.G. Verapamil reversal of chloroquine resistance in the malaria parasite *plasmodium falciparum* is specific for resistant parasites and independent of the weak base effect. *J. Biol. Chem.* **1995**, 270(38), 22393- 22398.

Mavuso, W. W. Synthetic haemozoin: characterisation, mechanism of formation from haematin and the effect of antimalarilal drugs. PhD Thesis, University of Cape Town, **2001**.

May, P.M., Murray, K., Williams, D.R. The use of glass electrodes for the determination of formation constants-II. *Talanta.* **1985**, 32(6), 483- 489.

May, P.M., Murray, K., Williams, D.R. The use of glass electrodes for the determination of formation constants-III. Optimisation of titration data: the ESTA library of computer programs. *Talanta.* **1988**, 35, 825- 830.

McGill, C. K., and Rappa, A. Advances in heterocyclic chemistry. Academic press. Inc, **1988**, Vol 4, 1-79.

Meisenheimer, J. Acylindazoles, *Ber.* **1926**, 59, 199-202

Moon, R.P., Tyas, L., Certa, U., Rupp, K., Bur, D., Jacquet, C., Matile, H., Loetscher, H., Grueninger-Leitch, F., Kay, J., Dunn, B.M., Berry, C., Ridley, R.G. Expression and characterisation of plasmepsin I from *Plasmodium falciparum*. *Eur. J. Biochem.* **1997**, 244, 552- 560.

Moreau, S., Perly, B., Biguet, J. Interactions de la chloroquine avec la ferriprotoporphyrine IX. *Biochimie.* **1982**, 64, 1015- 1025.

Moreau, S., Perly, B., Chachaty, C., Deleuze, C. A nuclear magnetic resonance study of the interactions of antimalarial drugs with porphyrins. *Biochim. Biophys. Acta.* **1985**, 840, 107- 116.
Moss, T.H., Bearden, A.J., Caughey, W.S. Mossbauer studies of bonding in iron porphyrin-ligand systems. *J. Chem. Phys.* **1969**, 51(6), 2624- 2631.

Mungthin, M., Bray, P.G., Ridley, R.G., Ward, S.A. Central role of hemoglobin degradation in mechanisms of action of 4-aminoquinolines, quinoline methanols, and phenanthrene methanols. *Antimicrob. Agents Chemother.* **1998**, 42(11), 2973- 2977.

Munro, O.Q. and Marques, H.M. Heme-peptide models for hemoproteins. 1. Solution chemistry of *N*-acetylmicroperoxidase-8. *Inorg. Chem.* **1996**, 35(13), 3752- 3767.

Murray, K., May, P. M. ESTA: equilibrium simulation for titration analysis, University of Wales Inststute of Science and Technology, Cardiff, **1984**.

O'Brien, R.L., Olenick, J.G., Hahn, F.E. Reactions of Quinine, Chloroquine and Quinacrine with DNA and their effects on the DNA and RNA polymerase reactions. *Proc. Natl. Acad. Sci. USA.* **1966**, 55, 1511- 1517.

O'Keeffe, D.H. and Barlow, C.H. Magnetic and spectroscopic probes for FeOFe linkages in hemin solutions. *Bioinorganic chemistry.* **1975**, 5, 125- 147.

O'Neill, P.M., Willcock, D.J., Hawley, S.R., Bray, P.G., Storr, R.C., Ward, S.A., Park, B.K. Synthesis, antimalarial activity, and molecular modeling of tebuquine analogues. *J. Med. Chem.* **1997**, 40, 437-448.

Ochiai, E. Recent Japanese work on the chemistry of pyridine-1-oxide and related compounds. *J. Org. Chem.* **1953**, 18, 534- 551.

Oliveira, M.F., Silva, J.R., Dansa-patreski, M., de Souza, W., Lin, U., Braga, C.M.S., Masuda, H., Oliveira, P.L. Haem detoxification by an insect. *Nature.* **1999**, 400, 517- 518.

Oliveira, M.F., Silva, J.R., Dansa-Petreski, M., de Souza, W., Braga, C.M.S., Masuda, H., Oliveira, P.L. Haemozoin formation in the midgut of the blood-sucking insect *rhodnius prolixus*. *FEBS Lett.* **2000a**, 477, 95- 98.

Oliveira, M.F., d'Avila, J.C.P., Torres, C.R., Oliveira, P.L., Tempone, A.J., Rumjanek, F.D., Braga, C.M.S., Silva, J.R., Dansa-Patretski, M., Oliveira, M.A., de Souza, W., Ferreira, S.T. Hemozoin in *Schistosoma mansoni*. *Mol. Biochem. Parasitol.* **2000b**, 111, 217- 221.

Omodeo-Sale, F., Monti, D., Olliaro, P., Taramelli, D. Prooxidant activity of beta-haematin (synthetic malaria pigment) in arachidonic acid micelles and phospholipid large unilamellar vesicles. *Biochem. Pharmacol.* **2001**, 61, 999- 1009.

Orjih, A.U., Banyal, H.S., Chevli, R., Fitch, C.D. Hemin lyses malaria parasites. *Science.* **1981**, 214, 667- 669.

Orjih, A.U., Kanjananggulpan, P., Fitch, C.D. Ferriprotoporphyrin IX and cell lysis: A protective role for hydrogen peroxide. *Life Sci.* **1988**, 42(25), 2603- 2607.

Pagola, S., Stephens, P.W., Scott Bohle, D., Kosar, A.D., Madsen, S.K. The structure of malaria pigment (β-haematin). *Nature.* **2000**, 404, 307- 310.

Parapini, S., Basilico, N., Pasini, E., Egan, T.J., Olliaro, P., Taramelli, D., Monti, D. Standardization of the physicochemical parameters to assess *in vitro* the β-hematin inhibitory activity of antimalarial drugs. *Exper. Parasitol.* **2000**, 96(4), 249- 256.

Pasvol.,Clinical Infectious Diseases: Malaria. London: Bailliere Tindall; **1995**; 211.

Peck, R.M., Preston, R.K., Creech, H.J. Nitrogen mustard analogues of antimalarial drugs. *J. Am. Chem. Soc.* **1959**, 81, 3984- 3989.

Peters, W. and Robinson, B.I. The chemotherapy of rodent malaria. LVIII. Drug combinations to impede the selection of drug resistance, part 2: the new generation-artemesinin or artesunate with long-acting blood schizontocides. *Ann. Trop. Med. Parasitol.* **2000**, 94(1), 23- 35.

Price, C.C., Leonard, N.J., Peel, E.W., Reitsema, R.H. Some 4-Amino-7-chloroquinoline derivatives. *J. Am. Chem. Soc.* **1946a**, 68, 1807- 1808.

Price, C.C. and Roberts, R.M. The synthesis of 4-hydroxyquinolines. I. Through ethoxymethylenemalonic ester. *J. Am. Chem. Soc.* **1946b**, 68, 1204- 1207.

Rawn, D, J. Biochemistry. I ed. Burlington, Neil Patterson Publishers, 1989; 6, Hemoglobin and myoglobin: oxygen binding proteins. 121-47.

Raynes, K., Galatis, D., Cowman, A.F., Tilley, L., Deady, L.W. Synthesis and activity of some antimalarial bisquinolines. *J. Med. Chem.* **1995**, 38, 204- 206.

Raynes, K., Foley, M., Tilley, L., Deady, L.W. Novel bisquinoline antimalarials. *Biochem. Pharmacol.* **1996**, 52, 551- 559.

Raynes, K. Bisquinoline antimalarials: their role in malaria chemotherapy. *Int. J. Parasitol.* **1999**, 29, 367- 379.

Ridley, R.G., Hofheinz, W., Matile, H., Jaquet, C., Dorn, A., Masciadri, R., Jolid èon, S., Richter, W.F., Guenzi, A., Girometta, M., Urwyler, H., Huber, W., Thaithong, S., Peters, W. 4-Aminoquinoline analogs of chloroquine with shortened side chains retain activity against chloroquine-resistant *plasmodium falciparum. Antimicrob. Agents Chemother.* **1996**, 40(8), 1846- 1854.

Ridley, R.G., Matile, H., Jaquet, C., Dorn, A., Hofheinz, W., Leupin, W., Masciadri, R., Theil, F., Richter, W., F., Girometta, M., Guenzi, A., Urwyler, H., Gocke, E., Potthast, J., Csato, M., Thomas, A., Peters, W. Antimalarial activity of the bisquinoloine *trans*-*N1*,*N2*-Bis(7-Chloroquinolin-4-yl)Cyclohexane-1,2-Diamine: Comparison of two stereoisomers and detailed evaluation of the *S*,S enantiomer, Ro 47-7737. *Antimicrob. Agents Chemother.* **1997**, 41(3), 677- 686.

Ridley, R.G. and Hudson, A.T. Quinoline antimalarials. *Exp. Opin. Ther. Patents.* **1998**, 8(2), 121- 136.

Riegel, B., Lappin, G.R., Adelson, B.H., Jackson, R.I., Albisetti, C.J., Dodson, R.M., Baker, R.H. The synthesis of some 4-quinolinols and 4-chloroquinolines by the ethoxymethylenemalonic ester method. *J. Am. Chem. Soc.* **1946**, 68, 1264- 1266.

Roseman, K.A., Gould, M.M., Linfield, W.M., Edwards, B.E. Antimalarials. 8-Chloro-4-(2'-N,N-dibutylamino-1'-hydroxyethyl)benzo[h]-1,6-naphthyridine. *J. Med. Chem.* **1970**, 13, 230- 233.

Rosenthal, P.J. and Meshnick, S.R. Hemoglobin catabolism and iron utilizatioby malaria parasites. *Mol. Biochem. Parasitol.* **1996**, 83, 131- 139.

Russell, P. F. Practical Malariology. 2nd ed. London: Oxford university press, 1963.

Sadasivan, N., Eberspaecher, H.I., Fuchsman, W.H., Caughey, W.S. Substituted deuteroporphyrins. VI. Ligand-exchange and dimerization reactions of deuterohemins. *Biochemistry.* **1969**, 8(2), 534-541.

Sanchez, C.P., Wunsch, S., Lanzer, M. Identification of a chloroquine importer in *Plasmodium falciparum*. *J. Biol. Chem.* **1997**, 272(5), 2652- 2658.

Schmitt, T.H., Frezzatti, W.A., Schreier, S. Hemin-induced lipid membrane disorder and increased permeability: a molecular model for the mechanism of cell lysis. *Arch. Biochem. Biophys.* **1993**, 307(1), 96- 103.

Scott Bohle, D., Debrunner, P., Jordan, P.A., Madsen, S.K., Schulz, C.E. Aggregated heme detoxification byproducts in malaria trophozoites: □-hematin and malaria pigment have a single S=5/2 iron environment in the bulk phase as determined by EPR and magnetic mossbauer spectroscopy. *J. Am. Chem. Soc.* **1998**, 120, 8253- 8254.

Shack, J. and Clarke, W.M. Metalloporphyrins VI. Cycles of changes in systems containing heme. *J. Biol. Chem.* **1947**, 171, 143- 187.

Sherman IW, Malaria: parasite biology, pathogenesis, and protection. Washington: American society for microbiology, 1998.

Shah, V.R., Bose, J.L., Shah, R.C. *J. Sci. Ind. Rec.* **1960**, 19(B), 176

Sijwali, P.S., Shenai, B.R., Gut, J., Singh, A., Rosenthal, P.J. Expression and characterisation of the *plasmodium falciparum* haemoglobinase falcipain-3. *Biochem. J.* **2001**, 360, 481- 489.

Silver, J. and Lucas, B. Mossbauer studies on protoporphyrin IX Iron(III) solutions. *Inorg. Chim. Acta.* **1983**, 78, 219- 224.

Simplicio, J. Hemin monomers in micellar sodium lauryl sulfate. A spectral and equilibrium study with cyanide. *Biochemistry.* **1972**, 11(13), 2525- 2528.

Simplicio, J. and Schwenzer, K. Hemin intercalated in micellar cetyltrimethylammonium bromide and triton X-100. A kinetic, spectral and equilibrium study with cyanide. *Biochemistry.* **1973**, 12(10), 1923-1929.

Simplicio, J., Schwenzer, K., Maenpa, F. Kinetics of cyanate and imidazole binding to hemin in micelles. *J. Am. Chem. Soc.* **1975**, 97(25), 7319- 7326.

Slater, A.F.G., Swiggard, W.J., Orton, B.R., Flitter, W.D., Goldberg, D.E., Cerami, A., Henderson, G.B. An iron-carboxylate bond links the heme units of malaria pigment. *Proc. Natl. Acad. Sci. USA.* **1991**, 88(biochemistry), 325- 329.

Slater, A.F.G. and Cerami, A. Inhibition by chloroquine of a novel haem polymerase enzyme activity in malaria trophozoites. *Nature.* **1992**, 355, 167- 169.

Slater, A.F.G. Chloroquine: Mechanism of drug action and resistance in *plasmodium falciparum*. *Pharmac. Ther.* **1993**, 57, 203- 235.

Snyder, H.R., Freier, H.E., Kovacic, P., Van Heyningen, E.M. Synthesis of 4-hydroxyquinolines. VIII. Some halogen containing 4-aminoquinoline derivatives. *J. Am. Chem. Soc.* **1947**, 69, 371- 374.

Srinivas, V. and Mohan Rao, C. Time profile of hemin aggregaton: and analysis. *Biochemistry international.* **1990**, 21(5), 849- 855.

Sterling drug inc., US2940974. 1960; EN,54,24813.

Sugioka, Y., Suzuki, M., Sugioka, K., Nakano, M. A ferriprotoporphyrin IX-chloroquine complex promotes membrane phospholipid peroxidation. *FEBS Lett.* **1987**, 223(2), 251- 254.

Sugioka, Y. and Suzuki, M. The chemical basis for the ferriprotoporphyrin IX-chloroquine complex induced lipid peroxidation. *Biochim. Biophys. Acta.* **1991**, 1074, 19- 24.

Sullivan, D.J., Gluzman, I.Y., Goldberg, D.E. Plasmodium hemozoin formation mediated by histidine-rich proteins. *Science.* **1996a**, 271, 219- 222.

Sullivan, D.J., Gluzman, I.Y., Russell, D.G., Goldberg, D.E. On the molecular mechanism of chloroquine's antimalarial action. *Proc. Natl. Acad. Sci. USA.* **1996b**, 93(Medical sciences), 11865-11870.

Sullivan, D.J., Matile, H., Ridley, R.G., Goldberg, D.E. A common mechanism for blockade of heme polymerization by antimalarial quinolines. *J. Biol. Chem.* **1998**, 273(47), 31103- 31107.

Surolina, N. and Padmanaban, G. Chloroquine inhibits heme-dependent protein synthesis in *Plasmodium falciparum*. *Proc. Natl. Acad. Sci. USA.* **1991**, 88, 4786- 4790.

Surrey, A.R. and Hammer, H.F. Some 7-substituted 4-aminoquinoline derivatives. *J. Am. Chem. Soc.* **1946**, 68, 113- 116.

Surrey, A.R. and Cutler, R.A. The role of phenol in the reaction of 4,7-dichloroquinoline with novol diamine. *J. Am. Chem. Soc.* **1951**, 73, 2623- 2626.

Surrey, A.R., Lesher, G.Y., Mayer, J.R., Webb, W.G. Hypotensive agents. II. The preparation of Quarternary salts of some 4-dialkylaminoalkylaminoquinolines. *J. Am. Chem. Soc.* **1959**, 81, 2894-2897.

Takahashi, Kazuhiko, Kohda, Kohfuku, Huang, Kawazoe, Yutaka; *Chem. Pharm. Bull.* **1983**, 31(3), 959- 965.

Tappel, A.L. The mechanism of the oxidation of unsaturated fatty acids catalyzed by hematin compounds. *Arch. Biochem. Biophys.* **1953**, 44, 378- 395.

Tappel, A.L. Unsaturated lipid oxidation catalysed by hematin compounds. *Arch. Biochem. Biophys.* **1955**, 721- 733.

The World Health Report 1999: making a difference. **1999**.

Tipping, E., Ketterer, B., Christodoulides, L. Interactions of small molecules with phospholipid bilayers. *Biochem. J.* **1979**, 180, 327- 337.

Tondys, H., Van der Plas, H.C., Wozniak, M. On the Chichibabin amination of quinoline and some nitroquinolines. *J. Heterocyclic Chem.* **1985**, 22, 353- 355.

Torrens, M.A., Straub, D.K., Epstein, L.M. Mossbauer studies on oxo-bridged iron (III) porphines. *J. Am. Chem. Soc.* **1972**, 94(12), 4160- 4167.

Trager, W. and Jensen, J.B. Human malaria parasites in continuous culture. *Science.* **1976**, 193, 674-675.

Tyas, L., Gluzman, I., Moon, R.P., Rupp, K., Westling, J., Ridley, R.G., Kay, J., Goldberg, D.E., Berry, C. Naturally-occurring and recombinant forms of the aspartic proteinases plasmepsins I and II from the human malaria parasite. *FEBS Lett.* **1999**, 454, 210- 214.

Van der Zee, J., Barr, D.P., Mason, R.P. ESR spin trapping investigation of radical formation from the reaction between hematin and *tert*-butyl hydroperoxide. *Free radical biology and medicine.* **1996**, 20(2), 199- 206.

Van der Jagt, D.L., Hunsaker, L.A., Campos, N.M. Comparison of proteases from chloroquine-sensitive and chloroquine-resistant strains of *P. falciparum*. *Biochem. Pharmacol.* **1987**, 36(19), 3285-3291.

Vennerstrom, J.L., Ellis, W.Y., Ager, A.L., Andersen, S.L., Gerena, L., Milhous, W.K. N,N-Bis(7-chloroquinolin-4-yl)alkanediamines with potential against chloroquine-resistant malaria. *J. Med. Chem.* **1992**, 35, 2429- 2134.

Vennerstrom, J.L., Ager, A.L., Dorn, A., Andersen, S.L., Gerena, L., Ridley, R.G., Milhous, W.K. Bisquinolines. 2. Antimalarial *N,N*-bis(7-chloroquinolin-4-yl)heteroalkanediamines. *J. Med. Chem.* **1998**, 41, 4360- 4364.

Vippagunta, S.R., Dorn, A., Matile, H., Bhattacharjee, A.K., Karle, J.M., Ellis, W.Y., Ridley, R.G., Vennerstrom, J.L. Structural specificity of chloroquine-hematin binding related to inhibition of hematin polymerization and parasite growth. *J. Med. Chem.* **1999**, 42, 4630- 4639.

Ward, S.A., Bray, P.G., Mungthin, M., Hawley, S.R. Current views on the mechanisms of resistance to quinoline-containing drugs in *plasmodium falciparum*. *Ann. Trop. Med. Parasitol.* **1995**, 89(2), 121-124.

Ward, S.A., Bray, P.G., Hawley, S.R. Quinoline resistance mechanisms in *P. falciparum*: the debate goes on. *Parasitology.* **1997**, 114(Suppl), s125- s136.

Ward, S.A and Bray, P.G. Definitive proof for a role of *pfmdr 1* in quinoline resistance in *Plasmodiam falciparum*. *Drug Res. Updat*, **2000**, 3, 80-81.

Warhurst, D.C. The quinine-haemin interaction and its relationship to antimalarial activity. *Biochem. Pharmacol.* **1981**, 30, 3323- 3327.

Warhurst, D.C. Antimalarial interaction with ferriprotoporphyrin IX monomer and its relationship to activity of the blood schizontocides. *Ann. Trop. Med. Parasitol.* **1987**, 81(1), 65- 67.

Warhurst, D.C. Mechanism of chloroquine resistance. *Parasitol. Today.* **1988**, 4(8), 211- 213.

Warhurst, D. New developments: chloroquine resistance in *plasmodiam falciparum*. *Drug Resist. Updat.* **2001**, 4(3), 141-144.

Watanabe, T., Tanaka, Y., Sekiya, K., Akita, Y., Ohta, A. A convenieny synthesis of methylamino and dimethylamino substituted aromatic compounds. *Synthesis Communications.* **1980**, 39- 41.

Wellems, T.E., Panton, L.J., Gluzman, I.Y., do Rosario, V.E., Gwadz, R.W., Walker-Jonah, A., Krogstad, D.J. Chloroquine resistance not linked to *mdr*-like genes in a *plasmodium falciparum* cross. *Nature.* **1990**, 345, 253- 258.

Wellems, T.E., Walker-Jonah, A., Panton, L.J. Genetic mapping of the chloroquine-resistance locus on *P. falciparum* chromosome 7. *Proc. Natl. Acad. Sci. USA.* **1991**, 88, 3382- 3386.

White, N.J., Warrell, D.A., Bunnag, D. Quinidine in falciparum malaria. *The Lancet.* **1981**, 1069- 1071.

White, Dolphin D,The porphyrins. New York: Academic press, **1978**.

Wilson, C.M., Serrano, A.E., Wasley, A., Bogenschutz, M.P., Shankar, A.H., Wirth, D.F. Amplification of a gene related to mammalian mdr genes in drug -resistant *P. falciparum*. *Science.* **1989**, 244, 1184- 1186.

Winstanley, P.A. and Breckenridge, A.M. Currently important antimalarial drugs. *Ann. Trop. Med. Parasitol.* **1987**, 81(5), 619- 627.

Wunsch, S., Sanchez, C.P., Gekle, M., Grobe-Wortmann, L., Wiesner, J., Lanzer, M. Differential stimulation of the Na^+/H^+ exchanger determines chloroquine uptake in *Plasmodium falciparum*. *J. Cell Biol.* **1998**, 140(2), 335- 345.

Yasuhara, T., Mori, M., Wakamatsu, K., Kubo, K. Isolation and identification of hemin as an endogeneous Na^+/K^+-atpase inhibitor from porcine blood cells. *Biochem. Biophys. Res. Commun.* **1991**, 178(1), 95- 103.

Yayon, A., Vande Waa, J.A., Yayon, M., Geary, T.G., Jensen, J.B. Stage-dependent effects of chloroquine on *P. falciparum* in vitro. *J. Protozool.* **1983**, 30(4), 642- 647.

Yayon, A., Cabantchik, Z.I., Ginsburg, H. Identification of the acidic compartment of *plasmodium falciparum*-infected human erythrocytes as the target of the antimalarial drug chloroquine. *EMBO J.* **1984**a, 3(11), 2695- 2700.

Yayon, A., Timberg, R., Friedman, S., Ginsburg, H. Effects of chloroquine on the feeding mechanism of the intraerythrocytic human malarial parasite *P. falciparum*. *J. Protozool.* **1984**b, 31(3), 367- 372.

Yayon, A., Cabantchik, Z.I., Ginsburg, H. Susceptibility of human malaria parasites to chloroquine is pH dependent. *Proc. Natl. Acad. Sci. USA.* **1985**, 82(Cell Biology), 2784- 2788.

Yennawar, H.P. and Viswamitra, M.A. Steric and rotational constraints in the x-ray structure of the antimalarial drug amodiaquine. *Curr. Sci.* **1991**, 61, 39- 43.

Yokomama, A., Ohwanda, T., Saito, S., Shudo, K. Nitration of quinoline-1-oxide: mechanism of regioselectivity. *Chem. Pharm. Bull.* **1997**, 45(2), 279- 283.

Zarchin, S., Krugliak, M., Ginsburg, H. Digestion of the host erythrocyte by malaria parasites is the primary target for quinoline containing antimalarials. *Biochem. Pharmacol.* **1986**, 35(14), 2435- 2442.

Zhang, J., Krugliak, M., Ginsburg, H. The fate of ferriprotoporphyrin IX in malaria infected erythrocytes in conjunction with the mode of action of antimalarial drugs. *Mol. Biochem. Parasitol.* **1999**, 129-141.

Zhang, L., Dresser, M.J., Chun, J. K., Babbit, P. C., Giacomini, K. M. Cloning and functional characterisation of a rat renal organic cation transporter isoform (rOCTIA). *J. Biol. Chem.*, **1997**, 272, 16548-16554.

Zhang, Y. Inhibition of hemoglobin degradation in *P. falciparum* by chloroquine and ammonium chloride. *Exper. Parasitol.* **1987**, 64, 322- 327.